

**VOLCANIC GEOLOGY
AND
HYDROTHERMAL SYSTEMS
OF THE
YELLOWSTONE CALDERA**

**PREPARED FOR
UNION GEOTHERMAL DIVISION
UNION OIL COMPANY OF CALIFORNIA**

**DENNIS L. NIELSON
DUNCAN FOLEY
REGINA M. CAPUANO**

Earth Science Laboratory

**University of Utah Research Institute
420 Chipeta Way, Suite 120
Salt Lake City, Utah 84108
(801) 581-5283**

JUNE 13-18, 1983



Volcanic Geology and
Hydrothermal Systems of the
Yellowstone Caldera

June 13-18, 1983
Revised Schedule

Sunday

Assemble in West Yellowstone, MT.

Monday

morning

Lectures

1. Introduction to volcanic setting of Yellowstone - Foley
2. Magmatism and Petrology of volcanic systems - Nielson
3. Tectonic environments and physical spectrum of volcanism - Foley

afternoon

Field Trip

Mt. Washburn - andesite vent facies and regional geology

evening

Lecture

Examples of eruptive processes from Central America, Hawaii, and others - Nielson

Tuesday

morning

Lectures

4. Caldera Cycles - Nielson
5. Ash-flow tuffs and their relations - Foley
6. Tertiary calderas of Nevada - Foley

afternoon

Field Trip

Gardiner River - ash flow tuff cooling zone
Virginia Cascades
Firehole River drive

evening

Lecture

Valles Caldera - Nielson

Wednesday

morning

Lectures

7. Hydrothermal Systems - Nielson
8. Geology of Hydrothermal features - Foley

Introduction to volcanic setting of Yellowstone area

- I. Regional geological setting
- II. Absaroka volcanism
 - A. Location and nature of volcanism
 - B. Facies distribution
- III. Fossil forest controversy
 - A. Classical interpretation as simple layers
 - B. Interpretation of complex stratigraphy
- IV. Pre-Yellowstone Miocene volcanism
 - A. Regional trends
 - B. Snake River Plain
 - 1. Occurrence of calderas
 - 2. Occurrence of basaltic volcanism
 - 3. Plate tectonic setting
- V. Yellowstone volcanic field
 - A. Eruptive sequence
 - B. Evidence for magma

BATHOLITH

**NORTHERN
ROCKY
MOUNTAINS CV**

BEARTOOTH

YNP

**BIGHORN
BASIN**

ABSAROKA

IP

**TETONS
GROS
VENTRE**

**SNAKE RIVER
ID.**

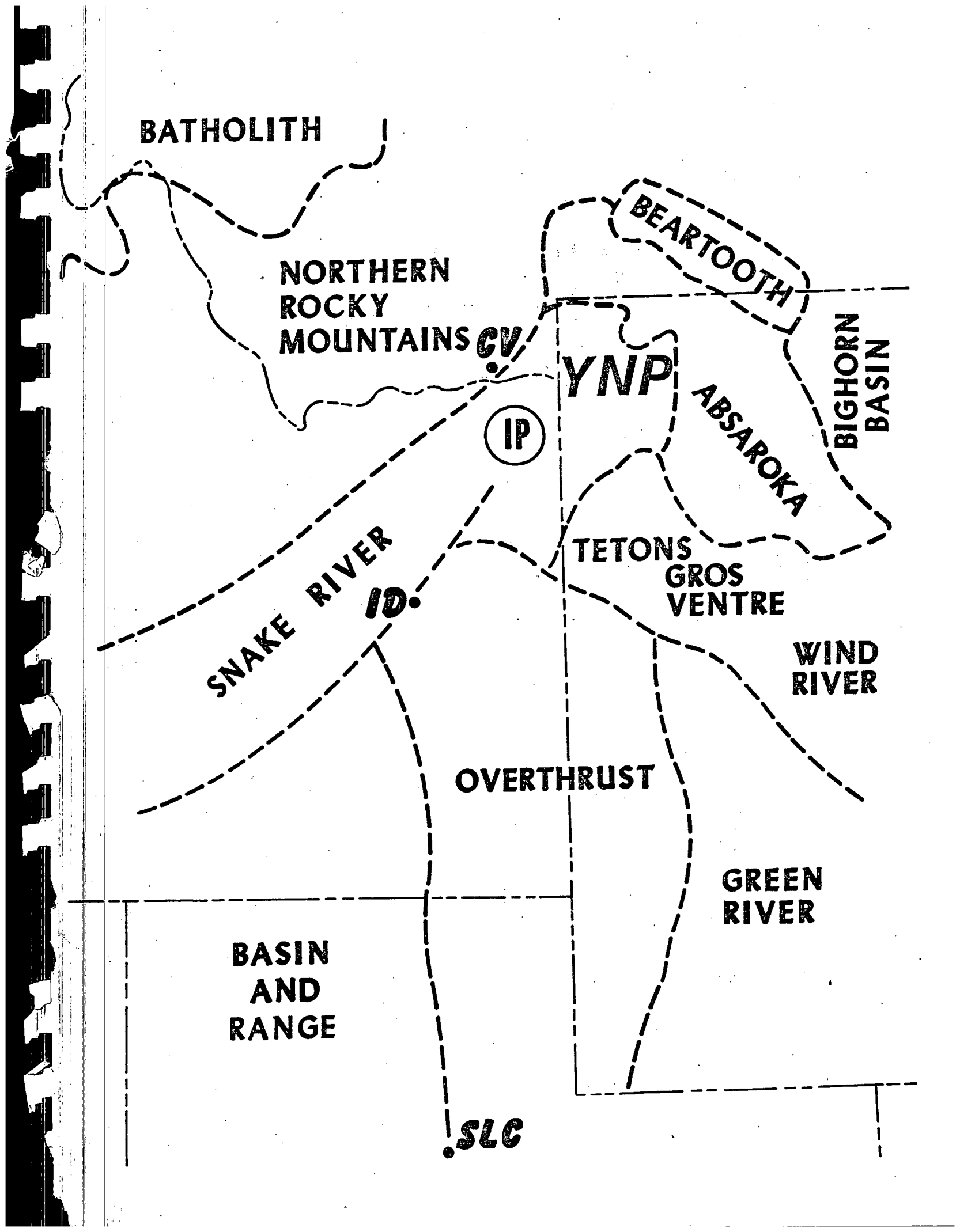
**WIND
RIVER**

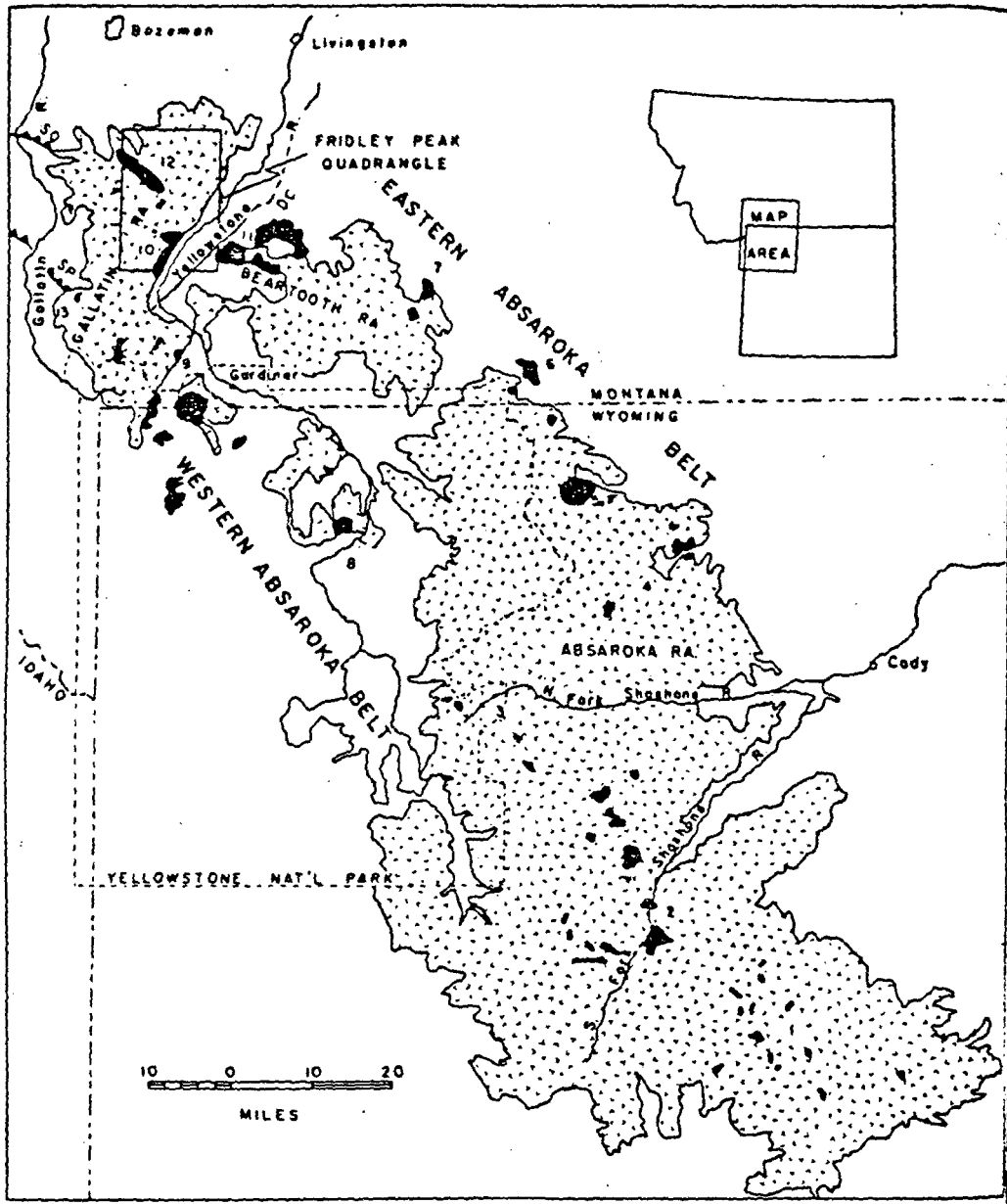
OVERTHRUST

**GREEN
RIVER**

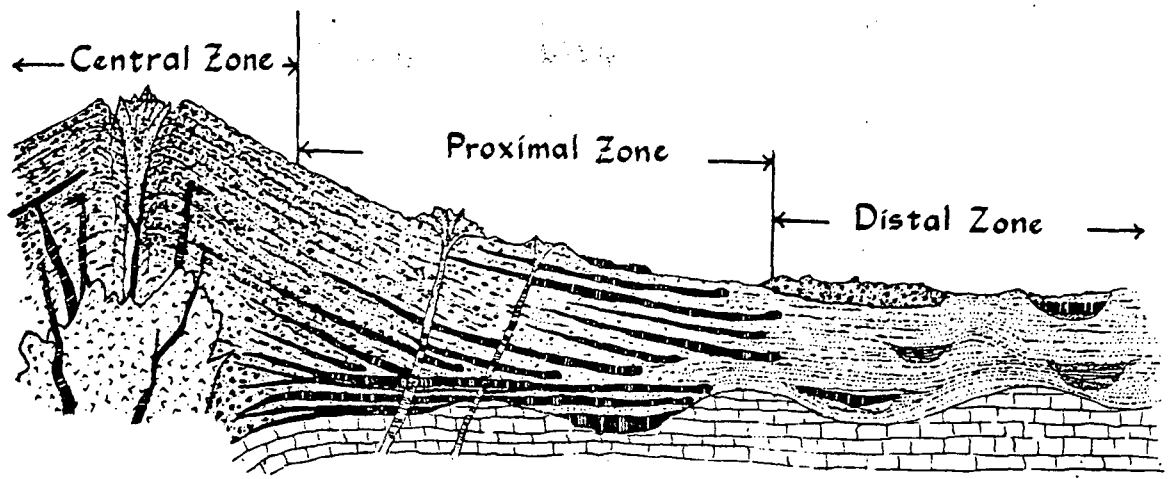
**BASIN
AND
RANGE**

.SLC





Chadwick, R.A., 1970, Belts of eruptive centers in the Absaroka-Gallatin volcanic province, Wyoming-Montana: Geol. Soc. Am. Bull., V. 81, p. 267-274



Central Facies (within about 0.5 to 2 km of central vents)

Volcanic rocks emplaced close to volcanic vents are normally easy to recognize in the field. Most are distinguished by some combination of the following features:

- dikes, especially those that are radial or randomly oriented
- sills that are concordant with moderate to steep initial dips
- breccia pipes and stocks
- hydrothermal alteration with steep lateral gradients
- coarse Strombolian ejecta
- thick, steeply banded siliceous lavas
- coarsely stratified but poorly sorted tephra
- steep initial dips
- thin lava flows that are volumetrically subordinate to fragmental ejecta
- ponded crater- and vent-fillings with sharply divergent cooling joints

Proximal Facies (up to 5 to 15 km from central vents)

The rocks laid down at increasing distances on the slopes and outer flanks of a large volcanic complex have many of the following features:

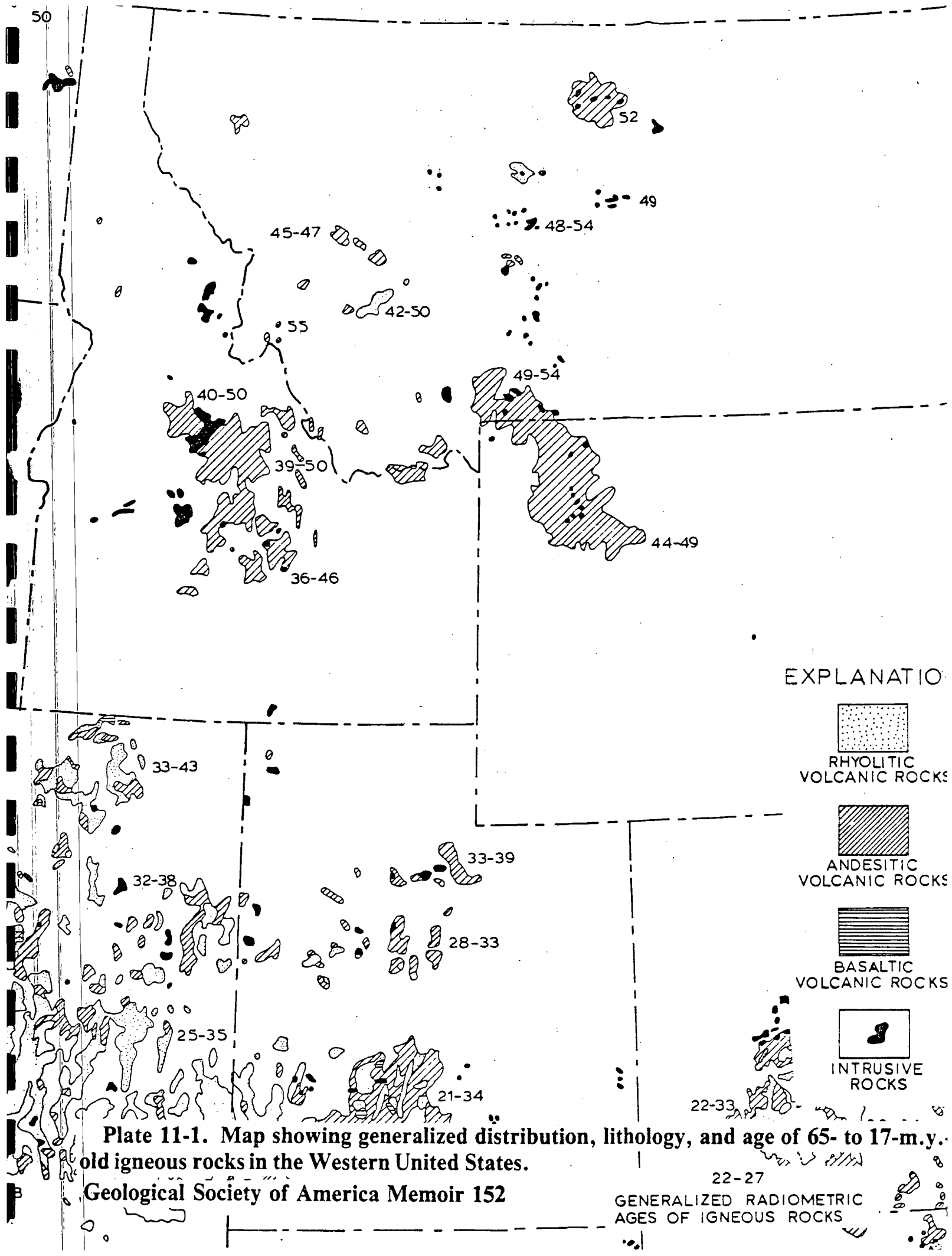
- broad, thick lavas
- lahars with angular or subangular blocks up to 10 m or so in diameter
- tephra layers with good sorting and grain-sizes mainly in the lapilli to coarse ash range
- zones of weathering and soil development between lava flows
- clastic debris reworked by water
- ignimbrites with moderate to strong welding and compaction

Distal Facies (more than about 5 to 15 km from central vents)

Volcanic rocks laid down well beyond the base of a large volcano tend to have a greater lateral continuity than those of inner zones and they conform more closely to conventional stratigraphic criteria. The features one finds in these outlying areas include:

- finely layered tephra with grain-sizes in the range of coarse to fine ash and with an outward-increasing ratio of glass to crystals
- lahars with blocks that rarely exceed a meter in diameter and have rounded or subrounded particles in their matrix
- ignimbrites with moderate to weak welding
- interlayered shallow-water sediments, soils, and organic debris
- lava flows restricted mainly to isolated vents, basaltic sheets, and intra-canyon flows

from: Williams and McBirney, *Volcanology*



EXPLANATION


 RHYOLITIC
 VOLCANIC ROCKS


 ANDESITIC
 VOLCANIC ROCKS


 BASALTIC
 VOLCANIC ROCKS

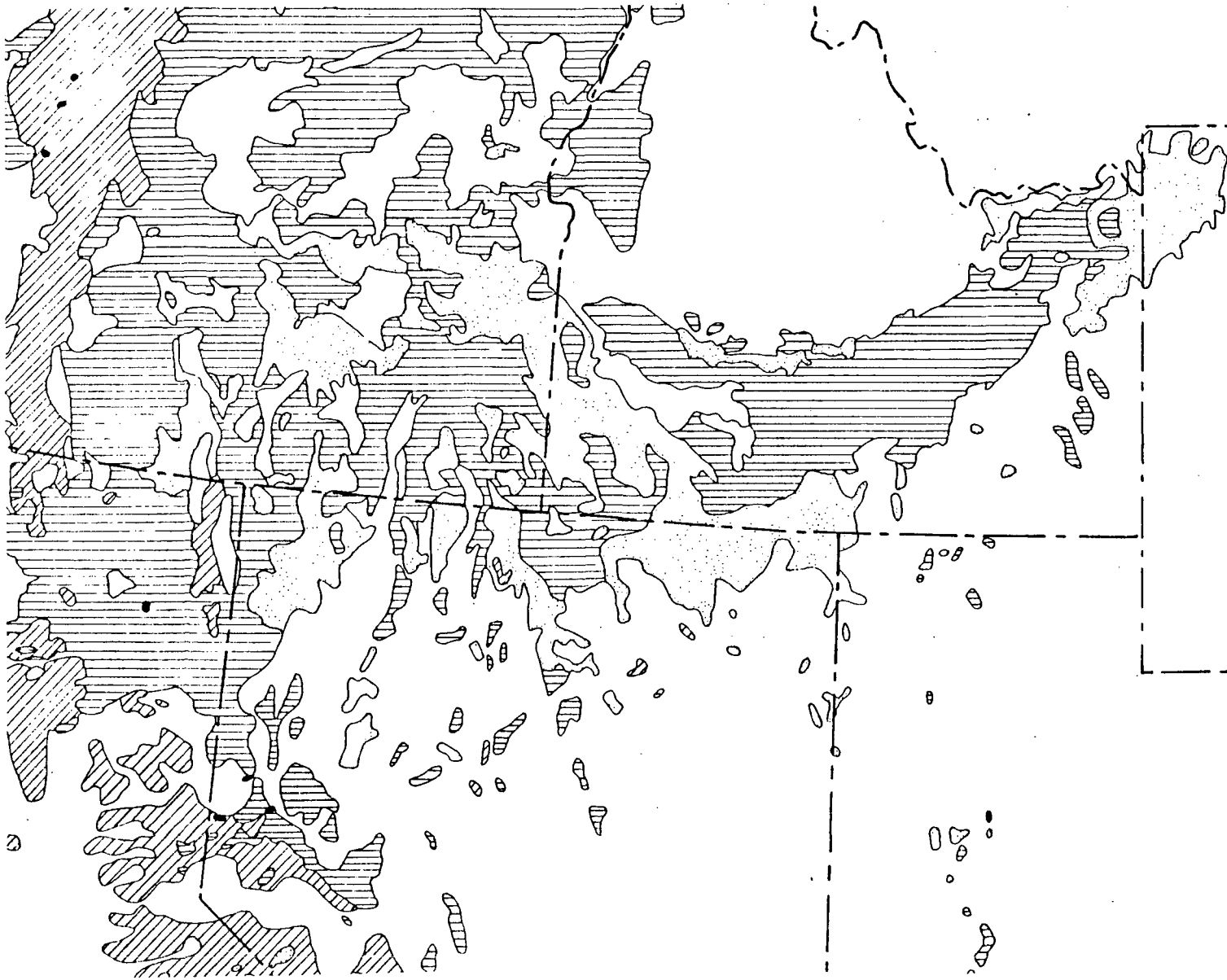

 INTRUSIVE
 ROCKS

22-27
 22-33
 25-35
 28-33
 32-38
 33-39
 33-43
 36-46
 39-50
 40-50
 42-50
 44-49
 45-47
 48-54
 49
 49-54
 52

Plate 11-1. Map showing generalized distribution, lithology, and age of 65- to 17-m.y. old igneous rocks in the Western United States.

Geological Society of America Memoir 152

GENERALIZED RADIOMETRIC
 AGES OF IGNEOUS ROCKS



EXPLANATION


 RHYOLITIC
 VOLCANIC ROCKS

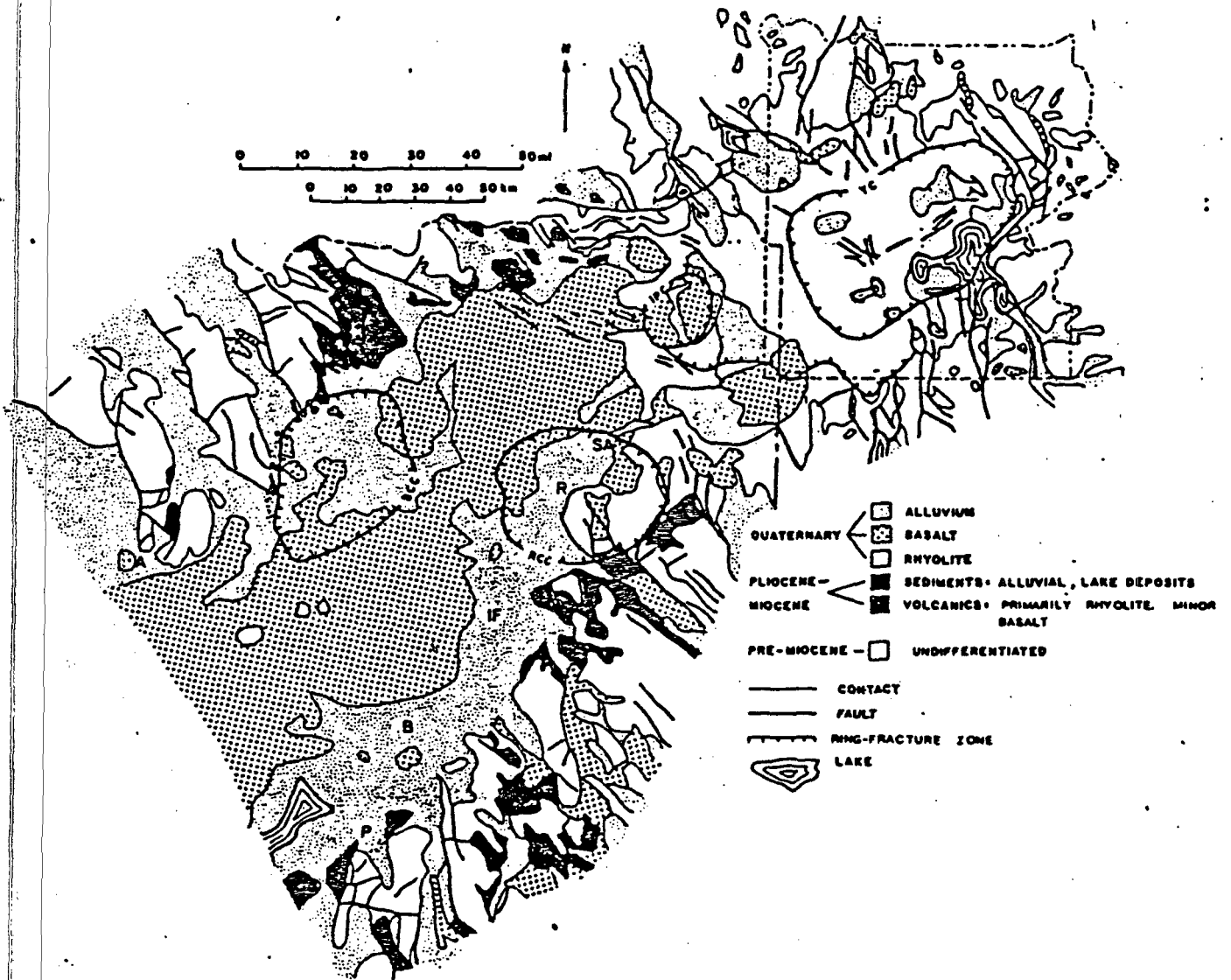

 ANDESITIC
 VOLCANIC ROCKS


 BASALTIC
 VOLCANIC ROCKS


 INTRUSIVE
 ROCKS

Plate 11-2. Map showing generalized distribution and lithology of igneous rocks less than 17 m.y. old in the Western United States.

Geological Society of America Memoir 152



McBroome and others, 1981

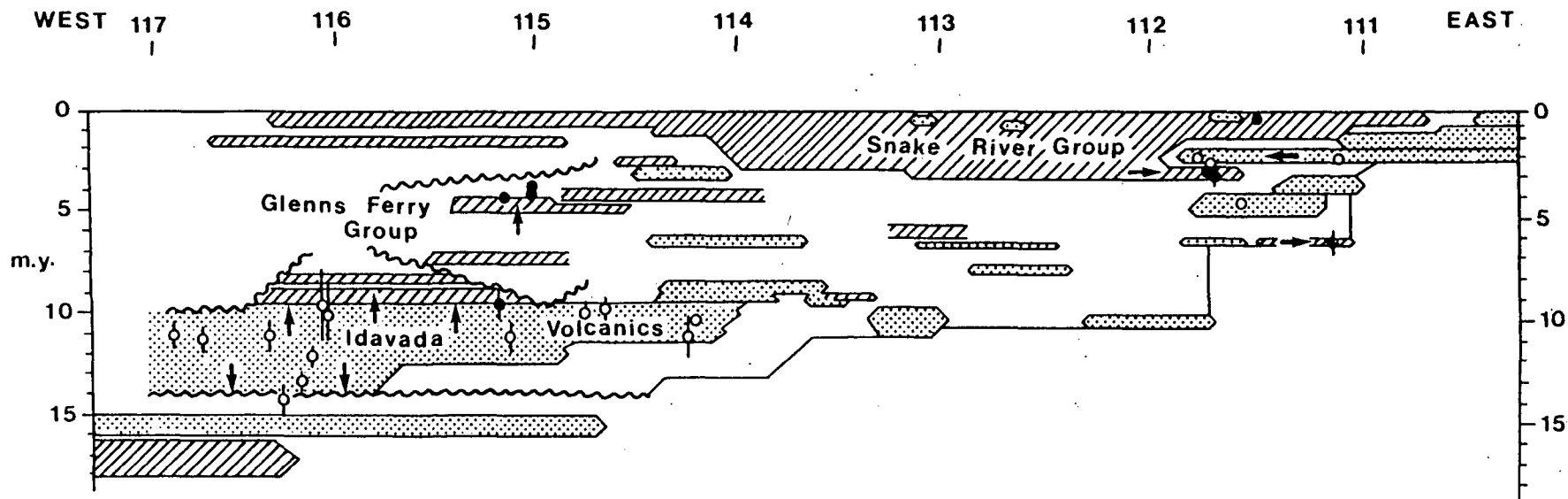


FIGURE 1. Space-time profile along the Snake River Plain, Idaho (simplified from Armstrong and others, 1975). New K-Ar dates are shown by black spots (for basalt) and open circles (for rhyolite). Unpatterned areas represent erosion intervals, sedimentary deposits, and minor volcanic units. Basalt formations are shaded with diagonal lines, rhyolite formations are stippled. The arrows highlight the changes caused by new information: expansion of the time span of eruption of Idavada Volcanics, shift of Glenns Ferry basalts to a younger date, and lateral extension of some units in the eastern Plain.

Armstrong and others, 1980

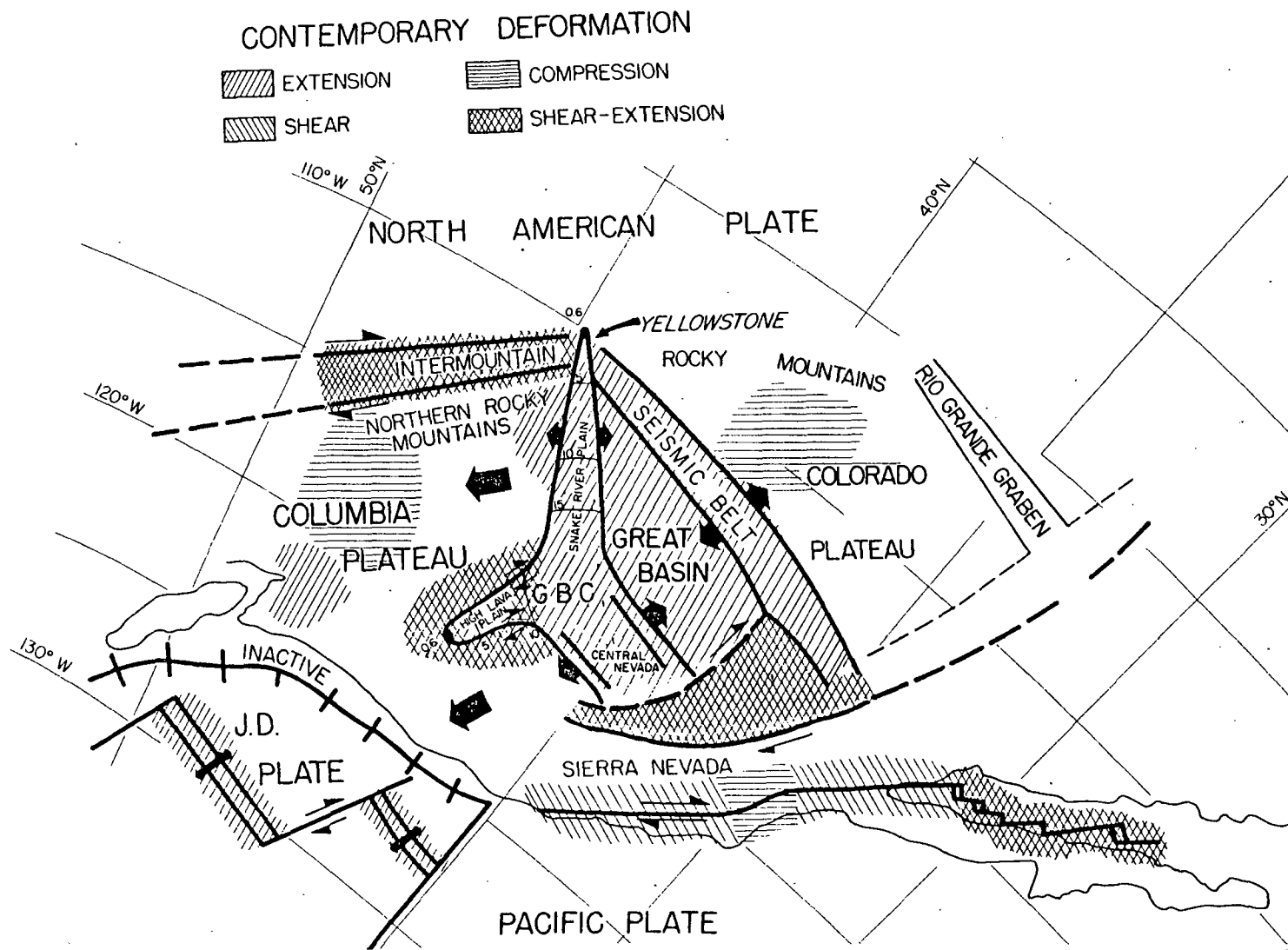


Figure 6-13. Summary of inferred contemporary deformation of the western North American plate. GBC = Great Basin Center of lithospheric uplift and divergence; J. D. = Juan de Fuca plate. Large arrows infer directions of subplate motions; small arrows indicate relative direction of motion on strike-slip fault zones. Fine lines across Snake River Plain-High Lava Plain indicate contours in m.y. B.P. of initiation of volcanism from Armstrong and others (1975) and MacLeod and others (1975).

Yellowstone Volcanic Field - Summary of eruptive history

Activity composed of three cycles, each marked by cataclysmic eruption of ash flow tuffs.

General sequence:

1. Rise of magma and doming
2. Rhyolite flows marking future ring fracture zone
3. \pm precursor basalts
4. Cataclysmic eruption
5. Caldera collapse and filling by rhyolites, \pm resurgence
6. Local basalts

The general sequence of Smith and Bailey (1968) holds, but details vary.

Cycle 1

Rise of three shallow pods of magma from deep source
Doming of surface
Eruption of rhyolites in east-central Yellowstone Park and north of Ashton, ID.
Eruption of basalts near Tower Falls and Mt. Everts, and along the W. Fork of the Madison River
Cataclysmic eruption of Huckleberry Ridge Tuff, 2 my, 2500 km³
Three members from vents in Yellowstone and Island Park area.
Caldera collapse
No resurgence (?)
Basalt in Narrows of Yellowstone River

Cycle 2

Early rhyolites in western part of Island Park
Eruption of Mesa Falls, Tuff, 1.2. my, 280 km³
Collapse
Rhyolite domes
Basalts, including much younger Snake River Plain type filling caldera

Cycle 3

Rise of two shallow magma bodies
Doming and emplacement of rhyolite flows along incipient ring of fracture zone
Lava Creek Tuff, 0.6 my, 1000 km³, two vents, Mallard Lake and Sour Creek
Collapse following eruption
Rhyolite flows and tuffs, within 10,000 years of eruption, along caldera margin
Three major younger sequences of rhyolite flows, and tuffs from W. Thumb
150, 110, 70 kybp
Basalts outside caldera, immediately post eruption and continuing

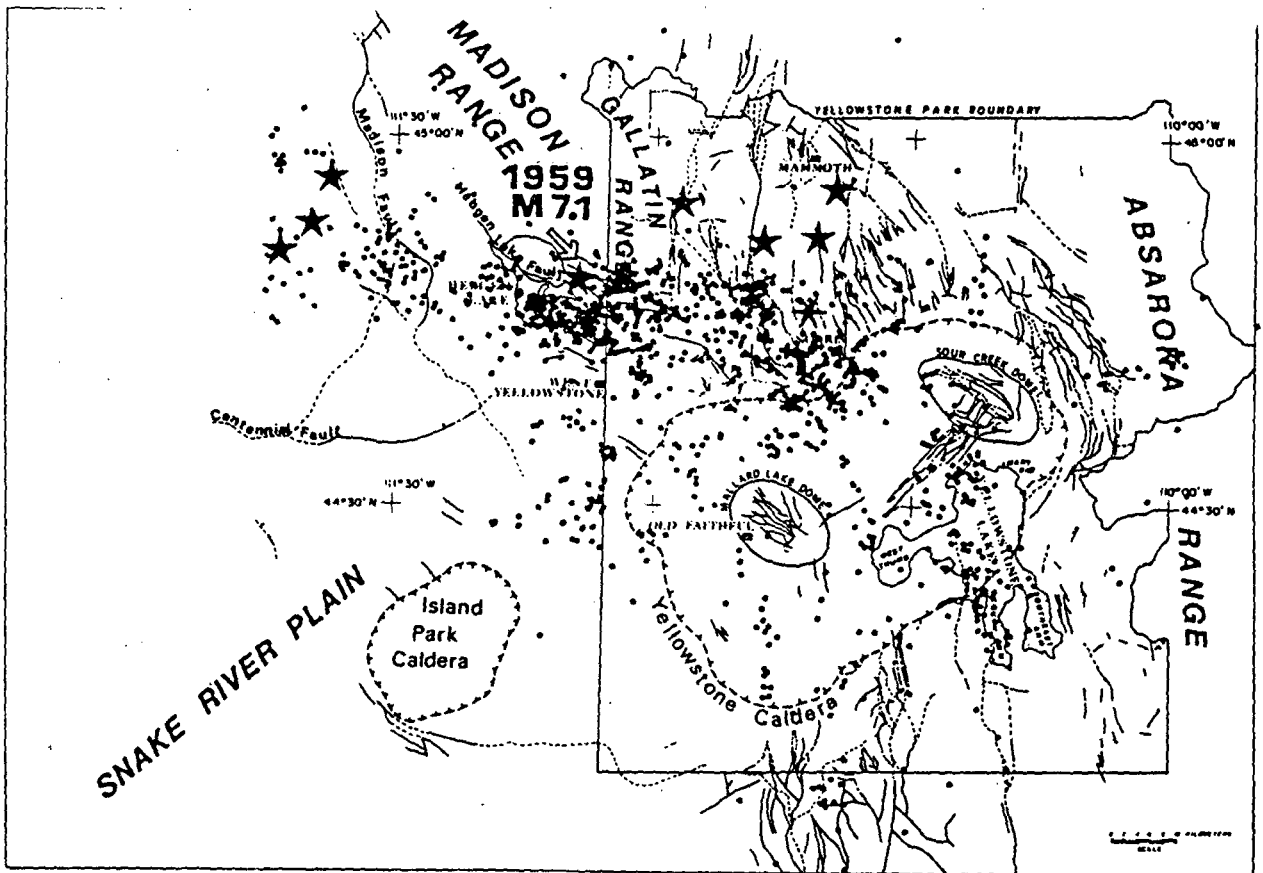


Figure 3: Earthquake distribution of the Yellowstone-Hebgen Lake region (1971-1979). Epicenters are those accurately determined from data of the University of Utah and the U.S. Geological Survey. Faults are taken from a compilation by R. L. Christiansen (U.S. Geological Survey, personal communication, 1978). Calderas are shown corresponding to their respective ages: I, 2.0 m.y.; II, 1.3 m.y.; and III, 0.6 m.y. Large stars correspond to epicenters of magnitude 6-7 historical earthquakes.

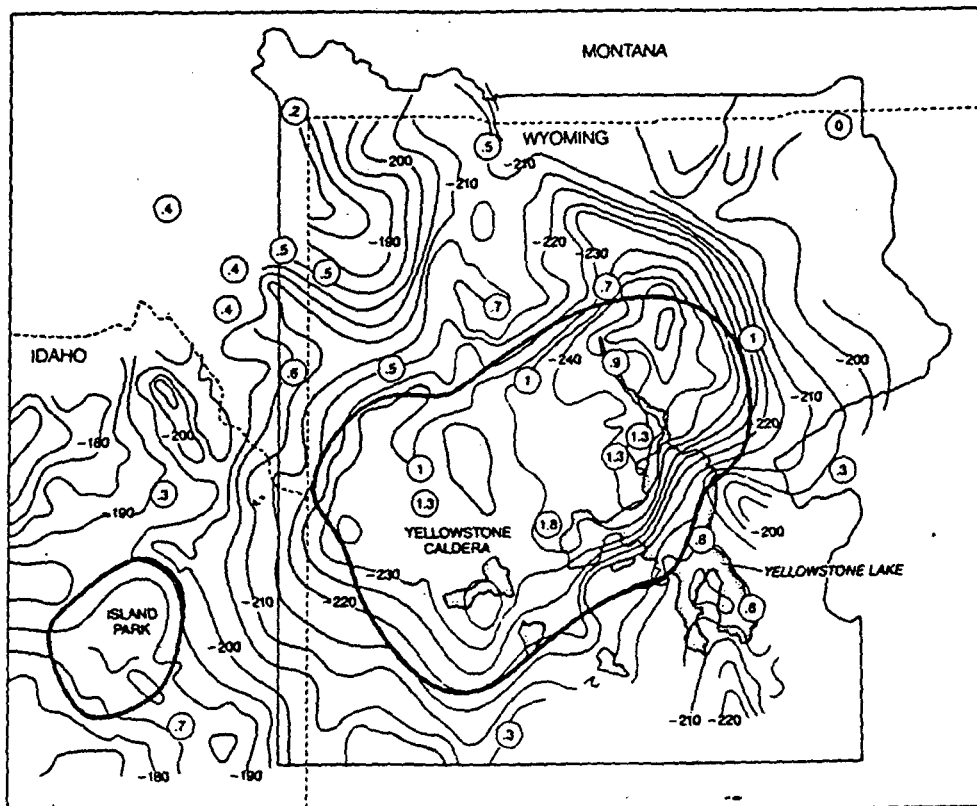
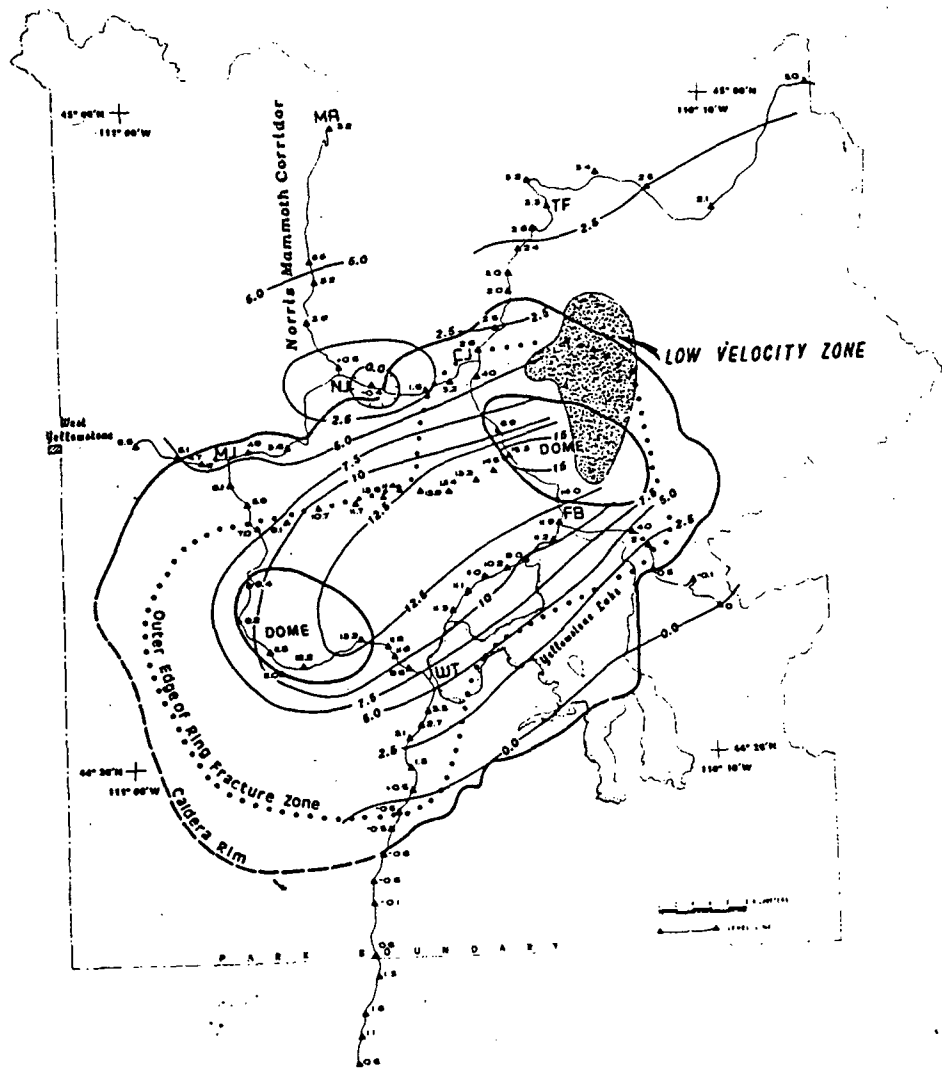


Figure 4: Bouguer gravity anomaly map at a contour interval of 5 mgal (map from Smith and Christiansen, 1980); data recontoured from Blank and Gettings, 1974). Open circles correspond to locations of seismograph stations that recorded teleseismic P-wave delays. Average delays are shown within the circles in seconds (from Iyer et al., 1981). P-wave delays were normalized to the seismograph station at the northeast side of Yellowstone National Park.



Smith and
Pelton, 1982

Figure 5: Contour map of relative uplift rates over the Yellowstone Plateau. Contours are in millimeters/year and were computed from the data of Smith and Pelton (1979, 1982). Bench-mark locations shown by triangles; MA, Mammoth; NJ, Norris Junction; CJ, Canyon Junction; FB, Fishing Bridge; WT, West Thumb; TF, Tower Falls.

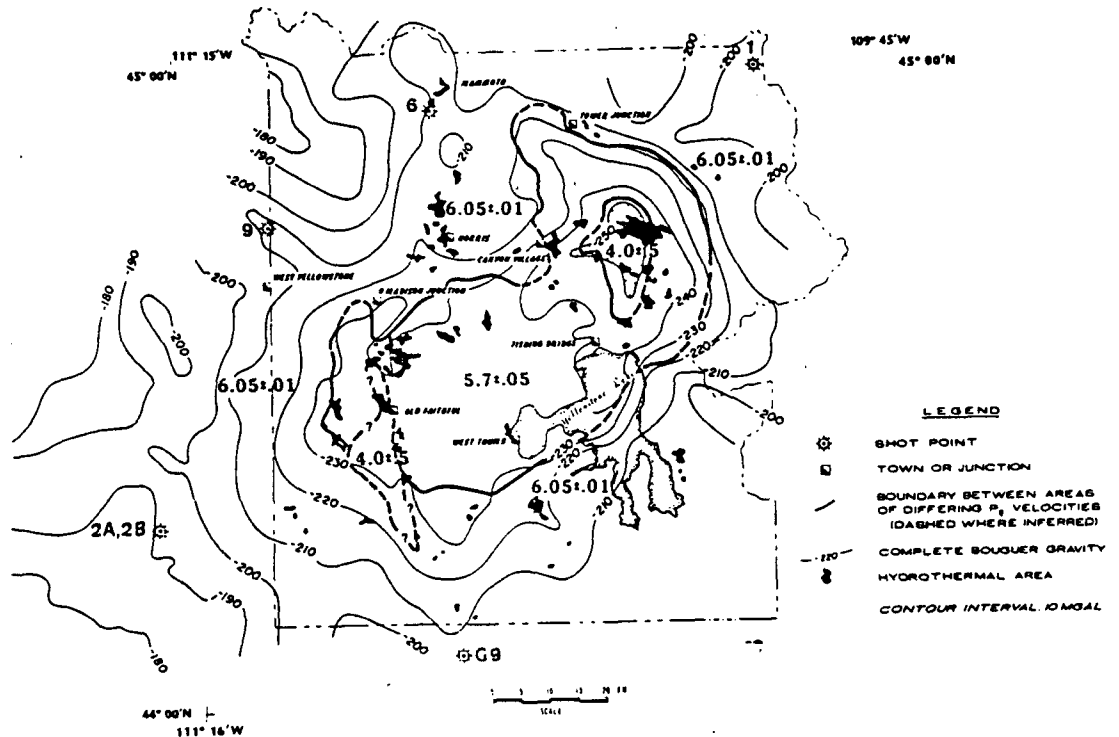


Figure 6: Areal extent of crystalline upper-crustal layer (2-10 km depth). P-wave velocities from Lehman et al. (1982) were determined from delay-time analyses. Velocities are in kilometers/second.

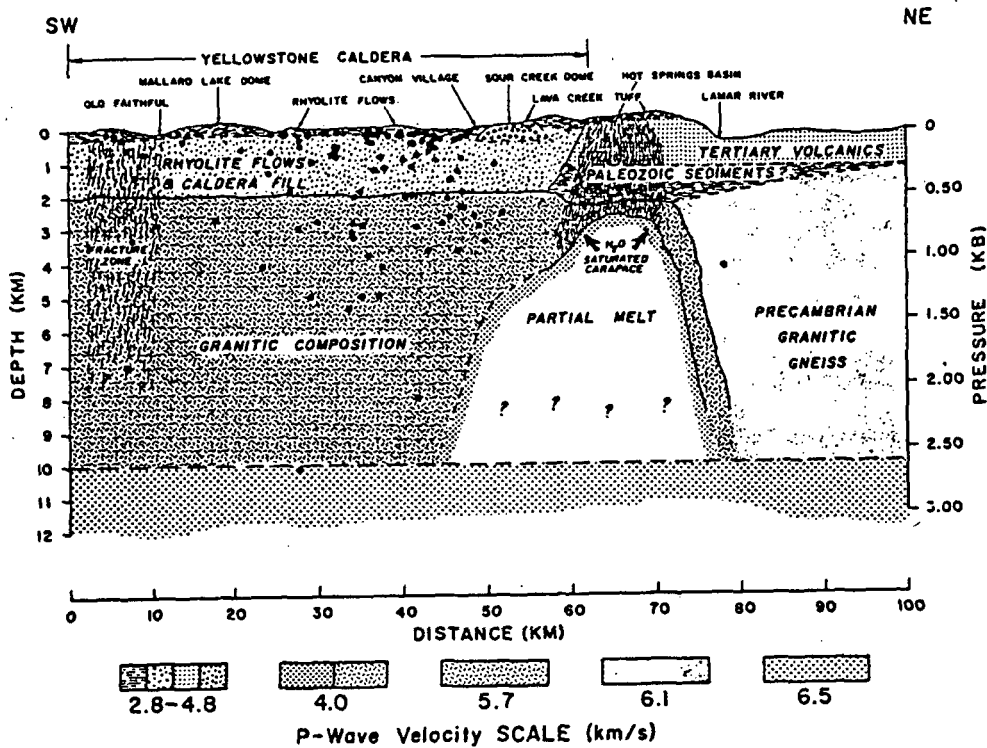


Figure 8: Generalized SW-NE upper-crustal cross section parallel to the axis of the Yellowstone caldera. Focal depths (shown by black dots) were projected from outside the low-velocity body. Velocities correspond to sources in Figure 7. Relative P-wave seismic attenuations are averaged from data of Clawson and Smith (1981).

Smith and
Braille, 1982

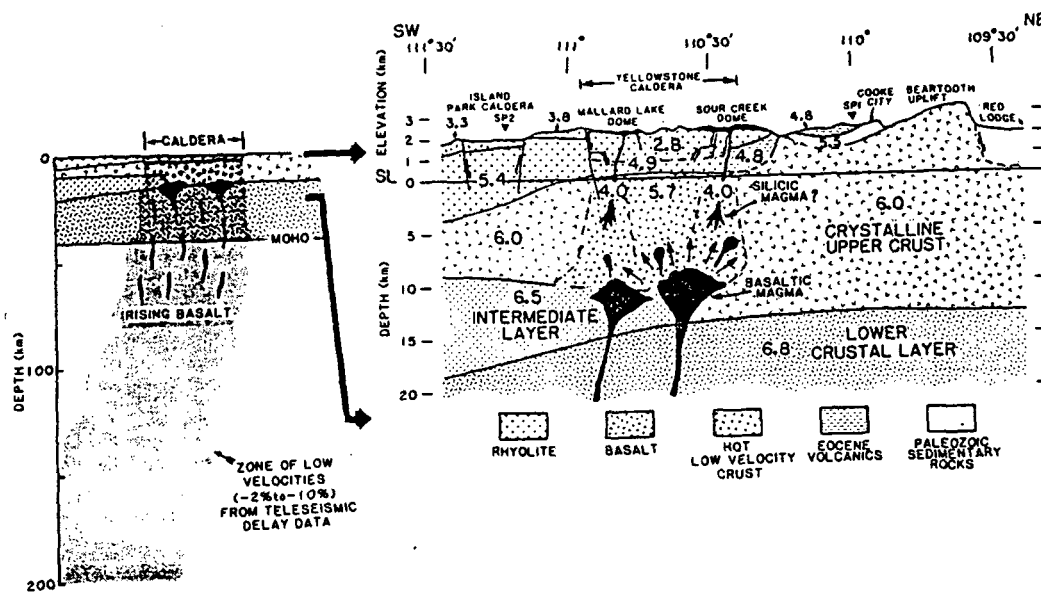


Figure 9: Idealized NE-SW geologic-seismic velocity model for the crustal structure of the Yellowstone-Island Park - Snake River Plain region. P-wave velocities are in kilometers/second (from Braille et al., 1982; Smith et al., 1982). Geologic interpretations are based on constraints of the Quaternary history and the petrologic models of Leeman (in press) and Christiansen (U.S. Geological Survey, personal communication, 1978; in press).

- Arct, M. J., and Chadwick, A. V., 1983, Dendrochronology in the Yellowstone fossil forest: Geol. Soc. of Am., Abstr. with Progs., v. 15, p. 408.
- Armstrong, R. L., Leeman, W. P., and Malde, H. E., 1975, K-Ar dating, Quaternary and Neogene volcanic rocks of the Snake River Plain, Idaho: Am. Jour. Sci., v. 275, p. 225-251.
- Armstrong, R. L., Harakal, J. E., and Neill, W. M., 1980, K-Ar dating of Snake River Plain (Idaho) volcanic rocks - new results: Isochron/West, n. 27, p. 5-10.
- Baker, R. G., 1976, Late Quaternary vegetation history of the Yellowstone Lake Basin, Wyoming: U.S. Geol. Surv. Prof. Paper 729-E, 48 p.
- Brott, C. A., Blackwell, D. D., and Ziagos, J. P., 1981, Thermal and tectonic implications of heat flow in the eastern Snake River Plain, Idaho: Jour. Geophys. Res., v. 86, p. 11709-11734.
- Chadwick, R. A., 1970, Belts of eruptive centers in the Absaroka-Gallatin volcanic province, Wyoming-Montana: Geol. Soc. of Am. Bull., v. 81, p. 267-274.
- Christiansen, R. L., Blank, H. R., Jr., 1972, Volcanic stratigraphy of the Quaternary rhyolite plateau in Yellowstone National Park: U.S. Geol. Surv. Prof. Paper 729-B, 18 p.
- Christansen, R. L., and Love, J. D., 1978, The Pliocene Conant Creek Tuff in the northern part of the Teton Range and Jackson Hole, Wyoming: U.S. Geol. Surv. Bull. 1435-6, 9 p.
- Coffin, H. G., 1976, Orientation of trees in the Yellowstone petrified forests: Jour. Paleo., v. 50, p. 539-543.
- Coffin, H. G., 1983, Erect floating stumps in Spirit Lake, Washington: Geology, v. 11, p. 298-299.
- Dorf, E., 1960, Tertiary fossil forests of Yellowstone National Park, Wyoming: Billings Geol. Soc., 11th Ann. Field Conf., p. 253-260.
- Fournier, R. O., 1983, Yellowstone National Park as an opportunity for deep continental drilling in thermal regions: Geol. Soc. Am. Abstr. with Progs., v. 15, p. 434.
- Fritz, W. J., 1980, Reinterpretation of the depositional environment of the Yellowstone "fossil forests": Geology, v. 8, p. 309-313.
- Fritz, W. J., 1980, Stratigraphic framework of the Lamar River Formation in Yellowstone National Park: Northwest Geology, v. 9, p. 1-18.
- Fritz, W. J., 1982, Geology of the Lamar River Formation, Northeast Yellowstone National Park, in, Reid, S. G., Foote, D. J., eds., Geology of the Yellowstone Park Area: Wyo. Geol. Assoc. 33rd Ann. Field Conf. Guidebook, p. 73-101.

- Froggatt, P. C., Wilson, C. J. N., and Walker, G. P. L., 1981, Orientation of logs in the Taupo Ignimbrite as an indicator of flow direction and vent position: *Geology*, v. 9, p. 109-111.
- Hauge, T. A., 1982, The Heart Mountain detachment fault, northwest Wyoming: Involvement of Absaroka volcanic rock, in, Reid, S. G., Foote, D. J., eds., *Geology of the Yellowstone Park Area: Wyo. Geol. Assoc. 33rd Ann. Field Conf. Guidebook*, p. 175-183.
- Iyer, H. M., Evans, J. R., Zandt, G., Stewart, R. M., Coakley, J. M., and Roloff, J. N., 1981, A deep low-velocity body under the Yellowstone caldera, Wyoming: Delineation using teleseismic P-wave residuals and tectonic interpretation: Summary: *Geol. Soc. Am. Bull.*, v. 92, part 1, p. 792-798.
- Keefer, W. R., 1971, The geologic story of Yellowstone National Park: *U.S. Geol. Surv. Bull.* 1347, 92 p.
- Love, J. D., and Good, J. M., 1970, Hydrocarbons in thermal areas, Northwestern Wyoming: *U.S. Geol. Surv. Prof. Paper* 644-B, 23 p.
- Love, J. D., and Keefer, W. R., 1975, Geology of sedimentary rocks in southern Yellowstone National Park, Wyoming: *U.S. Geol. Surv. Prof. Paper* 729-D, 60 p.
- Love, L. L., Kudo, A. M., and Love, D. W., 1976, Dacites of Bunsen Peak, the Birch Hills, and the Washakie Needles, northwestern Wyoming, and their relationship to the Absaroka volcanic field, Wyoming and Montana: *Geol. Soc. of Am. Bull.*, v. 87, p. 1455-1462.
- McBroome, L. A., Doherty, D. J., and Embree, G. F., 1981, Correlation of major Pliocene and Miocene ash-flow sheets, eastern Snake River Plain, Idaho: *Mont. Geol. Soc. Field Conf. SW Mont.*, p. 323-330.
- Pelton, J. R., and Smith, R. B., 1982, Contemporary vertical surface displacements in Yellowstone National Park: *Jour. Geophys. Res.*, v. 87, p. 2745-2761.
- Pierce, K. L., 1979, History and dynamics of glaciation in the northern Yellowstone National Park Area: *U.S. Geol. Surv. Prof. Paper* 729-F, 90 p.
- Pierce, W. G., 1982, Relation of volcanic rocks to the Heart Mountain Fault, in, Reid, S. G., and Foote, D. J., eds., *Geology of the Yellowstone Park Area: Wyo. Geol. Assoc. 33rd Ann. Field Conf. Guidebook*, p. 181-183.
- Richmond, G. M., 1976, Surficial geologic history of the Canyon Village Quadrangle, Yellowstone National Park, Wyoming, for use with map I-652: *U.S. Geol. Surv. Bull.* 1427, 35 p.
- Ruppel, E. T., 1972, Geology of the pre-Tertiary rocks in the northern part of Yellowstone National Park, Wyoming: *U.S. Geol. Surv. Prof. Paper* 729-A, 66 p.

- Smedes, H. W., and Prostka, H. J., 1972, Stratigraphic framework of the Absaroka volcanic supergroup in the Yellowstone National Park region: U.S. Geol. Surv. Prof. Paper 729-C, 33 p.
- Smith, R. B., and Christiansen, R. L., 1980, Yellowstone Park as a window on the earth's interior: Sci. Am., v. 242, p. 194-217.
- Smith, R. B., and Braile, L. W., 1982, Crustal structure and evolution of an explosive silicic volcanic system at Yellowstone National Parks, in, Reid, S. G., and Foote, D. J., eds., Geology of the Yellowstone Park Area: Wyo. Geol. Assoc. 33rd Ann. Field Conf. Guidebook, p. 233-250.
- Stewart, J. H., and Carlson, J. E., 1978, Generalized maps showing distribution, lithology and age of Cenozoic igneous rocks in the Western United States, in, Smith, R. B., and Eaton, G. P., eds., Cenozoic tectonics and regional geophysics of the western Cordillera: Geol. Soc. Am. Mem. 152, p. 263-264.
- Williams, H., and McBirney, A. R., 1979, Volcanology: Freeman, Cooper and Co., San Fran., 397 p.

Chapter 1

REVIEW OF THE PETROLOGY OF VOLCANIC SYSTEMS

1.1 CLASSIFICATION AND NOMENCLATURE

"When I use a word, it means just what I
choose it to mean - neither more nor less."

Humpty Dumpty (Hunt, 1982)

"Much of the current activity in this field [rock nomenclature] consists of attempts to redefine and rearrange existing names, and inevitably suffers from the lack of widely accepted, reasonably objective criteria for deciding whether proposed modifications of terms already in the public domain are actually in the public interest."

F. Chayes (1979)

The classification of igneous rocks in general, and volcanic rocks in particular has been a topic of contention from the earliest days of geology. Indeed, the struggle continues to this day, although most geologists are reasonably comfortable with an imprecise classification scheme. For most cases, major and trace element geochemical analyses are the rule in the literature rather than the exception, allowing the reader to apply his own favorite scheme and the author to side step imprecise nomenclature and define a rock as quantitatively as possible.

The aphanitic or prophyritic nature of most volcanic rocks has required the use of chemical analyses in their classification. These analyses include at a minimum nine major oxide components and water. Recent work has emphasized the importance of trace elements in the genesis of volcanic rocks and these are often also included with the major elements. Examples of analyses for several major rock types which will be discussed in this book are presented in Table 1-1.

The classification of volcanic rocks generally is considered in two different ways: that of providing a name to a specific rock and that of

Table 1-1 Major element chemistry and CIPW norms of selected volcanic rock types (Carmichael et al, 1974).

	1	2	3	4	5	6	7
SiO ₂	47.01	51.57	50.83	48.27	52.28	46.53	43.52
TiO ₂	3.20	0.80	3.44	0.89	0.94	2.28	2.45
Al ₂ O ₃	15.57	15.91	12.67	18.28	15.75	14.31	15.76
Fe ₂ O ₃	2.32	2.74	3.10	1.04	3.28	3.16	2.82
FeO	11.57	7.04	11.39	8.31	4.88	9.81	7.14
MnO	0.20	0.17	0.25	0.17	0.16	0.18	0.16
MgO	5.25	6.73	4.19	8.96	4.76	9.54	9.57
CaO	9.77	11.74	8.18	11.32	8.30	10.32	12.28
Na ₂ O	3.00	2.41	3.24	2.80	3.44	2.85	3.02
K ₂ O	0.31	0.44	0.87	0.14	2.08	0.84	1.43
P ₂ O ₅	0.32	0.11	0.75	0.07	0.36	0.28	0.41
Rest*	1.64	0.45	0.94	0.22	3.57	0.14	1.16
Total	100.16	100.11	99.85	100.47	99.80	100.24	99.72
<i>Q</i>	—	2.26	4.44	—	3.98	—	—
<i>or</i>	1.87	2.60	5.56	0.56	12.29	5.28	8.45
<i>ab</i>	25.39	20.39	27.25	23.58	29.11	20.04	4.48
<i>an</i>	28.10	31.29	17.51	36.97	21.39	23.63	25.22
<i>ne</i>	—	—	—	—	—	2.20	11.42
<i>di</i>	15.17	21.32	15.75	15.23	6.41	20.89	25.93
<i>hy</i>	11.92	16.05	16.04	—	13.76	—	—
<i>ol</i>	5.93	—	—	20.55	—	18.48	13.25
<i>mt</i>	3.36	3.97	4.41	1.39	4.76	4.53	4.09
<i>il</i>	6.08	1.52	6.54	1.67	1.79	4.41	4.65
<i>ap</i>	0.76	0.26	1.68	0.17	0.85	0.67	0.97

Explanation of column headings

- 1 Olivine tholeiite, Albemarle Island, Galápagos (McBirney and Williams, 1969, p. 121, no. 63)
- 2 Tholeiite, Talasea, New Britain (Lowder and Carmichael, 1970, p. 27, no. 311)
- 3 Tholeiitic lava, Thingmuli, Iceland (Carmichael, 1964b, p. 439, no. 10)
- 4 High-alumina basalt, Medicine Lake Highlands, California (Yoder and Tilley, 1962, p. 363, no. 16)
- 5 Hypersthene shoshonite lava, Yellowstone Park, Wyoming (J. Nicholls and Carmichael, 1969a, p. 60, no. 118A)
- 6 Alkali olivine basalt, prehistoric flow, Hualalai, Hawaii (Yoder and Tilley, 1962, p. 362, no. 20)
- 7 Basaltic flow, Korath Range, Lake Rudolph, Kenya (F. H. Brown and Carmichael, 1969, p. 251, no. k8)

* Includes H₂O, CO₂, and so on.

	1	2	3	4	5	6
SiO ₂	58.57	62.74	67.73	72.19	76.21	70.13
TiO ₂	0.64	0.56	0.50	0.33	0.07	0.30
Al ₂ O ₃	19.87	16.53	15.44	12.62	12.58	7.97
Fe ₂ O ₃	3.20	1.71	0.69	3.14	0.30	2.77
FeO	2.73	2.14	2.40	1.12	0.73	5.27
MnO	0.15	0.07	0.06	0.05	0.04	0.26
MgO	1.74	3.24	1.30	0.58	0.03	0.07
CaO	7.51	6.20	3.35	2.07	0.61	0.55
Na ₂ O	4.25	4.08	3.85	3.45	4.05	7.46
K ₂ O	0.74	1.18	3.25	3.70	4.72	4.24
P ₂ O ₅	0.10	0.16	0.15	0.02	0.01	0.04
Rest	0.63	1.31	1.15	0.80	0.52	1.19
Total	100.13	99.92	99.87	100.07	99.87	100.25
<i>Q</i>	12.67	17.43	22.98	33.18	33.06	28.75
<i>or</i>	4.37	6.97	18.90	21.86	27.80	25.06
<i>ab</i>	35.96	34.52	32.49	29.19	34.06	17.39
<i>an</i>	32.96	23.30	15.29	8.02	2.50	—
<i>di</i>	2.93	5.09	—	1.64	0.30	2.19
<i>hy</i>	4.52	7.38	6.82	0.68	0.92	8.68
<i>ac, ns</i>	—	—	—	—	—	15.90
<i>mt</i>	4.64	2.48	0.93	2.82	0.46	—
<i>il</i>	1.21	1.06	0.91	0.63	0.15	0.57
<i>ap</i>	0.24	0.38	0.34	0.15	—	0.09

Explanation of column headings

- 1 Andesite flow, Mt. Misery, St. Kitts, West Indies (P. E. Baker, 1968b, table 6, no. 15)
- 2 Andesite, Mt. Shasta, California (A. L. Smith and Carmichael, 1968, table 2, no. 72)
- 3 Pyroxene dacite, Medicine Lake Highlands (Carmichael, 1967b, table 5, no. 13)
- 4 Rhyodacite, Talasea, New Britain (Lowder and Carmichael, 1970, table 2, no. 279B)
- 5 Rhyolitic obsidian, Mono Craters, California (Carmichael, 1967a, table 5, no. 18)
- 6 Pantellerite obsidian, Lake Naivasha, Kenya (Nicholls and Carmichael, 1969a, table 1, no. 121R)

classifying suites of rock that are genetically related (magma series).

The actual mineral composition of a rock may be quantified by point-counting the abundance of the different phases present. This quantification of volume percent is termed the mode of the rock. The glassy and fine-grained nature of most volcanic rocks places limits on the value of this method for classification, but as we will see later, it can be used to characterize and correlate the products of different pyroclastic eruptive events.

A normative or norm calculation mathematically derives a standard suite of minerals from the major element chemical analysis of a rock. The most common norm calculation in the U.S. is the CIPW (Cross Iddings Pirson Washington) norm. The procedure for the calculation of this norm is given in Barth (Barth, 1966). The calculation is somewhat tedious by hand but is easily programmed on a computer. The CIPW norms of major rock types are given with the chemical analyses in Table 1-1.

The classification of rocks in the field generally relies on textures and observable minerals. An example of this is given in Table 1-2 which is adapted from Travis (1955). This system is based upon the composition and percentage of total feldspar and the presence and abundance of quartz or a feldspathoid (such as nepheline or leucite). This chart also equates fine-grained volcanic rocks with coarser grained plutonic equivalents. The obvious advantage of such a classification scheme is that it can be used by the field geologist to characterize rocks and communicate his findings to other geologists. Other more specialized rock names are in common usage and many archaic terms will crop up from time to time. These names can be easily found in reliable geological dictionaries.

ESSENTIAL MINERALS		POTASH FELDSPAR > 2/3 TOTAL FELDSPAR			POTASH FELDSPAR 1/3 - 2/3 TOTAL FELDSPAR		
		QUARTZ > 10%	QUARTZ < 10% FELDSPATHOID < 10%	FELDSPATHOID > 10%	QUARTZ > 10%	QUARTZ < 10% FELDSPATHOID < 10%	FELDSPATHOID > 10%
CHARACTERIZING ACCESSORY MINERALS		CHIEFLY: HORNBLLENDE, BIOTITE, PYROXENE, MUSCOVITE ALSO: SODIC AMPHIBOLES, AEGIRINE, CANCRINITE, SODALITE, TOURMALINE			CHIEFLY: HORNBLLENDE, BIOTITE, PYROXENE ALSO: SODIC AMPHIBOLES, AEGIRINE		
COLOR INDEX		10	15	20	20	25	30
AVERAGE CHEMICAL COMPOSITION (DALY)		SiO ₂ 71.5 Al ₂ O ₃ 14.0 Fe ₂ O ₃ 1.5 FeO 1.4 MgO 0.6 CaO 1.6 Na ₂ O 3.4 K ₂ O 4.3	SiO ₂ 60.4 Al ₂ O ₃ 17.0 Fe ₂ O ₃ 2.7 FeO 2.9 MgO 1.8 CaO 1.7 Na ₂ O 4.2 K ₂ O 5.1	SiO ₂ 56.0 Al ₂ O ₃ 19.2 Fe ₂ O ₃ 2.9 FeO 1.6 MgO 0.6 CaO 2.0 Na ₂ O 8.5 K ₂ O 5.3	SiO ₂ 66.8 Al ₂ O ₃ 15.8 Fe ₂ O ₃ 2.3 FeO 1.3 MgO 1.0 CaO 2.8 Na ₂ O 3.7 K ₂ O 4.2	SiO ₂ 57.0 Al ₂ O ₃ 17.1 Fe ₂ O ₃ 3.4 FeO 3.6 MgO 2.3 CaO 5.4 Na ₂ O 4.7 K ₂ O 3.7	SiO ₂ 54.1 Al ₂ O ₃ 21.0 Fe ₂ O ₃ 1.8 FeO 3.3 MgO 1.1 CaO 3.2 Na ₂ O 6.2 K ₂ O 5.9
PHENOCRYSTALLIC	EQUIGRANULAR Euhedral, lapilli, stocks, large laccoliths, thick dikes, and sills	GRANITE ALASKITE—few dark minerals GRAPHIC GRANITE—graphic texture ALKALI GRANITE—abundant albite and sodic amphibole or pyroxene CHARNOCKITE—with orthopyroxene LUXULLIANITE—tourmalinized	SYENITE QUARTZ SYENITE—a little quartz ALKALI SYENITE—no plagioclase except albite PULASKITE—a little nepheline NORDMARKITE—a little quartz LARVIKITE—with "blue" feldspar SPONKINITE—abundant FeMg minerals	NEPHELINE SYENITE LEUCITE SYENITE—suedoleucite only feldspathoid SODALITE SYENITE—sodalite only feldspathoid FOYATITE—abundant feldspar MALIGNITE—abundant FeMg minerals DITROITE—with nepheline and sodalite	QUARTZ MONZONITE (ADAMELLITE)	MONZONITE	NEPHELINE MONZONITE
	PHANERITIC GROUNDMASS Euhedral dikes, sills, plugs, small stocks, margins of larger masses	GRANITE PORPHYRY	SYENITE PORPHYRY	NEPHELINE SYENITE PORPHYRY	QUARTZ MONZONITE PORPHYRY	MONZONITE PORPHYRY	NEPHELINE MONZONITE PORPHYRY
	APHANITIC GROUNDMASS Flow, sills, laccoliths, surface flows, margins of larger masses, welded tuffs	RHYOLITE PORPHYRY	TRACHYTE PORPHYRY	PHONOLITE PORPHYRY	QUARTZ LATITE PORPHYRY	LATITE PORPHYRY	NEPHELINE LATITE PORPHYRY
	MICROCRYSTALLINE Flow, sills, surface flows, margins of larger masses, welded tuffs	RHYOLITE	TRACHYTE	PHONOLITE (LEUCITE PHONOLITE (leucite trachyte)—leucite only feldspathoid TINGUATE—abundant aegirine WYOMINGITE—leucite and plagioclase	QUARTZ LATITE (DELLENITE)	LATITE (TRACHY-ANDESITE)	NEPHELINE LATITE
GLASSY Surface flows, margins of tuffs and sills, welded tuffs	OBSIDIAN—black PITCHSTONE—reddish VITROPHYRE—porphyritic FELSITE—concentric fractures PUMICE—finely cellular, light colored SCORIA—coarsely cellular, dark colored	Normally it is not possible to determine the composition of these rocks. They are customarily designated by the names at the left of this column. Basic glass is rare so rocks named, except scoria, will normally be silica. If the approximate composition (by close association) or silica content (by refractive index or analysis), can be determined, the name may be prefixed by the name of the appropriate aphanitic rock, for example, "trachyte obsidian," or "latite vitrophyre." In general, scoria is basic; basic obsidian is called "tachylite", and spherulitic tachylite is "variolite."					

4

Table 1-2 (cont.)

CLASSIFICATION OF IGNEOUS ROCKS

Russell B. Travis

PLAGIOCLASE FELDSPAR > 2/3 TOTAL FELDSPAR					LITTLE OR NO FELDSPAR		SPECIAL TYPES	
POTASH FELDSPAR > 10% TOTAL FELDSPAR QUARTZ > 10%	POTASH FELDSPAR < 10% TOTAL FELDSPAR				CHIEFLY PYROXENE AND/OR OLIVINE	CHIEFLY FERRO-MAGNESIAN MINERALS AND FELDSPATHOIDS		
	SODIC PLAGIOCLASE		CALCIC PLAGIOCLASE					
	QUARTZ > 10%	QUARTZ < 10% FELDSPATHOID < 10%	QUARTZ < 10% FELDSPATHOID < 10%	FELDSPATHOID > 10% PYROXENE > 10%				
CHIEFLY: HORNBLLENDE, BIOTITE, PYROXENE (IN ANDESITE) ALSO: PYROXENE FELDSPATHOID SODIC AMPHIBOLES		CHIEFLY: PYROXENE URALITE, OLIVINE ALSO: HORNBLLENDE, BIOTITE, QUARTZ, ANALCITE, AEGIRINE, SODIC AMPHIBOLES			CHIEFLY: SERPENTINE, IRON ORE ALSO: HORNBLLENDE, BIOTITE		HORNBLLENDE BIOTITE IRON ORE	
20	20	25	50	60	95	55		
65.3 16.1 2.1 2.3 1.7 3.9 3.8 2.7	61.6 16.2 2.5 3.8 2.8 5.4 3.4 2.1	58.2 17.0 3.2 3.7 3.5 6.3 3.5 2.1	48.6 16.8 4.8 6.0 5.1 8.9 3.7 1.9	47.4 15.4 4.9 5.4 5.0 9.7 3.8 3.5	41.1 4.8 4.0 7.1 32.2 4.4 0.5 1.0	42.0 17.9 5.7 5.7 3.4 10.3 8.0 2.4		
GRANODIORITE	QUARTZ DIORITE (TONALITE)	DIORITE	GABBRO GABBRO—with clinopyroxene NORITE—with orthopyroxene OLIVINE GABBRO— with olivine TROCTOLITE— olivine and plagioclase only ANORTHOSITE— plagioclase only QUARTZ GABBRO— with quartz	DIABASE (Dolerite of British Columbia) Phenocrystic, diabasic texture, normally medium or fine-grained	THERALITE THERALITE NEPHELINE (GABBRO) TESCHERITE— andesine only OLIVINE THERALITE— with olivine	PERIDOTITE PERIDOTITE—clinopyroxene and olivine HARZBURGITE—orthopyroxene and olivine PICRITE—pyroxene and olivine with some plagioclase DIJNITE—olivine only PYROXENITE—pyroxene only SERPENTINE (SERPENTINITE)— chiefly serpentine	MISSOURITE— pyroxene, olivine and nepheline NOLITE— pyroxene and nepheline FINGERSITE—pyroxene and nepheline UNCOMPARAGITE (MELLITE PYROXENITE)—pyroxene and melilite	PEGMATITE— phenocrystalline rock, mostly siliceous, alkali-rich, for small crystals (usually having a coarser texture than parent) APLITE— phenocrystalline rock having sugary (fine-grained) matrix (plagioclase granular texture) LAMPROPHYRE— dark rock with fine-grained phenocrysts and a highly felsic matrix (granular texture)
GRANODIORITE PORPHYRY	QUARTZ DIORITE PORPHYRY	DIORITE PORPHYRY	GABBRO PORPHYRY		THERALITE PORPHYRY	PERIDOTITE PORPHYRY KIMBERLITE—peridotite porphyry or breccia		
DACITE PORPHYRY		ANDESITE PORPHYRY	BASALT PORPHYRY	TEPHRITE PORPHYRY	LIMBURGITE PORPHYRY			
DACITE	ANDESITE		BASALT OLIVINE BASALT— with olivine ANALCITE BASALT— with analcite QUARTZ BASALT— with quartz OCEANITE— with abundant olivine	TEPHRITE LEUCITE TEPHRITE— melilite only BASANITE— with olivine LEUCITE BASANITE— with olivine and leucite	LIMBURGITE	NEPHELINITE— pyroxene and nepheline LEUCITE— pyroxene and leucite MELLITE— pyroxene and melilite OLIVINE NEPHELINITE (NEPHELINE BASALT)— pyroxene, nepheline, and olivine ETC	TRAP— dark-colored aphanitic rock FELSITE— light-colored aphanitic rock ETC	

FREQUENCY OF OCCURRENCE:
This size type indicates COMMON ROCKS.
This size type indicates UNCOMMON ROCKS.
This size type indicates RARE ROCKS.

Streckeisen (1967) has presented a volcanic rock classification which is based on the modal abundance of quartz, alkali feldspar, plagioclase, feldspathoids, and mafic minerals. The rock name is defined by locating the modal abundances on the double triangles shown in Figure 1-1.

Rock nomenclature has also been based upon chemistry and on factors calculated from that chemistry. Figure 1-2 is a classification of andesites, dacites, and rhyolites which is based on weight percent K_2O and SiO_2 . Other classifications may be based on normative mineral content or calculations involving the normative mineral content such as the differentiation index (DI).

DI = normative quartz + albite + orthoclase + leucite + nepheline + kalsilite.

Thus a benmoreite is defined as "a silica-saturated to undersaturated igneous rock intermediate between mugearite and trachyte, with a differentiation index between 65 and 75 and $K_2O:Na_2O$ less than 1:2. (American Geological Institute Glossary of Geologic Terms).

It has long been recognized that certain types of igneous rocks occur together and indeed are genetically related to each other. This understanding is the basis for the definition of petrologic province and what we may call magma series. One of the most widely used classifications based on magma series was that proposed by Peacock (1931). This scheme involves the construction of a "Peacock Diagram" by plotting weight percent CaO versus SiO_2 and $(Na_2O + K_2O)$ versus SiO_2 . The point of intersection of these two lines defines the alkali-lime index of the suite. If the index is greater than 61% SiO_2 the suite is termed calcic; 56-61% is calc-alkaline; 51-56% is alkali-calcic; and less than 51% is alkalic.

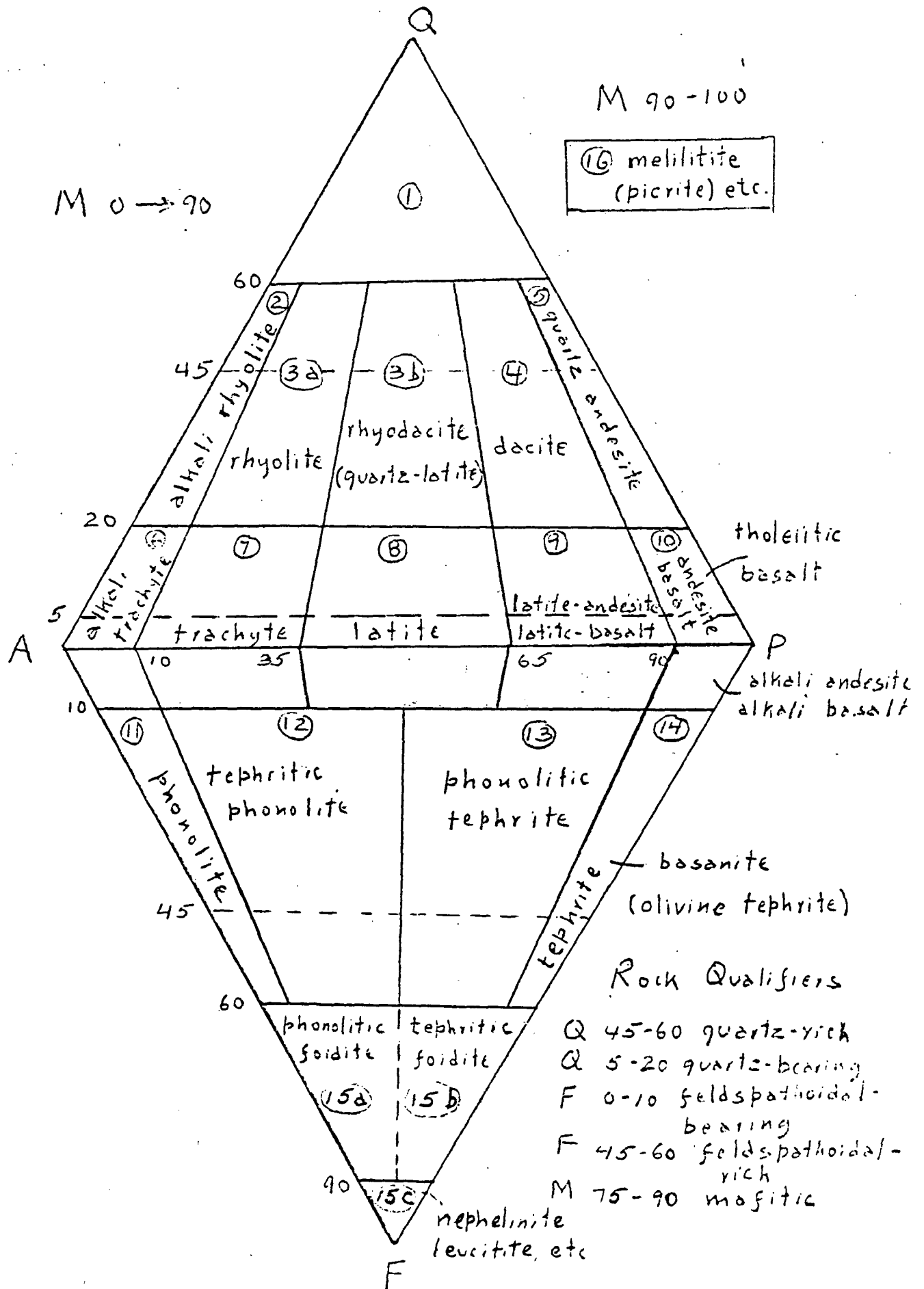


Fig. 1-1 Volcanic rock classification
(Streckeisen 1967)

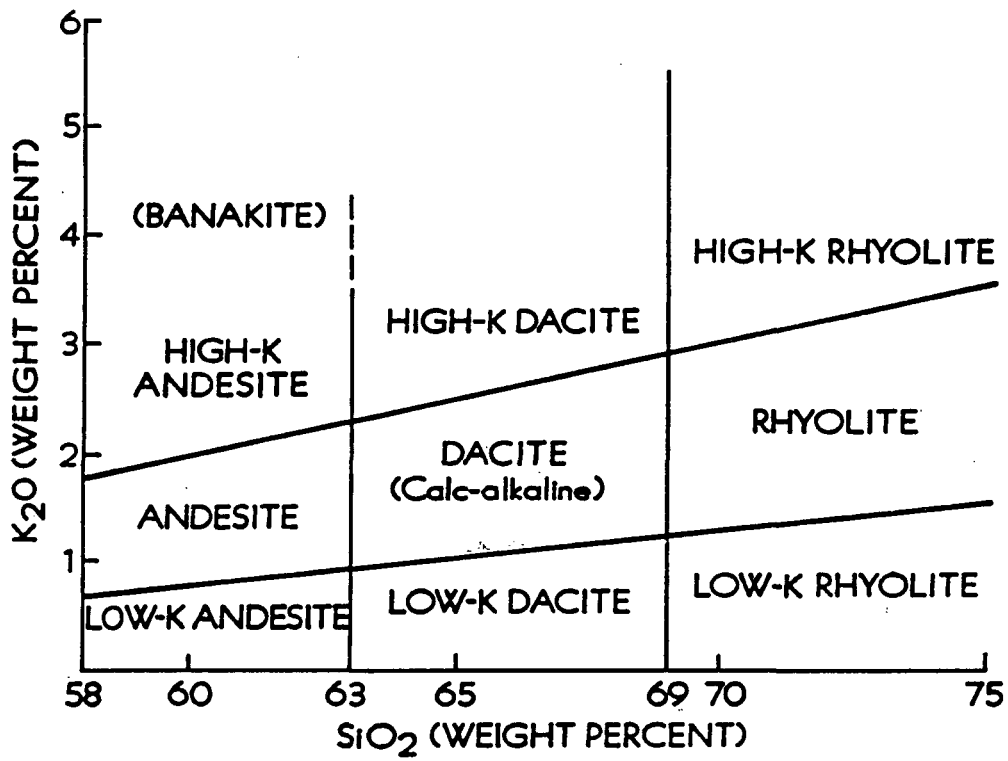


Fig. 1-2 Classification of andesite, dacite, and rhyolite by K₂O and SiO₂ contents (ewart, 1979).

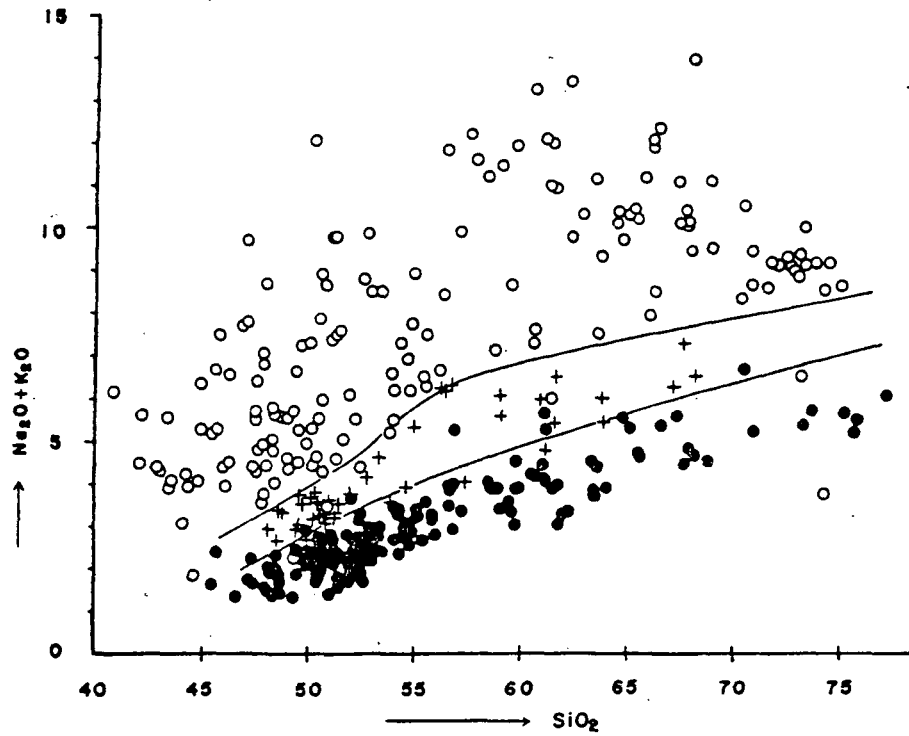
From the study of the chemistry of volcanic rocks in Japan, Kuno (1960, 1968) determined that there were three igneous rock series. He felt each series represented rocks which varied in composition, but which were derived from a single parental magma. He called the three series 1) tholeite, 2) high-alumina basalt, and 3) alkali olivine basalt and defined the boundaries between the series on the $\text{Na}_2\text{O} + \text{K}_2\text{O}$ or SiO_2 diagram (Fig. 1-3). Yoder and Tilley (1962) felt that high-alumina basalts were variations of both the tholeite and alkali olivine basalt series and did not represent a distinct series.

Irving and Barager (1971) have reviewed chemical data for a large number of volcanic rocks and have proposed a guide for the classification of the rocks on the basis of chemistry. They have attempted to subdivide the rocks on the basis of natural boundaries and give them rock names which are consistent with names originally proposed on the basis of mineralogy. They emphasize that although the classification may follow lines of magmatic evolution the proposed classification scheme is non-genetic. The basis of the classification is as follows.

- I. Subalkaline
 - A. Tholeitic basalt series
 - B. Calc-alkali series
- II. Alkaline
 - A. Alkali olivine basalt series
 - B. Nephelinitic, leucitic, and analcitic rocks
- III. Peralkaline

Within the series, individual rock names are defined on the basis of plots of normative color index (% mafic minerals in the norm) versus normative plagioclase composition.

Fig. 1-3 From Kuno (1968)



Alkali-silica diagram for tholeiite (solid circles) and high-alumina basalt (crosses) of central Japan and alkali olivine basalt (open circles) of central to southwestern Japan, Korea, and Manchuria, all of Cenozoic age. Their fractionation products in the same provinces—namely andesite, dacite, and rhyolite derived from the tholeiite (the pigeonitic rock series) and those derived from the high-alumina basalt (the high-alumina basalt series) and mugearite, trachyandesite, trachyte, and alkali rhyolite derived from the alkali olivine basalt—are also plotted by the respective marks. Both aphyric and porphyritic rocks are included. General boundaries between the fields of the three types of basalt and their fractionation products are shown by curves.

1.2 PHYSICAL PROPERTIES OF SILICATE MELTS

1.2.1 Spectrum of Volcanic Eruptions

During a volcanic eruption mass and energy are transferred from depth to the surface of the earth. The character of eruptions depends on the physical properties of the magmas which are a function of both their chemistry and to a large extent their interaction with their surroundings. This may involve especially the interaction of the magmas with meteoric waters as well as the contained magmatic water.

In this chapter we will explore why basaltic eruptions are common and produce large volumes of flow material but are generally not violent. On the other hand, rhyolitic through andesitic eruptions are less common, but violent and can lead to large losses of life. In addition, we will explore why some rhyolites produce viscous domes and flows in quiet eruptions while other magmas of essentially the same geochemical composition erupt violently and produce ash flow tuffs and calderas. Many volcanic centers produce the extremes of eruptive character during their lifetimes.

1.2.2 Review of Fluid Mechanics

The study of both magmatism and hydrothermal activity has its basis in the behavior of fluids. This section will review some of the concepts and terminology from elementary fluid mechanics. The discussion will be applied at this time to the behavior of silicate melts, but later in this book we will be applying much of the same information to describe the behavior of hydrothermal fluids.

Fluids in general possess elastic properties only under direct tension or compression. When pressure on the fluid is released the fluid will assume its

original volume. The elasticity of a fluid is quantified by its bulk modulus (E). The bulk modulus of a fluid increases with increasing confining pressure. Application of a shear stress will result in the permanent deformation of a fluid. Fluids will not transmit a shear stress. This inability to support shear stress allows fluids to flow. In a flowing fluid there are two fundamental types of motion, laminar flow and turbulent flow. Laminar flow results in an orderly motion in which fluid elements slide over each other in laminae. There is molecular motion and chemical and thermal diffusion, but no large-scale mixing between layers. Observations of fluids in laminar flow reveal the situation shown in Figure 1-4, with velocities equal to zero at boundaries and increasing with distance from the boundary. Turbulent flow is characterized by random motion of fluid elements and mixing throughout the fluid. A velocity profile of a fluid in turbulent flow is shown in Figure 1-5. At the boundary the flow is again zero. Within an extremely thin boundary layer the flow is laminar. This boundary layer is a very important factor in both the resistance to flow and in the heat flux between the fluid and the confining medium. Within the portion undergoing turbulent flow, in the strict sense, the motion of fluid elements is random, but the fluid has an average component of fluid velocity.

Fluid flow is often characterized by a dimensionless quantity called the Reynolds Number (R_e) where

$$R_e = \frac{\rho v D}{\eta}$$

In this equation ρ is the fluid density, v is the forward velocity, D is the diameter of the conduit, and η is the viscosity of the fluid. It has been determined empirically that flow is laminar for $R_e < 2000$ and turbulent for $R_e > 3000$. For values between 2000 and 3000 fluid flow fluctuates between

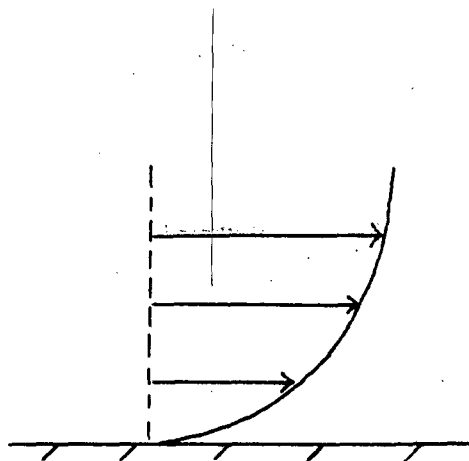


Fig. 1-4 Velocity profile of a fluid in laminar flow showing a velocity of zero at a fixed boundary and increasing with distance from that boundary.

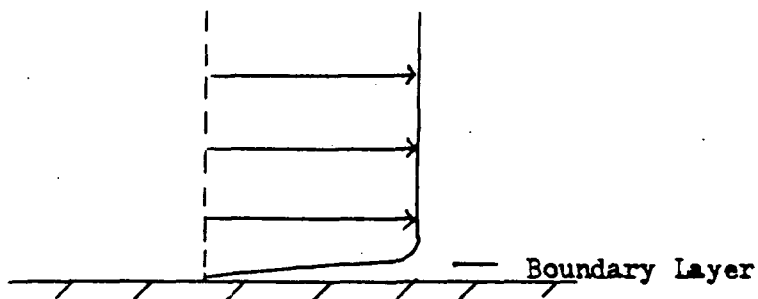


Fig. 1-5 Velocity profile of a fluid in turbulent flow showing a velocity of zero at a fixed boundary, a boundary layer in laminar flow and turbulent flow with an average forward velocity.

laminar and turbulent. Under most conditions silicate melts will exhibit laminar flow. The Reynolds number forms the basis of the study of fluid systems through the use of scaled models.

One of the fundamental properties of a fluid is viscosity (η), which is a constant relating shear stress (λ) to strain ratio or velocity gradient (dv/dx) or

$$\tau = \eta \left(\frac{dv}{dx} \right) .$$

Viscosity varies with temperature, but temperature has the opposite effect on liquids and gases. Viscosity increases with temperature in gases and decreases with temperature in liquids. The importance of viscosity in igneous processes has long been recognized and discussed (Bowen, 1934; Shaw, 1965, 1972; Bartlett, 1969; Bottinga and Weill, 1972; Kushiro, 1980). Among other things, the viscosity of a melt will determine flow morphology, convection in magma chambers, rates of ascent through the crust and crystal settling in magma chambers. In short, it is one of the most important factors in defining the chemistry and eruptive character of volcanic rocks.

If the fluid strictly follows the above relationship it is classed as a Newtonian fluid. However, in the case of silicate melts, it is often necessary for shear stresses to reach a critical value prior to the onset of flow. Silicate melts, then, generally behave as Bingham fluids. The behavior of these different fluid types can be generalized in Figure 1-6.

Shaw et al (1968) determined that basalts in an Hawaiian lava lake behaved as a Bingham fluid with critical shear stresses of 700 and 1200 dy/cm² at two different levels within the lake. The viscosities of these liquids were found to be 7.5×10^3 and 6.5×10^3 poise respectively. Rice (1981) has

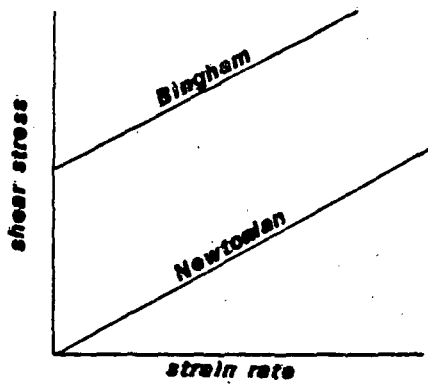


Fig. 1-6 Generalized diagram of the behavior of Newtonian and Bingham fluids.

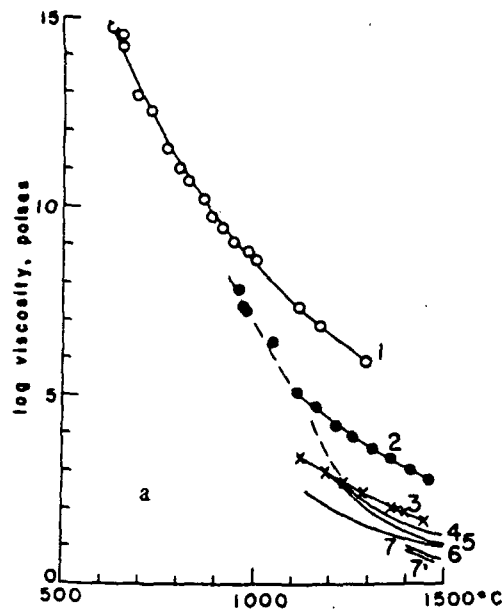


Fig. 1-7 Laboratory determinations of viscosity of various rock types as a function of temperature (Murase and McBirney, 1973).

suggested that crystals in a less dense Bingham fluid must reach a critical size before they will sink.

Murase and McBirney (1973) have studied the variation in viscosity of a spectrum of igneous rocks as a function of temperature. Their study was done in the laboratory using natural rock samples. They found that above the liquidus temperature, the viscosity decreases logarithmically with increase in temperature (Fig. 1-7) for these molten rocks they found the viscosity could be represented by the empirical relationship

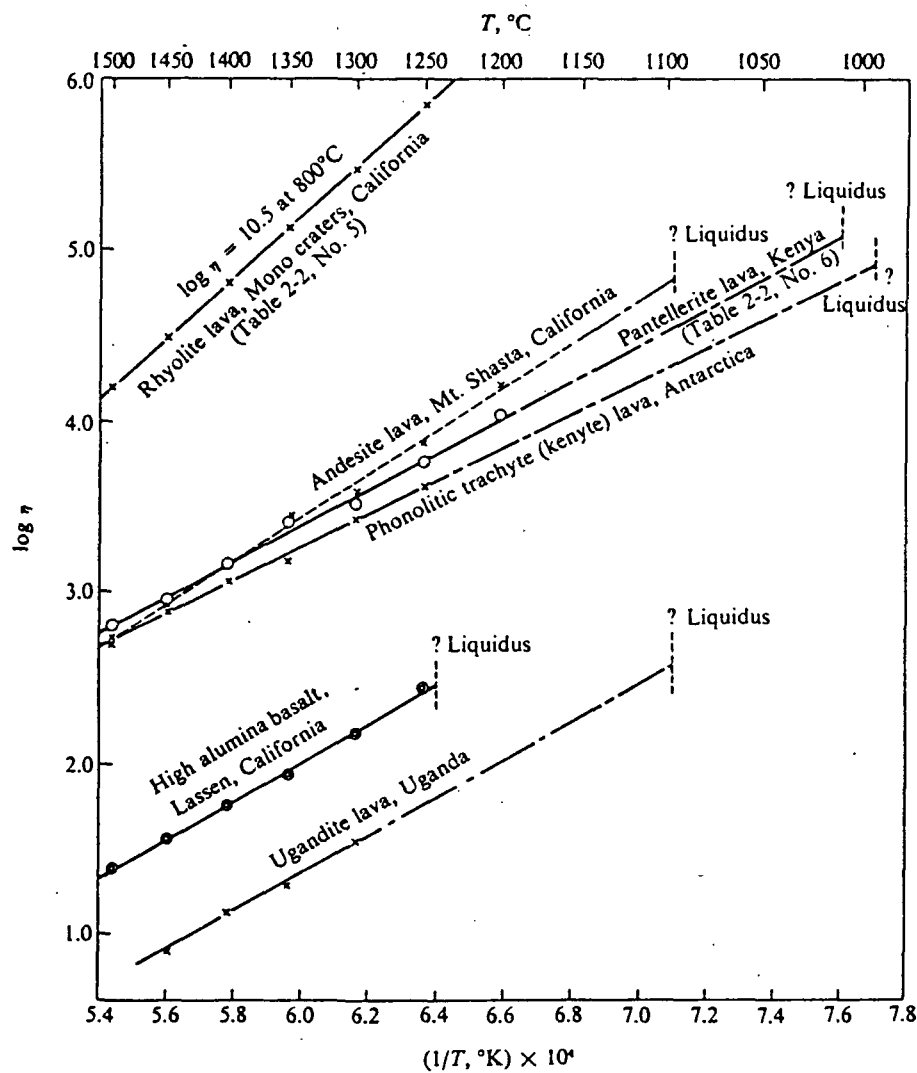
$$\eta = A_{\eta} \exp E_{\eta}/RT$$

where η is viscosity; E_{η} is the activation energy for viscous flow; R the gas constant; and A_{η} a constant. When temperatures fall below the liquidus the above relationship is no longer applicable, and viscosities increase rapidly with decrease in temperature. This is thought to result from the strength of temporary bonds. In natural systems, the presence of crystals, vapor bubbles, or xenoliths will also increase the viscosity of the melt.

Kushiro (1980) has studied the variation of viscosity and density of some silicate melts as a function of pressure. He has shown that viscosity in silicate melts is a function of pressure as well as temperature, with a general decrease in viscosity with increasing pressure. This viscosity change is often not linear, reflecting probable structural changes within the melt. He points out that these changes may influence trace element partitioning, the trend of crystal fractionation, and the locus of formation of plutons.

Figure 1-8 shows the variation in viscosity as a function of temperature of a number of rock types. These are calculated curves which demonstrate several valuable points. All the melts show an increase in viscosity with

Fig. 1-8 From Carmichael et al (1974).



Logarithms of calculated viscosities of various lava types plotted against $(1/T) \times 10^4$. Possible liquidus temperatures for each lava are also shown. Calculations are based on the data of Bottinga and Weill (1972).

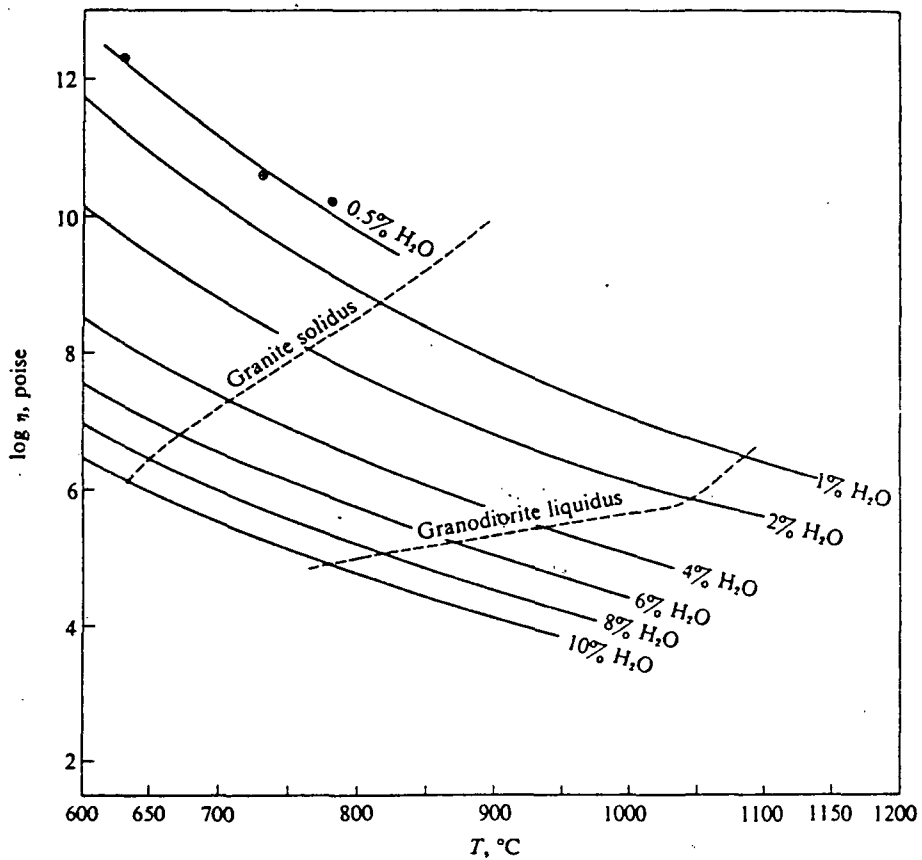
decreasing temperature as was demonstrated in Figure 1-7. The influence of chemistry is clearly seen with more siliceous rocks being more viscous than less siliceous rocks at the same temperature. In addition, the viscosity of less siliceous rocks increases more rapidly than the less siliceous rocks with a decrease in temperature. These changes are largely a result of polymerization of SiO_4^{-4} tetrahedra. In melts which are relatively deficient in cations such as calcium, sodium, and magnesium, the SiO_4 molecules combine to form chains with a resulting viscosity increase.

An increase in the water content of a magma will decrease its viscosity as shown in Figure 1-8. Thus the loss of water from an ascending magma may terminate the ascent of the body due solely to the increase in viscosity of the melt.

The viscosity will largely determine the morphology of a volcanic flow. Basalts and andesites, for instance, have a relatively low viscosity (Fig. 1-9) and thus form flows that tend to follow topographic lows and be areally extensive. Dacites and rhyolites, on the other hand, tend to form volcanic domes and short, stubby flows due to their relatively high viscosity.

Density (ρ) is another important factor in the behavior of igneous rocks. The densities of igneous rocks can be correlated with their SiO_2 content with more mafic rocks being more dense than rocks with higher SiO_2 content. Murase and McBirney (1973) have determined with densities of silicate liquids, as a function of temperature, and their curves are reproduced in Figure 1-10. These show a general decrease in density with an increase in temperature. As would be expected from the elastic behavior of liquids, density will increase with increasing pressure. This has been confirmed experimentally (Kushiro, 1980). Pressure has a more profound

Fig. 1-9 From Carmichael et al (1974).



Generalized curves after H. R. Shaw (1965) showing the viscosity of water-saturated acid magma (obsidian) as a function of temperature. The concentration of water, in wt %, is shown. Three values for obsidian with 0.5% H₂O are taken from Friedman et al. (1963). Burnham (1967) gives a similar plot; and the position of the granite solidus and granodiorite liquidus are taken from his paper.

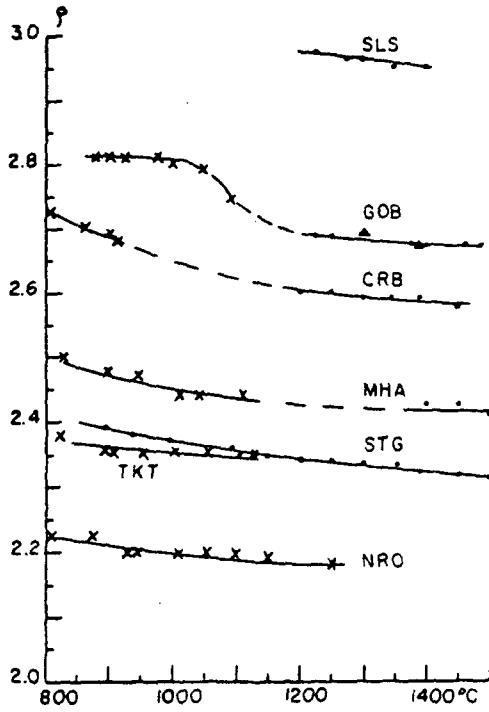


Fig. 1-10 Experimental determinations of the densities of various rock types as a function of temperature (Murase and McBirney, 1973).

influence on the density of a melt than does temperature.

1.2.3 Thermal Considerations

Rocks are effective thermal insulators. This allows molten rock to efficiently transfer thermal energy from depths to the upper reaches of the crust. In addition, it allows non-molten rock to serve as effective thermal reservoirs. Circulation of meteoric waters through these thermal reservoirs results in hydrothermal systems, which will be discussed in more detail later in this volume.

One of the basic thermal properties of rocks is thermal conductivity, which is a constant relating the quantity of heat (dQ) conducted in unit time across a surface (dS), or

$$dQ = -K \frac{dT}{dn} dS ,$$

where dT/dn is the thermal gradient, and K is the thermal conductivity. Some thermal conductivities of selected rock types are given in Table 1.3.

The thermal conductivity of rocks varies as a function of temperature, as shown in Figure 1-11. These data are from studies by Murase and McBirney (1973). They have interpreted the changes in slope of most of these samples as a result of change in the conduction mechanism from phonon conduction at lower temperatures to photon conductivity at higher temperatures.

Heat Capacity (Cp) or Specific Heat is another important property of rocks. It is defined as the quantity of heat necessary to raise the temperature of 1 gram of a substance 1°C. The heat capacity is temperature dependent and will increase with increasing temperature of rocks.

Table 1-3 Thermal conductivities of selected rocks
(From Geol. Soc. America Memoir 97).

Rock type and locality	Number of determinations	Conductivity (10^{-2} cal/cm sec $^{\circ}$ C)	
		Mean	Range
Granite and Quartz Monzonite Adams Tunnel, Colo.	59	7.89	6.7- 8.6
Granite Loetschberg Tunnel, Switzerland	12	7.77	6.2- 9.0
Granodiorite Steamboat Springs, Nev.	5	6.64	6.2- 6.9
Granodiorite Grass Valley, Calif.	14	7.61	7.0- 8.3
Quartz-Feldspar Porphyry Jacoba Bore, Orange Free State, S. Africa (25 $^{\circ}$ C)	5	8.0	7.6- 8.6
Syenite and Syenite Porphyry Kirkland Lake, Ont.	37	7.66	6.3- 9.5
Altered Rhyolite Timmins, Ont.	6	8.23	7.4- 8.8
Norite Sudbury, Ont.	5	6.42	5.5- 7.3
Serpentinized Peridotite Thetford Mines, Quebec	5	6.34	5.7- 7.0
Agglomerate Roodepoort Bore, Transvaal, S. Africa	5	7.4	7.1- 8.0
Karoo Dolerite Kestell Bore, Orange Free State (35 $^{\circ}$ C)	9	4.8	4.0- 5.5
Ventersdorp Lava Jacoba Bore, Orange Free State (25 $^{\circ}$ C)	9	7.4	6.3- 8.6
Ventersdorp Lava Roodepoort Bore, Transvaal	15	7.2	6.4- 8.0
Portage Lake Lava Calumet, Mich.	27	5.01	4.1- 6.6
Dense Flows Amygdaloidal Tops	10	6.4	5.5- 9.0
Porphyrite and Diabase Grass Valley, Calif.	21	7.14	6.2- 8.2
Quartz Diorite Gneiss Adams Tunnel, Colo.	17	7.75	6.6- 8.5
Injection Gneiss and Schist Adams Tunnel, Colo.	41	7.74	4.0-11.0
Gneiss Gotthard Tunnel, Switzerland	15	6.68	5.1- 8.0
Gneiss Simplon Tunnel, Switzerland	22	6.34	4.6- 7.7
Perpendicular Parallel	8	8.90	6.0-11.4
Schistes Lustrées Simplon Tunnel, Switzerland	8	5.74	4.1- 6.8
Perpendicular Parallel	7	7.50	6.8- 8.9

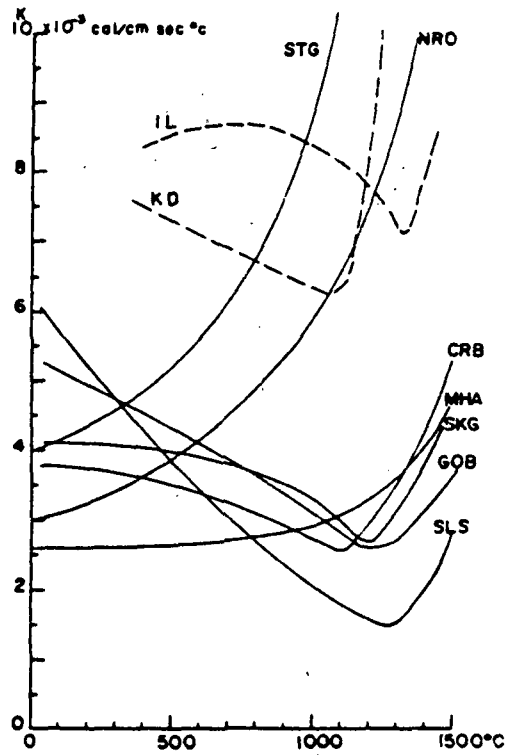


Fig. 1-11 Thermal conductivity of rocks as a function of temperature (Murase and McBirney, 1973).

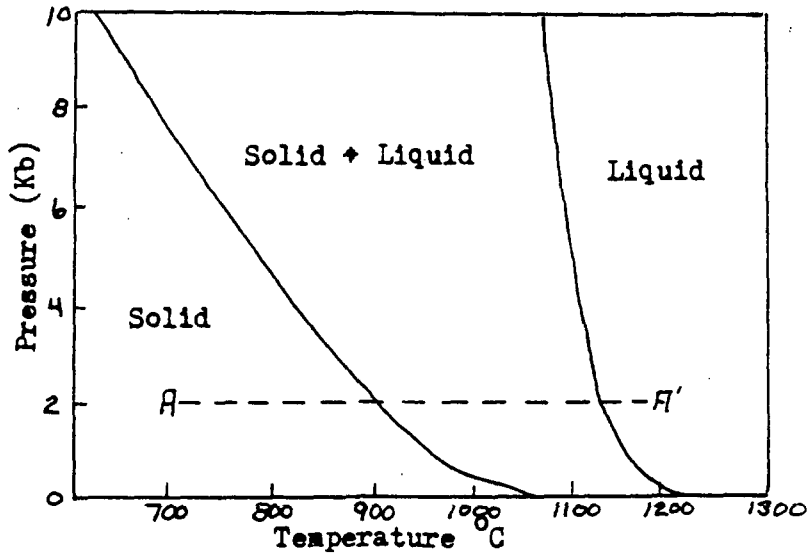


Fig. 1-12 Pressure-temperature relations of olivine tholeiite under saturated conditions (Yoder and Tilley, 1962).

The expansion and contraction of rocks during heating and cooling is defined by the coefficient of thermal expansion (α), which can be directly related to the change in density with temperature.

The latent heat of fusion (ΔH_f) is the heat required for the transformation from a solid to a liquid state. Correspondingly, when a molten rock is crystallized, ΔH_f represents the heat given off through the transformation from a liquid to a solid. Since rocks are multicomponent systems composed of minerals of different compositions and different melting temperatures, the melting or crystallization process takes place over a temperature interval as shown in Figure 1-12. The solidus in Figure 1-12 marks the beginning of melting and separates the pressure-temperature field where the rock is solid from that where solid and liquid coexist under equilibrium conditions. The liquidus defines the temperature above which the rock has been completely melted. The area between the solidus and liquidus defines a zone of partial melting. Heating a rock at a constant pressure of 2Kb (A-A', Fig. 1-12) then involves the following thermal considerations. Heating up to about 900°C will be dependent upon the specific heat of the rock. Through the interval between the liquidus and solidus, additional thermal input equivalent to the heat of fusion will be required and an amount of heat equivalent to the specific heat of the mixture will be necessary to continue the temperature increase. Above the liquidus, an increase in temperature will be dependent solely on the specific heat of the liquid.

The term convection is applied to both the heat and mass transfer within a fluid body. Convection is generally considered as forced convection where the fluid is under some sort of driving head or free convection where the movement of mass and resultant heat transfer is largely a result of

temperature dependent density differences.

Convection within an igneous melt will help determine the amount of homogenization and thus the path of chemical evolution as well as the thermal budget of the magma body. The Rayleigh Number (Ra) is a dimensionless quantity which is the ratio between buoyant and viscous forces.

$$R_a = \frac{g \alpha \rho d^3 \beta \Delta T}{7k \eta}$$

where α is the coefficient of thermal expansion, β is the temperature gradient, d is the thickness of the fluid layer, C_p is the heat capacity at constant pressure, k is the thermal conductivity, g is the gravitational constant, and η is the fluid viscosity. Convection will occur when $R_a > \sim 1700$ for an infinite horizontal layer of Newtonian fluid. Thus the principal variables controlling the onset of crystallization within a given magma body will be the temperature gradient (William and McBirney, 1979).

Mathematical modeling of the transfer of heat by conduction through igneous melts and adjacent wall rocks has been discussed by Lovering (1935, 1936) and Jaeger (1964) among others. The assumption of Lovering's (1935) cooling model are that the intrusion is instantaneous, the temperatures within the intrusion and within the wall rock are uniform, the wall rock is isotropic with the same thermal diffusivity as the intrusion, the thermal diffusivity and conductivity are constant, and heats of fusion are neglected. For a one-dimensional case, an infinite slab of finite thickness, the temperature at any distance from the center of the slab is given by the equation

$$\theta_{xt} = \theta_w + \frac{\theta_0}{2} \left\{ \operatorname{erf} \left(\frac{1-x}{2\sqrt{kt}} \right) + \operatorname{erf} \left(\frac{x+1}{2\sqrt{kt}} \right) \right\}$$

where x is the distance from the center of the dike, θ_w is the initial wall

rock temperature, θ_0 is the difference between the initial and the wall rock temperature, h is the thermal diffusivity ($h = k/\rho C_p$), and t is time in seconds.

Figure 1-13 shows a solution to the above equation for an infinite dike 3km thick with an initial intrusion temperature of 625°C intruded into wall rocks of 25°C. Equations for two- and three-dimensional intrusive bodies are also given in Lovering (1935).

1.2.4 Pressure

Pressure has an important role in the determination of the physical properties of silicate melts as well as melting relationships. The pressure that results from the overlying column of rock is termed the lithostatic pressure and that resulting from an overlying column of water is termed the hydrostatic pressure. These pressures at any depth can be calculated from

$$P = \rho gh$$

where ρ is the average density of the column of rock or water, h is its height and g is the gravitational constant.

Actual pressures will generally lie between lithostatic and hydrostatic pressures. If total pressure exceeds lithostatic pressure, the rock will fail through natural hydrofracturing or, if produced by the intrusion of magma, magmafracturing (Yoder, 1976).

Kushiro (1980) has experimented with the viscosities and densities of silicate melts at high pressures. In general viscosity decreases and density increases with an increase in pressure. With some types of melts (Fig. 1-14) there is a region between 7.5 and 10 Kb where changes of viscosity and density

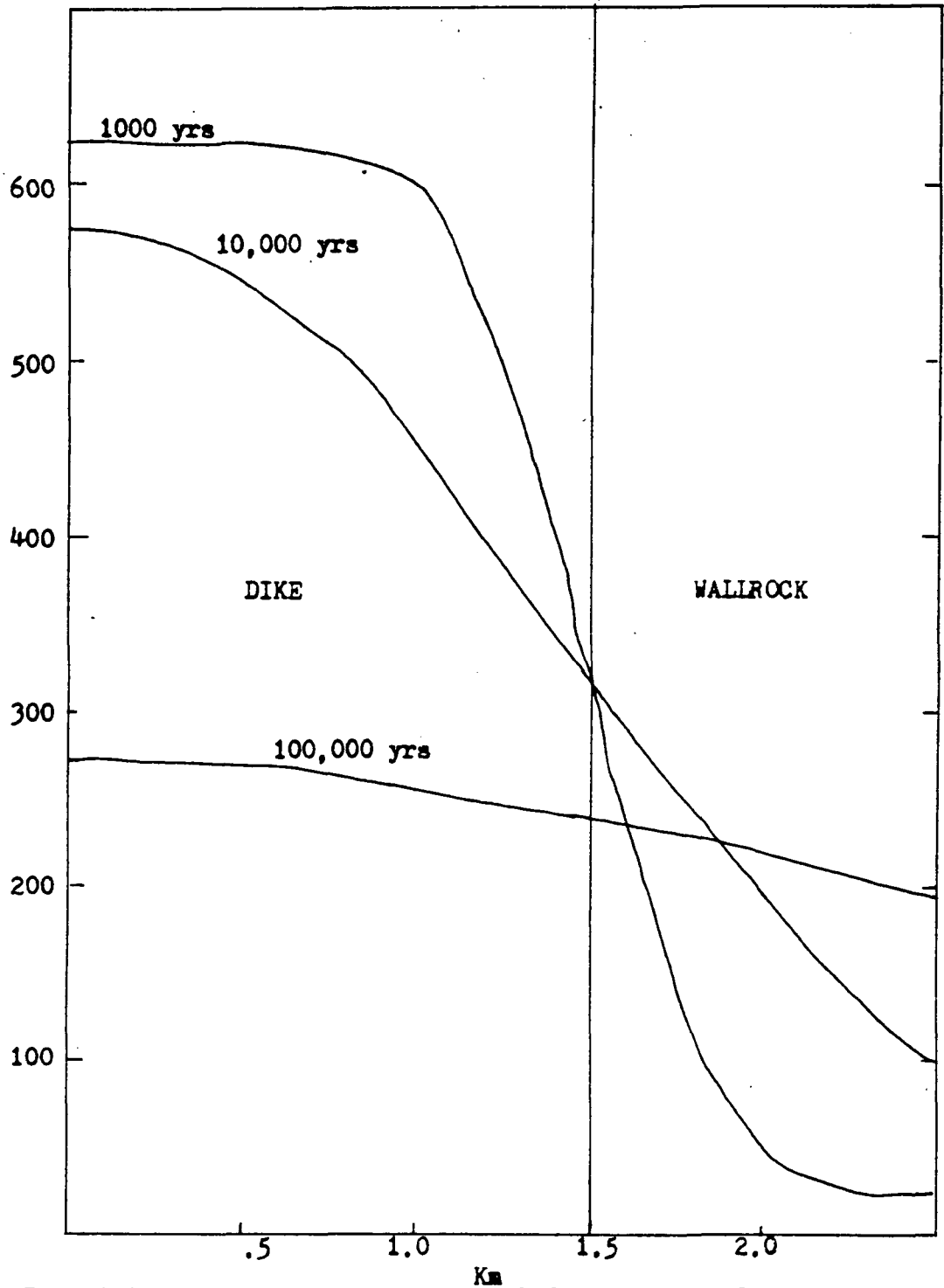
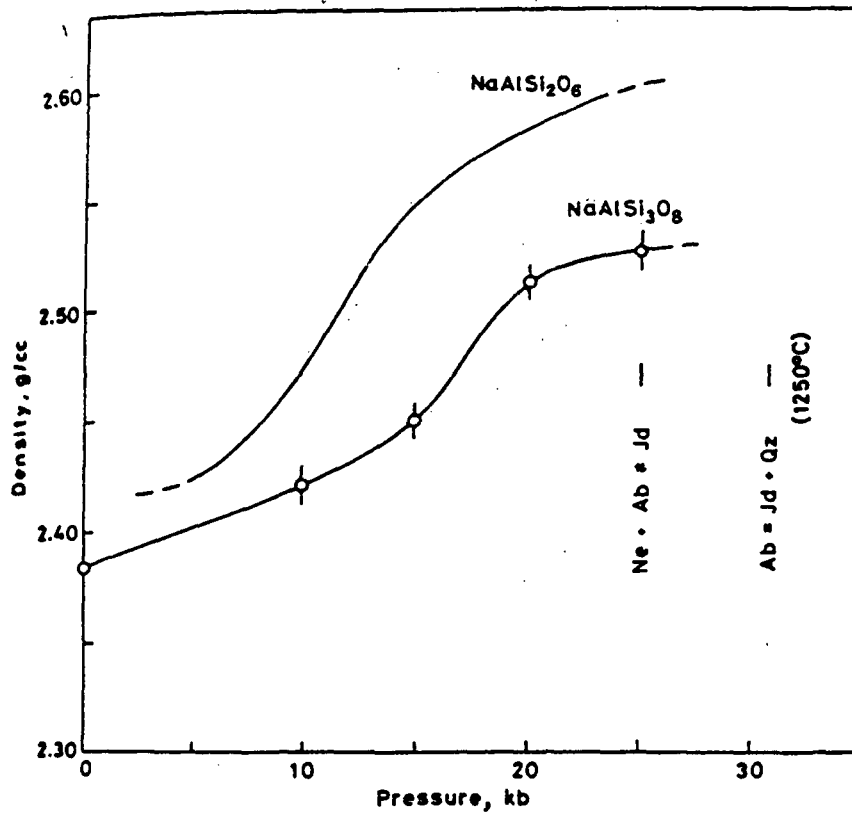
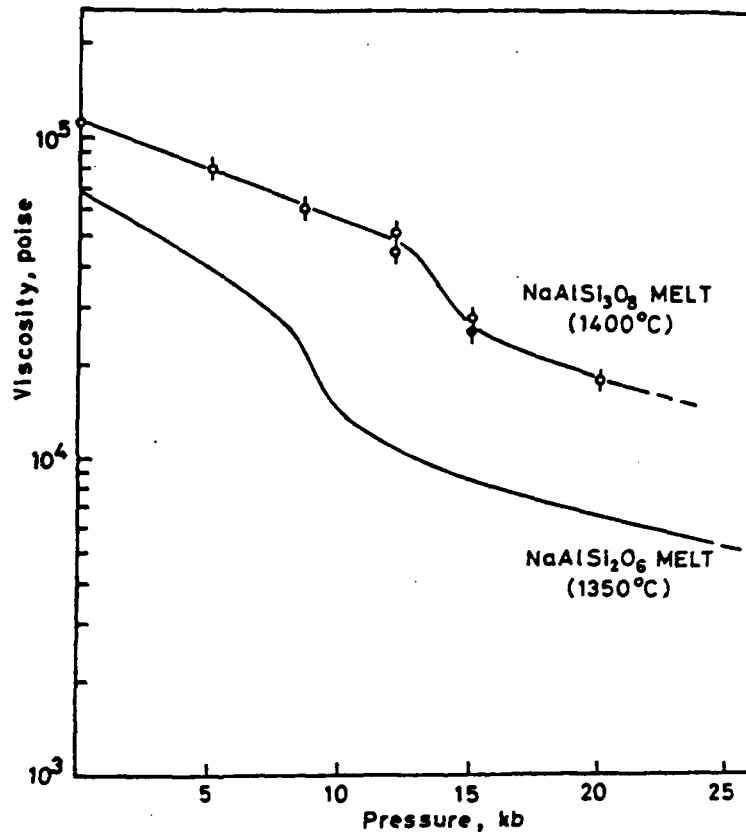


Fig. 1-13 Thermal conduction model for cooling of an infinite dike, 3km thick with an initial temperature of 625°C and a wallrock temperature of 25°C.



Density change of quenched melt (glass) of NaAlSi₃O₈ composition as a function of pressure of quenching (Kushiro, 1978). That of NaAlSi₂O₆ composition is shown for comparison. Two short vertical bars indicate the pressures for the reactions nepheline (Ne) + albite (Ab) = 2 jadeite (Jd) and albite = jadeite + quartz (Qz) at 1,250°C.



Viscosity change of NaAlSi₃O₈ (albite) melt with pressure at 1,400°C determined by Kushiro (1978a). That of NaAlSi₂O₆ melt at 1,350°C is shown for comparison.

Fig. 1-14 Changes in density and viscosity with pressure (Kushiro, 1980).

are much more rapid with increases in pressure. These zones are thought to represent changes in the structure of the melt itself. Kushiro has also pointed out that the change in density, with increasing pressure, of a basaltic melt is more rapid than for plagioclase feldspar. And whereas at low pressures plagioclase will sink in a basalt melt, at higher pressures, which depend upon the anorthite content of the plagioclase, crystals will tend to float. Thus changes in the total pressure on the system can influence the path of crystal fractionation. In addition the partitioning of trace elements between crystalline phases and the melt can be influenced by pressure (Kushiro, 1980, Fig. 11). Thus the trends of both major and trace elements can be expected to differ as a function of pressure. We will consider the importance of pressure further when discussing specific minerals or rock composition and the fractionation of igneous rocks.

1.2.5 Ascent of Magma

The ascent of a body of magma from its depth of formation toward the surface is controlled by "overburden squeeze" resulting from the weight of the overlying column of rock and also by buoyancy (Yoder, 1976). Yoder feels that overburden squeeze is the more important of the two.

From consideration of density differences, however, the velocity of an ascending magma body can be approximated by

$$v = \frac{(\rho - \rho') g \Delta x^2}{12\eta}$$

where ρ and ρ' are densities of the wall rock and melt, g is the gravitational constant, Δx is the width of the crack along which the magma is ascending, and η is the viscosity of the melt (Kushiro, 1980).

Thermal considerations for the ascent of magma through the crust have been dealt with by Marsh and Kantha (1978) and Turcotte (1981). Ramberg (1982) has pioneered the study of magma ascent using scaled models.

1.3 FUSION AND CRYSTALLIZATION OF SILICATE MELTS

The chemical composition and chemical variation of igneous rocks the world over is strikingly uniform. This uniformity implies that the processes which are active in the formation and subsequent evolution of these rocks are themselves fundamental. In this section we will discuss these processes in the context of melting and crystallization of igneous rocks and the chemical changes which can result from the fractionation of silicate melts during the melting or crystallization process.

1.3.1 Equilibrium Fusion or Crystallization

Equilibrium fusion or crystallization is the process by which an igneous melt is created or crystallized without a change in bulk composition. That is neither crystals nor liquid are separated from the system during the fusion or crystallization process. This is the least complex situation and we will use examples to review basic principles before dealing with the more complex topics of fractional crystallization and partial fusion. The approach of using experimental systems and equilibrium diagrams to explain fusion and crystallization of igneous melts was pioneered by Bowen (1928).

Figure 1-15 shows the equilibrium diagram for the system diopside-anorthite which can be used to illustrate crystallization and fusion in a relatively simple system. Since diopside is a pyroxene and anorthite a plagioclase feldspar there is no solid solution between the two end members. Mixtures of the two will, however, effect each others melting point as indicated by the position of the liquidus lines in Figure 1-15.

Assume that a melt has a composition of $An_{60}Di_{40}$ and has a temperature of $1450^{\circ}C$ (as in Fig. 1-15). As the melt is cooled it remains liquid until the

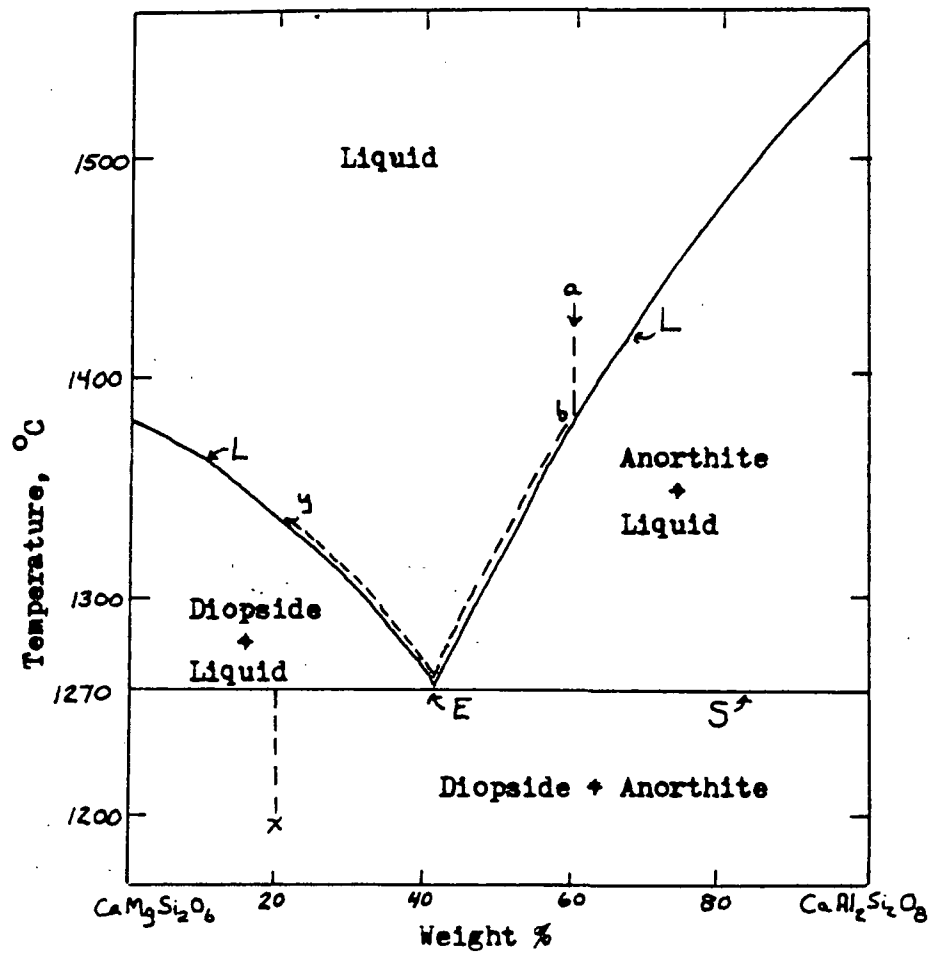


Fig. 1-15 Phase relations in the system diopside-anorthite (Bowen, 1915). L marks the liquidus, S the solidus, and E the eutectic. See text for a discussion of crystallization and fusion paths.

solidus is intersected (b, Fig. 1-15). At this point anorthite crystals begin to form and thus the liquid becomes more enriched in the diopside component. As cooling continues, anorthite crystals continue to form and the composition of the remaining liquid moves down the liquidus until it reaches the eutectic at 1270°C. At this point both diopside and anorthite crystallize from the melt. Further cooling does not take place until all the liquid has been consumed. The final solid is made up of 60% anorthite and 40% diopside, the original composition of the liquid. If anorthite had been separated from the melt during the crystallization process, the liquid would have followed the same path described above. However, the final composition of the system would have changed by the amount of anorthite removed.

Fusion in this system will follow the opposite path from that described above. This time consider a rock of composition $\text{Di}_{80}\text{An}_{20}$ (x, Fig. 1-15). As the temperature is increased, no melting takes place until the eutectic temperature (1270°C) is reached. At this point both diopside and anorthite begin to melt and the temperature will not increase until all of the anorthite has melted. The liquid will be of the eutectic composition ($\text{Di}_{58}\text{An}_{42}$). When the anorthite has melted, the liquid formed will change composition along the eutectic to point y (Fig. 1-15) at which time the system will be a liquid of composition $\text{Di}_{80}\text{An}_{20}$. Continued increases in temperature will have no effect on the composition of the liquid.

If a solid forms a liquid of identical composition upon the initiation of melting, the system is said to melt congruently. If a solid melts to a liquid plus a solid of a different composition it is said to melt incongruently. Incongruent melting takes place at a point which is called a peritectic on a phase diagram. Further discussion may be found in Bowen (1928).

Systems which have complete or partial solid solution are abundant and important in the study of igneous rocks petrogenesis. Figure 1-16 shows the phase diagram for the system Albite-anorthite. The crystallization of a melt of composition $Ab_{50}An_{50}$ is shown with cooling of the liquid following path a-b. When the temperature reaches b, crystals of composition c are formed. The liquid thus becomes relatively enriched in the albite component. As cooling proceeds, liquid and crystals continually re-equilibrate. The composition of the liquid moves along the liquidus to point d and the composition of the solid moves along the solidus to point e where crystallization is complete at a composition of $Ab_{50}An_{50}$. Fusion in this system will follow the opposite path.

The systems discussed so far have been relatively simple in that they contain only two phases. Rock systems are generally much more complex, but the consideration of a three phase system is not an unreasonable representation of some natural systems. Figure 1-17 shows the ternary system forsterite-anorthite-silica. This system has a join between anorthite and clinoenstatite. Compositions below that line will contain the assemblage forsterite + clinoenstatite + anorthite \pm spinel. Compositions above the line will contain the assemblage clinoenstatite + anorthite + SiO_2 . The crystallization of a melt of composition a (Fig. 1-17) will precipitate forsterite on cooling to the liquidus. As forsterite crystallizes the composition of the liquid moves directly away from forsterite. At b the composition of the liquid intersects the clinoenstatite begins to precipitate and forsterite begins to react with the remaining fluid to form enstatite. The composition of the remaining fluid moves down the forsterite-clinoenstatite boundary to c where anorthite begins to precipitate. The temperature will remain constant while clinoenstatite and anorthite are

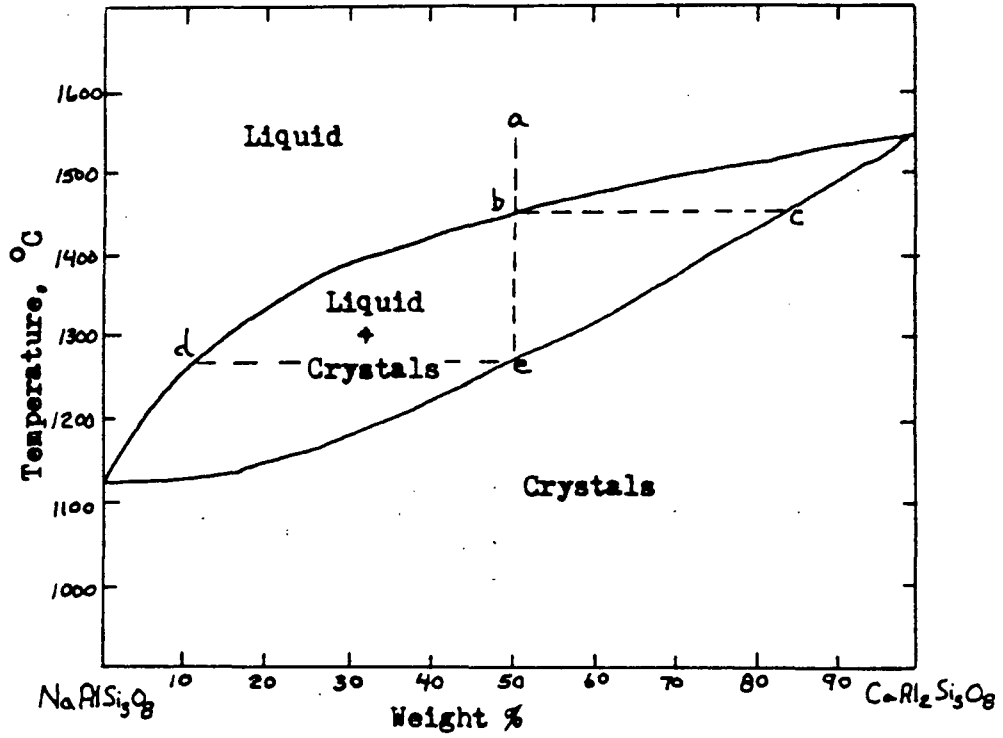


Fig 1-16 Phase relations in the system albite-anorthite (Bowen, 1913). See text for a discussion of crystallization and fusion paths.

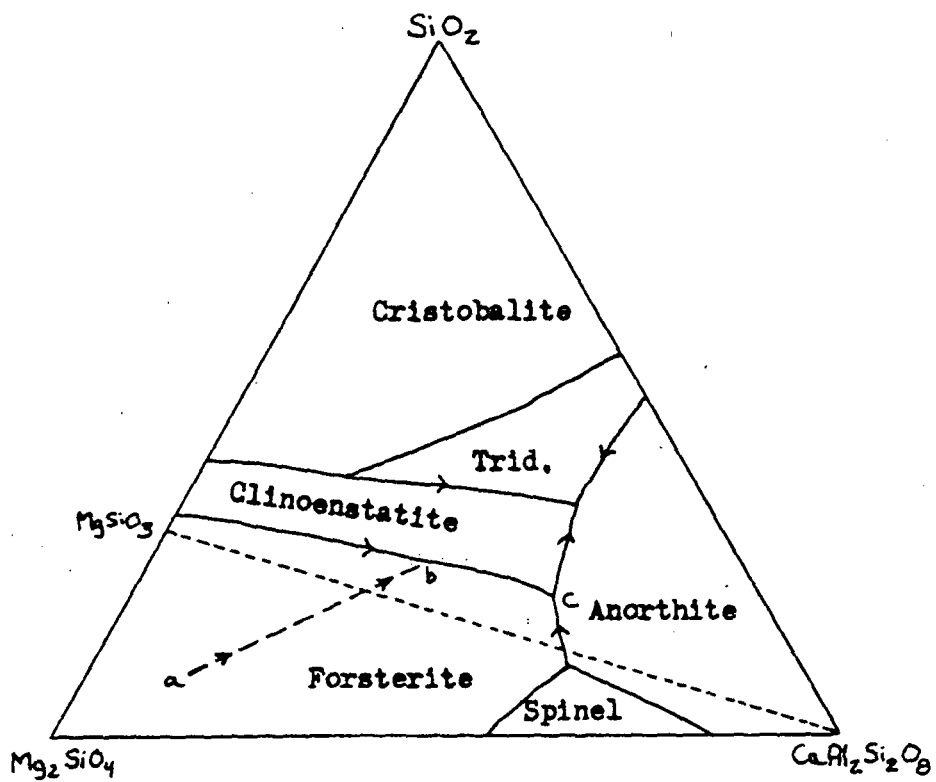


Fig. 1-17 Phase diagram of the system forsterite-anorthite-silica (Anderson, 1915).

precipitated and forsterite reacts to form clinoenstatite. After the fluid is exhausted the assemblage forsterite + clinoenstatite + anorthite continues to cool. Again, melting paths will be the opposite of the crystallization paths.

Note that Figure 1-17 offers explanations for many of the relationships seen in natural systems such as the mantling of forsterite by clinoenstatite and the mutual exclusion of forsterite and quartz in the same rock.

More complex quaternary systems are often displayed in the literature. The principles for following the cooling paths in these systems are the same as for simpler systems. More detailed discussions may be found in Carmichael et al (1974) or Ehlers (1972) among others.

The system $\text{NaAlSi}_3\text{O}_8\text{-KAlSi}_3\text{O}_8\text{-SiO}_2\text{-H}_2\text{O}$ is of great importance to our understanding of felsic magma systems. This system has been investigated by a number of authors (Tuttle and Bowen, 1958; Luth et al, 1964) and is shown in Figure 1-18. The system is somewhat complicated by the partial solid solution between potassium feldspar and albite. In addition the location of the eutectic and isobaric minima migrate away from Ab with a decrease in H_2O pressure.

The paths of crystallization are shown in Figure 1-18. Note that for composition falling within the field QE'E the first mineral to crystallize is quartz. The composition of the fluid will migrate directly away from quartz to the thermal trough represented by E-E'. From this point the fluid will move to the thermal minimum or the eutectic depending upon its composition.

A liquid leaving the composition X on the other hand, will initially crystallize K-fs-Albite solid solution. The initial crystals will react with the remaining melt as was demonstrated for the Ab-An system (Fig. 1-16). Thus

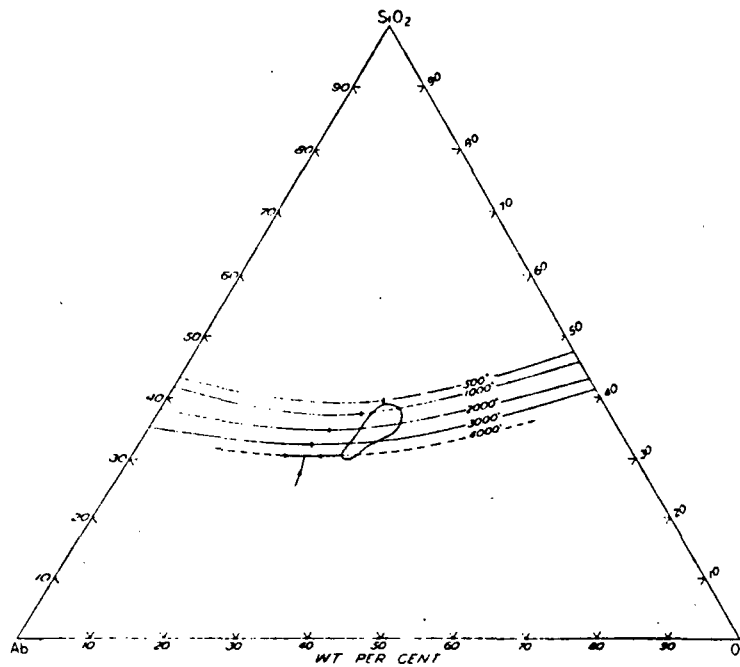
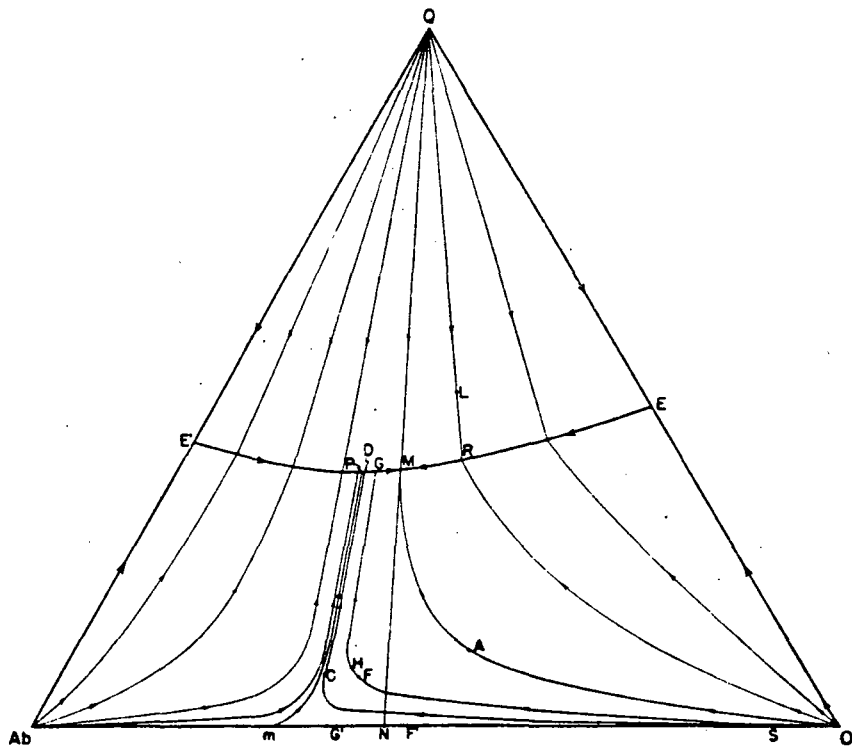


Fig. 1-18 The system $\text{NaAlSi}_3\text{O}_8\text{-KAlSi}_3\text{O}_8\text{-SiO}_2\text{-H}_2\text{O}$ (Tuttle and Bowen, 1958). a. Isobaric fractionation curves for water vapor pressure of 1000 kg/cm^2 ; b. effect of water vapor pressure on the isobaric minimum.

the fluid path will be curved as shown in Fig. 1-18.

Tuttle and Bowen point out that in order for the crystallization to remain isobaric, water must be continuously released from the system. This water can be responsible for the formation of hydrothermal ore deposits, hydrothermal alteration, or the presence of a magmatic water component in a geothermal system.

Lipman (1966) has applied the data from Tuttle and Bowen (1958) to demonstrate that several major Tertiary ash flow tuff sheets from Nevada crystallized under water pressures of 500 to 1200 bars. He has done this by plotting the normative Ab-Or-Q (albite-orthoclase-quartz) content, normalized to 100%, on Tuttle and Bowen isobaric fractionation curves (Fig. 1-19). Assuming that the continuing pressure is lithostatic and equal to water pressure, the range of conditions of generation of these ash flow sheets is from 3% H₂O, 750°C and depth to the top of the magma chamber of 1 mile to 5% H₂O, 700°C, and 2-5 miles to the top of the magma chamber. These water pressures are lower than had been proposed by previous investigators, leading Lipman to suggest that the key to ash flow magmatism and resultant calderas may be the evacuation of large shallow magma chambers rather than eruption resulting from high magmatic water pressures.

1.3.2 Fractional Crystallization

In contrast with equilibrium crystallization discussed in the preceding section, fractional crystallization involves the separation of crystals from the melt. In this way the bulk composition of the rock is changed and minerals that have a reaction relationship with the magma do not have the opportunity to do so. Various processes such as crystal settling, crystal

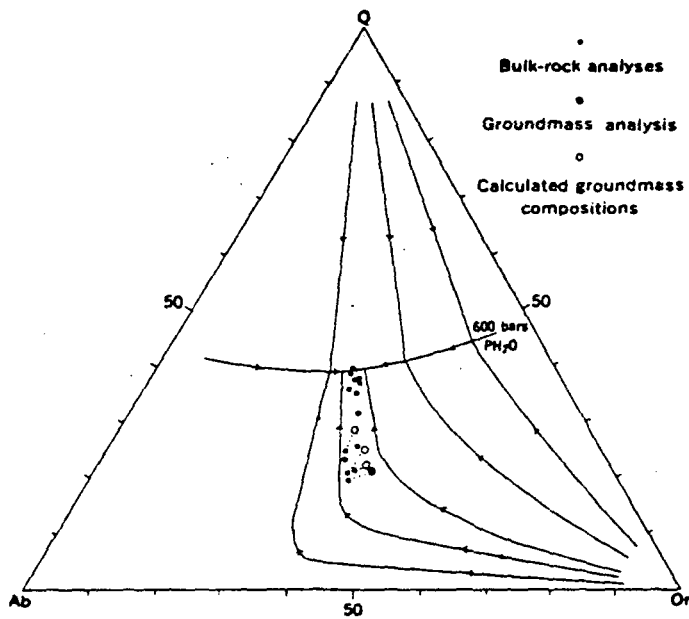


Fig. 1-19 Normative compositions of the Topopah Spring Member in the system Q-Or-Ab. Isobaric fractionation curves for 600 bars water pressure interpolated from Tuttle and Bowen (1958). From Lipman (1966).

floating, and filter pressing can be cited as mechanisms of fractional crystallization, but in general it is brought about by any mechanism which separates newly formed crystals from the remaining melt.

Bowen (1928) proposed the process of fractional crystallization to form andesitic through rhyolitic liquids from parental melts of basaltic composition. It has often been pointed out that this mechanism produces a relatively small volume of granitic liquid in proportion to the basaltic starting material. It is difficult to explain large volume felsic batholithic complexes by the fractional crystallization of basalt (Presnall, 1979). More realistic proposals center around the process of partial fusion which will be discussed in more detail in the next section. However, most petrologists would agree that the process of fractional crystallization is of fundamental importance in understanding the chemical variations of igneous rocks (Presnall and Bateman, 1973).

1.3.3 Fractional Fusion

Presnall (1969) has defined two end-member fusion processes, equilibrium and fractional fusion. Equilibrium fusion of an igneous rock will follow the reverse of the liquid path defined by equilibrium crystallization. The melt and crystalline residue react with each other during this process. During fractional fusion the melt and crystalline material are separated immediately and do not react with each other. Partial fusion involves the fusion of some portion of the rock and can thus involve equilibrium fusion, fractional fusion or some combination of these processes.

Yoder (1976) suggests that basalts are derived from the fractional fusion of a garnet peridotite. Experiments have shown that a substantial amount of

liquid of basaltic composition is derived from garnet peridotite at its fusion temperature.

1.4 CRYSTALLIZATION AND DIFFERENTIATION IN MAGMA CHAMBERS

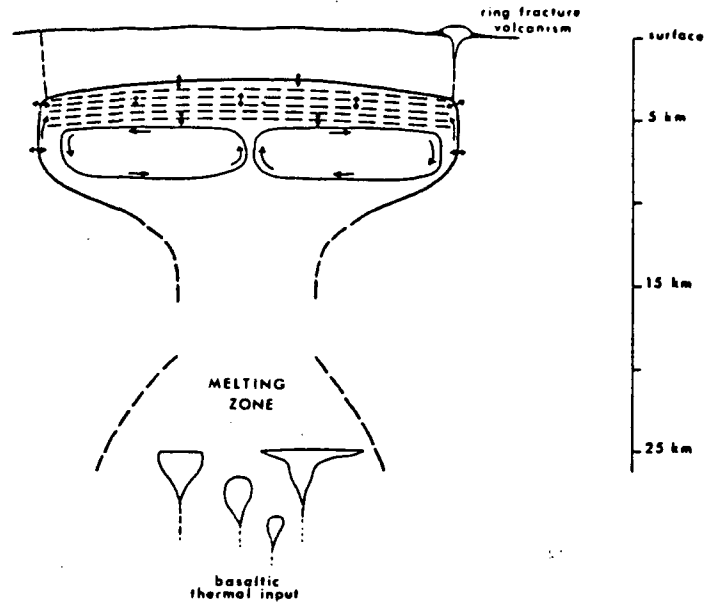
In previous sections we have considered the basic physical-chemical processes of melting and crystallization of silicate melts. The classical view of the crystallization process is that it takes place in a large magma chamber which is relatively uniform upon emplacement and subsequently is modified by fractional crystallization. Recently, however, studies of fluid mechanics have suggested some additional considerations for some of the processes influencing zoning in magma chambers. In addition, authors have also considered the effects of assimilation, mixing of different types of magmas, and separation of magmas into immiscible components to explain the chemical variations within volcanic rock suites.

Layered mafic intrusions have for many years served to exemplify important processes of differentiation in magma chambers. The layered nature of these intrusives has, in the past, been largely explained as resulting from fractionation by the process of crystal settling. However, recent work has suggested that a process called double-diffusive convection may be of importance (Turner and Gustafson, 1978; McBirney and Noyes, 1979; Chen and Turner, 1980). The process is based on the fact that if a thermal gradient is imposed on a fluid with a concentration gradient, horizontal layers of uniform concentration and temperature will be generated (Chen and Turner, 1980). Thus a magma chamber could become stratified. These stratified layers can be sustained because the diffusivity of heat between the layers is more rapid than the diffusivity of chemical components. The interfaces between layers are relatively static, but due to the net upward flux of heat, convection systems develop within the layers. Thus density, temperature, and composition will change downward in a magma body as a series of steps.

Much of the emphasis in the study of ash flow tuffs has centered on understanding the processes within the felsic magma chambers from which these rocks were derived (Smith, 1979; Hildreth, 1979, 1981). As we will see in subsequent sections, an ash-flow tuff is formed by the partial evacuation of felsic magma chambers and is thus the inverse of the layering developed within the chamber. The process of thermogravitational diffusion has been outlined by Hildreth (1979, 1981) and is called on to explain repeated thermal and compositional gradients which are apparently established in large felsic magma chambers. This process is based upon the establishment of compositional gradients in a magma chamber which is in the presence of a thermal gradient. The process is summarized in Figure 1-20.

Fig. 1-20 From Hildreth (1981).

Schematic portrayal of the convection-aided thermogravitational diffusive mechanism envisaged for differentiation of large silicic magma chambers; modified from Shaw and others (1976). A progressively stagnating high-silica roof zone, stabilized by a water concentration gradient, experiences both internal mass transfer and diffusive exchange with wall rocks and with the still-convecting subjacent magma volume. Compositional gradients are established in accordance with potentials imposed upon each constituent species in the melt by the thermal gradient, the gravitational field, and by systematic changes in melt structure resulting in turn from the gradients in T , P , X_{H_2O} , and $O/(Si + Al)$. Characteristic periods of time available for differentiation of such systems appear to range between 10^6 and 10^7 yr for epicratonic Valles-type calderas, but down to $<10^3$ yr for small caldera-forming stratovolcanoes. Arrows along the walls signify upward buoyancy in thin chemical boundary layers, owing to diffusive influx of H_2O from wall rocks (see Fig. 11 of Shaw, 1974). Underplating of the silicic focus by mantle-derived mafic magma is thought to supply the principal thermal input responsible for large-scale crustal melting and for driving the convective regime within the chamber. The schematic ponding might more realistically be portrayed by a plethora of dikes and gabbroic stocks. Such injections may sometimes trigger eruptions in small-volume systems and could produce both synplutonic dikes and many of the mafic inclusions so abundant in granodioritic and tonalitic parts of major plutons. Release of CO_2 and S from such basalts could affect mass transfer in the overlying silicic system.



1.5 REFERENCES

- Andersen, O., 1915, The system anorthite-forsterite-silica: *Am. Jour. Sci.*, v. 39, p. 407-454.
- Barth, T. F. W., 1966, *Theoretical Petrology*: Wiley, New York, 416 p.
- Bartlett, R. W., 1969, Magma convection, temperature distribution, and differentiation: *Am. Jour. Sci.*, v. 267, p. 1067-1082.
- Bottinga, Y., and Weill, D. F., 1972, The viscosity of magmatic silicate liquids: A model for calculation: *Am. Jour. Sci.*, v. 272, p. 438-475.
- Bowen, N. L., 1913, The melting phenomena of the plagioclase feldspars: *Am. Jour. Sci.*, v. 35, p. 577-599.
- Bowen, N. L., 1915, The crystallization of haplobasaltic, Naplodioritic, and related magmas: *Am. Jour. Sci.*, v. 40, p. 161-185.
- Bowen, N. L., 1928, *The evolution of the igneous rocks*: Princeton Univ. Press (reprinted 1956, Dover Publication, New York).
- Bowen, N. L., 1934, Viscosity data for silicate melts: *EOS Transactions*, 15 Annual Mtg. AGU, p. 249-255.
- Camichael, I. S. E., Turner, F. J., and Verhoogan, J., 1974, *Igneous Petrology*: New York, McGraw-Hill, 739 p.
- Chayes, F., 1979, Partitioning by discriminant analysis: a measure of consistency in the nomenclature and classification of volcanic rocks, in Yoder, H. S. (ed.), *The evolution of the igneous rocks, fiftieth anniversary perspectives*: Princeton University Press, p. 521-532.
- Chen, C. F. and Turner, J. S., 1980, Crystallization in a double-diffusive system: *Jour. Geophys. Res.*, v. 85, p. 2573-2593.
- Ehlers, E. G., 1972, *The interpretation of geological phase diagrams*: San Francisco, Freeman and Co., 280 p.
- Ewart, A., 1979, A review of the mineralogy and chemistry of Tertiary-Recent dacitic, latitic, rhyolitic, and related silicic volcanic rocks, in Barler, F. (ed) *Trondhjemites, Dacites and Related Rocks*: Elsevier, Amsterdam, p. 13-121.
- Hildreth, W., 1979, The Bishop Tuff: evidence for the origin of compositional zonation in silicic magma chambers, in Chapin, C. E. and Elston, W. E. (eds), *Ash-flow tuffs*: *Geol. Soc. America*, Special Paper 180, p. 43-75.
- Hildreth, W., 1981, Gradients in silicic magma chambers: implications for lithospheric magmatism: *Jour. Geophys. Res.*, v. 86, p. 10153-10192.
- Hunt, C.B., 1982, Overthrust belt - need for a definition, in Nielson, D. L. (ed) *Overthrust belt of Utah*: *Utah Geol. Assoc. Publication* 10, p. 119.

- Irvine, T. N. and Barager, W. R. A., 1971, A guide to the chemical classification of the common volcanic rocks: *Can. Jour. Earth Sciences*, v. 8, p. 523-548.
- Jaeger, J. C., 1964, Thermal effects of intrusions: *Rev. of Geophys.*, v. 2, p. 443-466.
- Kuno, H., 1960, High-alumina basalt: *Jour. Petrology*, v. 1, p. 121-145.
- Kuno, H., 1968, Differentiation of basaltic magmas, in *Basalts*, v. II, p. 623-688.
- Kushiro, I., 1980, Viscosity, density, and structure of silicate melts at high pressures, and their petrological applications, in Hargraves, R. B. (ed) *Physics of Magmatic Processes*: Princeton Univ. Press, Princeton, p. 93-120.
- Lipman, P. H., 1966, Water pressures during differentiation and crystallization of some ash-flow magmas from southern Nevada: *Am. Jour. Sci.*, v. 264, p. 810-826.
- Lovering, T. S., 1935, Theory of heat conduction applied to geological problems: *Geol. Soc. America, Bull.*, v. 46, p. 69-94.
- Lovering, T. S., 1936, Heat conduction in dissimilar rocks and the use of thermal models: *Geol. Soc. America Bull.*, v. 47, p. 87-100.
- Luth, W. C., Jahns, R. H., and Tuttle, O. F., 1964, The granite system at pressures of 4 to 10 kilobars: *Jour. Geophys. Res.*, v. 69, p. 759-773.
- Marsh, B. D. and Kantha, L. H., 1978, On heat and mass transfer from an ascending magma: *Earth Planet. Sci. Lett.*, v. 39, p. 435-443.
- McBirney, A. R. and Noyes, R. M., 1979, Crystallization and layering of the Skaegaard intrusion: *Jour. Petrol.*, v. 20, p. 487-554.
- Murase, T. and McBirney, A. R., 1973, Properties of some common igneous rocks and their melts at high temperatures: *Geol. Soc. America Bull.*, v. 84, p. 3563-3592.
- Peacock, M. A., 1931, Classification of igneous rock series: *J. Geol.*, v. 39, p. 54-67.
- Presnall, D. C., 1969, The geometrical analysis of partial fusion: *Am. Jour. Sci.*, v. 267, p. 1178-1194.
- Presnall, D. C., 1979, Fractional crystallization and partial fusion, in Yoder, H. S., *The evolution of the igneous rocks, fiftieth anniversary perspectives*: Princeton Univ. Press, p. 59-75.

- Presnall, D. C. and Bateman, P. C., 1973, Fusion relations in the system $\text{NaAlSi}_3\text{O}_8$ - $\text{CaAl}_2\text{Si}_2\text{O}_8$ - KAlSi_3O_8 - SiO_2 - H_2O and the generation of granitic magmas in the Sierra Nevada Batholith: *Geol. Soc. America Bull.*, v. 84, p. 3181-3202.
- Rice, A., 1981, Convective fractionation: a mechanism to provide cryptic zoning, layering, crescumulates, banded tuffs and explosive volcanism in igneous processes: *Jour. Geophys. Res.*, v. 86, p. 405-417.
- Shaw, H. R., 1965, Comments on viscosity, crystal settling, and convection in granitic magmas: *Am. Jour. Sci.*, v. 263, p. 120-152.
- Shaw, H. R., 1972, Viscosities of magmatic silicate liquids: An empirical method of prediction: *Am. Jour. Sci.*, v. 272, 870-893.
- Shaw, H. R., Wright, T. L., Peck, D. L., and Okamura, R., 1968, The viscosity of basaltic magma; an analysis of field measurements in Makaopuhi Lava Lake, Hawaii: *Am. Jour. Sci.*, v. 266, p. 225-264.
- Smith, R. L., 1979, Ash-flow magmatism, in Chapin, C. E. and Elston, W. E., *Ash-flow tuffs*: *Geol. Soc. America, Spec. Paper 180*, p. 5-27.
- Streckeisen, A., 1967, Classification and nomenclature of igneous rocks: *Neues Jb. Miner. Abb.*, v. 107, p. 144-240.
- Travis, R. B., 1955, Classification of Rocks: *Quarterly of the Colorado School of Mines*, v. 50, no. 1, 98 p.
- Turcotte, D. L., 1981, Some thermal problems associated with magma migration: *Jour. Volcanol. and Geoth. Res.*, v. 10, p. 267-278.
- Turner, J. S. and Gustafson, L. B., 1978, The flow of hot saline solutions from vents in the sea floor--some implications for exhalative massive sulfide and other ore deposits: *Econ. Geology*, v. 73, p. 1082-1100.
- Turner, J. S. and Gustafson, L. B., 1981, Fluid motions and compositional gradients produced by crystallization or melting at vertical boundaries: *Jour. Volcanol. and Geoth. Res.*, v. 11, p. 93-125.
- Tuttle, O. F. and Bowen, N. L., 1958, Origin of granite in light of experimental studies in the system $\text{NaAlSi}_3\text{O}_8$ - KAlSi_3O_8 - SiO_2 - H_2O : *Geol. Soc. America, Memoir 74*.
- Williams, H. and McBirney, A. R., 1979, *Volcanology*: San Francisco, Freeman, Cooper, 397 p.
- Yoder, H. S., 1976, *Generation of basaltic magma*: Washington, D.C., National Academy of Sciences, 265 p.
- Yoder, H. S. and Tilley, C. E., 1962, Origin of basalt magmas: an experimental study of natural and synthetic rock systems: *Jour. Petrology*, v. 3, p. 342-532.

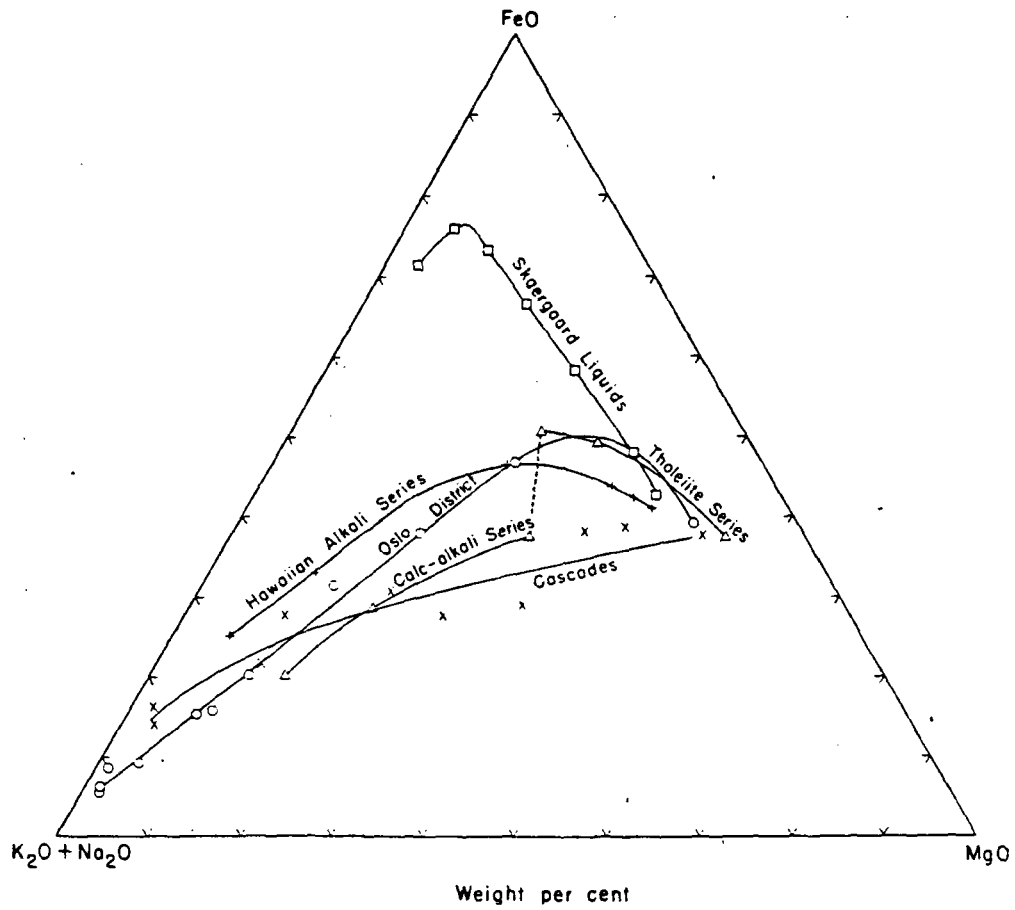


FIG. 18. An FMA plot of the rock series presented in Fig. 17.

YODER AND TILLEY, 1962

TABLE 4-1. Compositions of volcanic gases (In volume percent)

	1	2	3	4	5	6	7	8	9
CO ₂	21.4	46.2	40.9	4.6	10.1	2.1	15.3	10.4	25.9
CO	0.8	0.7	2.4	0.3	2.0	0.6	1.4	8.3	•
H ₂	0.9	0.03	0.8	2.8	0.2	0.4	4.4	1.1	—
SO ₂	11.5	14.3	4.4	4.1	—	0.01	—	—	0.0
S ₂	0.7	0.0	—	—	0.5	0.9	0.2	1.3	—
SO ₃	1.8	38.8	—	—	—	—	—	—	—
Cl ₂	0.1	0.0	—	—	0.4	0.3	0.2	0.4	—
F ₂	0.0	0.0	—	—	3.3	1.5	0.0	0.0	—
HCl	—	—	—	0.6	—	—	—	—	—
N + rare gases	10.1	16.6	8.3	4.5	0.9	0.6	5.2	7.2	11.1
H ₂ O	52.7	71.4	43.2	83.1	82.5	93.7	73.2	71.3	63.0

• Included with N.

1. Kilauea, Hawaii; average of the best 10 collections of gas from Halemaumau lava lake in 1917-1919 (Jaggard, 1940).
2. Mauna Loa, Hawaii; average of two samples collected from molten lava in 1926 (Shepherd, 1938).
3. Nyiragongo, Congo; the single "excellent" analysis of gas from the lava lake in 1959 for which water was determined (Chaigneau, Tazieff, and Fabre, 1960).
4. Surtsey, Iceland; average of 11 analyses of samples taken between Oct. 15, 1964, and March 31, 1967 (Sigvaldason and Elisson, 1968).
5. Mt. Pelée, West Indies; gas extracted from lava (hypersthene andesite) of the spine formed in 1902 (Shepherd and Merwin, 1927).
6. Lassen Peak, California; gas extracted from lava (dacite) erupted in 1915 (Shepherd, 1925).
7. Mauna Loa, Hawaii; gas extracted from pumice (basalt) of the 1926 eruption (Shepherd, 1938).
8. Niuafou'ou; gas extracted from lava (basalt) of the 1929 eruption (Shepherd, 1938).
9. Kozu-shima, Japan; gas extracted from rhyolite lava (Iwasaki, Katsura, and Sakato, 1955).

from: Macdonald (1972)

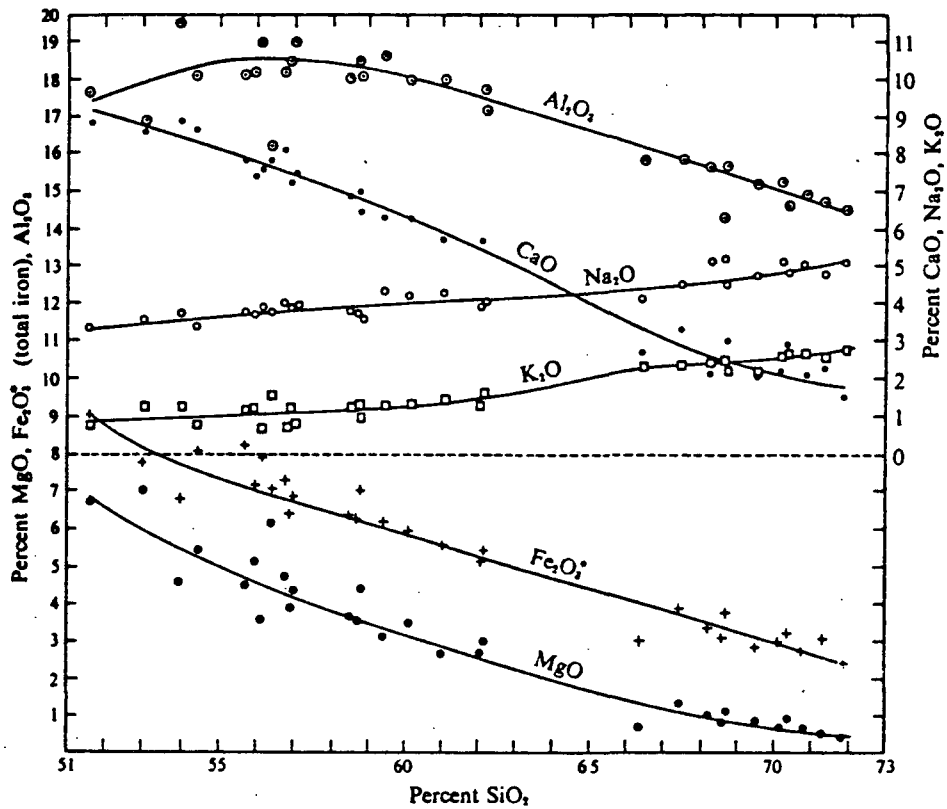


Fig. 2-1 Variation diagram (Harker type) for volcanic rocks of Crater Lake, Cascades volcanic province, northwestern United States. (After Williams, 1942.)

CARMICHAEL AND OTHERS, 1974

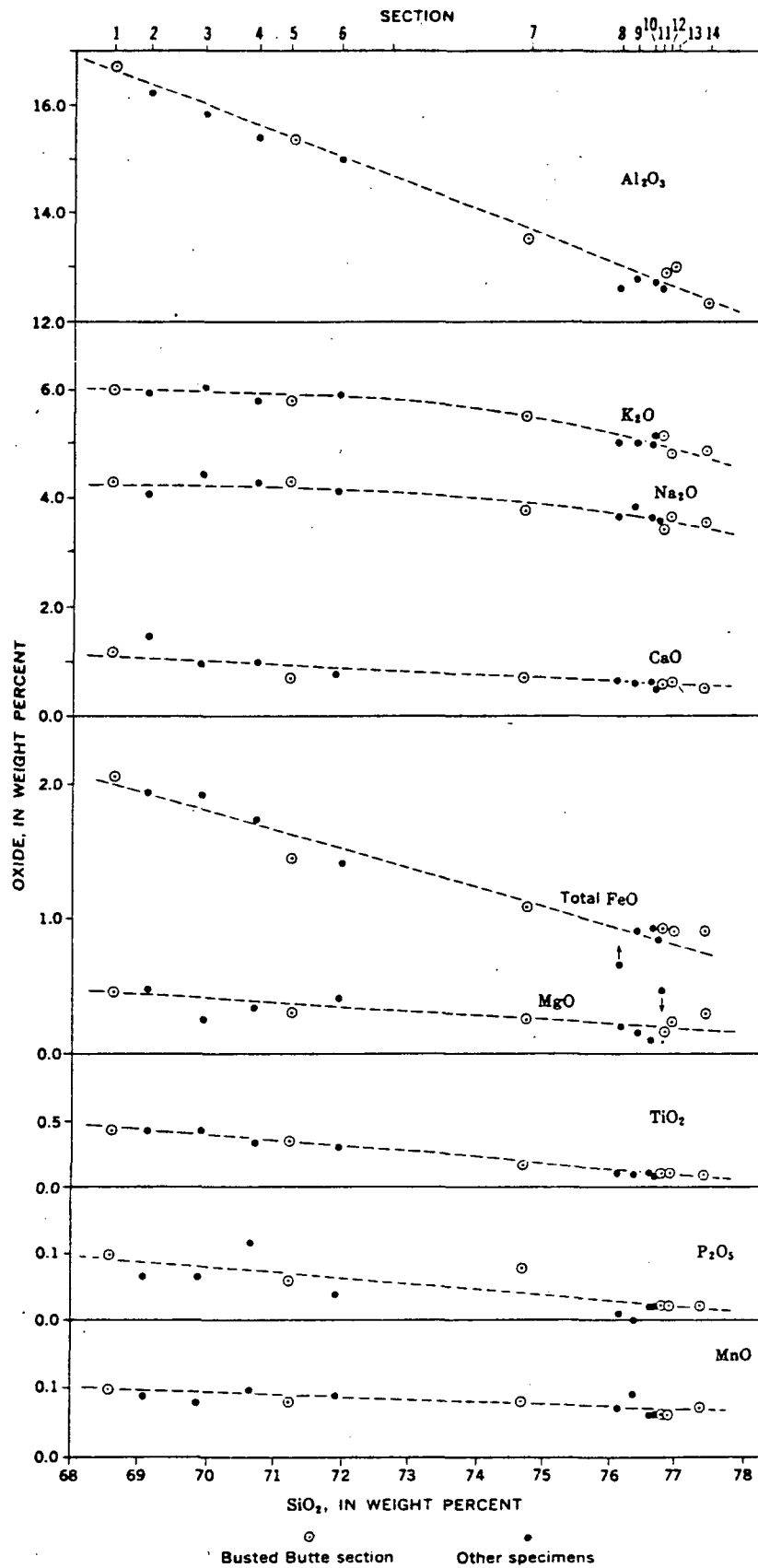
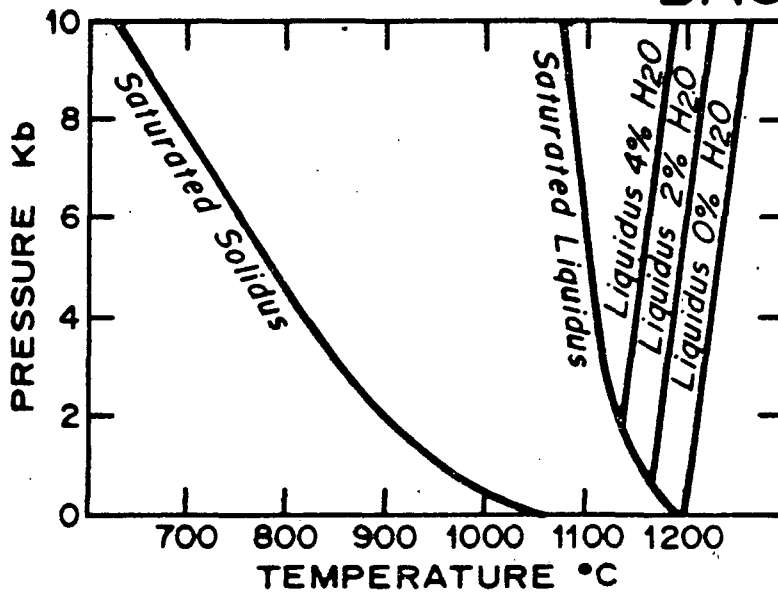
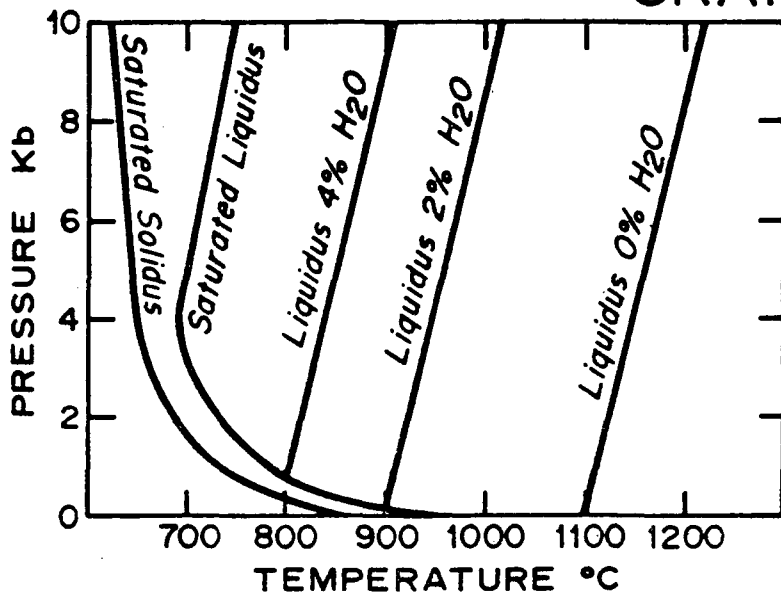


FIGURE 22.—SiO₂-variation diagrams for weight percent of major oxides of tuffs of the Topopah Spring Member, free of volatiles. Data are from table 2.

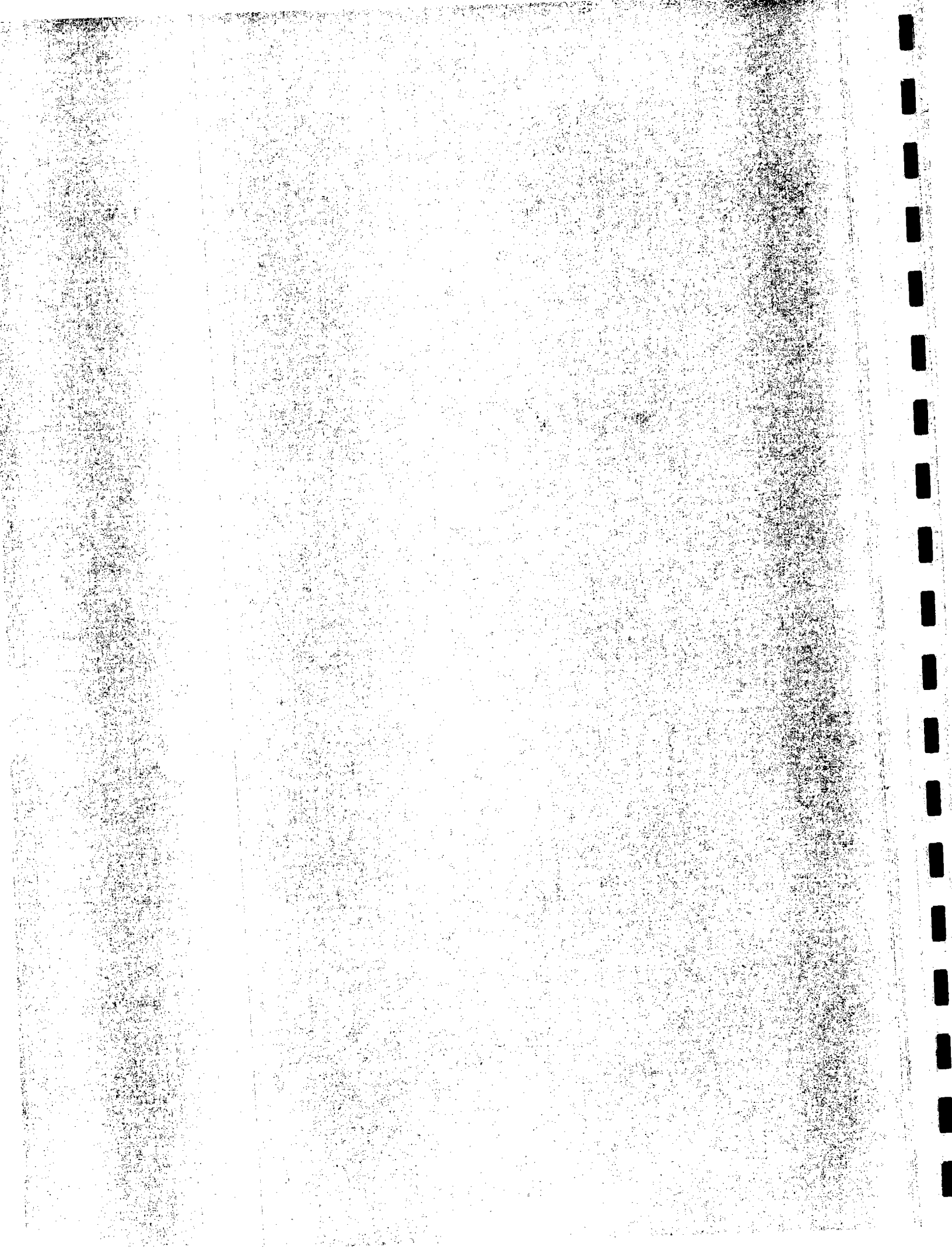
BASALT



GRANITE



from Harris, Kennedy and Scarfe (1970)

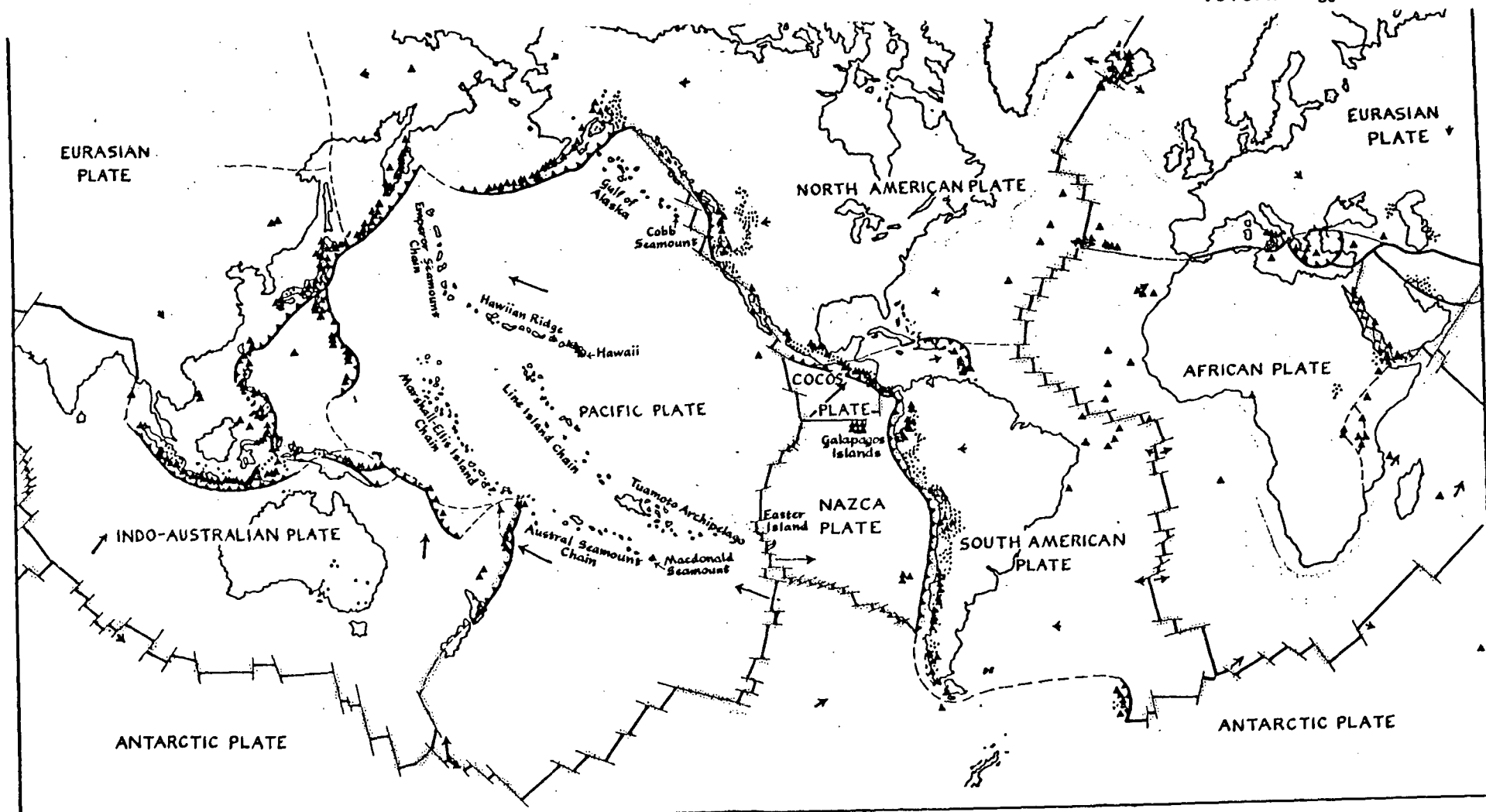


Tectonic Environments and Physical Spectrum of Volcanism

- A. Volcanic activity and plate boundaries
- B. Intraplate volcanism
- C. Classification of eruptive types

ACTIVE VOLCANOES OF THE WORLD

Williams and McBirney, 1979
Volcanology



-  Deep Oceans
-  Deep Earthquakes
-  Volcano
-  Spreading Axis
-  Continental Shelves
-  Shallow Earthquakes
-  Trench
-  Plate Motion

TABLE 10-1. Classification of volcanic eruptions

<i>Eruption type</i>	<i>Physical nature of the magma</i>	<i>Character of explosive activity</i>	<i>Nature of effusive activity</i>	<i>Nature of dominant ejecta</i>	<i>Structures built around vent</i>
Basaltic flood	Fluid	Very weak ejection of very fluid blebs; lava fountains	Voluminous wide-spreading flows of very fluid lava	Cow-dung bombs and spatter; very little ash	Spatter cones and ramparts; very broad flat lava cones; broad lava plain
Hawaiian	Fluid	Weak ejection of very fluid blebs; lava fountains	Thin, often extensive flows of fluid lava	Cow-dung bombs and spatter; very little ash	Spatter cones and ramparts; very broad flat lava cones
Strombolian	Moderately fluid	Weak to violent ejection of pasty fluid blebs	Thicker, less extensive flows of moderately fluid lava; flows may be absent	Spherical to fusiform bombs; cinder; small to large amounts of glassy ash	Cinder cones
Vulcanian	Viscous	Moderate to violent ejection of solid or very viscous hot fragments of new lava	Flows commonly absent; when present they are thick and stubby; ash flows rare	Essential, glassy to lithic, blocks and ash; pumice	Ash cones, block cones, block-and-ash cones
Peléean	Viscous	Like Vulcanian, commonly with glowing avalanches	Domes and/or short very thick flows; may be absent	Like Vulcanian	Ash and pumice cones; domes
Plinian (exceptionally strong Vulcanian)	Viscous	Paroxysmal ejection of large volumes of ash, with accompanying caldera collapse	Ash flows, small to very voluminous; may be absent	Glassy ash and pumice	Widespread pumice lapilli and ash beds; generally no cone building
Rhyolitic flood	Viscous	Relatively small amounts of ash projected upward into the atmosphere	Voluminous wide-spreading ash flows; single flows may have volume of tens of cubic miles	Glassy ash and pumice	Flat plain, or broad flat shield, often with caldera
Ultravulcanian	No magma	Weak to violent ejection of solid fragments of old rock	None	Accessory and accidental blocks and ash	Block cones; block-and-ash cones
Gas eruption	No magma	Continuous or rhythmic gas release at vent	None	None; or very minor amounts of ash	None
Fumarolic	No magma	Essentially nonexplosive weak to moderately strong long-continued gas discharge	None	None; or rarely very minor amounts of ash	Generally none; rarely very small ash cones

MacDonald, 1972

Tectonics and Volcanism

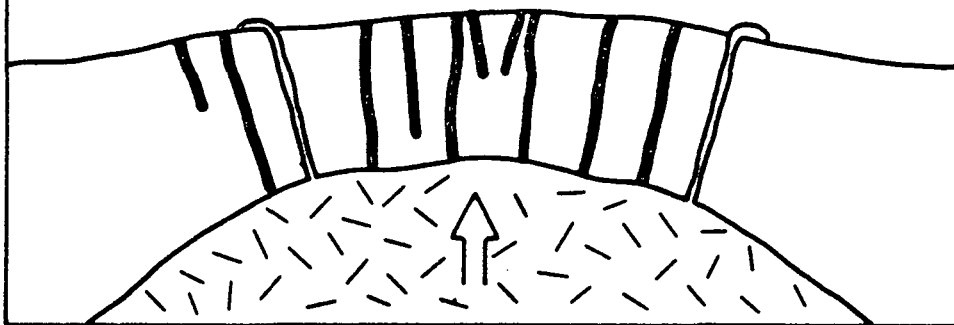
Bird, J.M., 1980, Plate Tectonics: American Geophysical Union, 986p

Carmichael, I.S.E., Turner, F.J., and John Verhoogen, 1974, Igneous Petrology: McGraw-Hill, p. 373-563

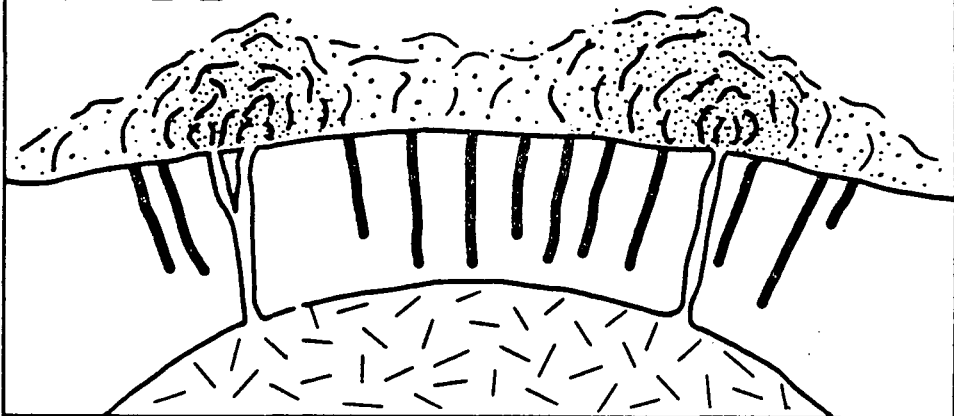
Williams, Howell, and A.R. McBirney, 1979, Volcanology: Freeman, Cooper & Co., San Francisco, 397p

CALDERA CYCLES

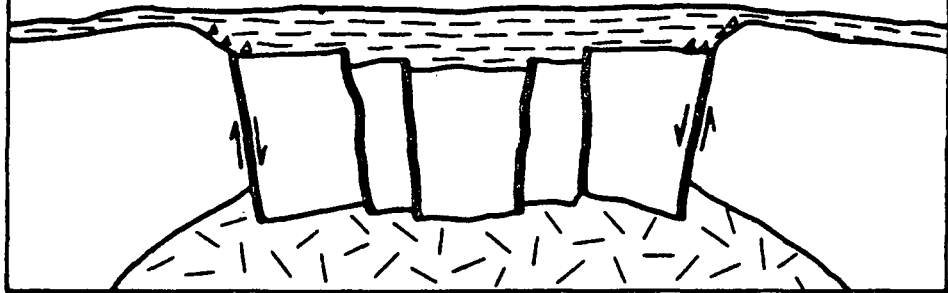
STAGE 1



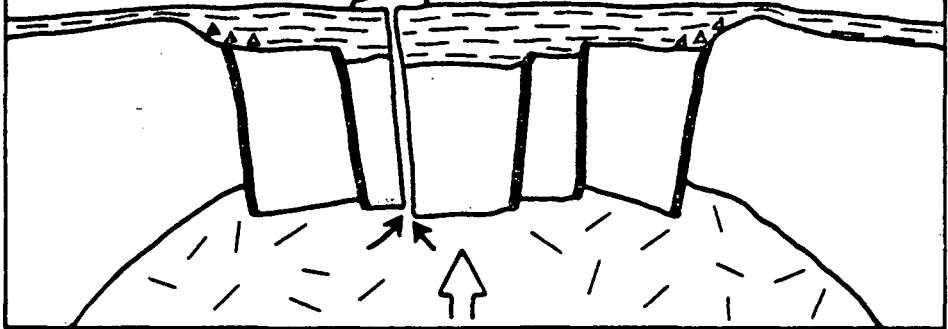
STAGE 2

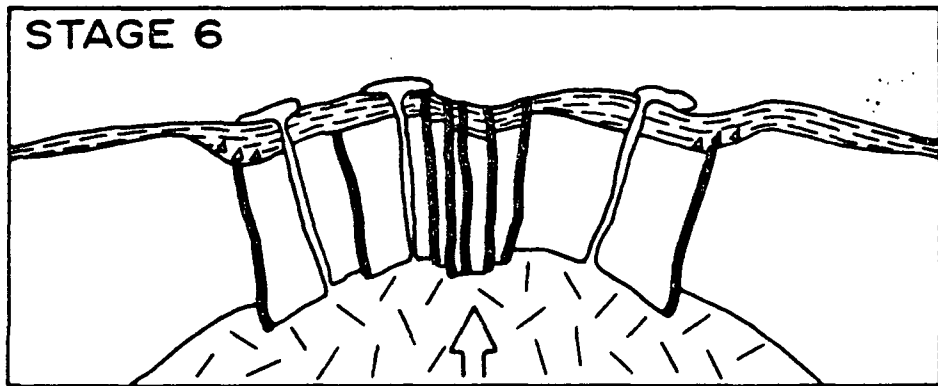
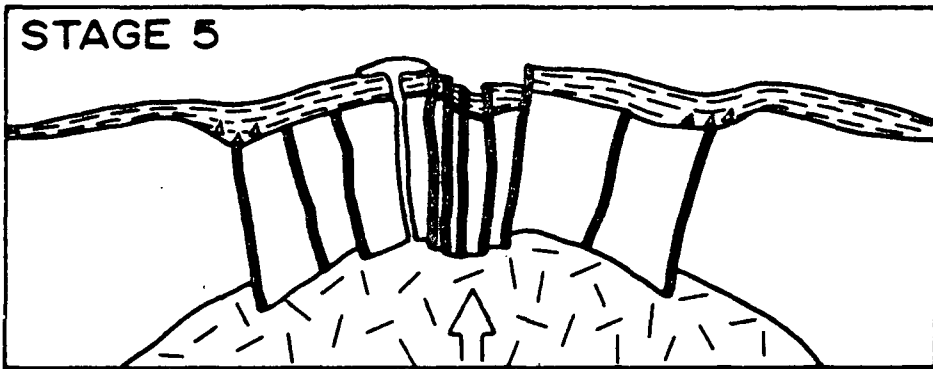


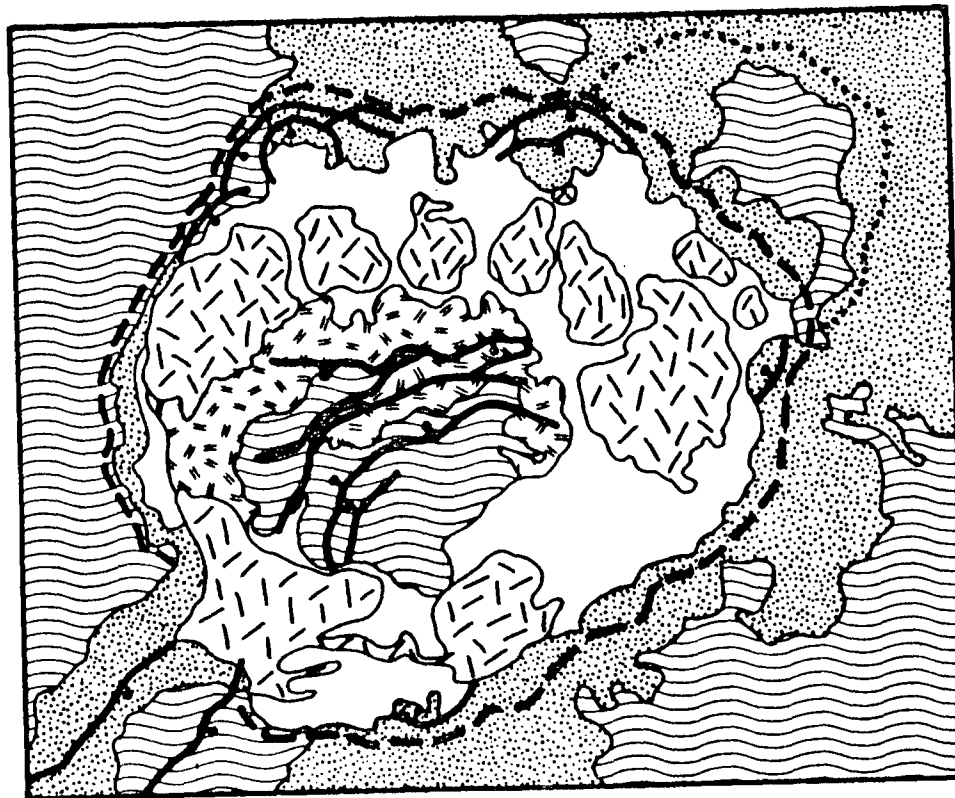
STAGE 3



STAGE 4

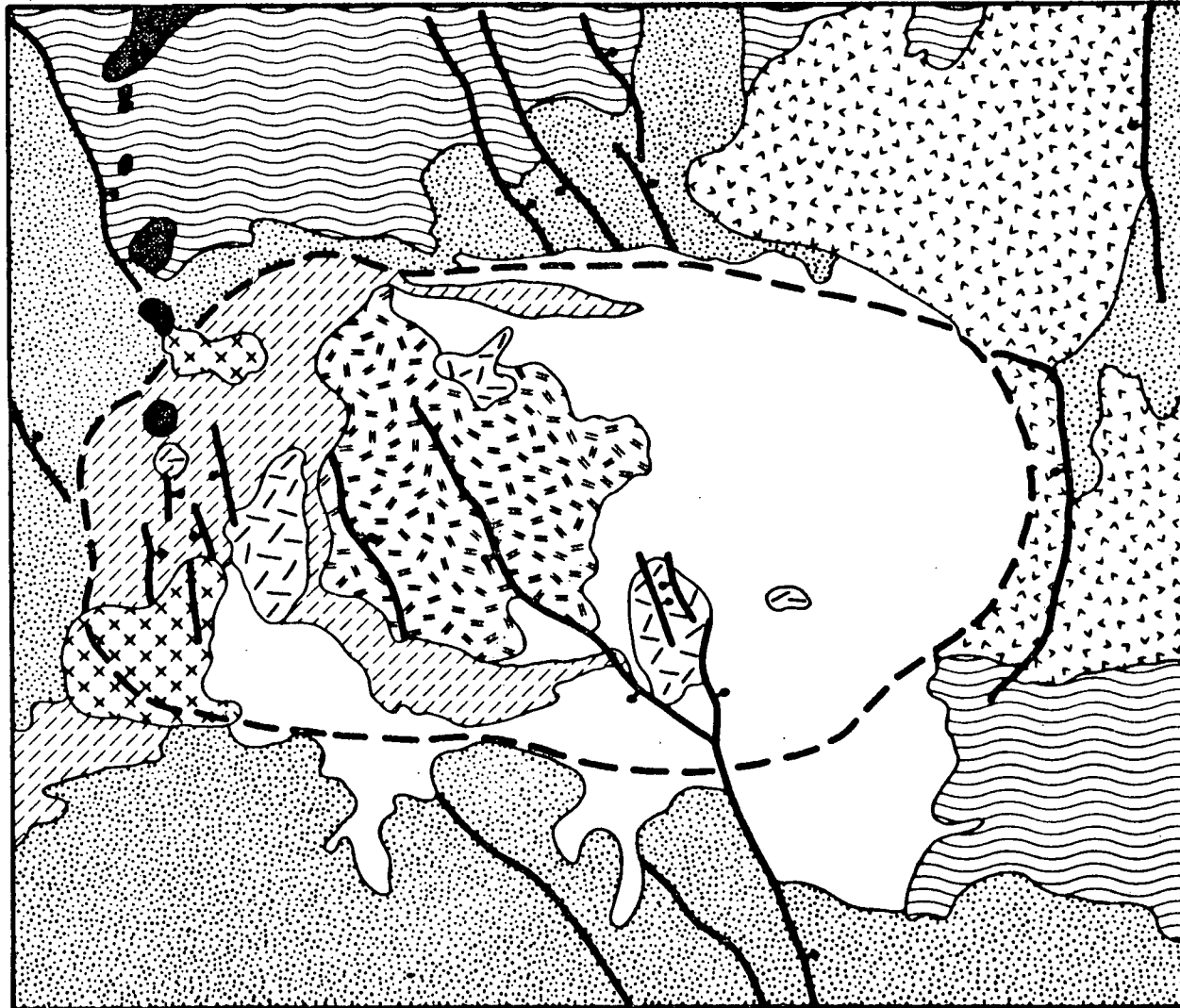






0 10 km

GENERALIZED GEOLOGIC MAP
of the
VALLES CALDERA
(from Smith & Bailey, 1968)



0 10 km

GENERALIZED GEOLOGIC MAP
of the
LONG VALLEY CALDERA, CALIFORNIA
(from Bailey & others, 1976)

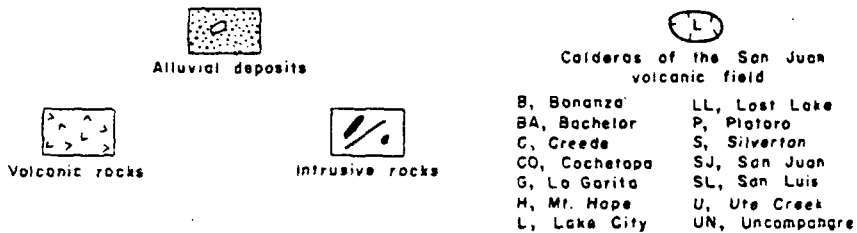
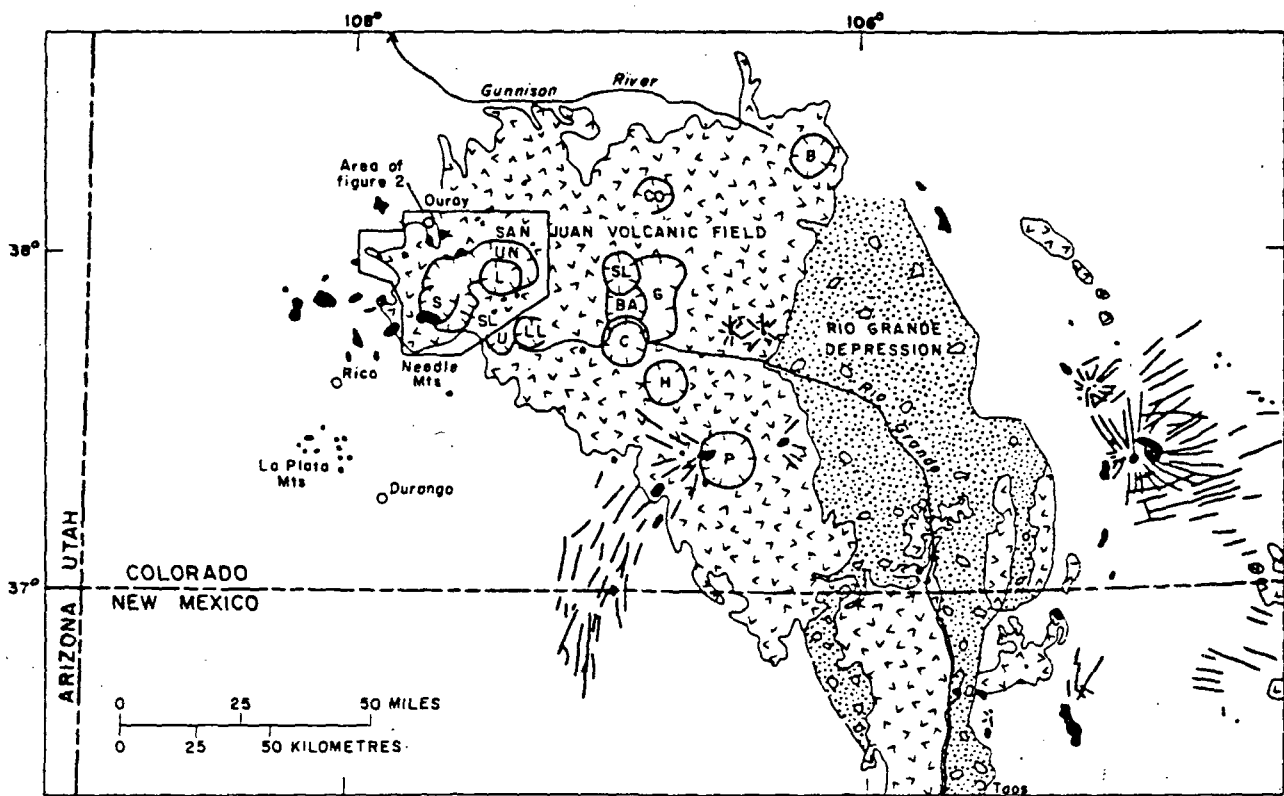
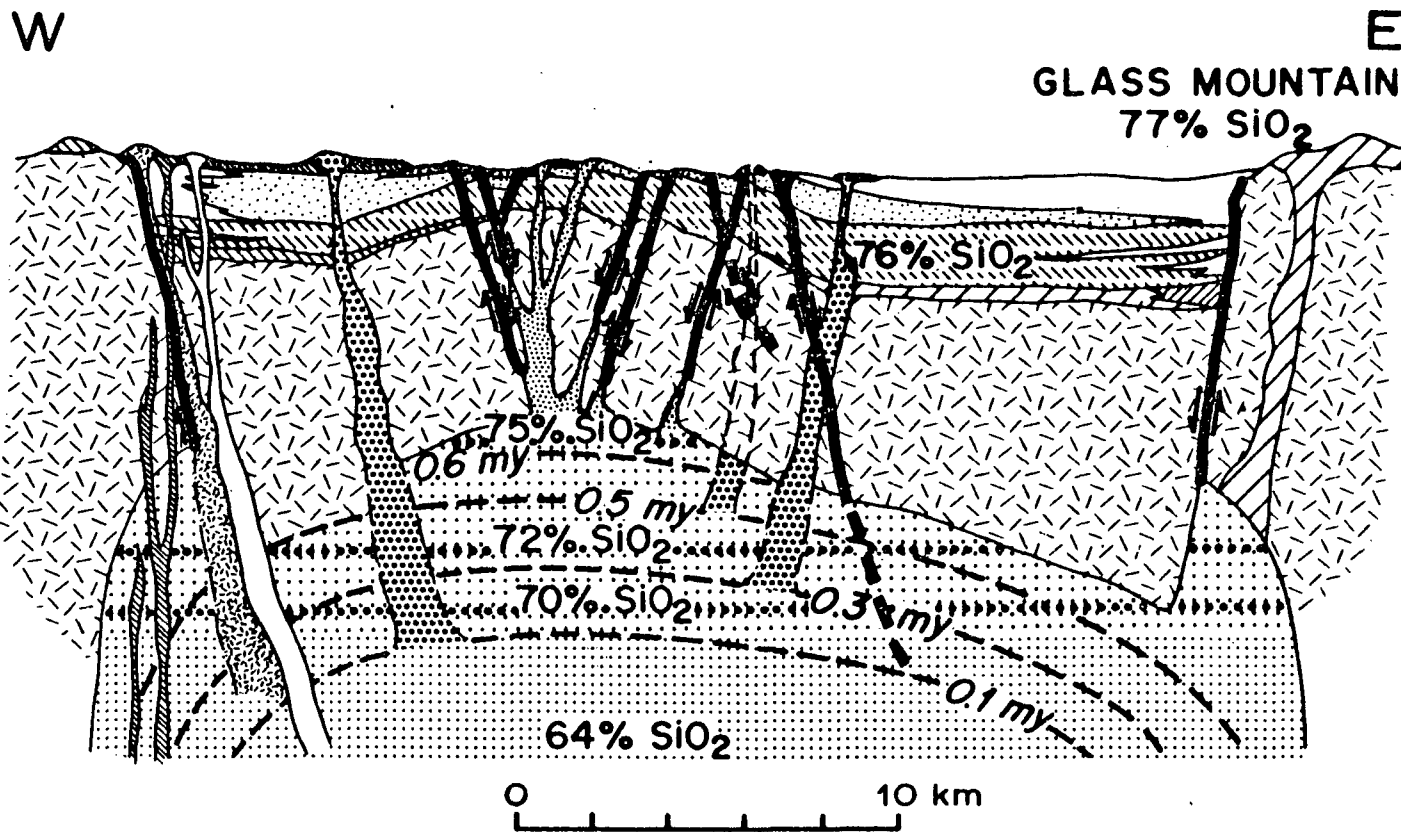


FIG. 1. Index map showing the San Juan volcanic field, the western San Juan caldera complex (illustrated in more detail in Fig. 2), and adjacent mineralized areas.

LIPMAN AND OTHERS, 1976



SCHMATIC CROSS-SECTION
of the
LONG VALLEY CALDERA, CALIFORNIA
(from Bailey & others, 1976)

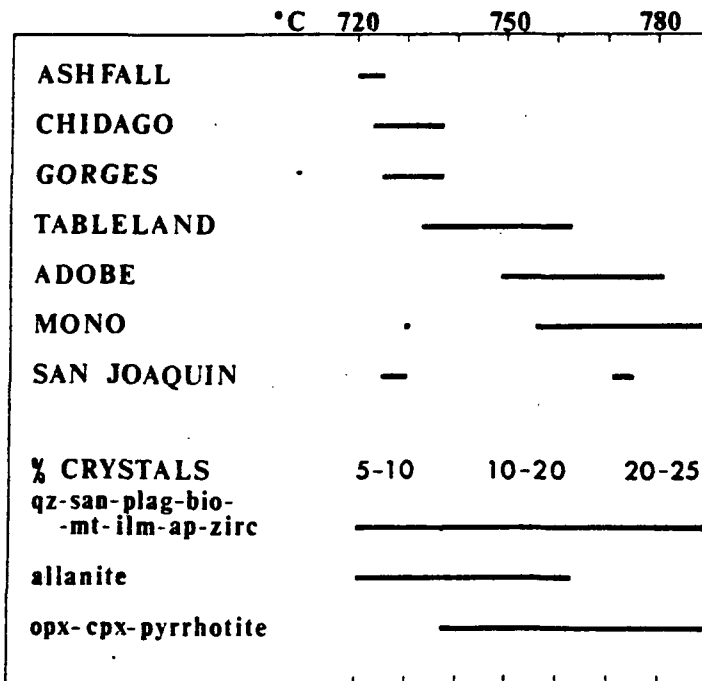


Figure 2. Phenocryst contents and ranges of Fe-Ti oxide temperature found for the several Bishop Tuff emplacement units. Two well-defined cooling units are conformably superimposed in the San Joaquin drainage. In the Mono Basin lobe the single low-temperature sample (B-75) is basal nonwelded pumice near the caldera margin.

Hildreth, 1979

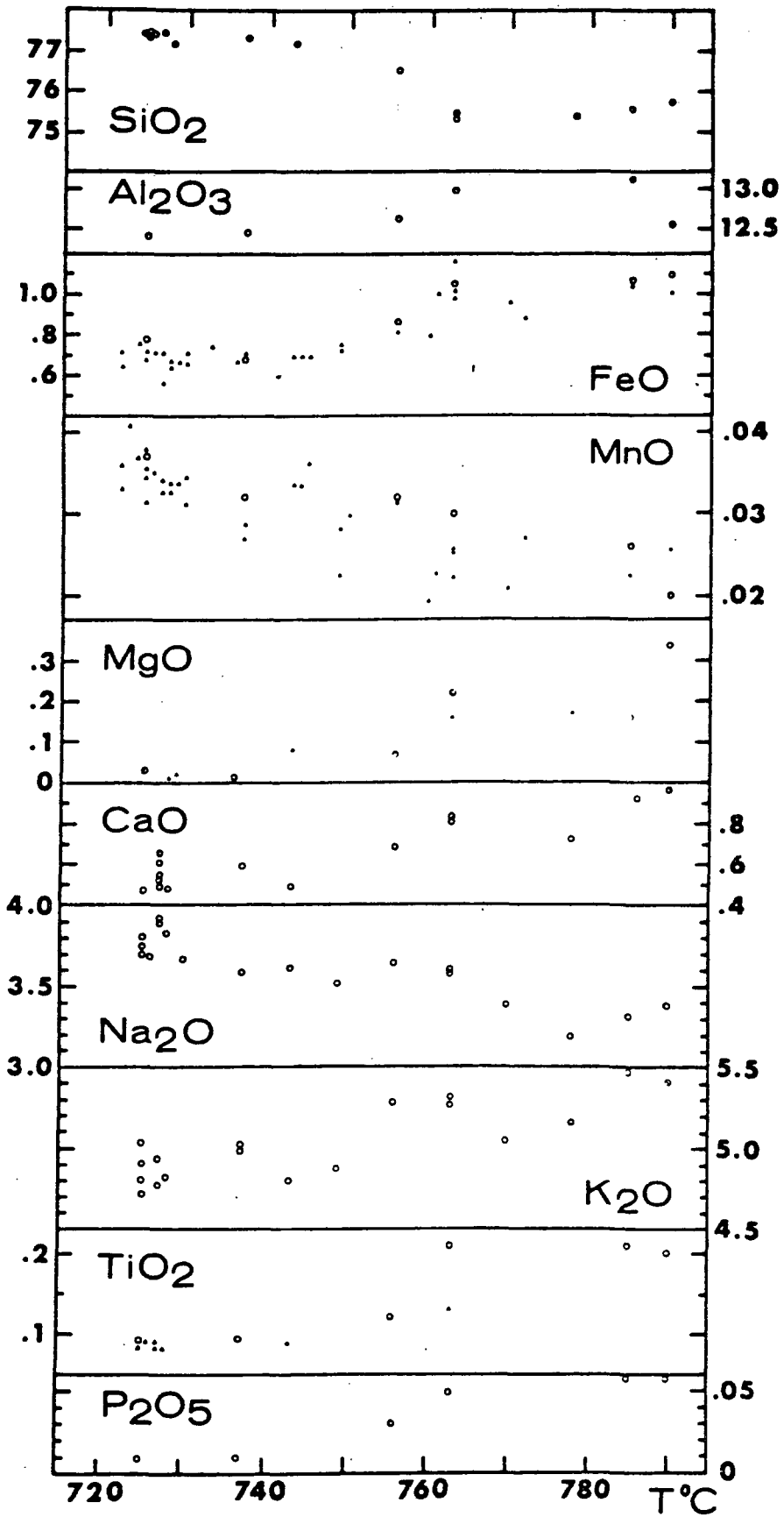


Figure 11. Whole-rock major-element variations with Fe-Ti oxide temperature. Open circles are wet chemical analyses by the methods of Carmichael (1970); filled symbols are INAA (Fe, Mn) or XRF (Mg, Ti) results.

THE BISHOP TUFF

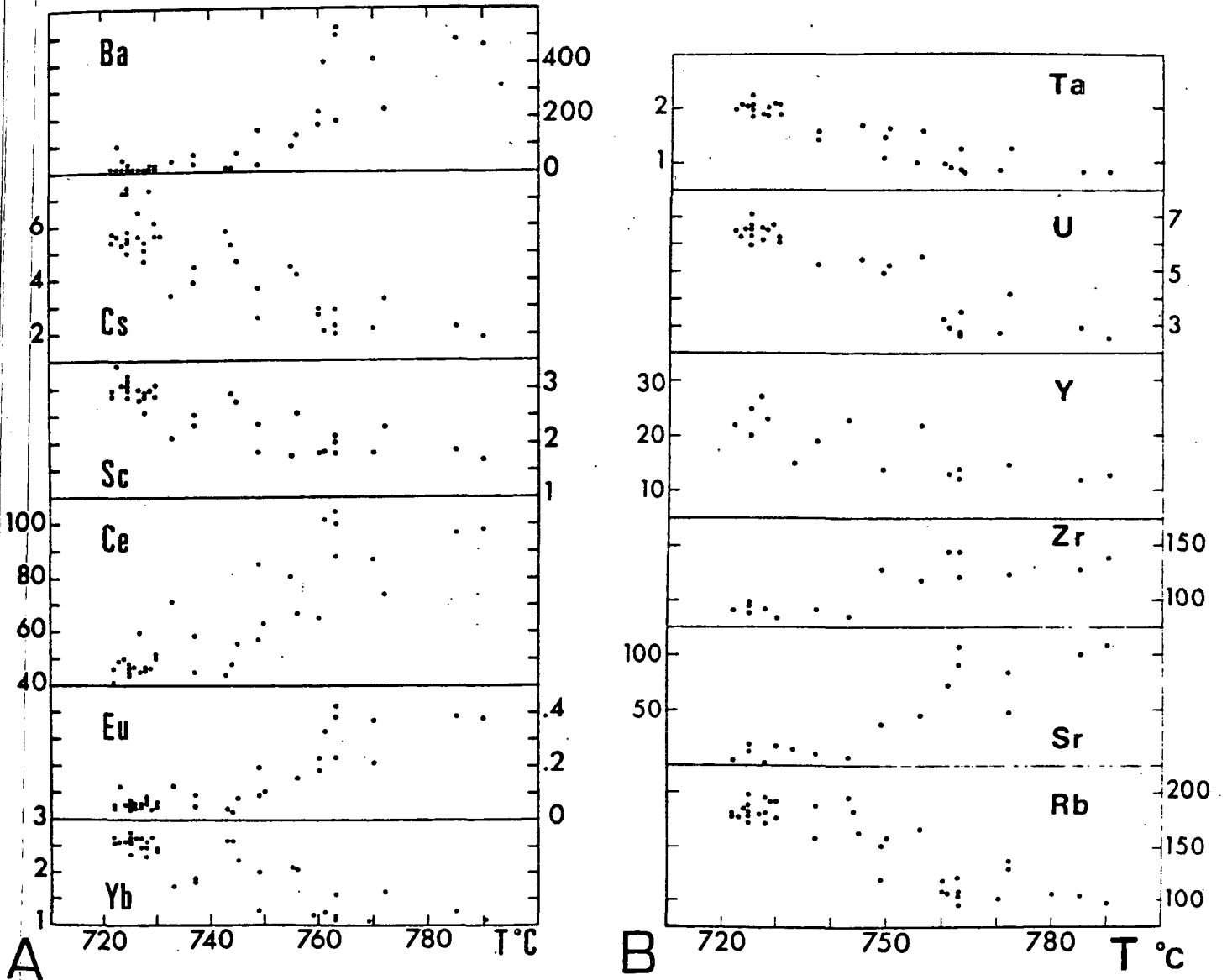


Figure 12. Variation of whole-rock trace-element contents with Fe-Ti oxide temperature. (A) Ba, Cs, Sc, Ce, Eu, and Yb. (B) Ta, U, Y, Zr, Sr, and Rb (INAA results, except Y, Zr, and Sr by XRF).

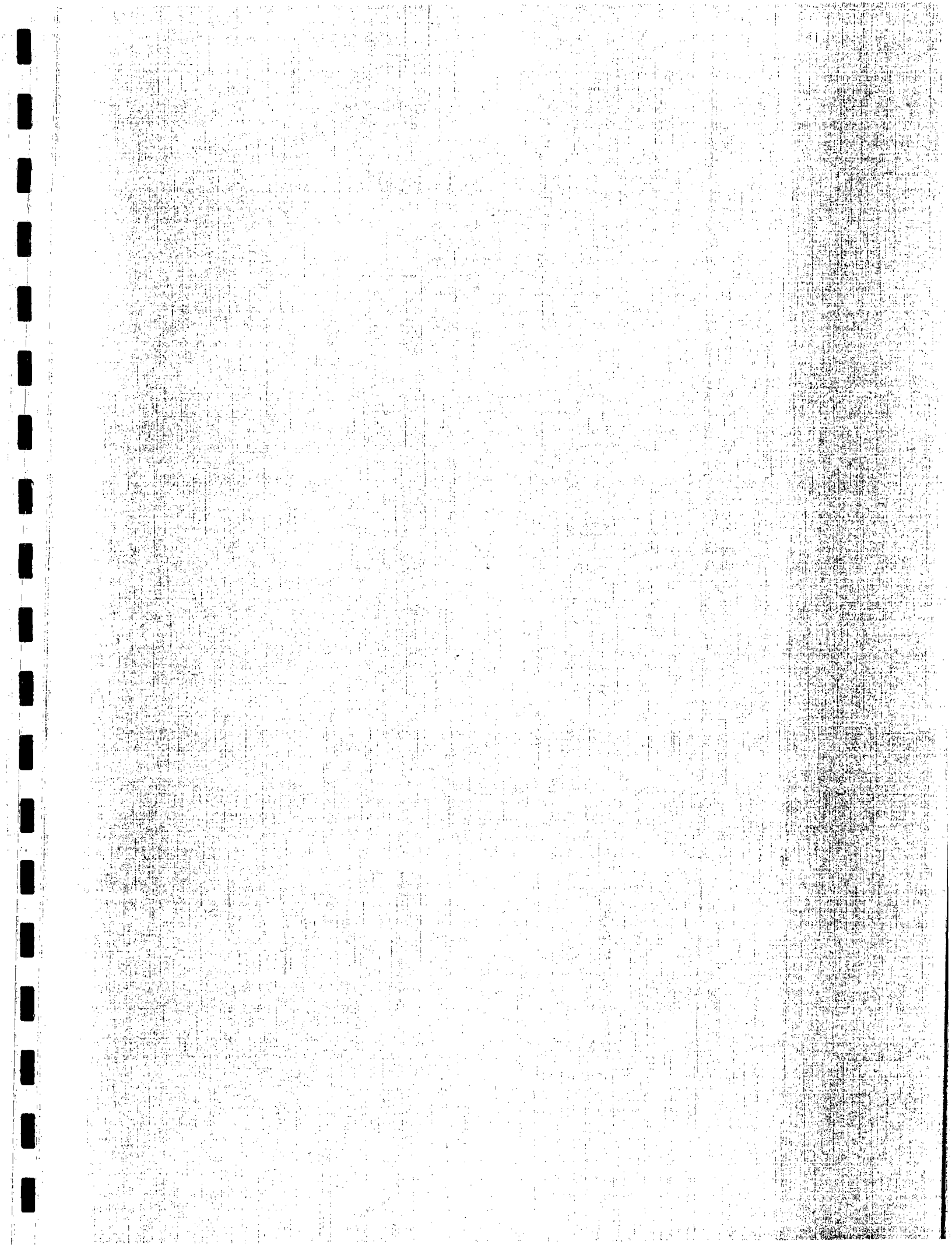
CALDERA CYCLES

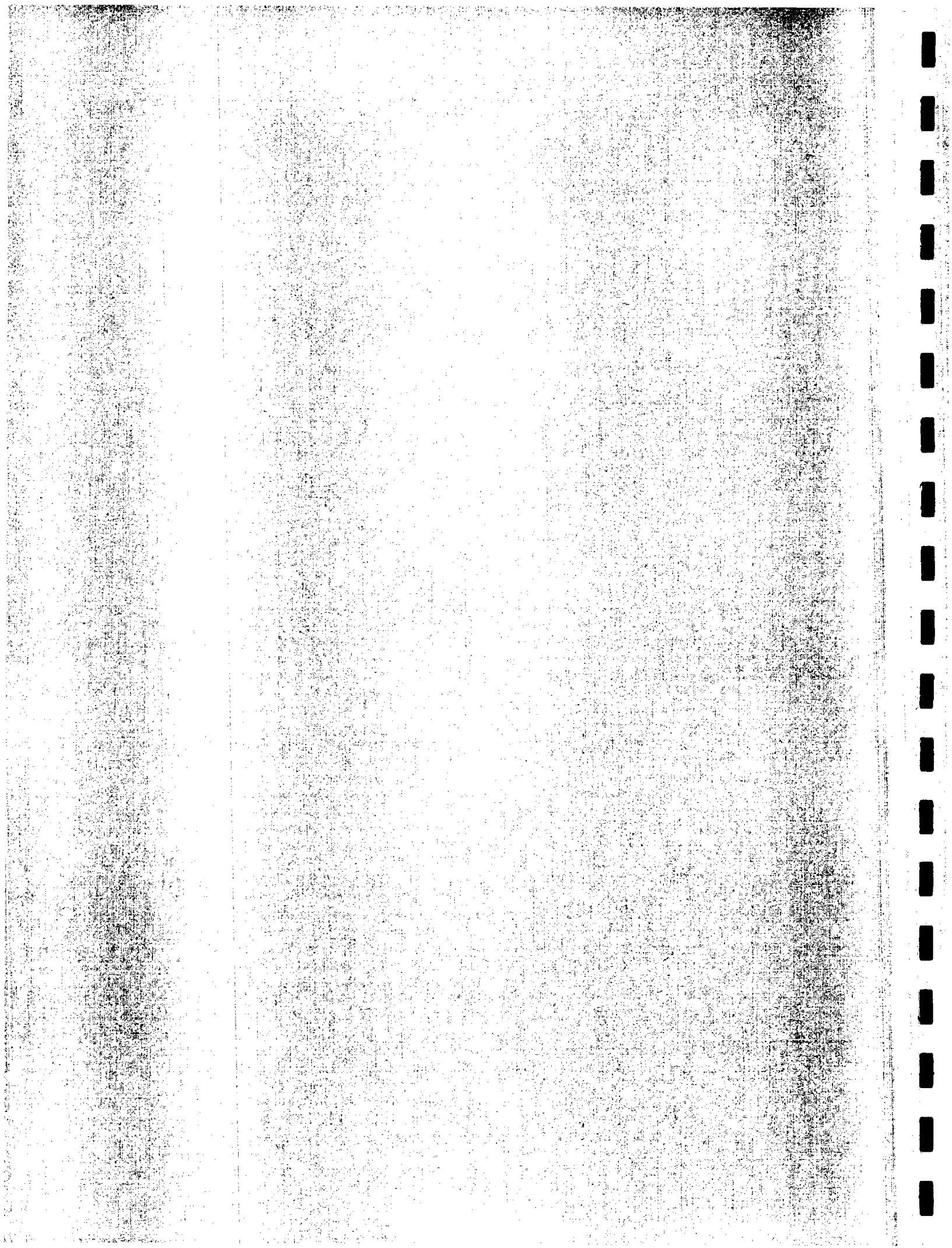
RÉFERENCES

- Anderson, A.T., 1976, Magma mixing: petrological process and volcanological tool: *Jour. Volcanol. Geoth. Res.*, v. 1, p. 3-33.
- Bailey, R.A., Dalrymple, G.B., and Lanphere, M.A., 1976, Volcanism, structure, and geochronology of Long Valley Caldera, Mono County, California: *Jour. Geophys. Res.*, v. 81, no. 5, p. 725-744.
- Blake, M.C., McKee, E.H., Marvin, R.F., Silberman, M.L., and Nolan, T.B., 1975, The Oligocene volcanic center at Eureka, Nevada: *Jour. Research U.S. Geol. Survey*, v. 3, p. 605-612.
- Bond, A. and Sparks, R.S.J., 1976, The Minoan eruption of Santorini, Greece: *Jour. Geol. Soc. London*, v. 132, p. 1-16.
- Boyd, F.R., 1961, Welded tuffs and flows in the Rhyolite Plateau of Yellowstone Park, Wyoming: *Geol. Soc. Amer. Bull.*, v. 72, p. 387-426.
- Carr, W. J. and Quinlivan, W.D., 1968, Structure of Timber Mountain resurgent dome, Nevada Test Site, in Eckel, E.B. (ed) Nevada Test Site: *Soc. America Mem.* 110, p. 99-108.
- Christiansen, R.L., 1979, Cooling units and composite sheets in relation to caldera structure, in Chapin, C.E. and Elston, W.E. (eds) Ash-flow tuffs: *Geol. Soc. Amer. Spec. Paper* 180, p. 29-42.
- Christiansen, R.L., Lipman, P.W., Carr, W.J., Byers, F.M., Orkild, P.P., and Sargent, K.A., 1977, Timber Mountain - Oasis Valley caldera complex of southern Nevada: *Geol. Soc. America Bull.*, v. 88, p. 943-959.
- Eaton, G.P., Christiansen, R.L., Iyer, H.M., Pitt, A.M., Mabey, D.R., Blank, H.R., Zietz, I., and Gettings, M.E., 1975, Magma beneath Yellowstone Park: *Science*, v. 188, p. 787-796.
- Eichelberger, J.C., 1975, Origin of andesite and dacite; evidence of mixing at Glass Mountain in California and at other circum - Pacific volcanoes: *Geol. Soc. Amer. Bull.*, v. 86, p. 1381-1391.
- Fenner, C.N., 1938, Contact relations between rhyolite and basalt on Gardiner River, Yellowstone Park: *Geol. Soc. Amer. Bull.*, v. 49, p. 1441-1484.
- Hildreth, W., 1979, The Bishop Tuff: evidence for the origin of compositional zonation in silicic magma chambers; in Chapin, C.E., and Elston, W.E. (eds), Ash-flow tuffs: *Geol. Soc. Amer. Spec. Paper* 180, p. 43-75.
- Hildreth, W., 1981, Gradients in silicic magma chambers: implications for lithospheric magmatism: *Jour. Geophys. Res.*, v. 86, p. 10153-10192.

- Huppert, H.E., Shepherd, J.B., Sigurdsson, H., and Sparks, R.S.J., 1982, On lava dome growth, with application to the 1979 lava extrusion of the Soufriere of St. Vincent: *Jour. Volcanol. Geoth. Res.*, v. 14, p. 199-222.
- Kohn, B.P. and Topping, W.W., 1978, Time-space relationships between late Quaternary rhyolitic and andesitic volcanism in the southern Taupo volcanic zone, New Zealand: *Geol. Soc. Amer. Bull.*, v. 89, p. 1265-1271.
- Lipman, P.W., 1966, Water pressures during differentiation and crystallization of some ash-flow magmas from southern Nevada: *Am. Jour. Sci.*, v. 264, p. 810-826.
- Lipman, P.W., 1971, Iron-titanium oxide phenocrysts in compositionally zoned ash-flow sheets from southern Nevada: *Jour. Geology*, v. 79, p. 438-456.
- Lipman, P.W. and Friedman, I., 1975, Interaction of meteoric water with magma: an oxygen-isotope study of ash-flow sheets from southern Nevada: *Geol. Soc. Amer. Bull.*, v. 86, p. 695-702.
- Lipman, P.W., Steven, T.A., Luedke, R.G. and Burbank, W.S., 1973, Revised volcanic history of the San Juan, Uncompahgre, Silverton, and Lake City calderas in the western San Juan Mountain, Colorado: *Jour. Res. U.S. Geol. Survey*, v. 1, p. 627-642.
- Michael, P.J., 1983, Chemical differentiation of the Bishop Tuff and other high-silica magmas through the crystallization process: *Geology*, v. 11, p. 31-34.
- Myers, J.S., 1975, Cauldron subsidence and fluidization mechanisms of intrusion of the coastal batholith of Peru into its own volcanic ejection: *Geol. Soc. Amer. Bull.*, v. 86, p. 1209-1220.
- Ofledahl, C., 1978, Cauldrons of the Permian Oslo Rift: *Jour. Volcanol. Geoth. Res.*, v. 3, p. 343-371.
- Ritchey, J.L., 1980, Divergent magmas at Crater Laker, Oregon: Products of fractional crystallization and vertical zoning in a shallow, water-undersaturated chamber: *Jour. Volcanol. Geoth. Res.*, v. 7, p. 373-386.
- Robinson, P.T., Elders, W.A., and Muffler, L.J.P., 1976, Quaternary volcanism in the Salton Sea geothermal field, Imperial Valley, California: *Geol. Soc. Amer. Bull.*, v. 87, p. 347-360.
- Smith, R.L., 1960, Ash flows: *Geol. Soc. America Bull.*, v. 71, p. 795-842.
- Smith, R.L., 1979, Ash-flow magmatism, in Chapin, C.E., and Elston, W.E., (eds) *Ash-flow tuffs*: *Geol. Soc. Amer. Special Paper 180*, p. 5-27.
- Smith, R.L. and Bailey, R.A., 1966, The Bandelier Tuff: a study of ash flow eruption cycles from zoned magma chambers: *Bull. Volcanol.*, v. 29, p. 83-103.

- Smith, R.L. and Bailey, R.A., 1968, Resurgent cauldrons: Geol. Soc. America Mem. 116, p. 613-662.
- Smith, R.L., Bailey, R.A., and Ross, C.S., 1970, Geologic map of the Jemez Mountains, New Mexico: U.S. Geol. Survey Misc. Invest. Map I-571.
- Spera, F.J. and Crisp, J.A., 1981, Eruption volume, periodicity, and caldera area: relationships and inferences on development of compositional zonation in silicic magma chambers: Jour. Volcanol. Geoth. Res., v. 11, p. 169-187.
- Williams, H., 1941, Calderas and their origin: Univ. Calif. Berkeley Pub. Geol. Sci., v. 25, p. 239-346.
- Wohletz, K.H. and Sheridan, M.F., 1983, Hydrovolcanic explosions II. Evolution of basaltic tuff rings and tuff cores: Am. Jour. Science: v. 283, p. 385-413.
- Yoder, H.S., 1973, Contemporaneous basaltic and rhyolite magmas: Am. Mineral., v. 58, p. 153-171.





An Introduction to Ash-Flow Tuffs and Their Relatives

I. Introduction

- A. terminology
- B. historical aspects of study

II. Eruption Column Dynamics

- A. eruptive type
 - 1. Plinian
 - 2. Pelean
- B. constituents
 - 1. magma
 - a) crystals
 - b) pumice and vitric materials
 - 2. gasses
 - a) water
 - b) others
 - 3. accidental fragments
 - a) lithic fragments
 - b) crystals
- C. flow regime
 - 1. higher velocity, larger particles, lower shear gradients toward center of pipe
 - 2. 2 part eruption column
 - 3. collapse

III. Depositional Mechanism

- A. fall
 - 1. characteristics
 - 2. distribution
- B. surge
 - 1. introduction
 - 2. deposits
 - 3. facies and bedding
- C. flow
 - 1. eruptive sequence
 - 2. composition
 - 3. deposition
 - a) components
 - b) sequence

IV. Cooling and Compaction

- A. thermal regime
 - 1. heat retention
 - 2. heat loss

- B. cooling unit concept
- C. welding
 - 1. thermal and pressure dependent process
 - 2. zonation superimposed on original stratigraphy
- D. secondary flowage
- E. post-emplacement mineralogical changes
 - 1. devitrification
 - 2. vapor phase crystallization
 - 3. granophyric alteration
 - 4. fumarolic alteration

- V. Field Characteristics
 - A. distinguishing air-falls from ash-flows
 - B. characteristics of rhyolite flows
 - C. vent identification

ASH-FLOW TUFFS

HISTORICAL DEVELOPMENT OF CONCEPTS

UNUSUAL ROCKS NOTED IN WESTERN U.S.
CANARY ISLANDS
ITALY

MT. PELEE, 1902, "NUEE ARDENTE" - ALSO 1929-1932

IDDINGS IN YELLOWSTONE - 1899

BISHOP TUFF - 1938

"NEW" CLASSIC PAPERS

SMITH, 1960A,B

ROSS AND SMITH, 1961

INTEGRATED MACROSCOPIC AND MICROSCOPIC FEATURES
IDENTIFIED NATURE OF VOLCANIC PROCESSES

ERUPTION TYPES

PLINIAN - EXCEPTIONALLY POWERFUL CONTINUOUS GAS BLAST
MUCH PUMICE
VESUVIUS, 79AD (PLINY THE ELDER)
KRAKATOA, 1883

PELEAN - DOMES AND GLOWING AVALANCHES
LESS AIRFALL THAN PLINIAN
MT. PELEE, 1902
SANTIAGUITO, GUATEMALA

CONTENTS OF ERUPTION

FROM MAGMA

CRYSTALS

PUMICE

ASH

GASSES

FROM VENT

LITHIC FRAGMENTS

XENOCRYSTS

FROM ENVIRONMENT

LITHIC FRAGMENTS

WATER

AIR

FLOW REGIME IN VENT AND CLOUD DYNAMICS

INTENSITY OF ERUPTION - PRESSURE OF GAS PHASE
VISCOSITY OF LIQUIDS

DRIVEN BY VESICULATION

2 PART ERUPTION COLUMN

LOWER GAS THRUST

1.5 - 4 KM MAX

UPPER CONVECTIVE THRUST

CONTROLLED BY DENSITY OF COLUMN (BUOYANCY)

SOLID/GAS RATIO & DENSITY

FALLOUT OF CLASTS, RISE OF FINES

ENTRAPMENT AND HEATING OF AIR (4 X WEIGHT)

ERUPTIVE COLUMN COLLAPSE

DENSITY EXCEEDS SURROUNDING ATMOSPHERE

REDUCTION IN VOLATILES - INCREASE IN PARTICLES

ADMIXING AIR REDUCED - COLUMN WARMER

COLLAPSE - INITIAL TURBULENT FLOW

SEPARATION - ASH TO CLOUD

LITHICS AND CRYSTALS TO FLOW

LOWER DENSE FLOW CONTINUES TO GIVE OFF ASH

LOWER GAS CONTENT OF ERUPTION -

LOWER COLUMN HEIGHT

MORE THERMAL RETENTION

HOTTER EMPLACEMENT TEMPERATURE OF UNITS

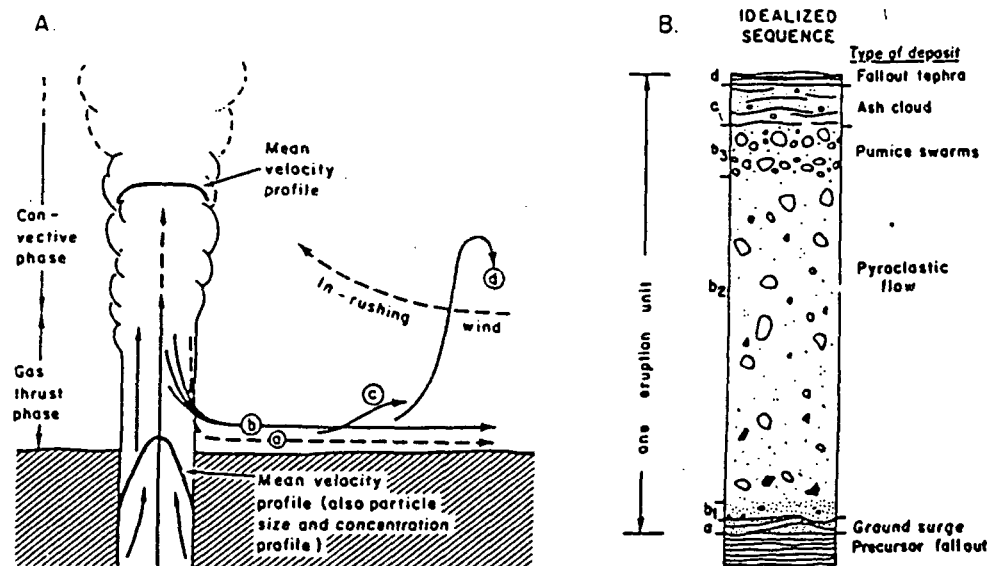


Fig. 8. Eruption column collapse related to idealized eruption unit. Letters a-d in Fig. 8A correspond to those in Fig. 8B. A. Outer part of column collapses to form a pyroclastic surge (a); followed by (b) progressive collapse of interior parts to give voluminous, high-concentration pyroclastic flow. Pyroclastic material segregates from surface of flow (dilute phase) to form an ash cloud (c). Finest-grained material continues to be elutriated into atmosphere from dilute phase flow (d). It falls back on flow deposits or is swept back to join main eruption column by inward rushing atmospheric winds. B. Idealized depositional sequence of one eruption unit showing ground surge deposit (a), fine-grained basal layer of pyroclastic flow developed by flowage processes (b_1), main body of the pyroclastic flow representing the main bulk of the collapsed eruption column (b_2), a zone of pumice swarms segregated at the top of the ash flow (b_3), an ash cloud deposit elutriated from the top of the moving pyroclastic flow (c) and a thin fallout deposit (d).

Fisher, 1979

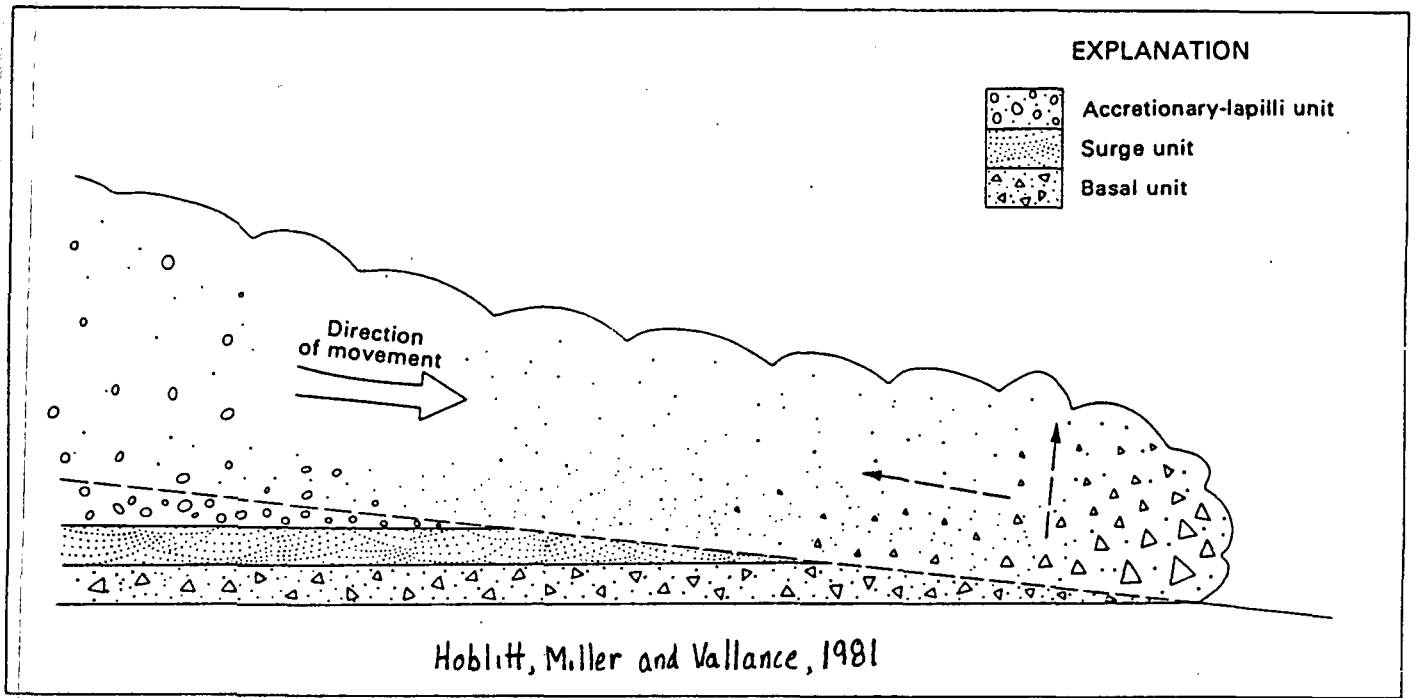


Figure 243.—Diagrammatic model showing deposition of basal, surge, and accretionary-lapilli units from blast cloud. Particle size and concentration decrease upward and backward (dashed arrows) in the cloud.

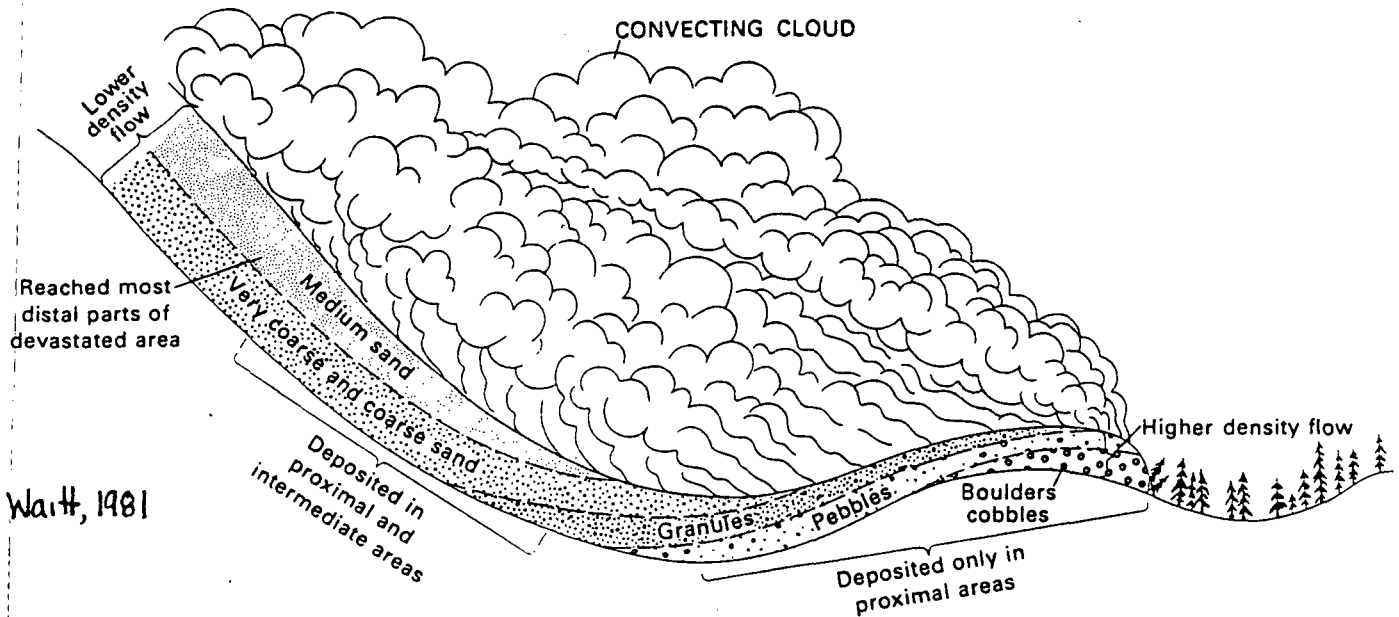


Figure 270.—Schematic diagram of pyroclastic density flow sweeping through proximal area, showing inferred maximum particle size and relative density within flow.

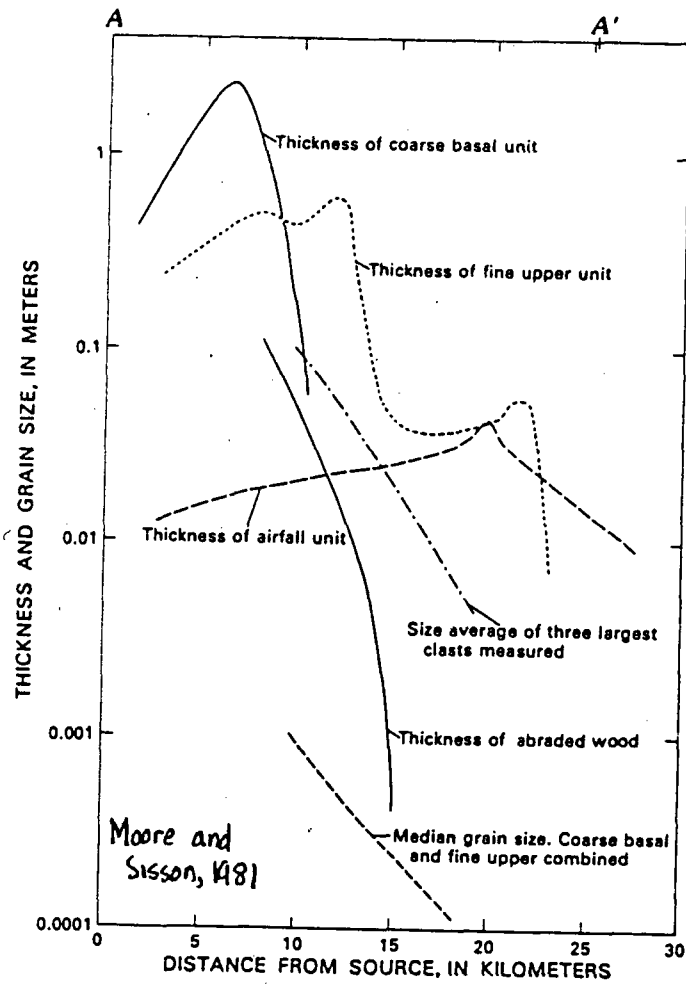


Figure 248.—Change in characteristics of the pyroclastic surge deposits as a function of distance from the source as measured on line A-A' (shown in fig. 244).

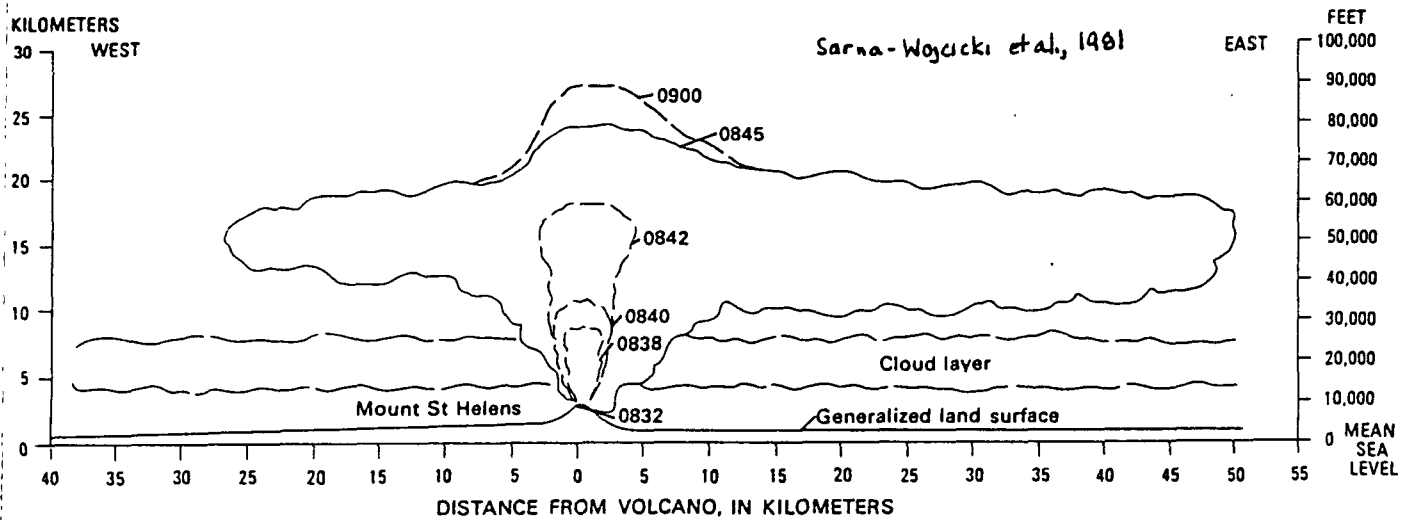


Figure 331.—Diagrammatic east-west profile showing early vertical growth and lateral expansion of plume from the May 18 eruption. Altitudes between 0838 and 0842 are from Rosenbaum and Waitt (this volume) and those between 0845 and 0900 are from Carl Rice (oral commun., 1980). Horizontal extent for 0845 is from NOAA satellite photograph taken at 0845 PDT, sector KB7.

DEPOSITION AS FALL

MANTLE TOPOGRAPHY

LAYERING - THIN TO THICK

MAY BE DISCONTINUOUS

SEEN IN GRAIN SIZE

LITHIC RICH ZONES

COARSE PUMICE

CONCENTRATION OF FINE-GRAINED MATERIALS

VITRICS

WIDE DISPERSAL

MAY CONTAIN 50% OF VOLUME OF ERUPTION

SURGES

RECOGNIZED FROM NUCLEAR STUDIES

PYROCLASTIC SURGE - TIME-TRANSIENT, UNSTEADY
FLOW OF TEPHRA

COMPOSED OF JUVENILE, ACCESSORY, ACCIDENTAL
COMPONENTS

THIN CONTINUOUS BEDS

LOW ANGLE CROSS BEDDING

PLANAR

MASSIVE

MODEL - FLUIDIZED CLOUD

COLLAPSE

NEAR VENT SALTATION

DEFLATION WITH GAS LOSS

LOSS OF FLUIDIZATION

SURGE DEPOSITS

SANDWAVES - UNDULATING SURFACE(S) OVER UNDERLYING SURFACE

DUNES

RIPPLES

CROSS BEDDING

CLOSEST TO VENT

DEPOSITION FROM SALTATION

MASSIVE - LOOK LIKE SMALL ASH-FLOW TUFFS

UNSTRATIFIED

UNGRADED

DEFLATING SURGE

OCCUR BOTH CLOSE TO AND DISTANT FROM VENT

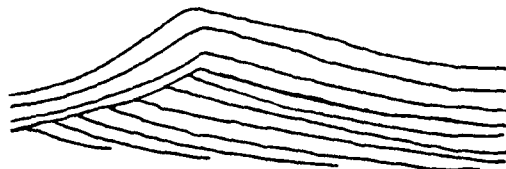
PLANAR - INVERSELY GRADED BEDDING

MOST DISTANT FROM VENT

Direction of Transport →



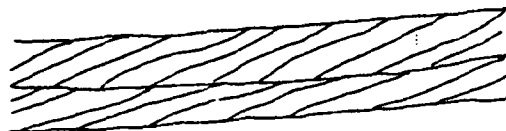
Gently sloped wave of generally long wavelength, low amplitude often grading laterally into planar beds, and found as faint laminations in fine-grained massive beds.



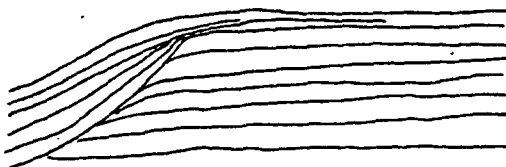
Relatively symmetrical antidune shape, built up on the stoss side, elongated on the lee side, and containing marked inner unconformities.



Festooned dunes; direction of transport is perpendicular to the plane of the paper.



Cross laminations occurring in bedding sets 2 to 8 cm thick.



Chute and pool structure of Schmincke and others (1973) with coarse-grained, steeply dipping stoss side.



Symmetrical dunes with lee side accumulations of coarse material.



Antidunes with rounded crest and internal unconformities.



Sinusoidal ripple-drift laminations of short wavelength.

Figure 3. Morphologies of sandwaves viewed in cross section. Variation of these types occur commonly in deposits of pyroclastic surge.

Wohletz and Sheridan, 1979

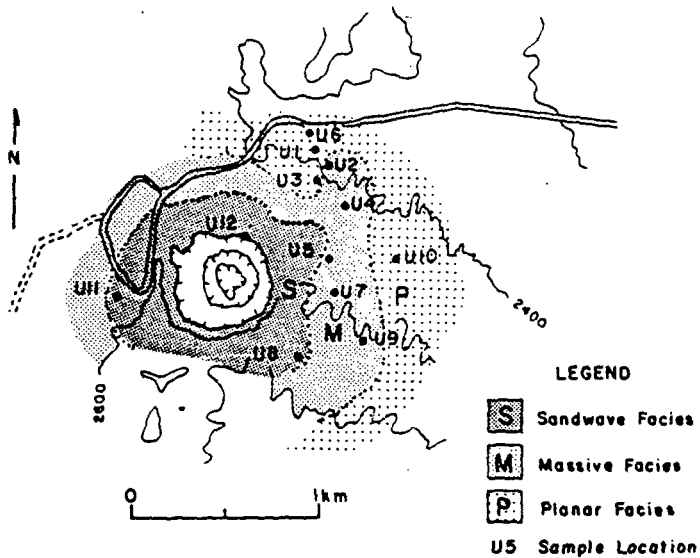
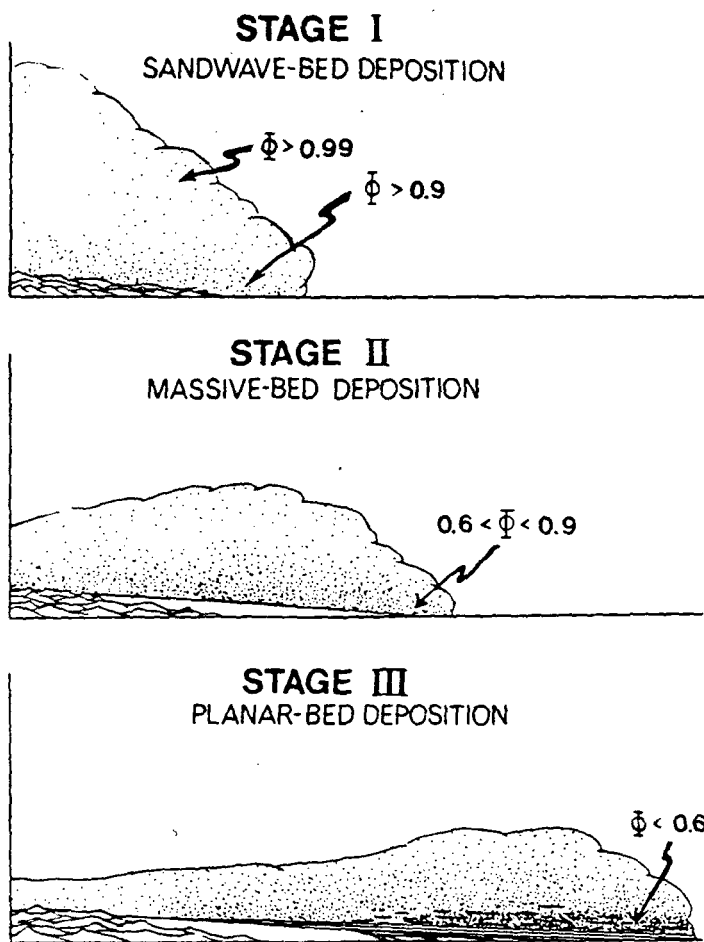


Figure 14. Pyroclastic-surge facies map of Ubehebe Crater.



Wohletz and
Sheridan, 1979

Figure 18. Diagrammatic illustration of a surge cloud at three stages of its development: Stage I near the vent, Stage II at intermediate distances from the vent, and Stage III near the terminus of its flow. During Stage I, flow is highly inflated ($\Phi > 0.9$), and deposition of sandwave beds results. At Stage II the cloud has deflated ($0.6 < \Phi < 0.9$), with massive bed deposition resulting. Finally, at Stage III, the cloud has deflated until it is an avalanching-type flow ($0.5 < \Phi < 0.6$), planar beds are deposited, and the flow stops.

Flows

ASH FLOW TUFFS DOMINATE

TYPICAL SEQUENCE:

- 1) BASAL BLAST
- 2) DEPOSITS FROM AVALANCHE
- 3) DEPOSITS FROM CLOUD

GREAT MOBILITY

FOLLOW TOPOGRAPHY

MAY CLIMB BARRIES (700 M AT 50 KM!)

MOVE RAPIDLY

COMPOSITION

PRIMARYLY RHYOLITIC

PERALKALINE

DACITE

ANDESITE

} NOT AS COMMON

ASH FLOW TUFFS

COMPONENTS - GAS - FLUIDIZATION

CRYSTALS

ASH

LITHIC FRAGMENTS

PUMICE

BOMBS

FLOW-BASAL LAYER

CM TO > 1 M THICK

REVERSE GRADING OF PUMICE AND \pm LITHICS

LARGER LITHICS ABSENT

FINER GRAINED THAN OVERLYING MATERIALS

MAIN BODY

90% FLOW BULK

POORLY SORTED

LITHICS MORE CONCENTRATED AT BASE
(NORMAL GRADING)

LARGER PUMICE RISE TOWARD TOP
(REVERSE GRADING)

OVERLYING ASH

ENRICHED IN VITRIC MATERIALS (10x)

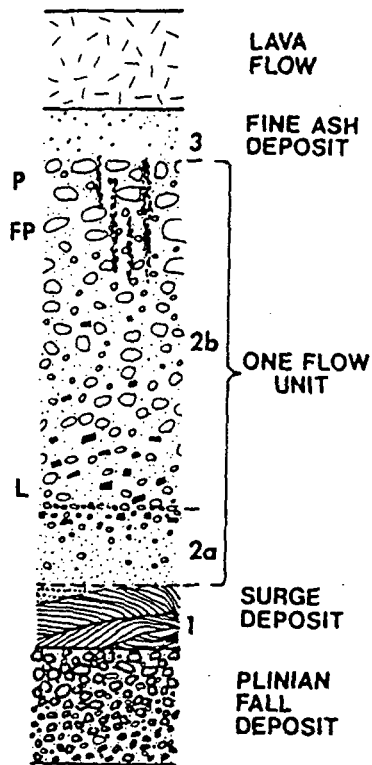


Figure 3. Schematic diagram showing the textural elements of a complete eruption episode. An inversely graded Plinian fall bed is overlain by a surge of deposit of (1) sand-wave, massive, or planar facies (Wohletz and Sheridan, this volume). The basal layer of the pyroclastic flow (2a) may show inverse grading, whereas the main part of the flow (2b) has double-grading. Lithic inclusions (L) are concentrated near the base, and pumice fragments (P) are concentrated toward the top. Fumarolic pipes (FP) may be present throughout the flow. Deposits of fine ash (3) from the cloud would occur above the flow unit. A lava flow might cap the sequence. Modified after Sparks and others (1973).

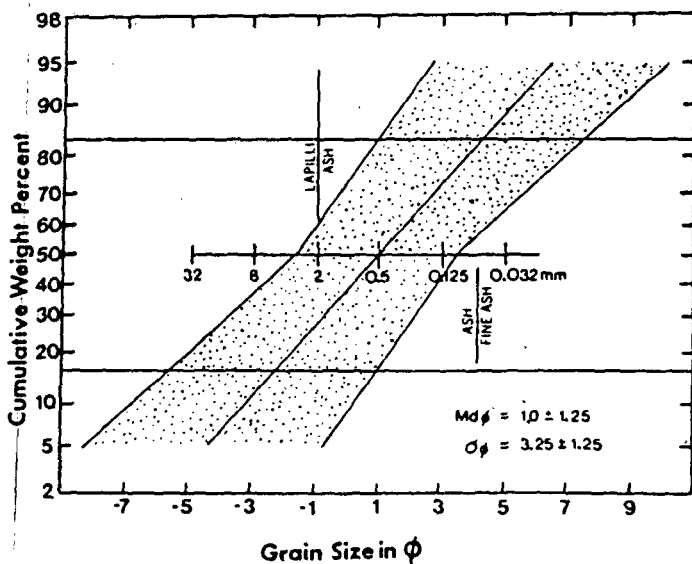


Figure 4. Range of particle sizes for pyroclastic flows. Average analysis is plotted, and two standard deviations are shown by stippled pattern. Data taken from Sparks (1976). Most pyroclastic flows are more than 50% (by weight) particles less than 2 mm and hence would be termed ash flows following Smith (1960a).

Sheridan, 1979

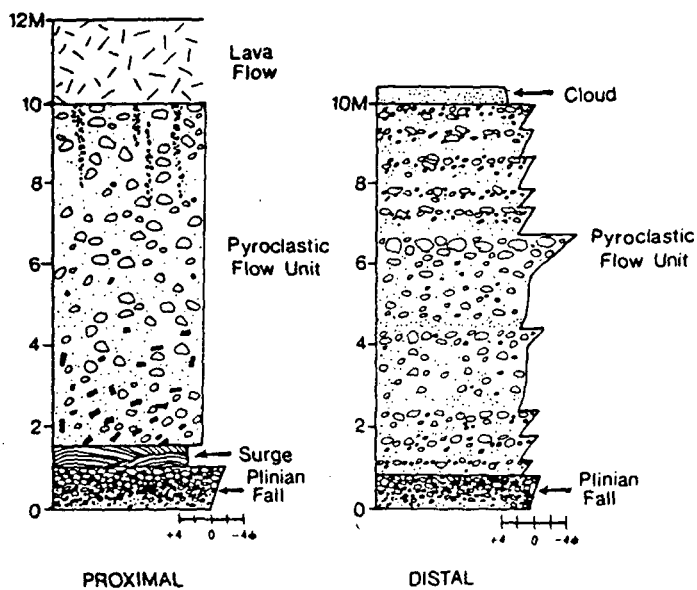


Figure 8. Proximal and distal facies of intermediate to large pyroclastic flow units. Scales show grain size.

COOLING AND COMPACTION

IMPOSE CHARACTERISTIC STRATIGRAPHY
OCCUR IN BOTH FALL AND FLOW DEPOSITS

EMPLACEMENT TEMPERATURES

>500°C

SHOW CHANGES THROUGH ERUPTIVE SEQUENCE

Welding

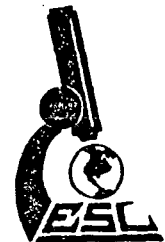
process which promotes union or cohesion of
glassy fragments (shards)

two major factors : temperature
thickness

creates zonation

doesn't change phenocrysts, but does
compress shards

develop eutaxitic structure



**Smith (1960b) identified 3 welding zones
boundries transitional, but may be abrupt
(under 1') zones change both vertically
and horizontally**

**NO welding - bottom (except in very hot flows)
and top of flow cooled quickly
pumice in unwelded zones may
represent magma**

**Partial welding - some loss of pore space,
pumice collapsing
shards becoming compressed**

**Dense welding - least amount of pore space
vitrophyre at base**

**pumice - darken as welding increases
(before matrix)**



Heat loss through : radiation

conduction to ground

conduction from cloud to

atmosphere

secondary factors – fumeroles,

etc.

Heat conserved by: gases – small mass

time – 60–100 mph emplacement

insulation – poor thermal

conductivity



Fiamme

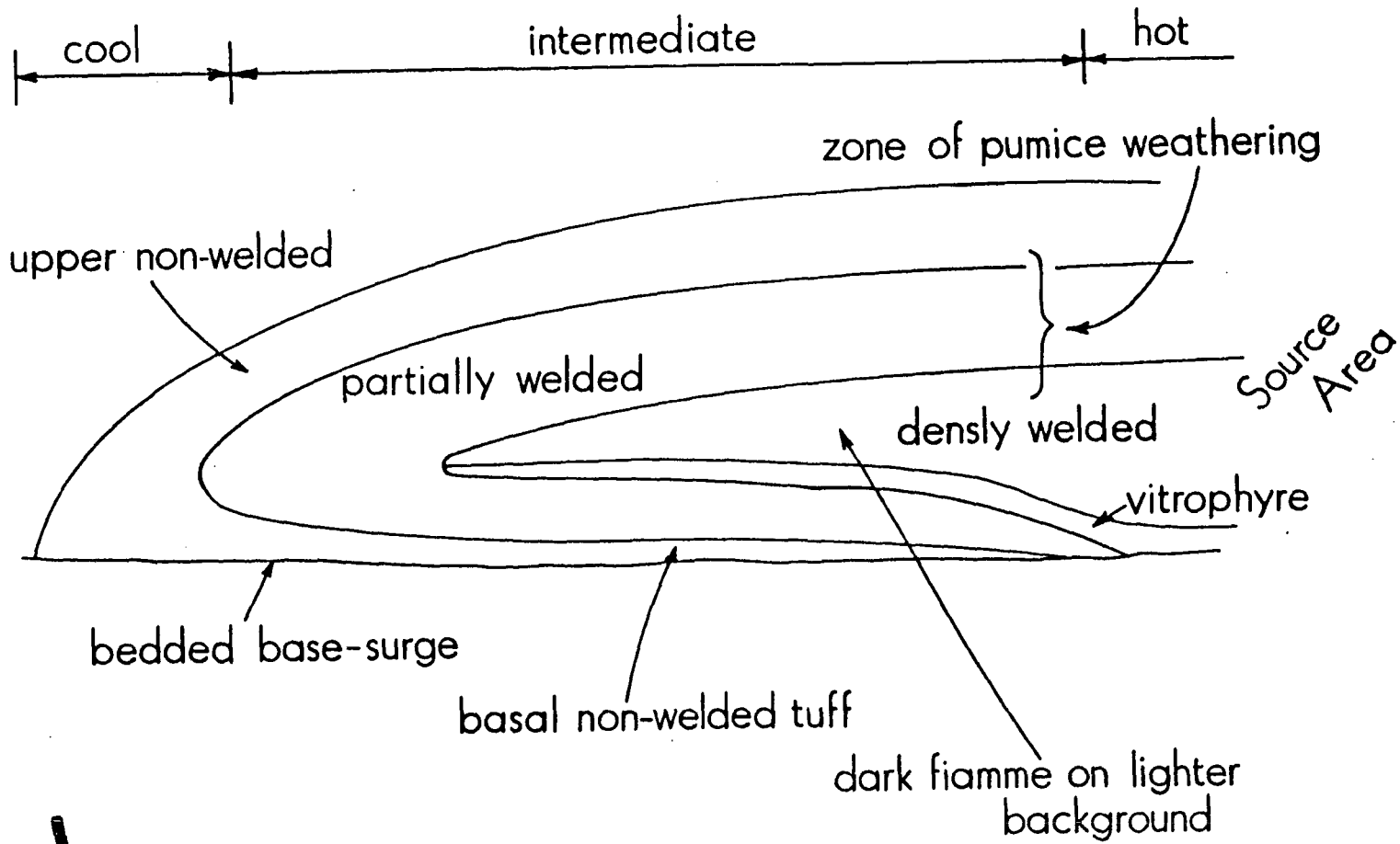
**formed from pumice - but not all flows have
sufficient pumice in unwelded
parts to account for fiamme
(Ross & Smith, 1960)**

unexpanded lumps of volatile rich very fluid glass

**increase in water vapor over fluvial channels
yielding secondary melting
(McBirney, 1968)**



ASH FLOW TUFF WELDING ZONES



DEFINITIONS

COOLING UNIT - SINGLE OR MULTIPLE FLOWS THAT COOL
TOGETHER

SIMPLE COOLING UNIT - "ESSENTIALLY" UNINTERRUPTED
COOLING HISTORY

COMPOUND COOLING UNIT - PARTIAL COOLING
BREAK BETWEEN FLOWS

COMPOSITE COOLING - GRADATIONAL FROM SIMPLE TO
COMPOUND TO SEPARATE SHEETS
GOING AWAY FROM SOURCE

Secondary Characteristics

superimposed on welding

devitrification - crystal formation in glass shards or pumice

cristobalite and feldspar

vapor phase crystallization - crystal formation in open spaces

tridymite and alkalic feldspar

granophyric alteration - only in thick, densely welded tuffs

groundmass quartz and alkalic feldspar

fumerolic alteration - near-surface vapor phase



Further Field Features

Flowage - primary : pumice swarms

rafted pumice

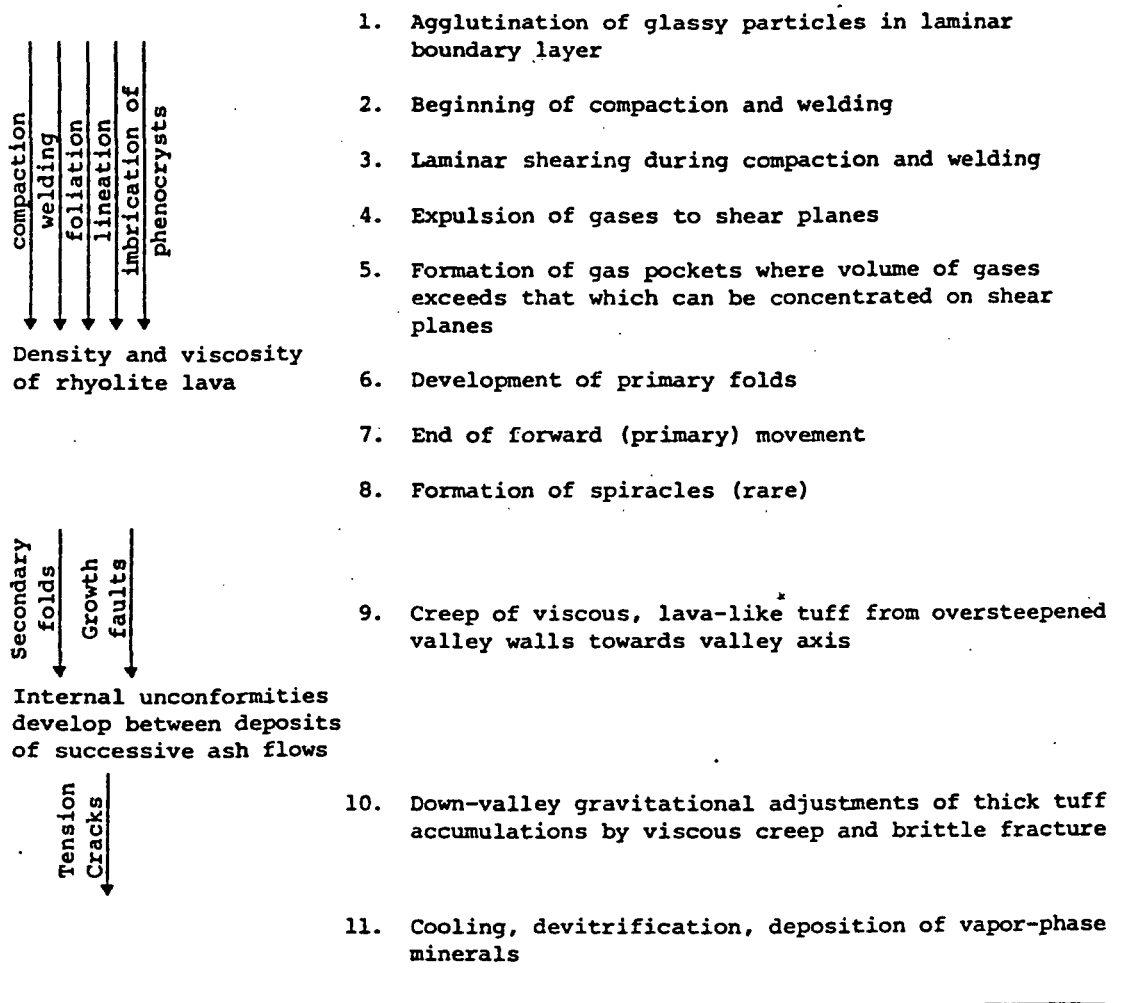
inclusion trains

secondary : radial stretching

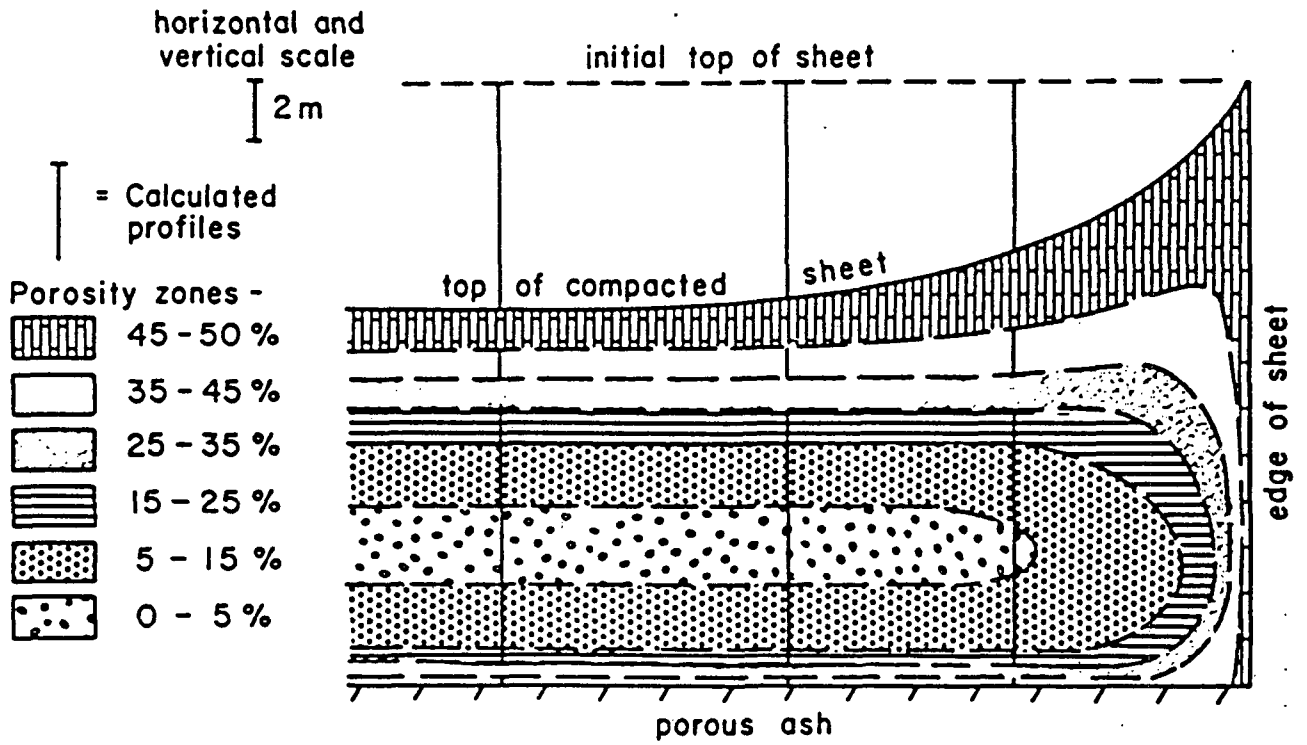
flow deformation (folds)



TABLE 2. SEQUENCE OF EVENTS DURING DEPOSITION OF THE WALL MOUNTAIN TUFF AS INTERPRETED FROM PRIMARY AND SECONDARY FLOW STRUCTURES AND THE ROCK FABRIC



a) $T_{(empl)} = 750^{\circ}\text{C}$
Initial thickness = 20 m



DISTINGUISHING LAVA FLOWS FROM ASH FLOWS

LAVA

CONTINUOUS FLOW BANDING
VISCIOUS EMPLACEMENT
HIGHLY CONTORTED STRUCTURES
POSSIBLE

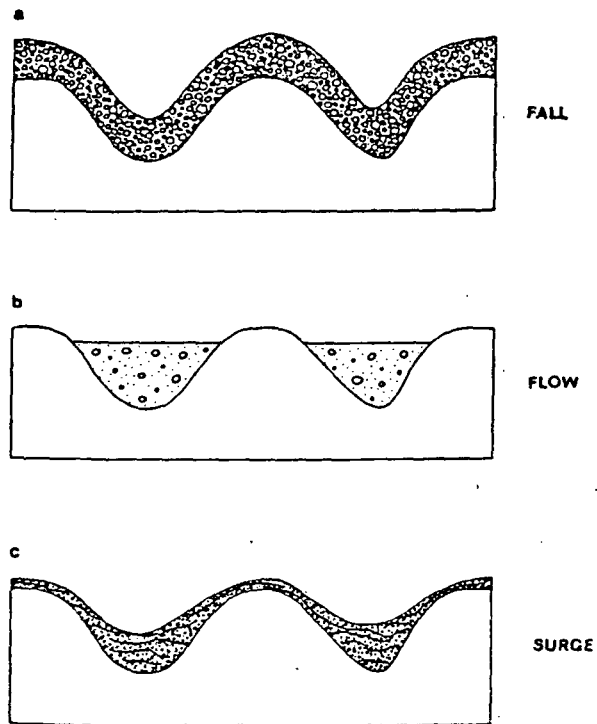
ASH

DISCONTINUOUS EUTAXITIC STRUCTURES
WIDESPREAD DEPOSITION
CHARACTERISTIC STRATIGRAPHY

Table 7-4. Distinguishing characteristics of ash flows and falls

Property	Ash flow	Ash Fall
Structures	Generally unbedded but may have "hot" flowage structures, welding, and fumaroles. Columnar structures in some zones.	Good horizontal bedding.
Size and size gradients	Clast size reduction commonly pronounced down dip. Most particles less than 4 mm.	Generally finer than ash flows. Strong lateral gradients and some vertical grading.
Sorting	Very poorly sorted with much variation within an outcrop. Marked tails on both ends of size curve.	Good sorting. Little variation within an outcrop. Tail of fines only.
Geometry	Elongate with shape controlled by major topographic lows. Flat top.	Wide spread, sheet-like and conformable, blanketing depositional surface.
Thickness and extent	May exceed several hundred feet near source and extend as much as 20 to 50 miles from it.	Commonly a few feet or less but exponentially thicker upwind; rarely more than 20 feet. May extend several hundred miles as very thin units.
Petrology	Welding common as is glass cement if not devitrified. Much welded and deformed pumice. Devitrified shards have axiolitic structure. Cristobalite.	Welding unusual.

Pettyjohn, Potter, Siever, 1973



Wright and others,
1980

Fig. 2. Geometric relations of the three main types of pyroclastic deposit overlying the same topography.

VENT IDENTIFICATION

STRATIGRAPHIC RELATIONS

COMPOSITE SHEETS

LAG FALL DEPOSITS

CENTER OF DISTRIBUTION

WITHIN UNITS

PHENOCRYSTS LARGER AND MORE ABUNDANT

LITHIC FRAGMENTS LARGER AND MORE ABUNDANT

UNITS THICKEN

STEEPLY INCLINED EUTAXITIC STRUCTURES AND

WELDING ZONES

(DON'T CONFUSE WITH TOPOGRAPHY)

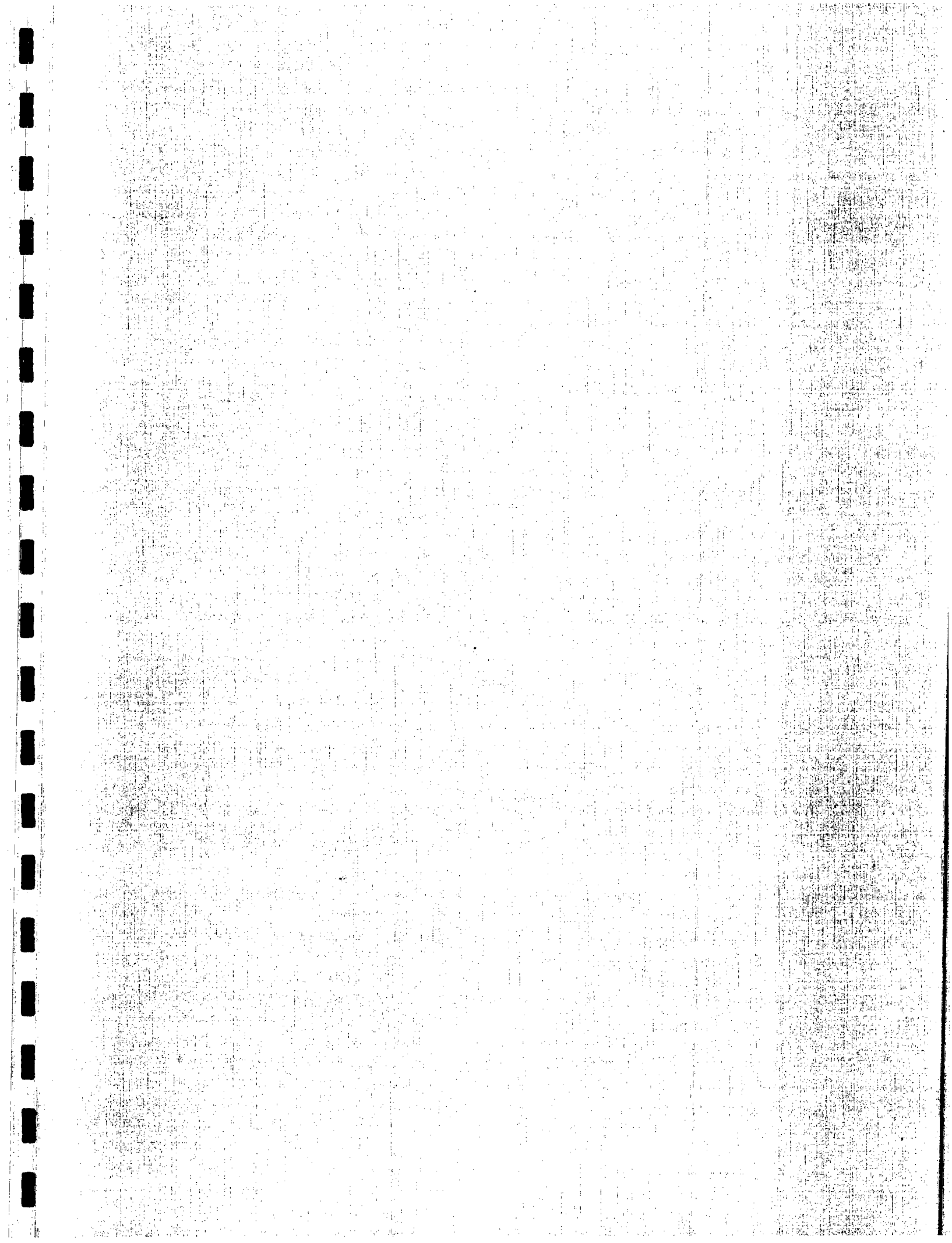
MORE DENSE WELDING

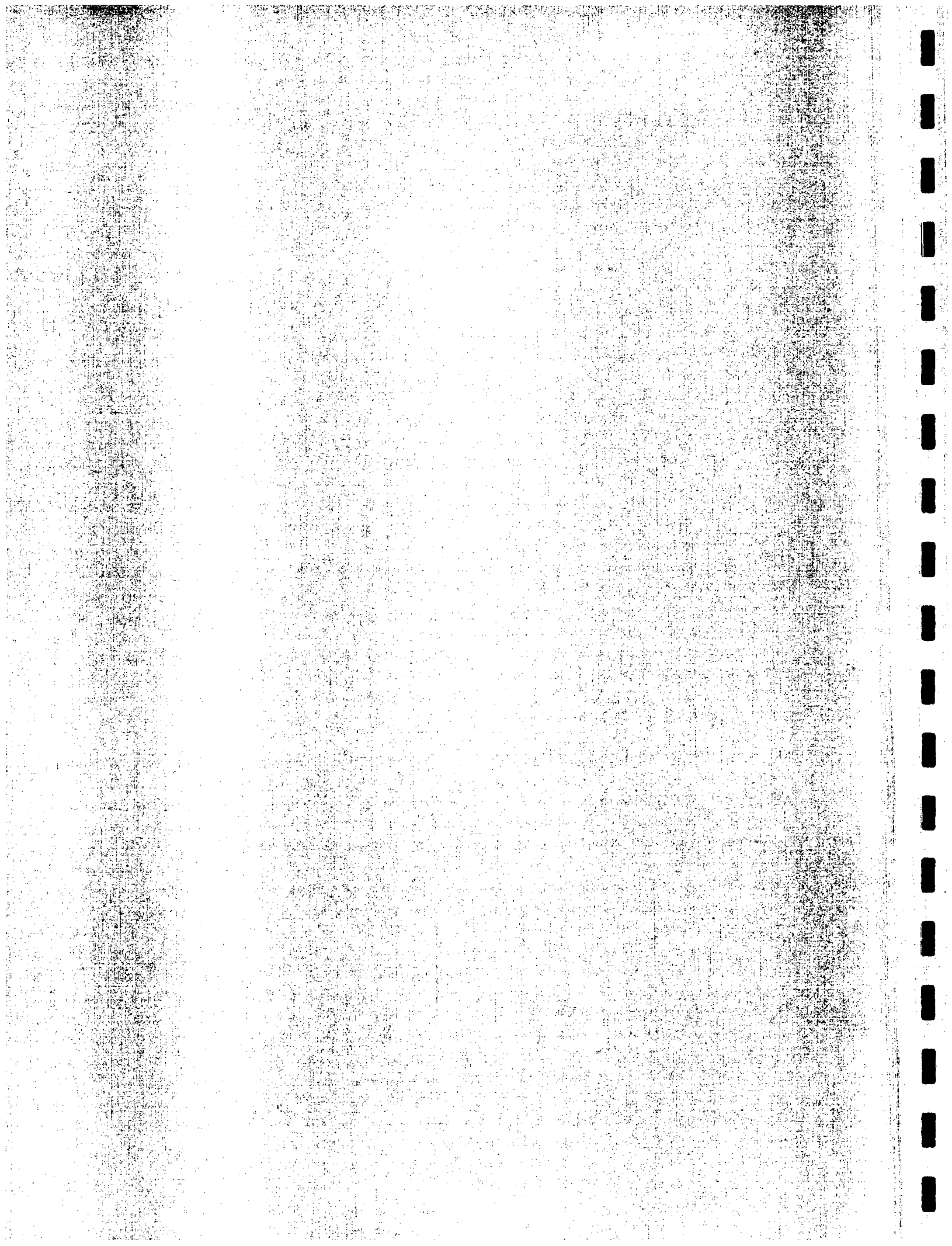
- Chapin, C. E., and Elston, W. E., eds., 1979, Ash-Flow Tuffs: Geol. Soc. Am. Spec. Paper 180, 211 p.
- Chapin, C. E., Lowell, G. R., 1979, Primary and secondary flow structures in ash-flow tuffs of the Gribbles Run paleovalley, central Colorado, in, Chapin, C. E., Elston, W. E., eds., Ash-Flow Tuffs: Geol. Soc. of Am. Spec. Paper 180, p. 137-154.
- Crowe, B. M., Fisher, R. V., 1973, Sedimentary structures in base-surge deposits with special reference to cross-bedding, Ubehebe Craters, Death Valley, California: Geol. Soc. of Am. Bull., v. 84, p. 663-682.
- Davies, D. K., Quearry, M. W., Bonis, S. B., 1978, Glowing avalanches from the 1974 eruption of the volcano Fuego, Guatemala: Geol. Soc. of Am. Bull., v. 89, p. 369-384.
- Druitt, T. H., and Sparks, R. S. J., 1982, A proximal ignimbrite breccia facies on Santorini, Greece: Jour. Volc. Geoth. Res., v. 13, p. 147-171.
- Eichelberger, J. C., and Koch, F. G., 1979, Lithic fragments in the Bandelier Tuff, Jemez Mountains, New Mexico: Jour. Volc. Geoth. Res., v. 5, p. 115-134.
- Fischer, R. V., 1977, Erosion by volcanic base-surge density currents: U-shaped channels: Geol. Soc. Am. Bull., v. 88, p. 1287-1297.
- Fisher, R. V., 1979, Models for pyroclastic surges and pyroclastic flows: Jour. Volc. Geoth. Res., v. 6, p. 305-318.
- Froggatt, P. C., Wilson, C. J. N., and Walker, G. P. L., 1981, Orientation of logs in the Taupo Ignimbrite as an indicator of flow direction and vent position: Geology, v. 9, p. 109-111.
- Gibson, L. L., and Tazieff, H., 1967, Additional theory of origin of fiamme in ignimbrites: Nature, Vol. 215, p. 1473-74.
- Heiken, G., 1978, Plinian-type eruptions in the Medicine Lake Highland, California, and the nature of the underlying magma: Jour. Volc. Geoth. Res., v. 4, p. 375-402.
- Izett, G. A., 1981, Volcanic ash beds: recorders of Upper Cenozoic silicic pyroclastic volcanism in the western United States: Jour. Geophys. Res., v. 86, p. 10200-10222.
- Izett, G. A., and Wilcox, R. E., 1982, Map showing localities and inferred distributions of the Huckleberry Ridge, Mesa Falls, and Lava Creek ash beds (Pearlette family ash beds) of Pliocene and Pleistocene age in the western United States and southern Canada: U.S. Geol. Surv. Misc. Inv. Map I-1325.
- Lipman, P. W., and Christiansen, R. L., 1964, Zonal Features of an ash-flow Sheet in the Piapi Canyon Formation, Southern Nevada: U.S. Geol. Surv. Prof. Paper 501-B, p. B74-B78.

- Lirer, L., Pescatore, T., Booth, B., and Walker, G. P. L., 1973, Two plinian pumice-fall deposits from Somma-Vesuvius, Italy: *Geol. Soc. of Am. Bull.*, v. 84, p. 759-772.
- Lofgren, G., 1971, Experimentally produced devitrification textures in natural rhyolitic glass: *Geol. Soc. of Am. Bull.*, Vol. 82, p. 111-124.
- McBirney, A. R., 1968, Second additional theory of origin of fiamme in ignimbrites: *Nature*, Vol. 217, p. 938.
- Miller, T. P., Smith, R. L., 1977, Spectacular mobility of ash flows around Aniakchak and Fischer calderas, Alaska: *Geology*, v. 5, p. 173-176.
- Noble, D. C., 1968, Laminar viscous flowage structures in ash-flow tuffs from Gran Canaria, Canary Islands: A Discussion: *Jour. Geol.*, v. 76, p. 721-3.
- Pettijohn, F. J., Potter, P. E., and Siever, R., 1972, *Sand and Sandstone*: Springer-Verlag, New York, p. 261-292.
- Ragan, D. M., and Sheridan, M. F., 1972, Compaction of the Bishop Tuff, California: *Geol. Soc. Am. Bull.*, v. 83, p. 95-106.
- Riehle, J. R., 1973, Calculated compaction profiles of rhyolitic ash-flow tuffs: *Geol. Soc. Am. Bull.*, v. 84, p. 2193-2216.
- Rose, W. I., Jr., 1972, Santiaguito volcanic dome, Guatemala: *Geol. Soc. of Am. Bull.*, v. 83, p. 1413-1434.
- Ross, C. L., and Smith, R. L., 1961, Ash-Flow Tuffs: Their origin, geologic relations and identification: *U.S. Geol. Surv. Prof. Paper 366*, 81 p.
- Sarna-Wojcicki, A. M., 1976, Correlation of late Cenozoic tuffs in the central Coast Ranges of California by means of trace- and minor-element chemistry: *U.S. Geol. Surv. Prof. Paper 972*, 30 p.
- Sarna-Wojcicki, A. M., Shipley, S., Waitt, R. B., Jr., Dzurisin, D., and Wood, S. H., 1981, Areal distribution, thickness, mass, volume, and grain size of air-fall ash from the six major eruptions of 1980, in, Lipman, P. W., Mullineaux, D. R., eds., *The 1980 eruptions of Mount St. Helens*, Washington: *U.S. Geol. Surv. Prof. Paper 1250*, p. 577-600.
- Schmincke, H. V., and Swanson, D. A., 1967, Laminar viscous flowage structures in ash-flow tuffs from Gran Canaria, Canary Islands: *Jour. Geol.*, v. 75, p. 641-664.
- Self, S., and Sparks, R. S. J., 1978, Characteristics of widespread pyroclastic deposits formed by the interaction of silicic magma and water: *Bull. Volc.*, v. 41-3, p. 196-212.
- Sheridan, M. F., 1970, Fumarolic mounds and ridges of the Bishop Tuff, California: *Geol. Soc. Am. Bull.*, v. 81, p. 851-868.
- Sheridan, M. F., 1971, Particle-size characteristics of pyroclastic tuffs: *Jour. Geophys. Res.*, v. 76, p. 5627-5634.

- Sheridan, M. F., 1979, Emplacement of pyroclastic flows: A review, in, Chapin, C. E., and Elston, W. E. eds., Ash-Flow Tuffs: Geol. Soc. Am. Spec. Paper 180, p. 125-136.
- Sheridan, M. F., and Wohletz, K. H., 1981, Hydrovolcanic explosions: the systematics of water-pyroclast equilibration: Science, v. 217, p. 1387-1389.
- Shulters, M. V., and Clifton, D. G., 1980, Mount St. Helens volcanic-ash fall in the Bull Run watershed, Oregon, March-June 1980: U.S. Geol. Surv. Circ. 850-A, 15 p.
- Smith, R. L., 1960a, Ash Flows: Bull. Geol. Soc. Am., v. 71, p. 795-842.
- Smith, R. L., 1960b, Zones and zonal variations in welded ash flows: U.S. Geol. Surv. Prof. Paper 354F, p. 149-158.
- Sparks, R. S. J., Self, S., and Walker, G. P. L., 1973, Products of Ignimbrite Eruptions: Geology, v. 1, p. 115-118.
- Sparks, R. S. J., and Wilson, L., 1976, A model for the formation of ignimbrite by gravitational column collapse: Jour. Geol. Soc. Lond., v. 132, p. 441-451.
- Sparks, R. S. J., and Walker, G. P. L., 1977, The significance of vitric-enriched air-fall ashes associated with crystal-enriched ignimbrites: Jour. Volc. Geoth. Res., v. 2, p. 329-341.
- Sparks, R. S. J., Wilson, L., and Hulme, G., 1978, Theoretical modeling of the generation, movement and emplacement of pyroclastic flows by column collapse: Jour. Geophys. Res., v. 83, p. 1727-1739.
- Sparks, R. S. J., and Wright, J. V., 1979, Welded air-fall tuffs, in, Chapin, C. E., and Elston, W. E., eds., Ash-Flow Tuffs: Geol. Soc. Am. Spec. Paper 180, p. 155-166.
- Taylor, P. S., and Stoiber, R. E., 1973, Soluble material on ash from active Central American volcanoes: Geol. Soc. of Am. Bull., v. 84, p. 1031-1042.
- Vicars, R. G., and Breyer, J. A., 1981, Sedimentary facies in air-fall pyroclastic debris, Arikaree Group (Miocene), northwest Nebraska, U.S.A: Jour. Sed. Pet., v. 51, p. 909-921.
- Waite, R. B., Jr., and Dzurisin, D., 1981, Proximal air-fall deposits from the May 18 eruption-stratigraphy and field sedimentology, in, Lipman, P. W., and Mullineaux, D. R., eds., The 1980 eruptions of Mount St. Helens, Washington: U.S. Geol. Surv. Prof. Paper 1250, p. 601-616.
- Walker, G. P. L., 1972, Crystal concentration in ignimbrites: Contr. Min. Pet., Vol. 36, p. 135-146.
- Walker, G. P. L., 1980, The Taupo pumice: product of the most powerful known (ultraplinian) eruption?: Jour. Volc. Geoth. Res., v. 8, p. 69-94.

- Walker, G. P. L., Heming, R. F., and Wilson, C. J. N., 1980, Low-aspect ratio ignimbrites: *Nature*, v. 243, p. 286-287.
- Walker, G. P. L., Wilson, C. J. N., and Froggatt, P. C., 1980, Fines-depleted ignimbrite in New Zealand - the product of a turbulent pyroclastic flow: *Geology*, v. 8, p. 245-249.
- Walker, G. P. L., Self, S., and Froggatt, P. C., 1981, The ground layer of the Taupo Ignimbrite: a striking example of sedimentation from a pyroclastic flow: *Jour. Volc. Geoth. Res.*, v. 10, p. 1-11.
- Walker, G. P. L., Wilson, C. J. N., and Froggatt P. C., 1981, An ignimbrite veneer deposit: the trail-marker of a pyroclastic flow: *Jour. Volc. Geoth. Res.*, v. 9, p. 409-421.
- Walker, G. W., and Swanson, D. A., 1968, Laminar Flowage in a Pliocene Soda Rhyolite Ash-Flow Tuff, Lake and Harney Counties, Oregon: *U.S. Geol. Surv. Prof. Paper 600B*, p. B37-B47.
- Williams, S. N., 1983, Plinian airfall deposits of basaltic composition: *Geology*, v. 11, p. 211-214.
- Wilson, C. J. N., 1980, The role of fluidization in the emplacement of pyroclastic flows: an experimental approach: *Jour. Volc. Geoth. Res.*, v. 8, p. 231-249.
- Wilson, C. J. N., and Walker, G. P. L., 1982, Ignimbrite depositional facies: the anatomy of a pyroclastic flow: *Jour. Geol. Soc. Lond.*, v. 139, p. 581-592.
- Wohletz, K. H., and Sheridan, M. F., 1979, A model of pyroclastic surge, in, Chapin, C. E., and Elston, W. E., eds., *Ash-Flow Tuffs: Geol. Soc. of Am. Spec. Paper 180*, p. 177-194.
- Wolff, J. A., and Wright, J. V., 1981, Rheomorphism of welded tuffs: *Jour. Volc. Geoth. Res.*, v. 10, p. 13-34.
- Wright, J. V., and Walker, G. P. L., 1977, The ignimbrite source problem: significance of a co-ignimbrite lag-fall deposit: *Geology*, v. 5, p. 729-732.
- Wright, J. V., Smith, A. L., and Self, S., 1980, A working terminology of pyroclastic deposits: *Jour. Volc. Geoth. Res.*, v. 8, p. 315-336.
- Wright, J. V., and Walker, G. P. L., 1981, Eruption, transport and deposition of ignimbrite: a case study from Mexico: *Jour. Volc. Geoth. Res.*, v. 9, p. 111-131.





Calderas of Nevada

- I. Regional geologic setting
- II. Volcanism of the Nevada Test Site
- III. Stonewall Mountain
 - A. Volcanic evolution
 - B. Age dating
 - C. Geochemistry

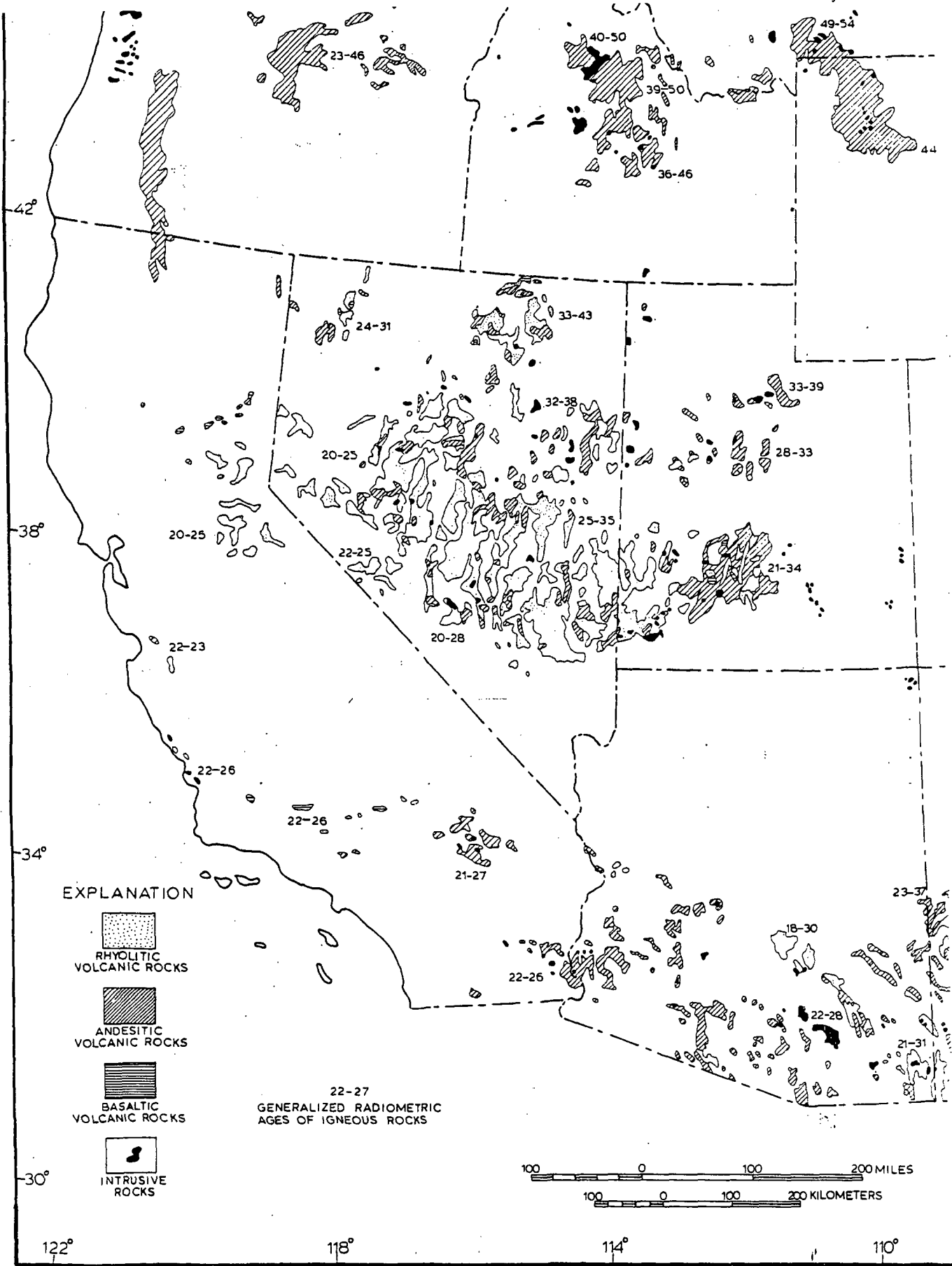


Plate 11-1. Map showing generalized distribution, lithology, and age of 65- to 17-m.y.-old igneous rocks in the Western United States. Sea-floor basalts in the Oregon-Washington coast ranges and Laramide intrusive rocks in California, Nevada, Arizona, Colorado, and Montana are omitted.

Stewart and Carlson, 1970

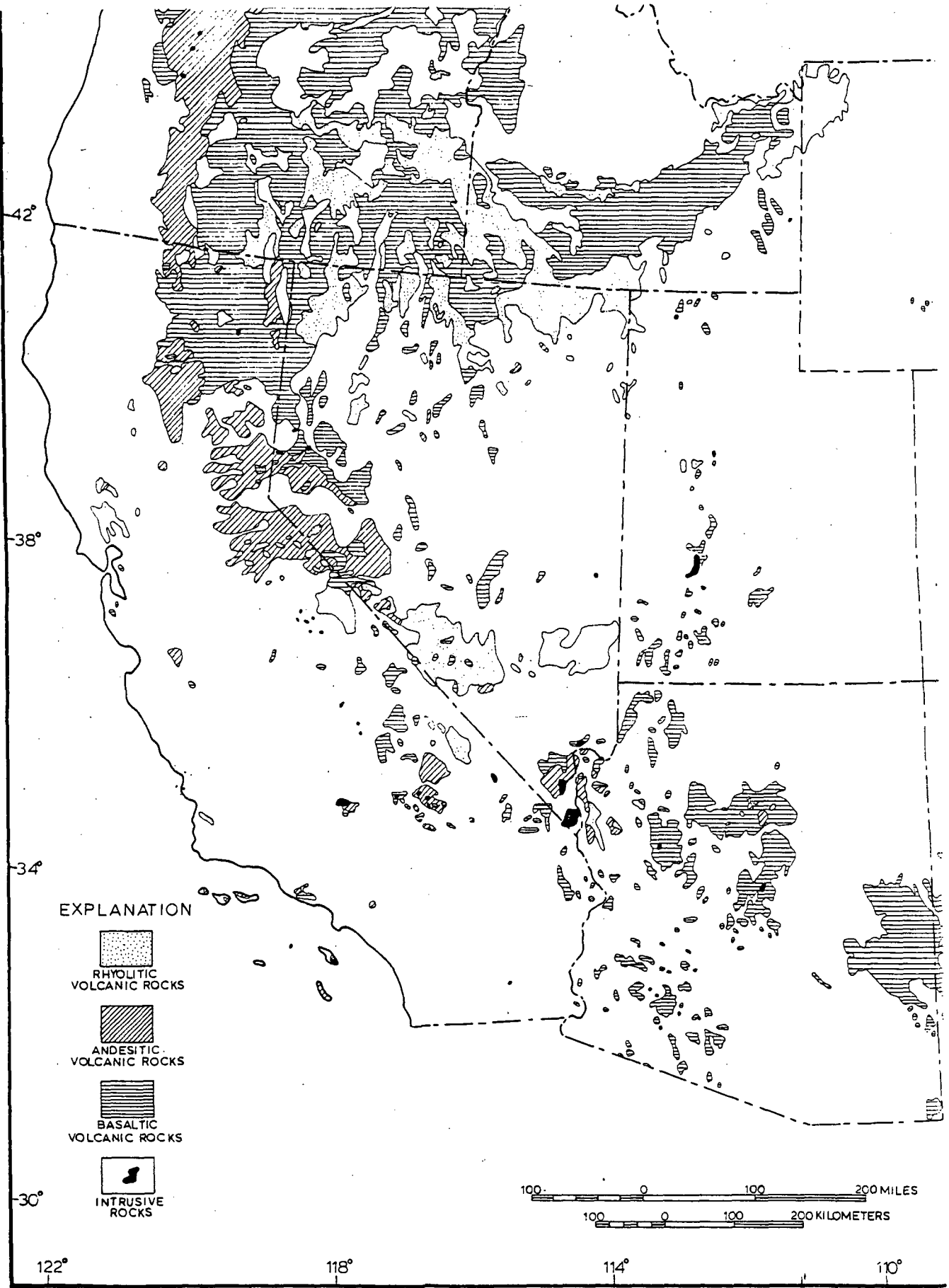
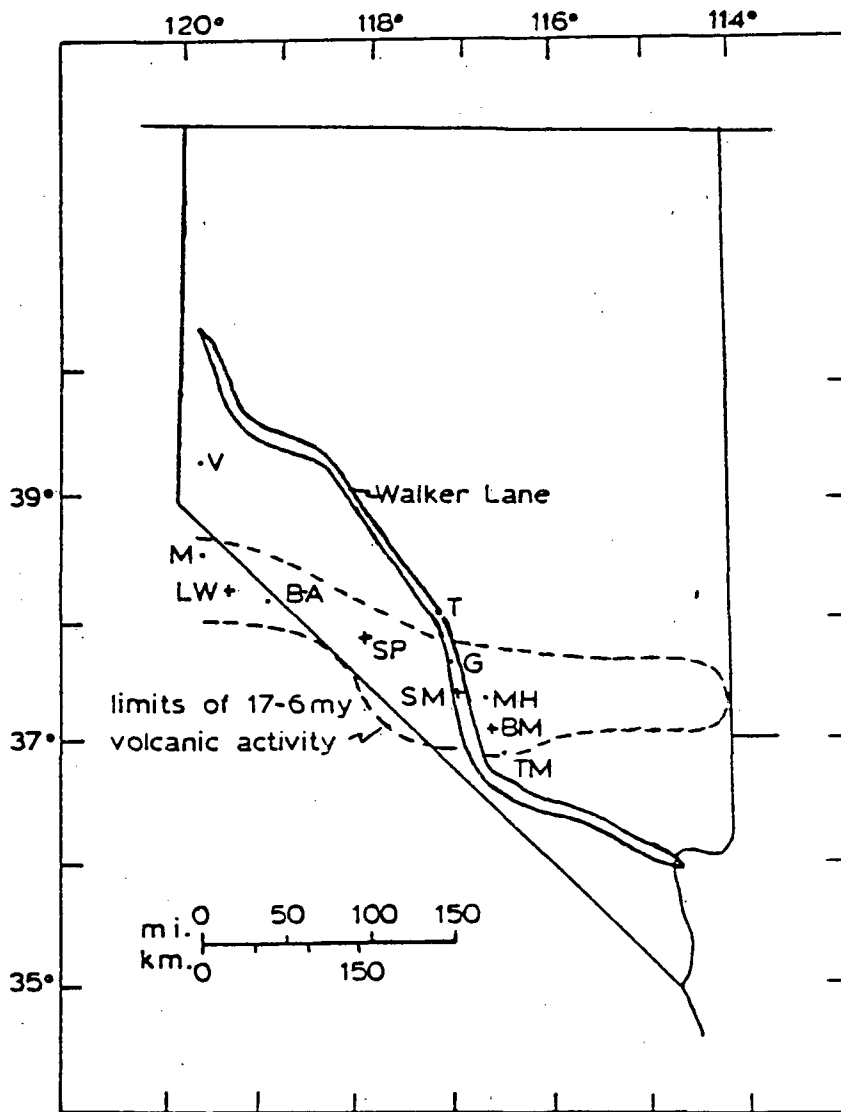


Plate 11-2. Map showing generalized distribution and lithology of igneous rocks less than 17 m.y. old in the Western United States.

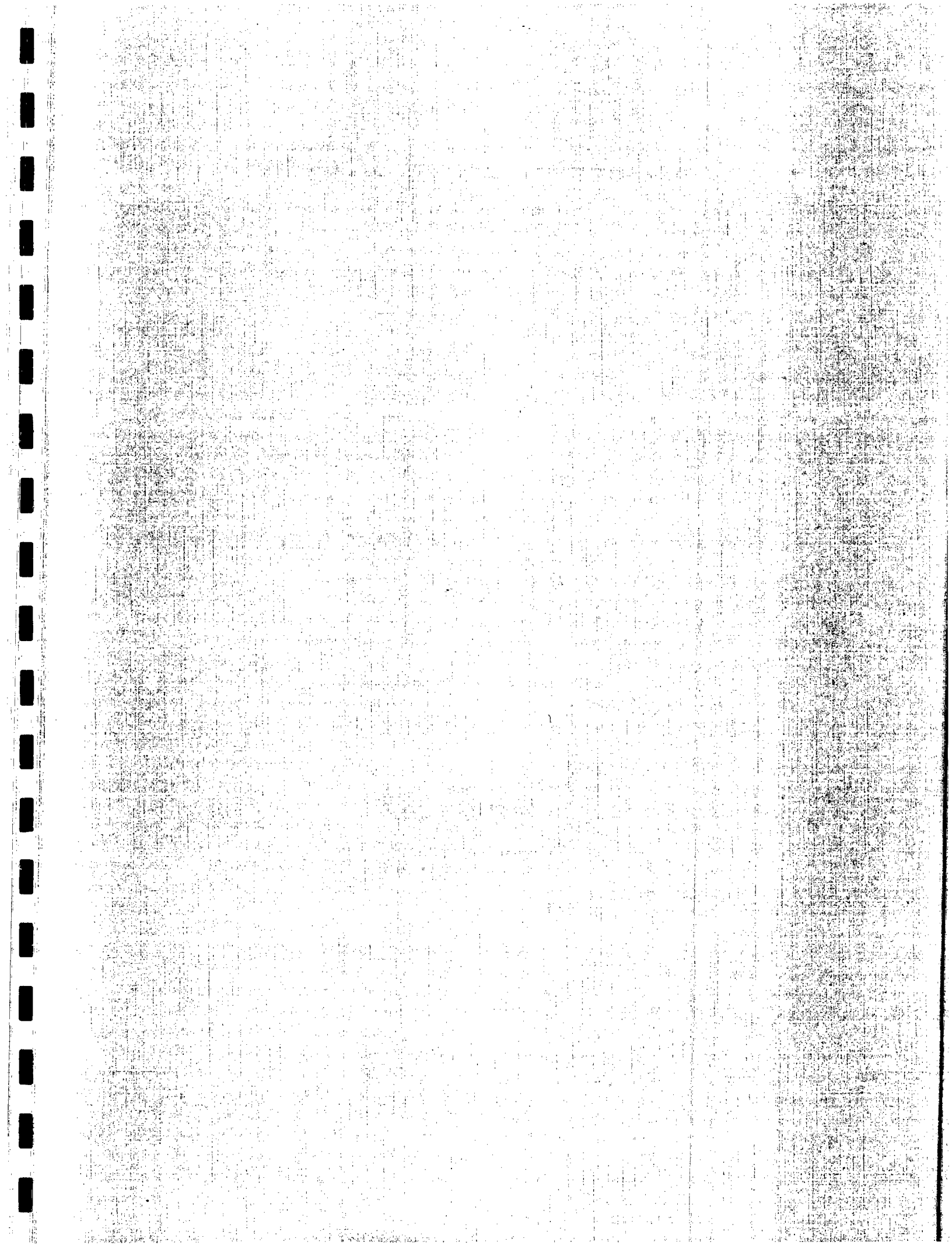
Stewart and Carlson, 1978

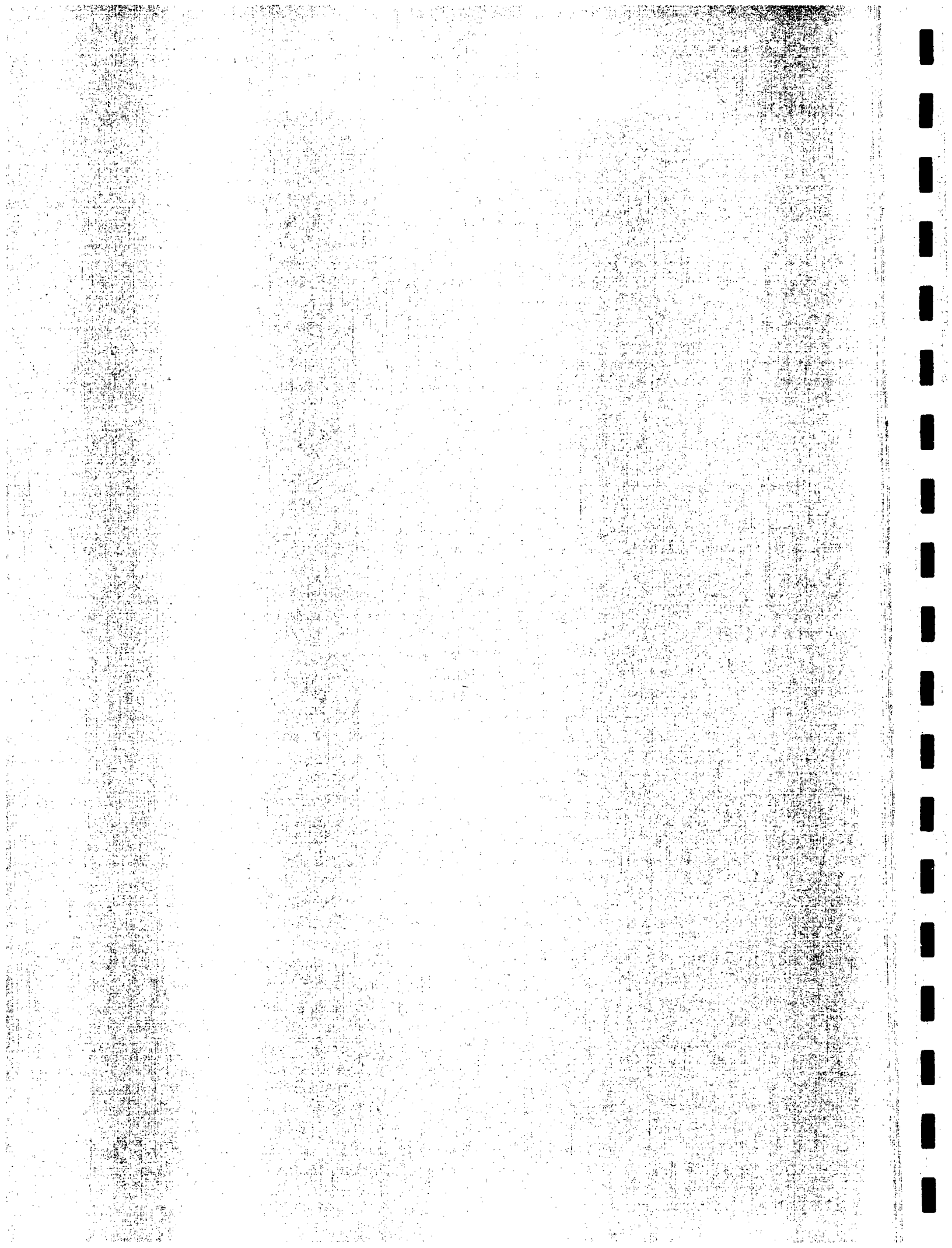


Selected Tertiary Volcanic Centers and the Walker Lane
 - centers "dominantly" older than 10 m.y.
 + centers "dominantly" younger than 10 m.y.
 V = Virginia City, M = Markleville, LW = Little Walker,
 B-A = Bodie - Aurora, T = Tenopah, SP = Silver Peak,
 G = Goldfield, SM = Stonewall Mountain, MH = Mount
 Helen, BM = Black Mountain, TM = Timber Mountain
 (after Ekren et al., 1971, Noble et al., 1976,
 Stewart et al., 1977).

- Albers, J. P., Stewart, J. H., 1972, Geology and mineral deposits of Esmeralda County, Nevada: Nev. Bu. Mines and Geology, Bull. 78, 80 p.
- Ashley, R. O., 1974, Road log and trip guide, Goldfield District: Nev. Bu. Mines and Geology, Report 19, p. 21.
- Byers, F. M., Carr, W. J., Christiansen, R. L., Lipman, P. W., Orkild, P. P., Quinlivan, W. D., 1976, Geologic map of the Timber Mountain caldera area, Nye County, Nevada: U.S. Geol. Surv. Misc. Inv. Map I-891.
- Byers, F. M., Carr, W. J., Orkild, P. P., Quinlivan, W. D., Sargent, K. A., 1976, Volcanic Suites and Related Cauldrons of Timber Mountain - Oasis Valley Caldera Complex, Southern Nevada: U. S. Geol. Surv. Prof. Paper 919, 70 p.
- Christiansen, R. L., Lipman, P. W., Carr, W. J., Byers, F. M., Orkild, P. P., and Sargent, K. A., 1977, Timber Mountain - Oasis Valley caldera complex of southern Nevada: Geol. Soc. America Bull., v. 88, p. 943-959.
- Cornwall, H. R., 1972, Geology and mineral deposits of southern Nye County, Nevada: Nev. Bu. Mines and Geology, Bull. 77, 49 p.
- Eckel, E. B., ed., 1968, Nevada Test Site: Geol. Soc. of Am. Memoir 110, 290 p.
- Ekren, E. B., Anderson, R. E., Rogers, C. L., and Noble, D. C., 1971, Geology of northern Nellis Air Force Bombing and Gunnery Range, Nye County, Nevada: U.S. Geol. Survey Prof. Paper 651, 91 p.
- Foley, D., 1978, The geology of the Stonewall Mountain volcanic center, Nye County, Nevada: unpub. Ph.D. dissert., Ohio State Univ., 139 p.
- Keith, W. J., 1977, Geology of the Red Mountain Mining District, Esmeralda County, Nevada: U.S. Geol. Survey Bull. 1423, 45 p.
- Marvin, R. F., Byers, F. M., Mehnert, H. H., Orkild, P. P., and Stern, T. W., 1970, Radiometric ages and stratigraphic sequence of volcanic and plutonic rocks, southern Nye and western Lincoln Counties, Nevada: Geol. Soc. of America Bull., v. 81, p. 2657-2676.
- McKee, E. H., 1970, Fish Creek Mountains Tuff and Volcanic Center, Lander County, Nevada: U.S. Geol. Surv. Prof. Paper 681, 17 p.
- Noble, D. C., Bath, G. D., Christiansen, R. L., Orkild, P. P., 1968, Zonal relations and Paleomagnetism of the Spearhead and Rocket Wash Members of the Thirsty Canyon tuff, Southern Nevada: U.S. Geol. Surv. Prof. Paper 600 C, p. C61-C65.
- Noble, D. C., and Christiansen, R. L., 1974, Black Mountain volcanic center, in, Guidebook to the geology of four Tertiary volcanic centers in central Nevada: Nev. Bu. Mines and Geology, Report 19, p. 27-34.

- Noble, D. C., Korringa, M. K., Church, S. E., Bowmal, H. R. Silberman, M. L., and Heropoulos, C. E., 1976, Elemental and isotopic geochemistry of nonhydrated quartz latite glasses from the Eureka Valley Tuff, east-central California: Geol. Soc. of America Bull., v. 87, p. 754-762.
- Noble, D. C., Vogel, T. A., Weiss, S. I., Erwin, J. W., 1983, Integrated field, trace-element, and paleomagnetic determination of the stratigraphic relations, distribution, and source areas of ash-flow sheets of the Black Mtn. and Stonewall Mtn. Volcanic Centers, Nevada: EOS, v. 64, p. 336 (abstr.).
- Robinson, P. T., McKee, E. H., and Moiola, R. J., 1968, Cenozoic volcanism and sedimentation, Silver Peak region, western Nevada and Adjacent California, in, Coats, R. R., Hay, R. L., and Anderson, C. A., eds., Studies in Volcanology: Geol. Soc. of America Memoir 116, p. 577-611.
- Stewart, J. H., Moore, W. J., and Zietz, I., 1977, East-west patterns of Cenozoic igneous rocks, aeromagnetic anomalies, and mineral deposits, Nevada and Utah: Geol. Soc. of America Bull., v. 88, p. 67-77.
- Stewart, J. H., Carlson, J. E., 1978, Generalized maps showing distribution, lithology, and age of Cenozoic igneous rocks in the Western United States, in, Smith, R. B., Eaton, G. P., eds., Cenozoic tectonics and regional geophysics of the western cordillera: Geol. Soc. Am. mem 152, p. 263-264.





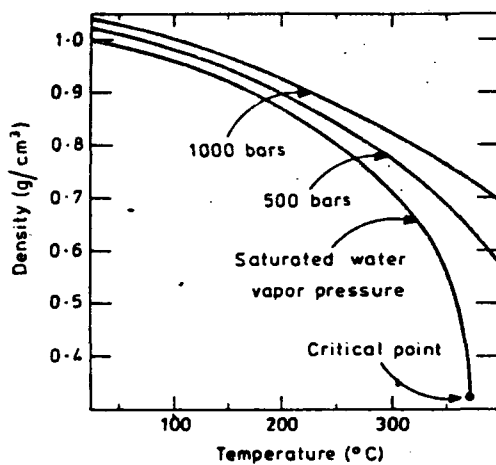


Fig. 4.1 Density of water at saturated vapor pressures and at 500 and 1000 bars.

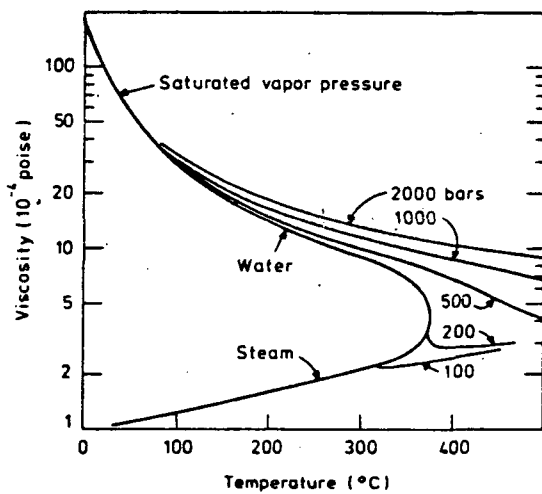


Fig. 4.5 The viscosity of water and steam at various temperatures and pressures.

Ellis and Mahon, 1977

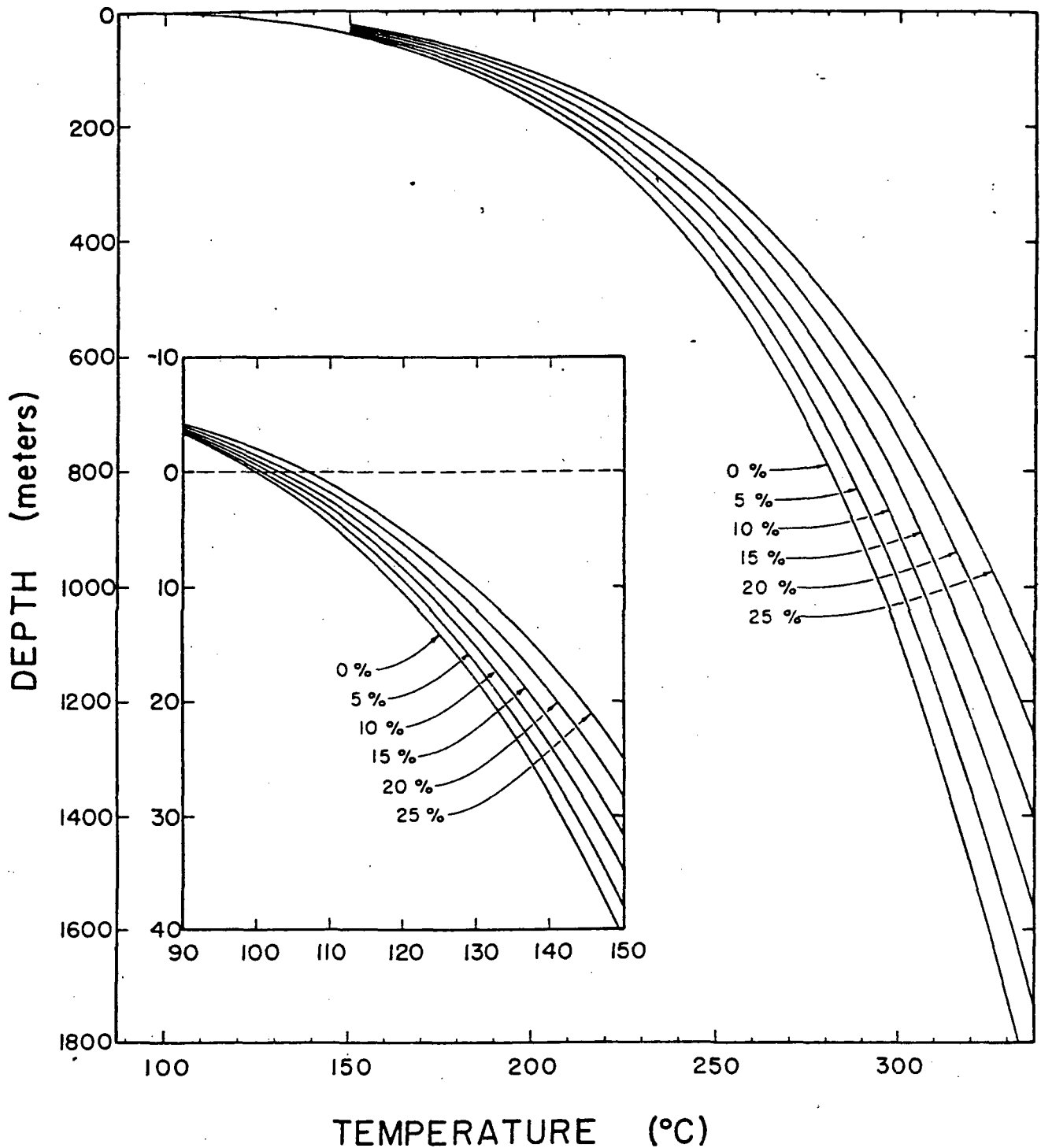


FIG. 2. Boiling-point curves for H_2O liquid (0 wt percent) and for brine of constant composition given in wt percent NaCl. Insert expands the relations between 100° and $150^\circ C$. The temperature at 0 meters of each curve is the boiling point for the liquid at 1.013 bars (1.0 atm) load pressure which is equivalent to the atmospheric pressure at sea level. The uncertainty is contained within the width of the lines.

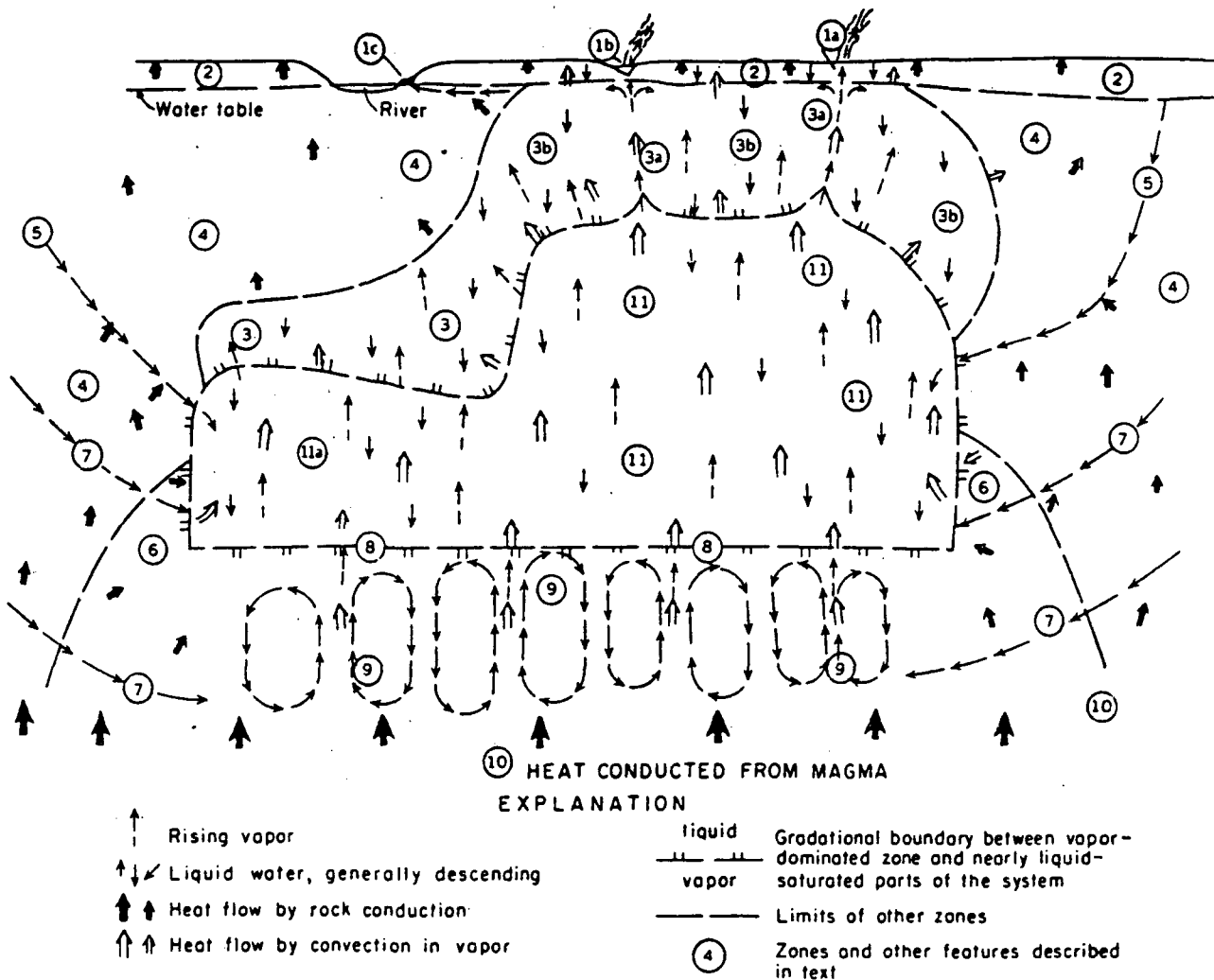


FIG. 7. Model of dynamic vapor-dominated geothermal reservoir surrounded by water-saturated ground. The most significant parts of the model, inward and downward by number, are: 4) zone of conductive heat flow; 3) zone of condensation of steam (conductive and convective heat flow equally important); 11) main vapor-dominated reservoir, with convective upflow of heat in steam in larger channels, and downflow of condensate in small pores and fractures (surface tension effects); 9) deep zone of convective heat transfer, probably in brine; 10) deep zone of conductive heat flow (too hot for open fractures to be maintained). Other features are discussed in text.

(White et al, 1971)

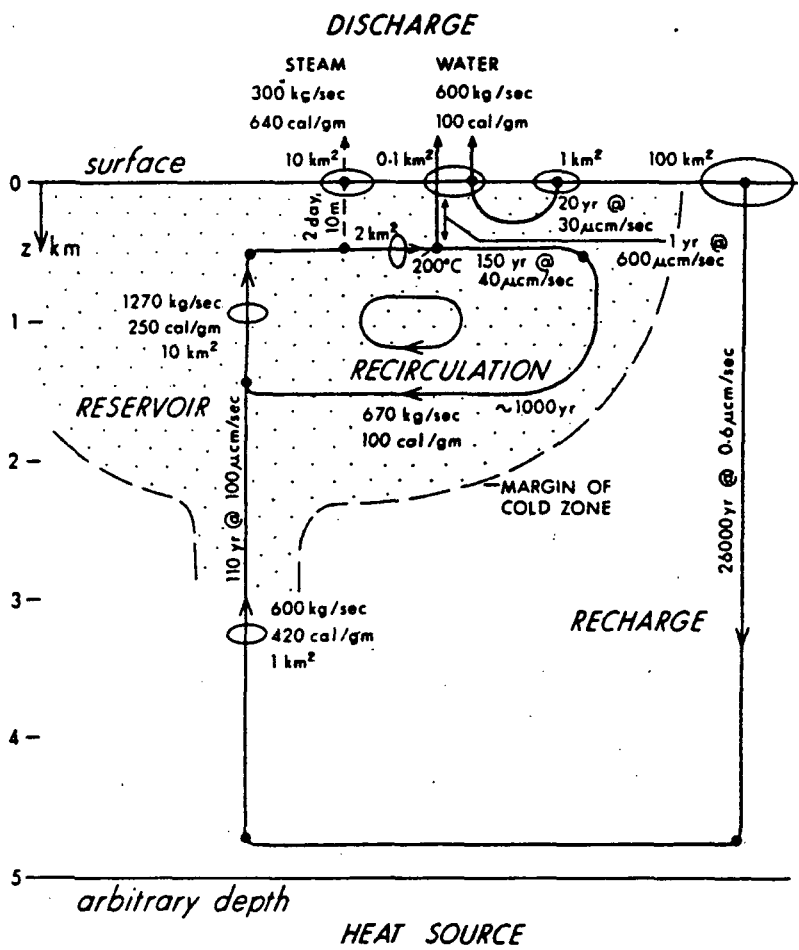


Fig. 14. Schema of a pipe model of Wairakei: flow in kilograms per second, enthalpy in calories per gram, cross-sectional areas in square kilometers, velocities in microcentimeters per second, time in years.

Elder, 1965

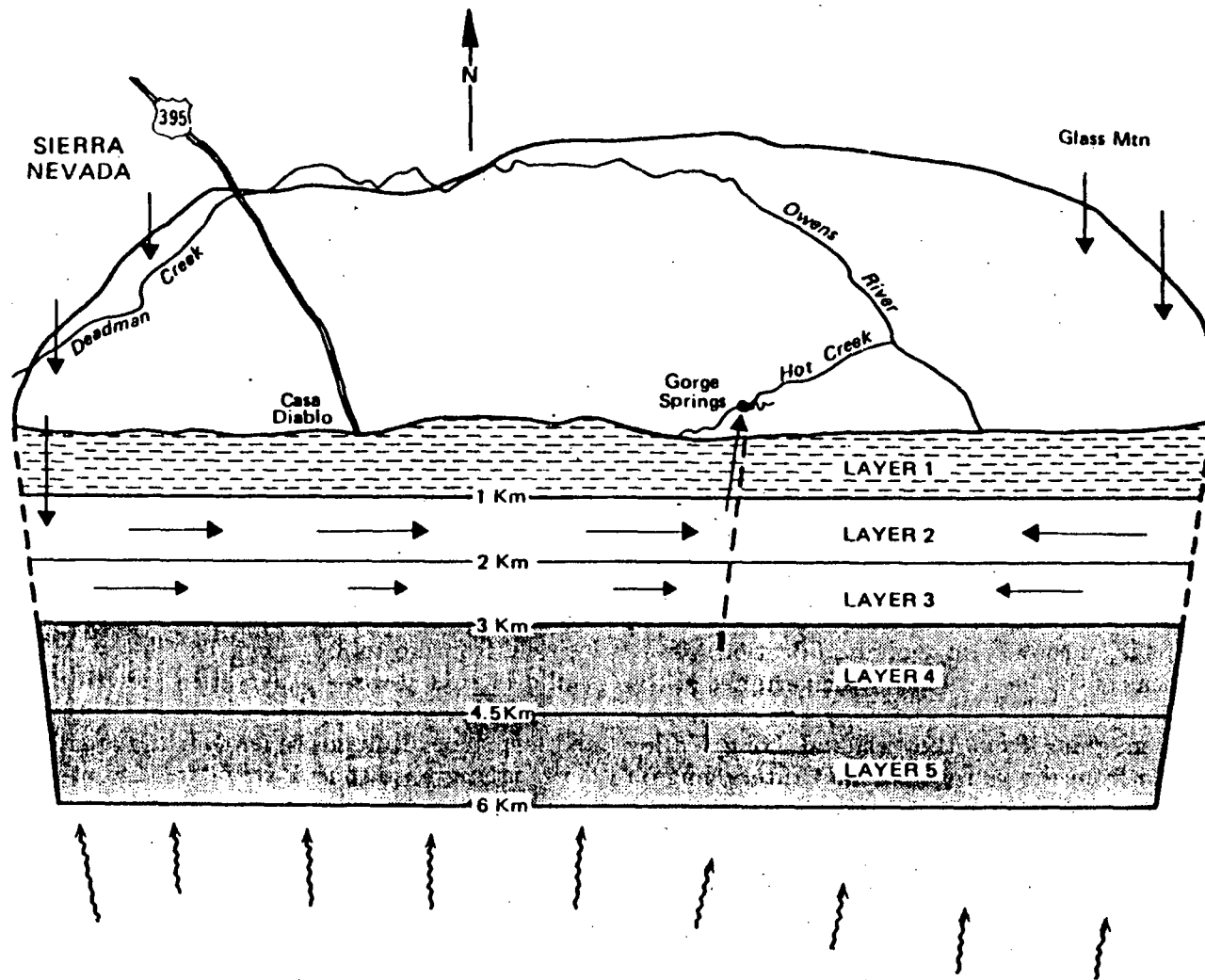


FIGURE 18.—Block diagram showing conceptual model of Long Valley hydrothermal system. Model consists of 5 horizontal layers having properties listed in table 15. Patternless layers between depths of 1 and 3 km represent the hydrothermal reservoir in fractured, densely welded Bishop Tuff. Recharge to reservoir is by way of caldera ring fault in the west and northeast. Discharge is by way of faults and fractures to springs in Hot Creek gorge. Straight arrows indicate ground-water flow, wavy arrows indicate heat flow. Vertical to horizontal exaggeration approximately 1.6 to 1.

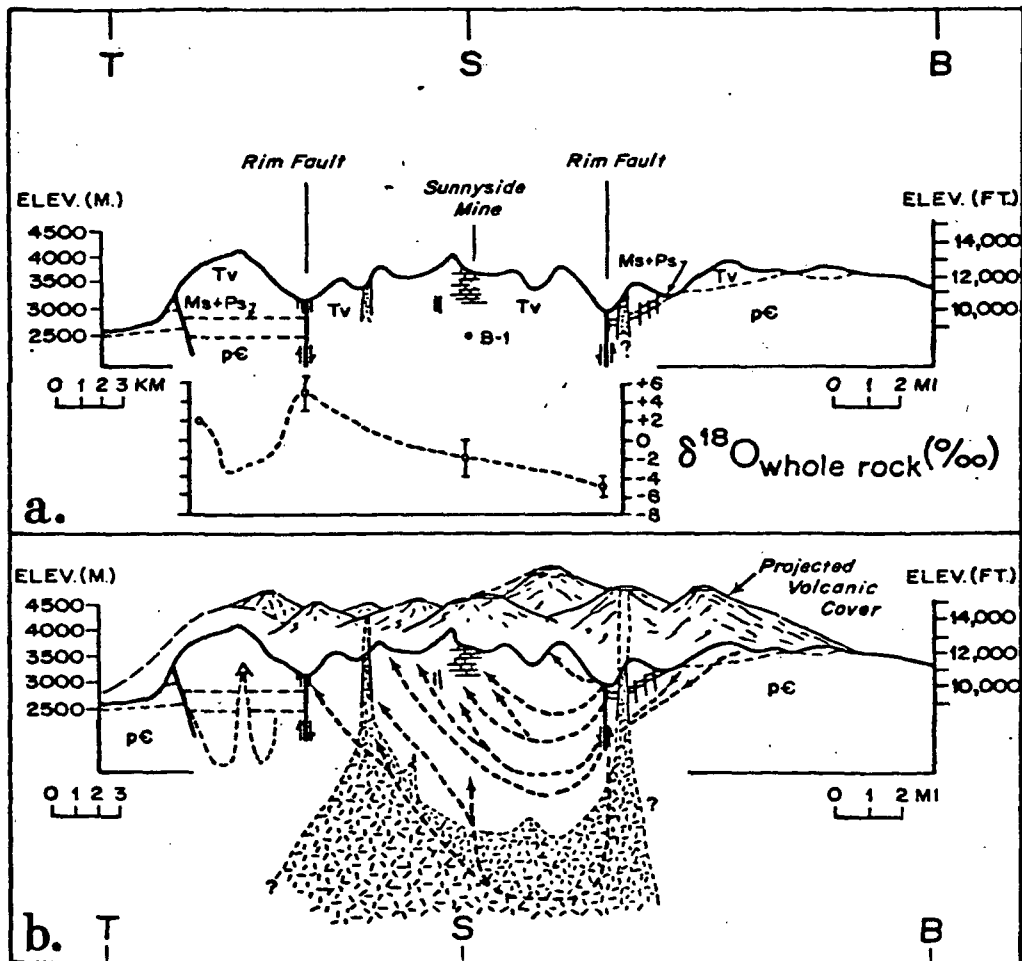
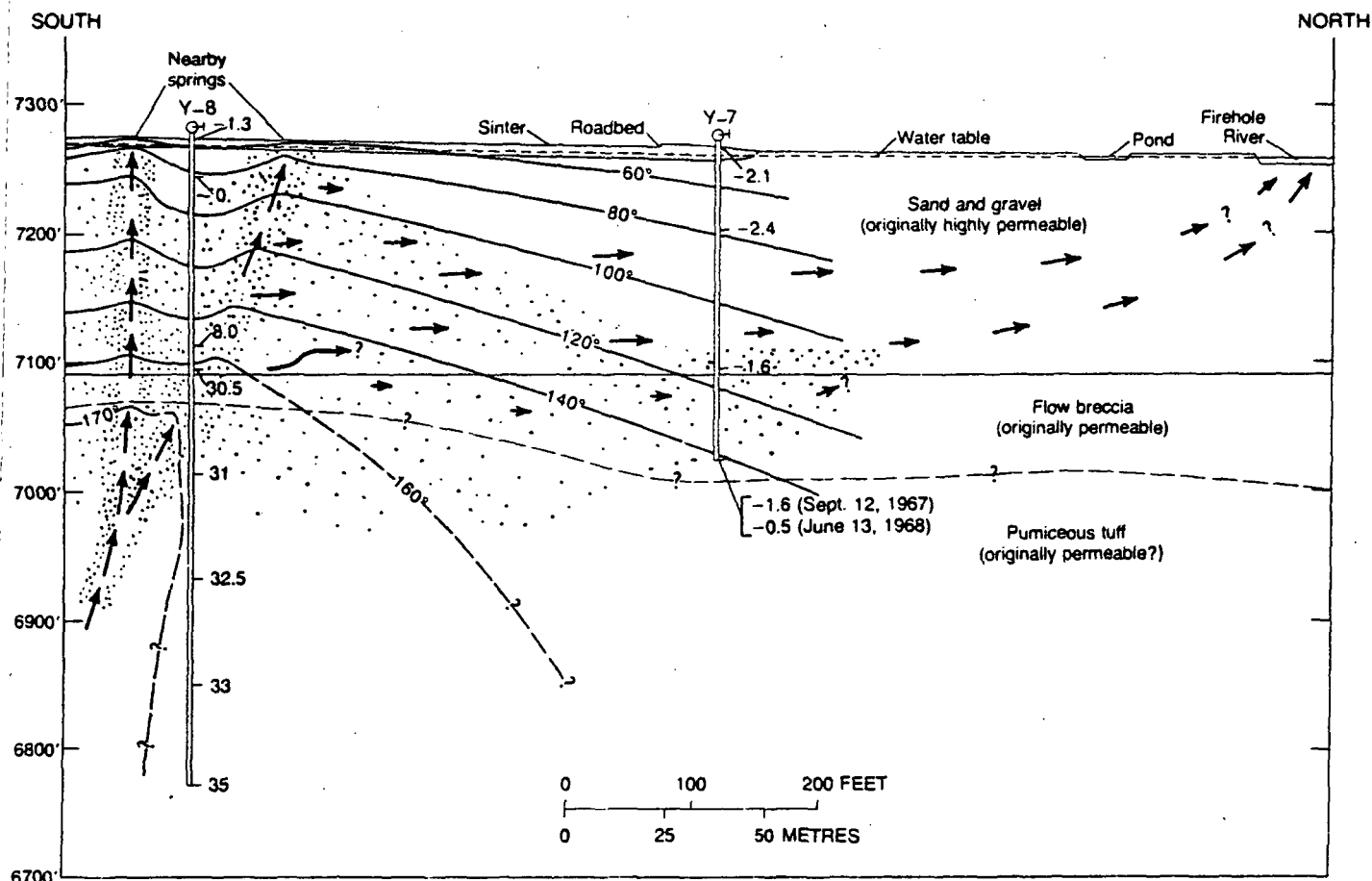


FIG. 22. a. Geologic and topographic cross section through the San Juan and Silverton calderas along section T-S-B (T = Telluride; S = Sunnyside; B = Beartown) of Figure 23 (compiled from Steven et al., 1974a; Mayor and Fisher, 1972; Burbank and Luedke, 1964, 1969; Varnes, 1963; Standard Metals Corporation Geology Department). Vertical exaggeration = 2.6. Oxygen isotope whole-rock values plotted below section are compiled from Taylor, 1974b; Forester and Taylor, 1972; this study. Cross-hatched areas indicate locations of intrusive rocks. "B-1" indicates the bottom of Standard Metals Corporation's exploration drill hole.

b. Geologic and topographic reconstruction. Surface cover has been reconstructed based on calculated depths from Nash (1975) and this study. Dashed arrows indicate suggested groundwater flow and convective fluid flow during mineralization.



EXPLANATION

- 33 Wellhead water pressure, in pounds per square inch (gage), as drilling progressed
- 2.4 Water level below ground expressed as negative wellhead water pressure
- Decreased permeability due to deposition of hydrothermal minerals
- 60° Contour, showing inferred ground temperature, in degrees celsius
- Direction and qualitative rate of flow of thermal water

FIGURE 13.—Section through Y-7 and Y-8 drill holes, showing pressures, temperature contours, and deduced self-sealing by deposition of hydrothermal minerals in originally permeable ground.

(White et al, 1975)

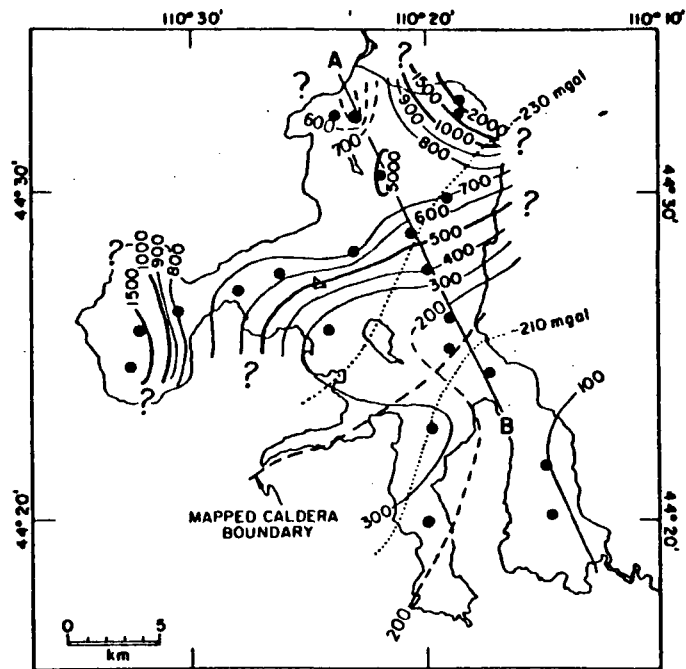


Fig. 9. Contour map of corrected heat flow from Yellowstone Lake: contour intervals are 100 mW m^{-2} ($2.4 \mu\text{cal cm}^{-2} \text{ s}^{-1}$) below, and 500 mW m^{-2} ($12 \mu\text{cal cm}^{-2} \text{ s}^{-1}$) above, 1000 mW m^{-2} ($24 \mu\text{cal cm}^{-2} \text{ s}^{-1}$). Not all contours are shown around the anomaly west of Stevenson Island or in Mary Bay. The mapped boundary of the caldera is shown as a dashed line. Two gravity contours [Eaton *et al.*, 1975] are shown by dotted lines, and the value of the contour is identified in milligals.

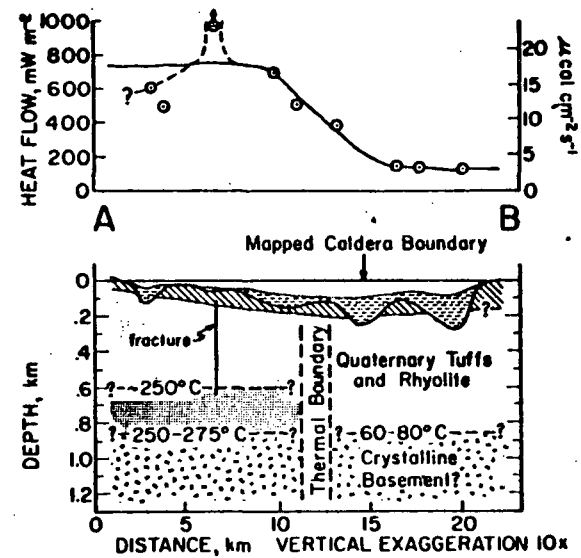


Fig. 10. Schematic cross section of the southeastern boundary of the Yellowstone caldera based on heat flow and seismic data. The location of the section is shown in Figure 9. Lake sediments are shown by the dashed pattern. Pre-erosion glacial, sedimentary, and volcanic units are indicated by the hatched pattern. The heat flow profile is shown above the section, and estimated temperatures are plotted on the major boundaries of the section. The heavy stippled area of Quaternary tuff and rhyolite is the depth where the thermal regime probably becomes nonconductive.

Morgan *et al.* 1977

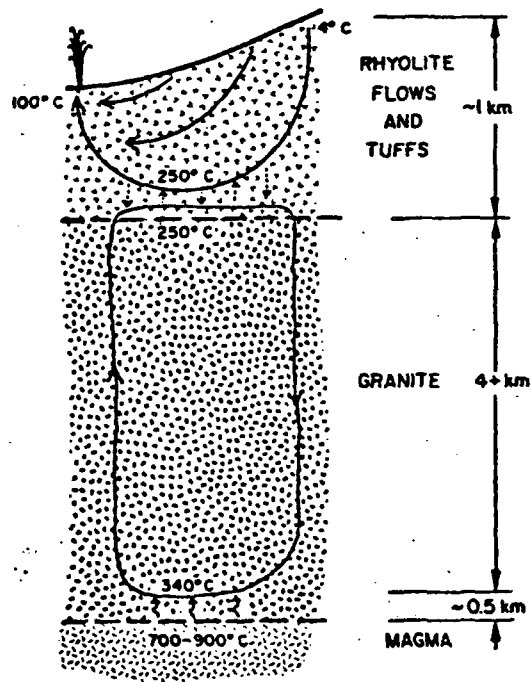


Fig. 11. Schematic model of heat transfer in the Yellowstone caldera. The model is explained in the text. The upper convective system is suppressed beneath the lake. The model assumes that the 5-km s^{-1} refractor beneath Yellowstone Lake is the solidified top of the granitic batholith associated with the caldera.

MORGAN AND OTHERS, 1977

HYDROTHERMAL SYSTEMS

REFERENCES

- Becker, K. and von Herzen, R.P., 1983, Heat transfer through the sediments of the Mounds hydrothermal area, Galapagos Spreading center at 86°W: Jour. Geophys. Res., v. 88, p. 995-1008.
- Berger, B.R. and Taylor, B.E., 1980, Pre-Cenozoic normal faulting in the Osgood Mountains, Humboldt County, Nevada: Geology, v. 8, p. 594-598.
- Casadevall, T. and Ohmoto, H., 1977, Sunnyside Mine, Eureka Mining District, San Juan Co., Colorado: Geochemistry of gold and base metal ore deposition in a volcanic environment: Econ. Geology, v. 72, p. 1285-1320.
- Donaldson, I.G., 1962, Temperature gradients in the upper layers of the earth's crust due to convective water flows: J. Geophys. Res., v. 67, p. 3449-3459.
- Dunn, J.C. and Hardee, H.C., 1981, Superconvecting geothermal zones: Jour. Volcan. Geoth. Res., v. 11, p. 189-201.
- Elder, J.W., 1965, Physical processes in geothermal areas: Am. Geophys. Union Managr. Ser. 8, p. 211-239.
- Elston, W.E., 1978, Mid-Tertiary cauldron and their relationship to mineral resources, southwestern New Mexico: A brief review: New Mexico Geological Society Special Publ. 7, p. 107-113.
- Elston, W.E., Rhodes, R.C., and Erb, E.E., 1976, Control of mineralization by mid-tertiary volcanic centers, southwestern New Mexico: New Mexico Geological Society Special Publ. #5, p. 125-130.
- Ewers, G.R. and Keays, R.R., 1977, Volatile and precious metal zoning in the Broadlands geothermal field, New Zealand: Econ. Geology, v. 72, p. 1337-1354.
- Haynes, F.M. and Titley, S.R., 1980, The evolution of fracture-related permeability within the Ruby Star Granodiorite, Sierrita porphyry copper deposit, Pima County, Arizona: Econ. Geology, v. 75, p. 673-683.
- Henley, R.W. and Ellis, A.J., 1983, Geothermal systems ancient and modern: a geochemical review: Earth-Science Rev., v. 19, p. 1-50.
- Lipman, P.W., Fisher, F.S., Mehnert, H.H., Naeser, C.W., Luedke, R.G., and Steven, T.A., 1976, Multiple ages of mid-Tertiary mineralization and alteration in the western San Juan Mountains, Colorado: Econ. Geology, v. 71, p. 571-588.
- Morgan, P., Blackwell, D.D., Spafford, R.E., and Smith, R.B., 1979, Heat flow measurements in Yellowstone Lake and the thermal structure of the Yellowstone caldera: Jour. Geophys. Res., v. 82, no. 26, p. 3719-3732.

- Norton, D. and Knapp, R., 1977, Transport phenomena in hydrothermal systems: the nature of porosity: *Am. Jour. Sci.*, v. 277, p. 913-936.
- Norton, D. and Knight, J., 1977, Transport phenomena in hydrothermal systems: coding plutons: *Am. Jour. Sci.*, v. 277, p. 937-981.
- Norton, D. and Taylor, H.P., 1979, Quantitative simulation of the hydrothermal systems of crystallizing magmas on the basis of transport theory and oxygen isotope data: an analysis of the Skaergaard intrusion: *Jour. Petrology*, v. 20, p. 421-486.
- Skinner, B.J., White, D.E., Rose, H.J., and Mays, R.E., 1967, Sulfides associated with the Salton Sea geothermal brine: *Econ. Geology*, v. 62, p. 316-330.
- Sleep, N.H. and Wolert, T.J., 1978, Egress of hot water from midocean ridge hydrothermal systems: some thermal constraints: *Jour. Geophys. Res.*, v. 83, p. 5913-5922.
- Snow, D.T., 1968, Rock fracture spacings, openings, and porosities: *Jour. Soil Mech. and Found. Div. Am. Soc. Civil Eng.*, v. 94, p. 73-91.
- Snow, D.T., 1970, The frequency and apertures of fractures in rock: *Int. Jour. Rock Mech. Min. Sci.*, v. 7, p. 23-40.
- Sorey, M.L., Lewis, R.E., and Olmsted, F.H., 1978, The hydrothermal system of Long Valley caldera, California: *U.S. Geol. Surv. Prof. Paper 1044-A*, 60p.
- Steven, T.A., Luedke, R.g., and Lipman, P.W., 1974, Relation of mineralization to calderas in the San Juan volcanic field, southwestern Colorado: *Jour. Res. U.S. Geol. Survey*, v. 2, no. 4, p. 405-409.
- Steven, T.A., and Ratte, J.C., 1965, Geology and structural control of ore deposition of the Creede district, San Juan Mountains, Colorado: *U.S. Geol. Survey Prof. Paper 487*, 87 p.
- Taylor, H.P. and Forester, R.W., 1979, An oxygen and hydrogen isotope study of the Skaergaard intrusion and its country rocks: a description of a 55-m.y. old fossil hydrothermal system: *Jour. Petrology*, v. 20, p. 355-419.
- Toulmin, P., and Clark, S.P., 1967, Thermal Asepts of ore formation, in Barnes, H.L. (ed), *Geochemistry of hydrothermal ore deposits*: New York, Holt, Rinehart, and Winston, p. 437-464.
- Truesdell, A.H. and Fournier, R.O., 1976, Conditions in the deeper parts of the hot springs systems of Yellowstone National park, Wyoming: *U.S. Geol. Survey open-file report 76-428*, 22 p.
- Truesdell, A.H., Nathenson, M., and Rye, R.O., 1977, The effects of subsurface boiling and dilution on the isotopic compositions of Yellowstone thermal waters: *Jour. Geophys. Res.*, v. 82, no. 26, p. 3694-3704.

- Villas, R.N. and Norton, D., 1977, Irreversible mass transfer between circulating hydrothermal fluids and the Mayflower stock: *Econ. Geology*, v. 72, p. 1471-1504.
- White, D.E., Fournier, R.O., Muffler, L.J.P. and Truesdell, A.H., 1975, Physical results of research drilling in thermal areas of Yellowstone National Park, Wyoming: U.S. Geol. Survey Prof. paper 892, 70 p.
- White, D.E., Muffler, L.J.P., and Truesdell, A.H., 1971, Vapor-dominated hydrothermal systems compared with hot-water systems: *Econ. Geology*, v. 66, p. 75-97.
- White, D.E., Thompson, G.A., and Sandberg, C.H., 1964, Rocks, structure, and geologic history of Steamboat springs thermal area, Washoe County, Nevada: U.S. Geol. Survey Prof. Paper 458-B, 63 p.
- Williams, D.L. and von Herzen, R.P., 1983, On the terrestrial heat flow and physical limnology of Crater Lake, Oregon: *Jour. Geophys. Res.*, v. 88, p. 1094-1104.

Geology of Hydrothermal Features

- I. Discussion of surface characteristics
 - A. Water dominated silica depositing
 - B. Water dominated carbonate depositing
 - C. Vapor dominated
- II. Hydrothermal explosion features
- III. Research drilling-physical results in Yellowstone
 - A. Silica systems
 - B. Carbonate system
 - C. Vapor dominated
- IV. Geysers
 - A. Definition
 - B. Eruption cycle

BASE T**FEATURES****CHEMISTRY****Silicia****180° C****springs
geysers
sinter terraces
high run off****high Si, Cl****Carbonate****73° C(Mammoth)****springs
travertine
high run off****high SO₄, HCO₃
CO₂ rich
inverse solubility****Vapor Dominated 236°C****mud pots
low run off
spatially
associated
with silicia
systems(?)****low Si, Cl
acid water
H₂S**

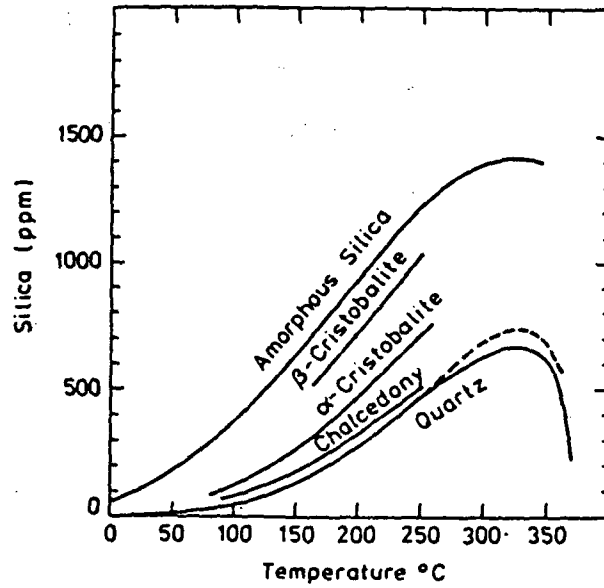


Fig. 4.18 The solubility of various forms of silica in water at saturated water vapor pressures (from Fournier, 1973).

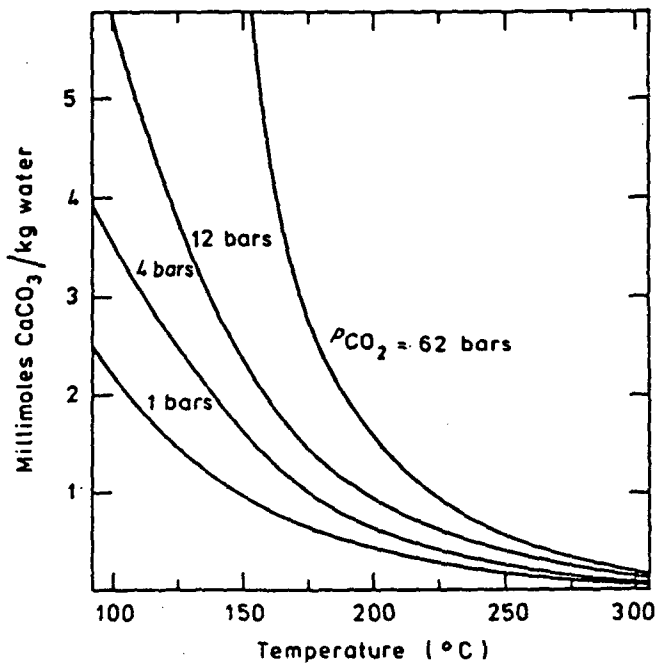
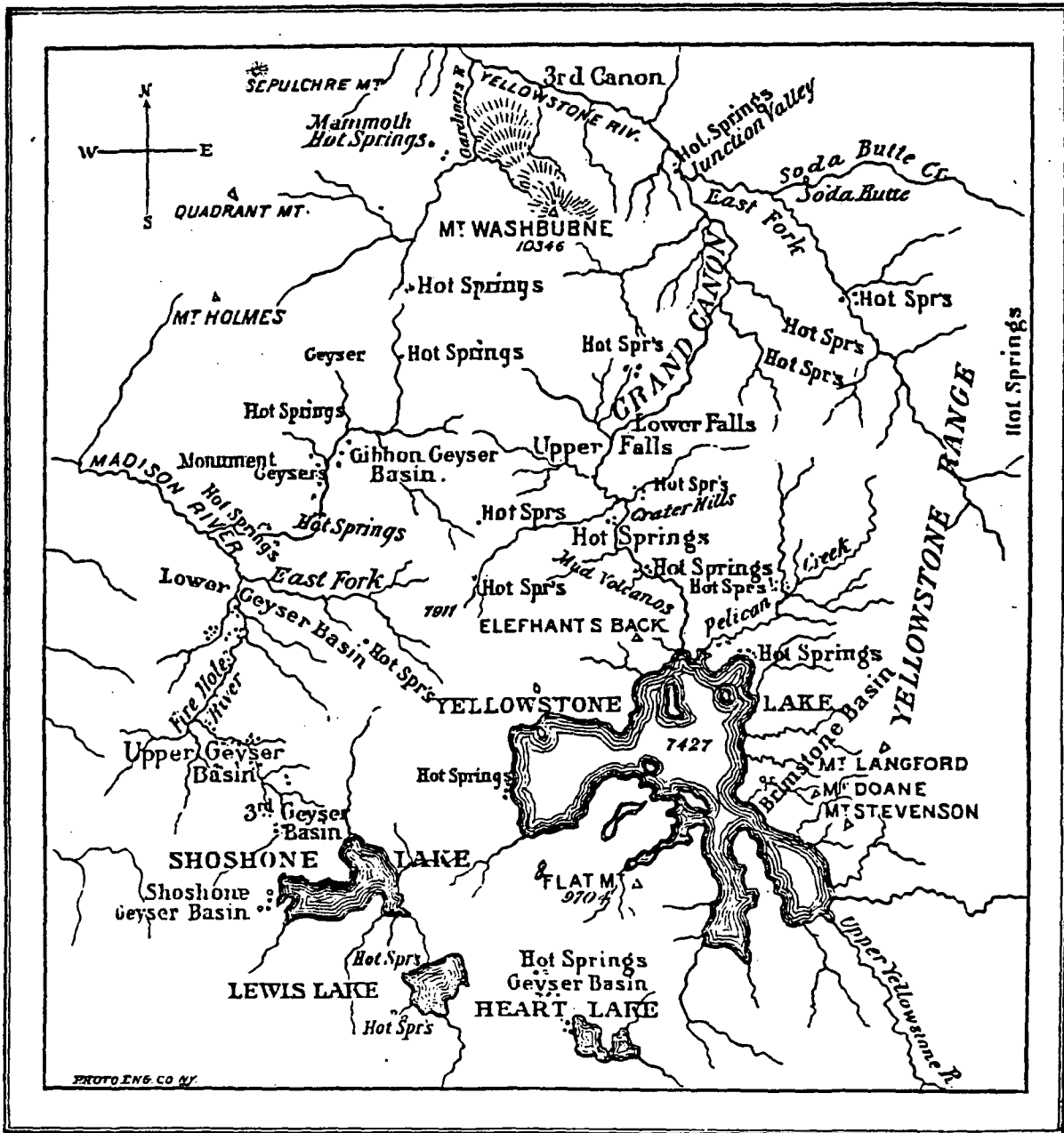


Fig. 4.14 The solubility of calcite in water at different partial pressures of carbon dioxide (from Ellis, 1959).

Ellis and Mahon, 1977



Map of Yellowstone National Park, showing distribution of Hot Springs.

Peale, 1883

Hydrothermal Explosion Craters

Characteristics of Pocket Basin

- 1200' x 2600' oval, surrounded by ridge
- inner slopes: 20-25°
- outer slopes: < 10°
- debris is hydrothermally cemented Bull Lake deposits
 - no primary volcanic rock
 - no bedrock rhyolite involved
- debris blown 3/4 mi
- waning stages of Pinedale

Many others in Yellowstone

Explosions occur in active hydrothermal areas

Triggered by rapid draining of glacial lake

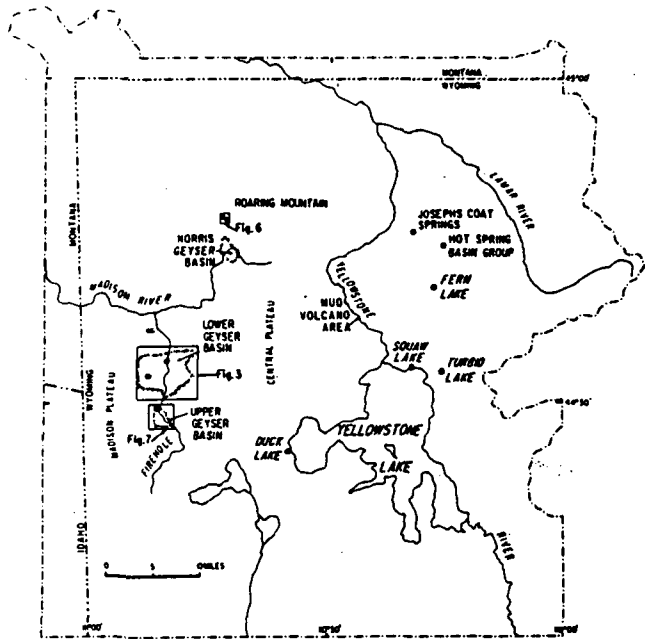


Figure 1. Map of Yellowstone National Park. Locations of hydrothermal explosion craters indicated by stars.

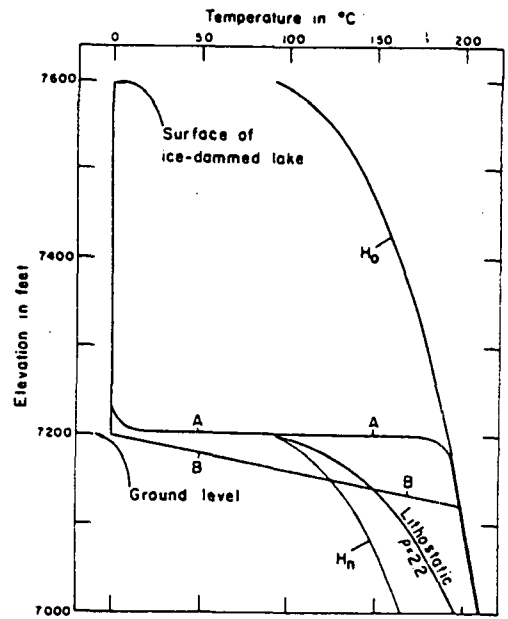
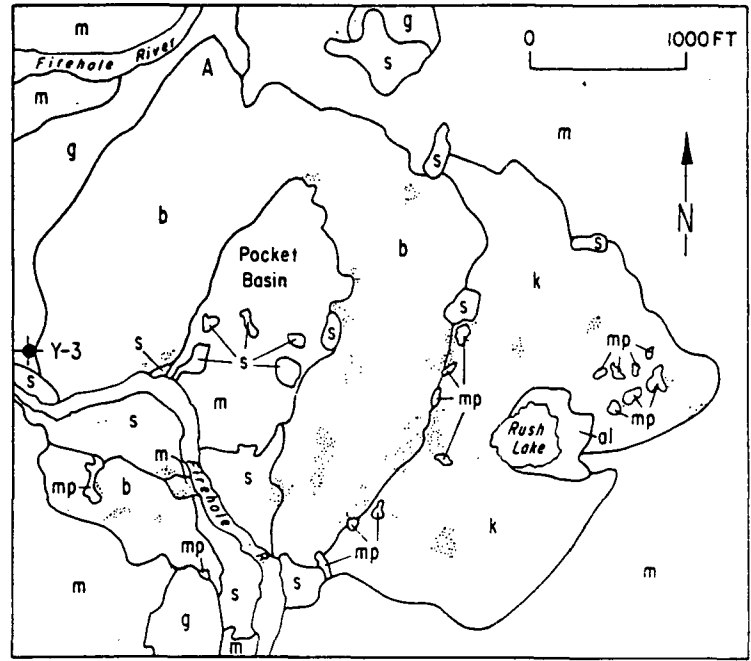


Figure 8. Graph illustrating how rapid draining of a glacially dammed lake could trigger a hydrothermal explosion. See text for explanation.



Figure 4. Annotated aerial photograph of Pocket Basin explosion crater. k, early Pinedale kames; b, hydrothermal explosion breccia; g, sand and gravel (early Pinedale outwash



deposits and subsequent alluvial deposits); s, sinter; m, silica mud; mp, mud pots; al, kaolinite alluvium. Dotted pattern denotes areas where

acid alteration is occurring. Locations of Y-3 drill hole and point A, probably a stubby mudflow, are also shown.

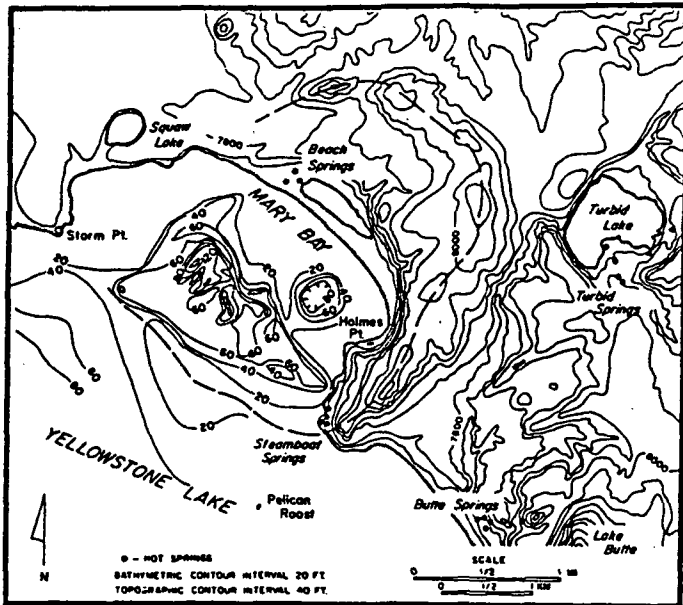


Fig. 3. Bathymetric contours of Mary Bay, offshore, are based on profiles 1-11. Topographic contours onshore are from the U.S. Geological Survey 15-min Canyon Village quadrangle sheet. Heavy dashed line is the outline of the Mary Bay hydrothermal explosion crater.

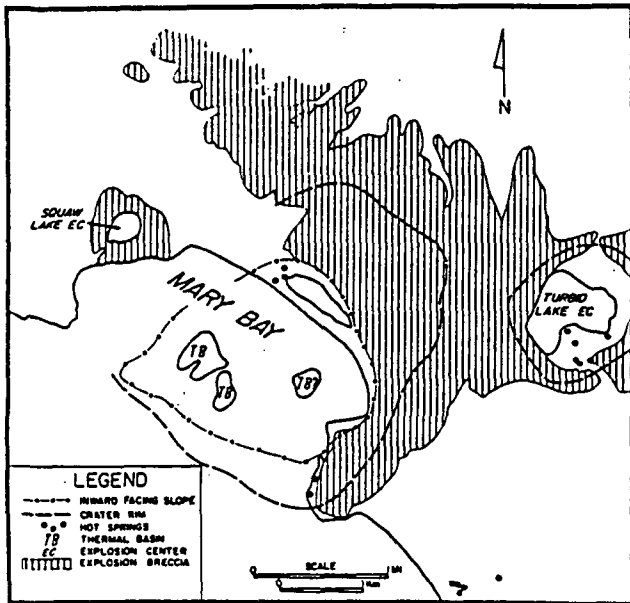


Fig. 5. Summary map of Mary Bay features. Distribution of explosion breccia from Christiansen and Blank (1973).

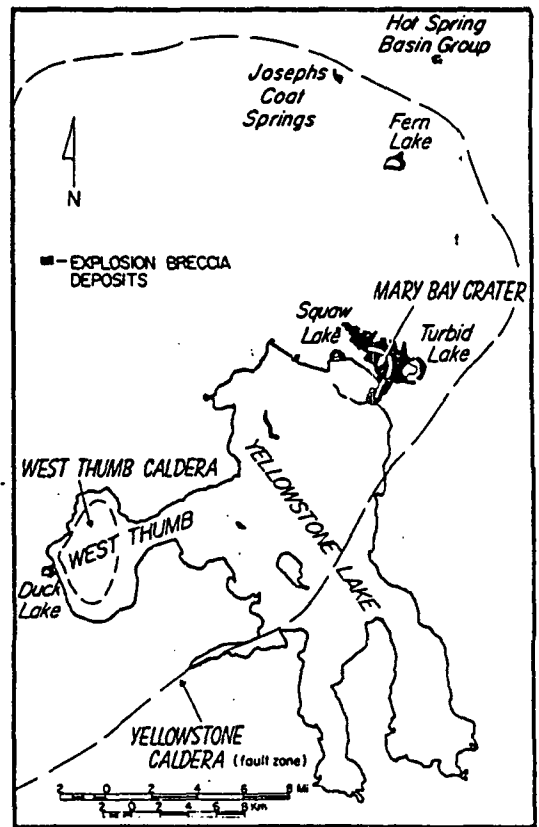


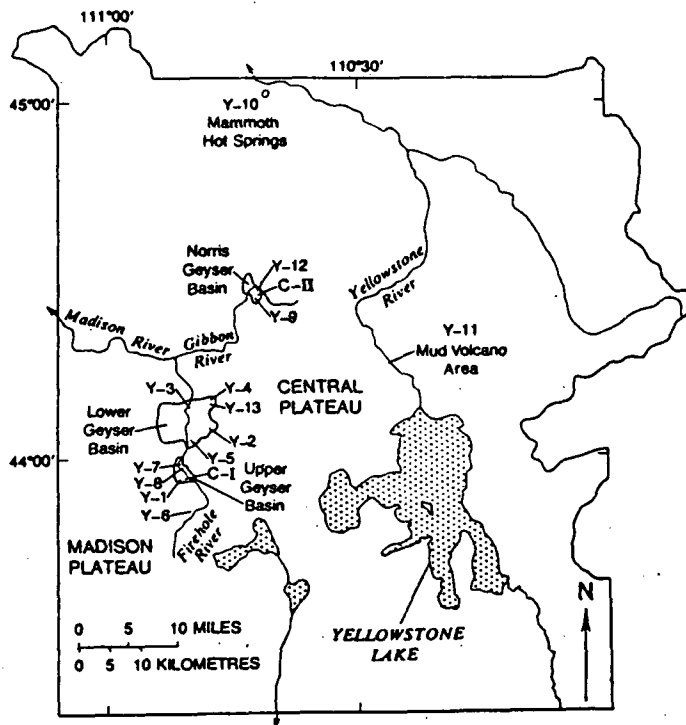
Fig. 6. Relation of Mary Bay to other hydrothermal explosion craters in Yellowstone Lake area (from Muffler et al., 1971).

Research Drilling

Carnegie Institute, 1929 and 1930 (Fenner, 1936)

Upper Basin
Norris Basin

U.S.G.S 1967, 1968 (White and others, 1975)



White and others,
1975

FIGURE 1—Map of Yellowstone National Park showing major geothermal areas and sites of research drill holes. U.S. Geological Survey holes are numbered Y-1 to Y-13 in order of drilling; holes drilled by the Carnegie Institution of Washington in 1929-30 are designated as C-I and C-II.

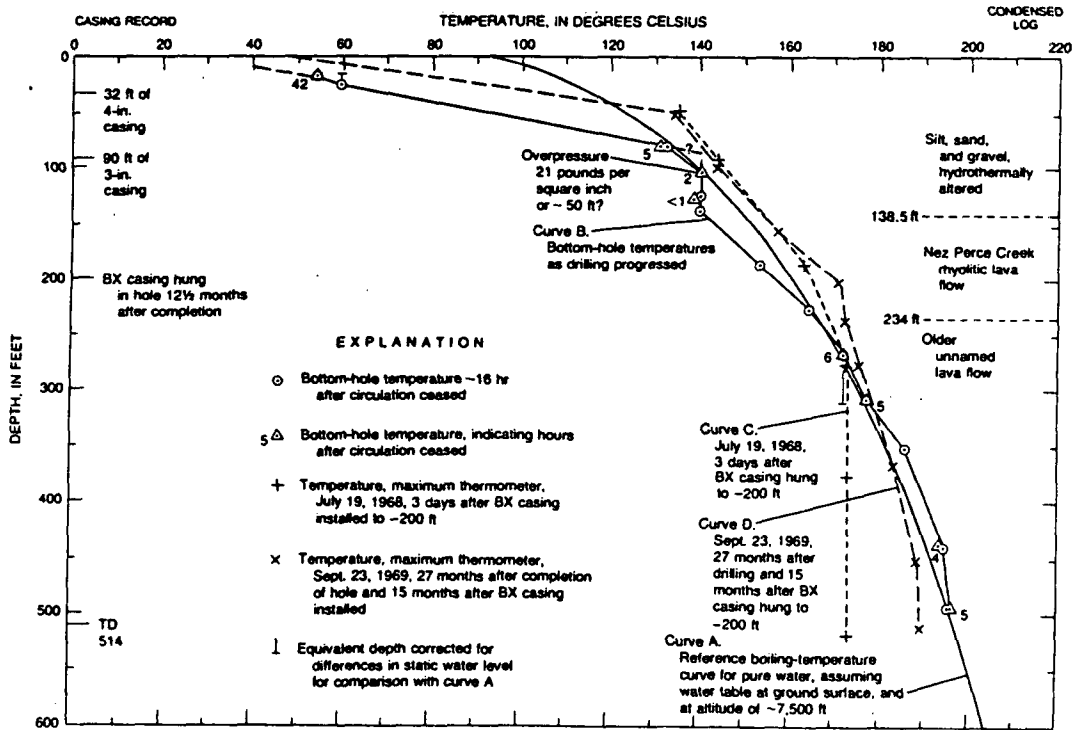


FIGURE 19.—Temperatures and other data, Y-3 (Ojo Caliente) drill hole, Lower Basin, near Pocket Basin

PHYSICAL RESULTS, DRILLING IN THERMAL AREAS, YELLOWSTONE NATIONAL PARK

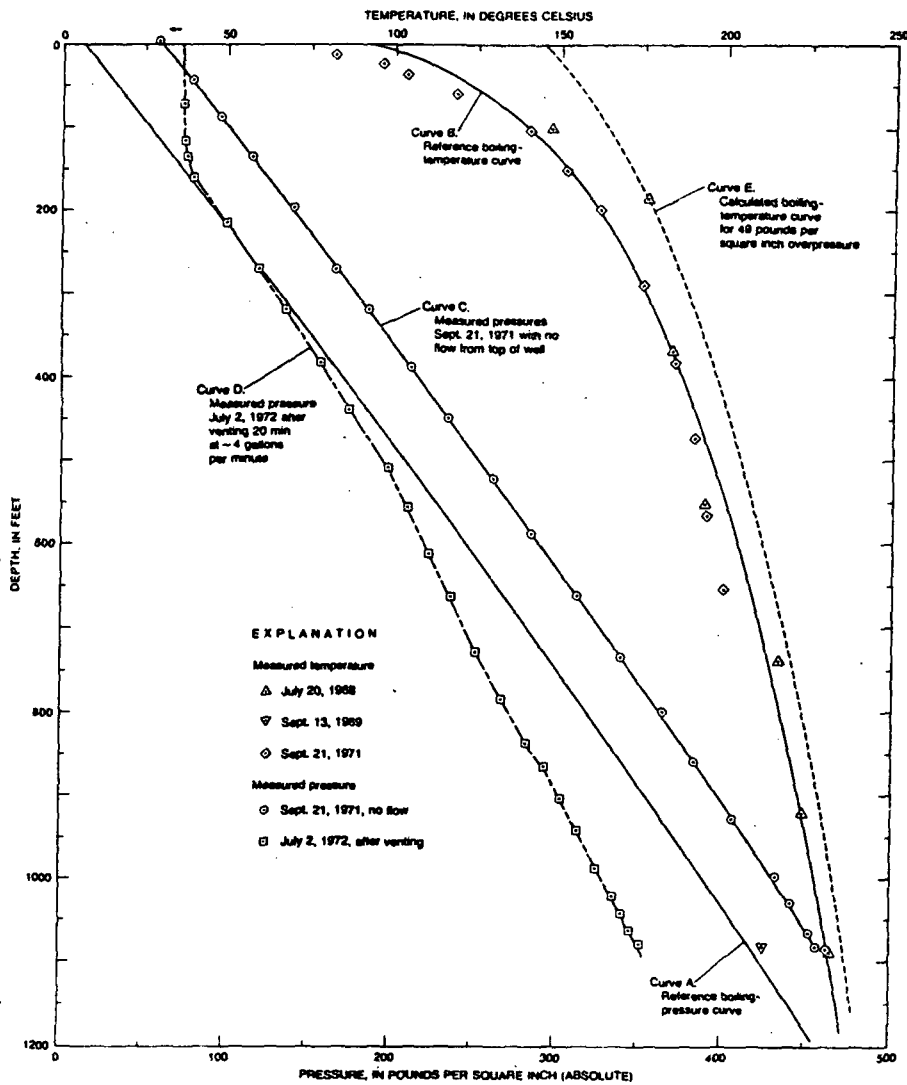


FIGURE 30.—In-hole temperatures and pressures of Y-12 drill hole after completion, compared with other data.

White and others,
1975

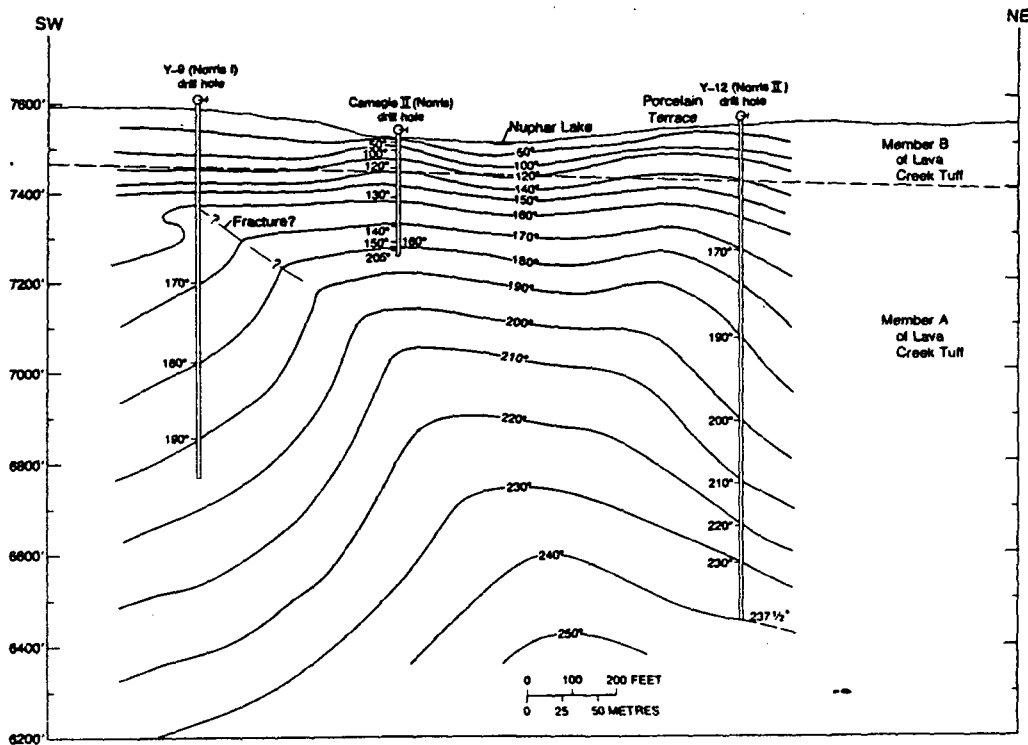


FIGURE 32.—Vertical section through Norris Basin drill holes Y-9, Carnegie II, and Y-12, showing bedrock, measured bottom-hole temperatures, and inferred temperature contours. Note contrast between measured and inferred temperatures in Carnegie II drill hole. The inferred fracture near Y-9 presumably connects with others (not shown) that account for the activity near Carnegie II and Congress Pool.

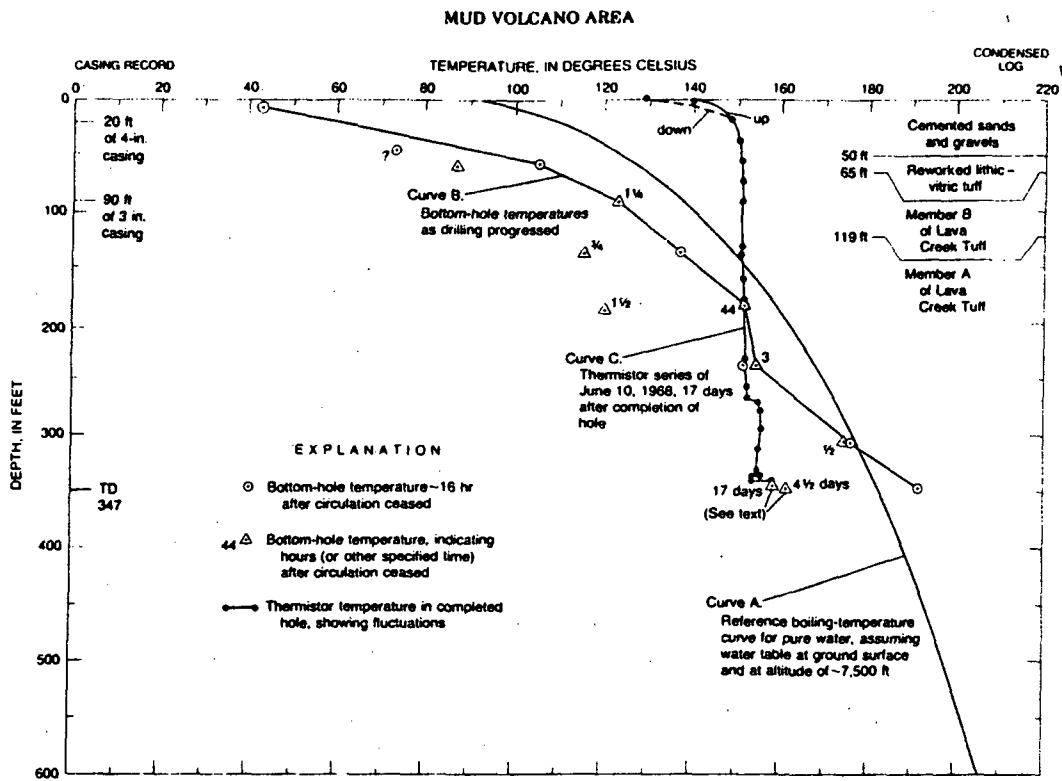


FIGURE 34.—Temperatures and other data, Y-11 (Sulphur Cauldron) drill hole, Mud Volcano area.

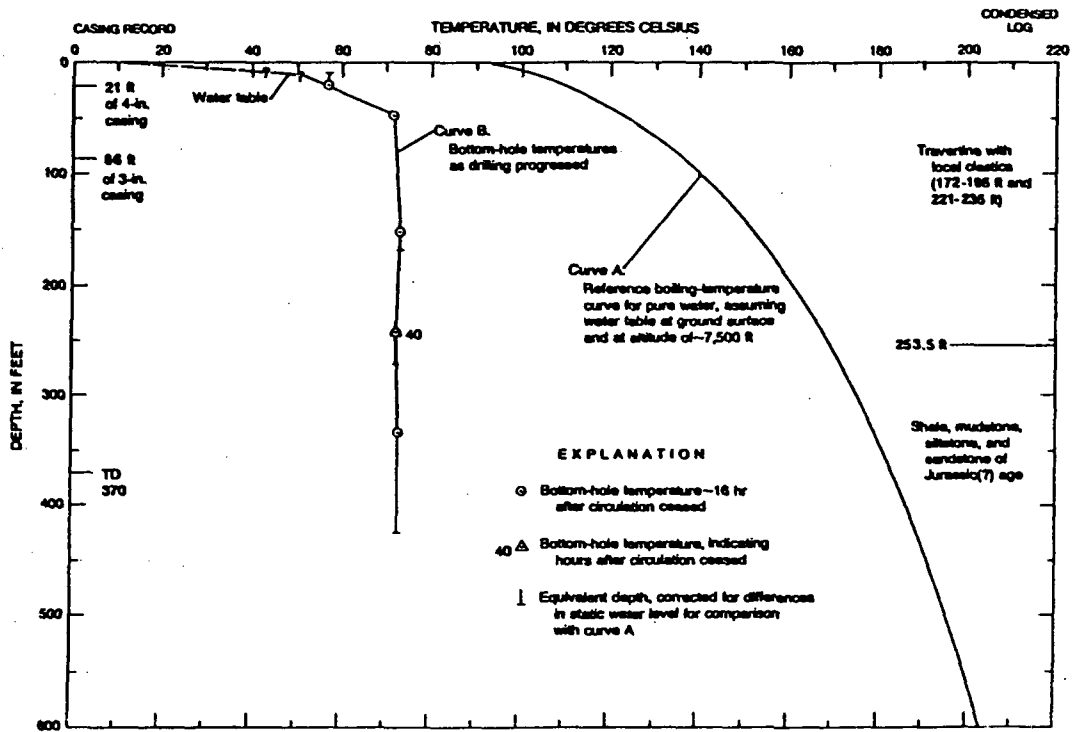


FIGURE 33.—Temperatures and other data, Y-10 (Mammoth Terrace) drill hole.

Geysers

Hot spring with intermittent eruption of hot water and steam

Requirements:

- thermal input
- water recharge
- proper plumbing

Associated with large convection systems

"Shallow" origin - base temp. $\sim 180^{\circ}\text{C}$

Natural eruptions follow sequence of White (1967)

Supercritical springs can be induced (Hague, 1889)

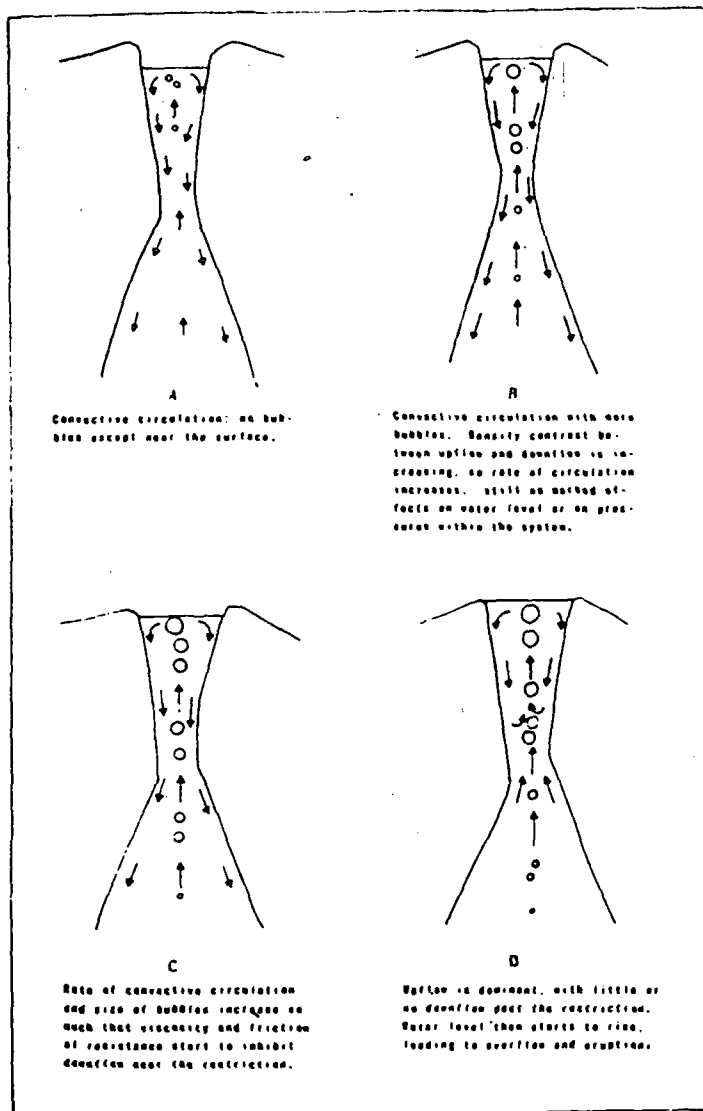


Fig. 12. Effects of increasing the number and size of bubbles in upflowing part of convection cell as temperatures increase, preliminary to overflow and eruption. Effects are most pronounced near restrictions but can also occur in vertical smooth-walled tubes of constant diameter.

White, 1967

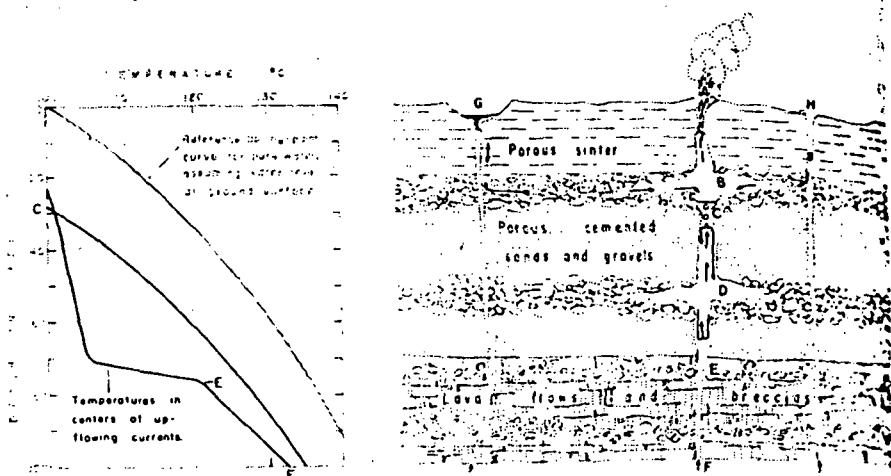


Fig. 13. Immediately after end of eruption and associated steam phase; water levels are at or near their minima, but temperatures are locally high.

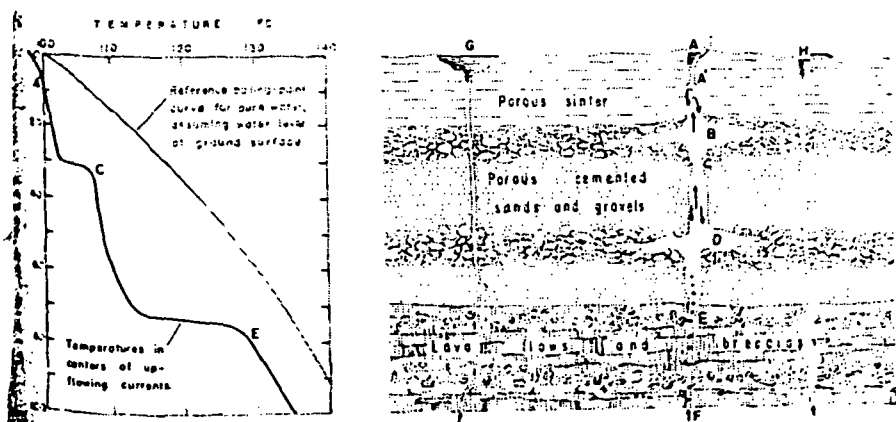


Fig. 14. End of water-recovery stage when one or more interconnected vents start to discharge again.

White, 1967

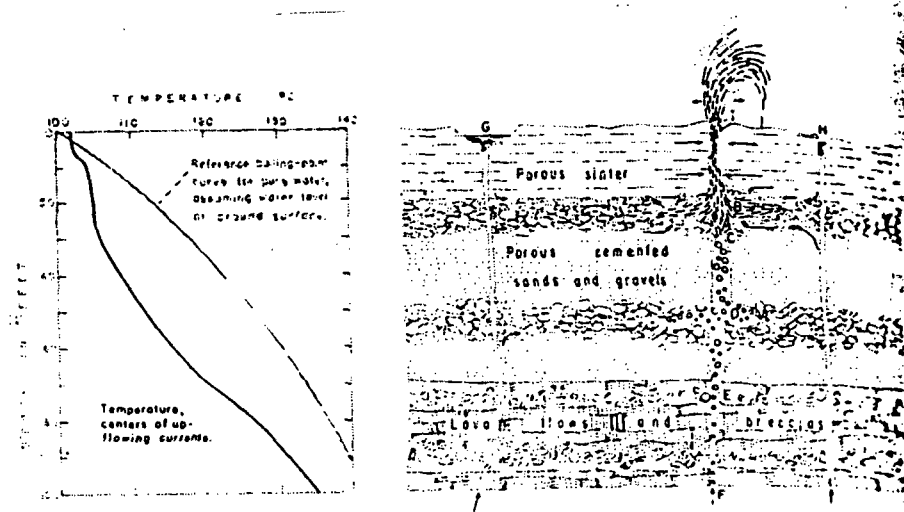


Fig. 15. Early bursting part of eruption phase; supplies of water and heat are abundant. A well-defined interface between liquid and vapor no longer exists, but a poorly defined zone in which vapor is the continuous phase migrates progressively downward during eruption and is here near point C.

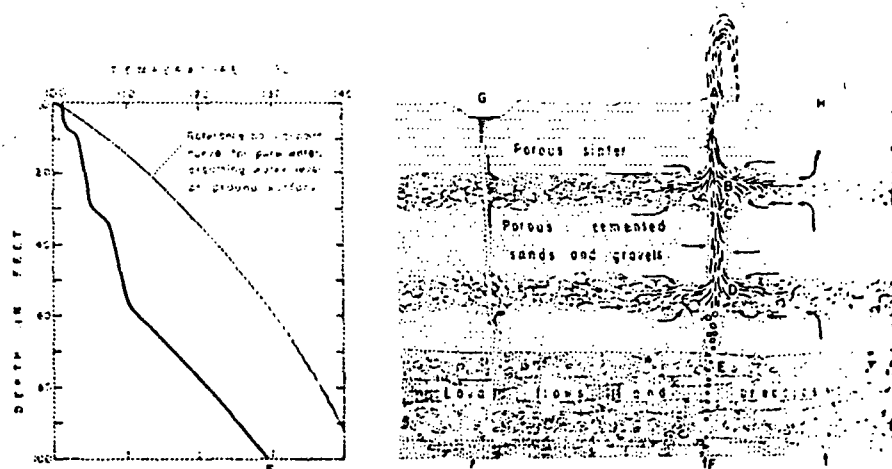


Fig. 16. Near the end of the eruption phase. Temperatures, pressures, and water supply are decreasing, and water must be erupted from increasingly greater average depth.

- Anderson, L. W., Anderegg, J. W., and Lawler, J. E., 1978, Model geysers: *Am. Jour. Sci.*, v. 278, p. 725-738.
- Bargar, K. E., 1978, Geology and thermal history of Mammoth Hot Springs, Yellowstone National Park, Wyoming: *U.S. Geol. Surv. Bull.* 1444, 55 p.
- Bargar, K. E., and Muffler, L. J. P., 1975, Geologic map of the travertine deposits, Mammoth Hot Springs, Yellowstone National Park, Wyoming: *U.S. Geol. Surv. Misc. Field Map* MF 659.
- Bryan, T. S., 1979, *The Geysers of Yellowstone*: Colo. Assoc. Univ. Press, 226 p.
- Ellis, A. J., and Mahon, W. A. J., 1977, *Chemistry and Geothermal Systems*: Academic Press, New York, 392 p.
- Fenner, C. N., 1936, Bore-hole investigations in Yellowstone Park: *Jour. Geol.*, v. 44, p. 225-315.
- Friedman, I., 1970, Some investigations of the deposition of travertine from hot springs - I. The isotopic chemistry of a travertine-depositing spring: *Geochem. Cosmochim. Acta*, v. 34, p. 1303-1315.
- Hague, A., 1889, Soaping geysers: *Science*, v. 13, p. 382-384.
- Hutchinson, R. A., 1982, Geologic and thermal highlights of Yellowstone, 1980-1982: unpub. MS., National Park Service, Mammoth, Wyoming, 12 p.
- Leeman, W. P., Doe, B. R., and Whelan, J., 1977, Radiogenic and stable isotope studies of hot-spring deposits in Yellowstone National Park and their genetic implications: *Geochem. Jour.*, v. 11, p. 65-74.
- Marler, G. D., 1973, Inventory of thermal features of the Firehole River Geyser Basins and other selected areas of Yellowstone National Park: N.T.I.S. PB-221 289, 639 p.
- Marler, G. D., and White, D. E., 1975, Seismic Geyser and its bearing on the origin and evolution of geysers and hot springs of Yellowstone National Park: *Geol. Soc. Am. Bull.*, v. 86, p. 749-759.
- Muffler, L. J. P., White, D. E., and Truesdell, A. H., 1971, Hydrothermal explosions craters in Yellowstone National Park: *Geol. Soc. Am. Bull.*, v. 82, p. 723-740.
- Muffler, L. J. P., White, D. E., Beeson, M. H., and Truesdell, A. H., 1982, Geologic map of Upper Geyser Basin, Yellowstone National Park, Wyoming: *U.S. Geol. Surv. Misc. Inv. Map* I-1371.
- Noguchi, K., and Nix, J., 1963, Geochemical studies of some geysers in Yellowstone National Park: *Japan Acad. Proc.*, v. 39, p. 370-375.

- Peale, A. C., 1883, The thermal springs of Yellowstone National Park, in, Hayden, F.V., 12th ann. rept. U.S. Geol. Geog. Surv. Territories, Part 11, p. 63-
- Pitt, A. M., and Hutchinson, R. A., 1982, Hydrothermal changes related to earthquake activity at Mud Volcano, Yellowstone National Park, Wyoming: Jour. Geophys. Res., v. 87, p. 2762-2766.
- Rinehart, J.S., 1980, Geysers and geothermal energy: Springer-Verlag, New York, 223 p.
- Rowe, J. J., Fournier, R. O., and Morey, G. W., 1965, Use of sodium iodide to trace underground water circulation in the hot springs and geysers of the Daisy Geyser Group, Yellowstone National Park: U.S. Geol. Surv. Prof. Paper 525B, p. B184-B186.
- Schoen, R., and Rye, R. O., 1970, Sulfur isotope distribution in solfataras, Yellowstone National Park: Science, v. 170, p. 1082-1084.
- Stauffer, R. E., Jenne, E. A., and Ball, J. W., 1980, Chemical studies of selected trace elements in hot-spring drainages of Yellowstone National Park: U.S. Geol. Surv. Prof. Paper 1044-F, 20 p.
- Truesdell, A. H., and Fournier, R. O., 1976, Conditions in the deeper parts of the hot spring systems of Yellowstone National Park, Wyoming: U.S. Geol. Surv. Open-file rept. 76-428, 29 p.
- White, D. E., 1967, Some principles of geyser activity mainly from Steamboat Springs, Nevada: Am. Jour. Sci., v. 265, p. 641-684.
- White, D. E., 1978, Conductive heat flows in research drill holes in thermal areas of Yellowstone National Park, Wyoming: Jour. Res. U.S. Geol. Surv., v. 6, p. 765-774.
- White, D. E., Muffler, L. J. P., and Truesdell, A. H., 1971, Vapor-dominated hydrothermal systems compared with hot-water systems: Econ. Geol., v. 66, p. 75-97.
- White, D. E., Fournier, R. O., Muffler, L. J. P., and Truesdell, A. H., 1975, Physical results of research drilling in thermal areas of Yellowstone National Park, Wyoming: U.S. Geol. Surv. Prof. Paper 892, 70 p.
- Wold, R. J., Mayhew, M. A., and Smith, R. B., 1977, Bathymetric and geophysical evidence for a hydrothermal explosion crater in Mary Bay, Yellowstone Lake, Wyoming: Jour. Geophys. Res., v. 82, p. 3733-3738.

Fluid-mineral equilibria in a hydrothermal system, Roosevelt Hot Springs, Utah

REGINA M. CAPUANO and DAVID R. COLE

Earth Science Laboratory Division, University of Utah Research Institute, 420 Chipeta Way, Suite 120, Salt Lake City, Utah 84108

(Received March 4, 1981; accepted in revised form March 30, 1982)

Abstract—The availability of fluids and drill cuttings from the active hydrothermal system at Roosevelt Hot Springs allows a quantitative comparison between the observed and predicted alteration mineralogy, calculated from fluid-mineral equilibria relationships. Comparison of all wells and springs in the thermal area indicates a common reservoir source, and geothermometer calculations predict its temperature to be higher ($288^{\circ}\text{C} \pm 10^{\circ}$) than the maximum measured temperature of 268°C .

The composition of the deep reservoir fluid was estimated from surface well samples, allowing for steam loss, gas release, mineral precipitation and ground-water mixing in the well bore. This deep fluid is sodium chloride in character, with approximately 9700 ppm dissolved solids, a pH of 6.0, and gas partial pressures of O_2 ranging from 10^{-32} to 10^{-35} atm, CO_2 of 11 atm, H_2S of 0.020 atm and CH_4 of 0.001 atm.

Comparison of the alteration mineralogy from producing and nonproducing wells allowed delineation of an alteration pattern characteristic of the reservoir rock. Theoretical alteration mineral assemblages in equilibrium with the deep reservoir fluid, between 150° and 300°C , in the system $\text{Na}_2\text{O-K}_2\text{O-CaO-MgO-FeO-Fe}_2\text{O}_3\text{-Al}_2\text{O}_3\text{-H}_4\text{SiO}_4\text{-H}_2\text{O-H}_2\text{S-CO}_2\text{-HCl}$, were calculated. Minerals theoretically in equilibrium with the calculated reservoir fluid at $>240^{\circ}\text{C}$ include sericite, K-feldspar, quartz, chalcedony, hematite, magnetite and pyrite. This assemblage corresponds with observed higher-temperature ($>210^{\circ}\text{C}$) alteration assemblage in the deeper parts of the producing wells. The presence of montmorillonite and mixed-layer clays with the above assemblage observed at temperatures $<210^{\circ}\text{C}$ corresponds with minerals predicted to be in equilibrium with the fluid below 240°C .

Alteration minerals present in the reservoir rock that do not exhibit equilibrium with respect to the reservoir fluid include epidote, anhydrite, calcite and chlorite. These may be products of an earlier hydrothermal event, or processes such as boiling and mixing, or a result of errors in the equilibrium calculations as a result of inadequate thermochemical data.

INTRODUCTION

ACTIVE geothermal systems provide a unique glimpse at the chemical and physical processes that take place during hydrothermal alteration and the influence that variations in temperature, pressure and chemical composition of thermal fluid have on the formation of alteration minerals. Detailed studies of the relationship between fluid chemistry and alteration mineralogy in geothermal systems are, however, lacking. In part, this represents the unavailability of complete fluid analyses and of detailed petrologic studies for most geothermal systems.

Extensive exploration in recent years at Roosevelt Hot Springs has made the necessary data available to study these processes. Seven wells, up to approximately 2000 m in depth, currently tap thermal fluids (Fig. 1). Chemical analyses of fluids and petrographic analyses of drill cuttings from several of these wells have been described (Ballantyne and Parry, 1978; Ballantyne, G., 1978; Nielson *et al.*, 1978; Parry, 1978; Rohrs and Parry, 1978; Glenn and Hulén, 1979; Bamford *et al.*, 1980; Glenn *et al.*, 1981). In most cases, however, these studies have focused on the individual wells rather than on the reservoir as a whole.

In this paper alteration mineralogy from the producing and nonproducing wells is compared and an alteration pattern characteristic of the reservoir rock

is defined. The composition of the deep reservoir fluid is calculated from analyses of liquid and steam samples from production well 14-2. Corrections are made for the effects of ground-water mixing, mineral precipitation, steam loss and gas release on the pH, gas partial pressures and element concentrations of the original reservoir fluid. Finally, mineral equilibria in the deep reservoir fluid are quantitatively evaluated at temperatures ranging from 150° to 300°C and compared to the alteration mineralogy of the reservoir rock.

GEOLOGY AND HYDROTHERMAL ALTERATION

Roosevelt Hot Springs thermal area, located in west-central Utah, covers approximately 32 sq km on the western margin of the Mineral Mountains (Fig. 1). The thermal reservoir occurs within fractured Precambrian gneisses and Tertiary granitic rocks of the Mineral Mountains pluton (Nielson *et al.*, 1978; Sibbett and Nielson, 1980). At least ten rhyolite domes occur along the crest of the Mineral Mountains, representing igneous activity between 0.5 and 0.8 million years ago. A deep-seated magma body related to this young rhyolitic volcanism is a possible heat source for the present geothermal system (Smith and Shaw, 1975).

The western boundary of the geothermal system is defined by the northeast-trending Opal Mound fault (Fig. 1). Wells drilled east of this fault, except 52-21 and 24-36, produce commercial quantities of fluid, whereas the two wells drilled west of the fault (9-1 and 82-33) do not (Fig. 1) (Forrest, 1980).

Drill cuttings are available for study from four geother-

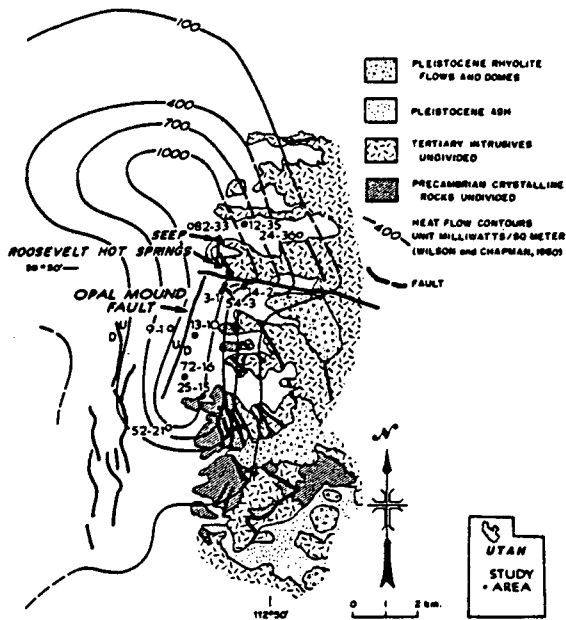


FIG. 1. Generalized geologic map of the Roosevelt Hot Springs thermal area, taken from Nielson and Moore (1979). Closed circles represent geothermal production wells and open circles represent nonproducing wells, as defined by Forrest (1980). Triangles indicate areas of surface seepage. The heat flow contours are taken from Wilson and Chapman (1980).

mal exploration wells, including the producing wells 72-16 and 14-2, and the nonproducing wells 52-21 and 9-1. Mineralogic descriptions of the cuttings from these wells are taken from the work of Ballantyne and Parry (1978), Bal-

lantyne, G. (1978), Nielson *et al.* (1978), Parry (1978), Rohrs and Parry (1978), Glenn and Hulen (1979) and Glenn *et al.* (1981). Petrographic studies of alteration mineralogy of these drill cuttings were limited by the small chip size which prohibited the accurate determination of paragenetic relationships.

Lithologies found in producing wells 72-16 and 14-2, and nonproducing wells 52-21 and 9-1, consist of arkosic alluvium overlying interfingering gneisses and granitic rocks. Alteration in these wells occurs mainly along faults and fractures that mark past and present fluid channels and appears to be largely independent of rock type.

Three alteration assemblages are recognized at depth in producing wells 72-16 and 14-2 (Fig. 2). These include an upper assemblage (I) characterized by the occurrence of montmorillonite, mixed-layer clays and epidote, a transition assemblage (II) present only in well 14-2, and a lower assemblage (III) that in contrast to the upper zones contains minor anhydrite and greater abundances of chlorite after plagioclase, pyrite and calcite. Despite these differences both zones contain chlorite after mafic minerals, limonite-hematite, quartz, sericite and traces of chalcocopyrite. Chalcocopyrite is present in both zones of well 72-16 but absent from well 14-2. K-feldspar is common in rocks of the reservoir and is described as an alteration phase in both 72-16 and 14-2. It is very difficult, however, to distinguish hydrothermal K-feldspar from perthitic, anti-perthitic and micrographic K-feldspar in gneisses and granitic rocks when examining only cuttings (Nielson *et al.*, 1978), and therefore it is considered as a questionable alteration product. Magnetite-ilmenite, although present as primary phases in wells 14-2 and 72-16, are also described as alteration products in 72-16.

Although these zones occur at considerably different depths in wells 72-16 and 14-2, their measured temperatures are very similar (Fig. 2). The highest measured temperatures for assemblage I in wells 72-16 and 14-2 are 196° and 210°C, respectively. The lower-most assemblage

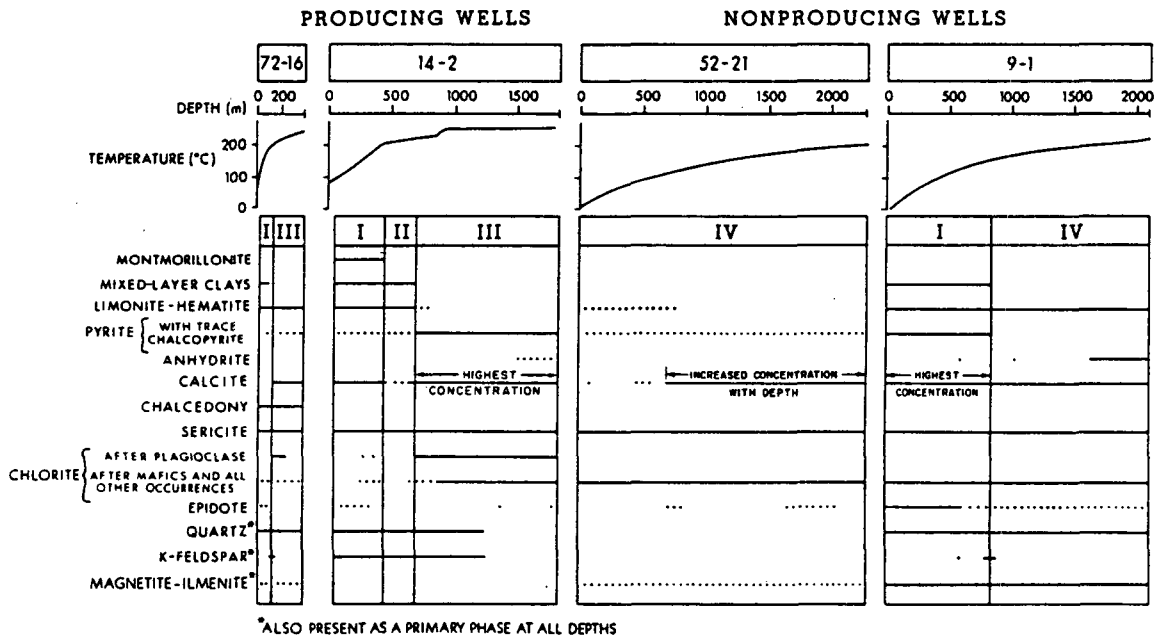


FIG. 2. Alteration mineralogy and temperature log data for wells 72-16, 14-2, 52-21 and 9-1, Roosevelt Hot Springs thermal area. Mineralogic and temperature-log data taken from Ballantyne and Parry (1978), Ballantyne, G. (1978), Nielson *et al.* (1978), Parry (1978), Rohrs and Parry (1978), Glenn and Hulen (1979) and Glenn *et al.* (1981). When more than one temperature log was available, the log that recorded the highest overall temperatures was used. A solid line indicates minor abundances; a dotted line indicates trace abundances.

(III) corresponds to temperatures ranging from 196°C to the bottom-hole temperature of 243°C in well 72-16 and from 224°C to the bottom-hole temperature of 268°C in well 14-2.

The alteration assemblage in nonproducing well 52-21 (assemblage IV) is markedly different from assemblages observed in the producing wells and includes sericite, chlorite (after mafic minerals), calcite and traces of hematite, pyrite, chalcopryrite, epidote and magnetite-ilmenite. The abundances of these alteration minerals are similar throughout the well with the exception of calcite and epidote which increase in concentration with depth, and hematite which only occurs above 762 m. Quartz and K-feldspar are present throughout the well, although not considered alteration products. The maximum measured temperature in well 52-21 is 204°C.

Alteration mineral assemblages in well 9-1 (although a nonproducing well) exhibit characteristics comparable to both nonproducing well 52-21 and the two producing wells 14-2 and 72-16. The upper mineral assemblage (I) in well 9-1 occurs above a major fault zone at 844 m and contains mixed-layer clays and epidote. This assemblage resembles the lower-temperature assemblages found in the producing wells (assemblages I and II). On the other hand, below 844 m in well 9-1, the lower alteration assemblage is characterized by the absence of chlorite after plagioclase and is most similar to the alteration assemblage observed in nonproducing well 52-21 (assemblage IV). An exception to this similarity, however, is the presence of trace amounts of anhydrite in assemblage IV of well 9-1. Measured temperatures in the upper zone of 9-1 (assemblage I) are less than 160°C, whereas in the lower portion of the well (assemblage IV) they range from 160°C to the bottom hole temperature of 224°C.

The apparent similarity between alteration minerals present in the upper portion of well 9-1 and the upper alteration assemblages found in the production wells suggests that at one time there was an influx of thermal fluid into the rocks above 844 m in well 9-1. Although well 9-1 is presently devoid of free-flowing thermal fluid, Glenn *et al.* (1981) have recognized a zone above the major fault at 844 m that is more fractured and altered than rock encountered in deeper portions of the well.

Several hydrothermal events have altered the rocks in the Roosevelt Hot Springs thermal area. Consequently, it is difficult to separate alteration assemblages produced by the present geothermal event from those of earlier events (i.e., Tertiary alteration associated with Cu-Pb-Zn mineralization (Bamford *et al.*, 1980)). Nevertheless the mineralogic relationships described for wells 72-16, 14-2, 52-21 and 9-1 suggest that alteration assemblages characteristic of the producing wells are related to the present thermal event. This argument is supported by the similarity in the zoning sequences found within the two producing wells, 14-2 and 72-16, and the differences between alteration assemblages found in producing and nonproducing wells.

FLUID CHEMISTRY

Chemical analyses of fluids from wells and springs in the Roosevelt Hot Springs area (Table 1) indicate that four types of water are present: 1) deep circulating thermal fluid tapped by producing wells 14-2, 54-3, and 72-16; 2) hot water from nonproducing wells 9-1 and 52-21; 3) recent discharge from the Roosevelt seep; and 4) water from the now dry Roosevelt Hot Spring. Fluid from wells that do not produce has a composition clearly different from production well fluid. The temperature and concentration of Na, K, F, Cl and total dissolved solids are lower

in fluid discharged from nonproductive wells, whereas Ca, Mg, Fe, SO₄ and HCO₃ are more concentrated. Spring water from the Roosevelt seep is similar to nonproducing well fluid, exhibiting greater concentrations of Ca, Mg and HCO₃ than producing well fluid. The total dissolved solids content of fluid discharged from the seep, however, is in the same range as that measured for production wells. Fluid from the now dry Roosevelt Hot Spring is similar to producing well fluid but has higher Mg and lower Si concentrations.

Comparison of the compositions of the Roosevelt fluids, however, suggests they are derived from a common reservoir source and that variations in composition are due largely to ground-water mixing. Local ground water is enriched in Ca, Mg, Fe, SO₄ and HCO₃ and depleted in Na, K, F and Cl relative to the thermal fluid (Mower and Cordova, 1974). This compares well with enrichments and depletions in nonproducing well fluids relative to production well fluid to indicate that nonproducing well fluid is mixed with local ground water.

The extent of ground-water mixing with thermal fluid in the Roosevelt geothermal system tends to increase with distance from well 54-3 (Fig. 3). The minimum mixing percents for fluid from wells 14-2, 72-16, 9-1 and 52-21 average 7, 12, 17 and 21%, respectively, whereas the maximum amounts of ground-water mixing with fluids discharged from the Roosevelt seep and hot spring average 25 and 11%, respectively. These relationships suggest that well 54-3 and other nearby producing wells have the most direct access to the reservoir. Contouring of heat flow data from the Roosevelt thermal area (Fig. 1) produces a similar pattern, with the highest heat flow corresponding to areas of least mixing.

An enthalpy-chloride diagram (Fig. 4) (Truesdell and Fournier, 1976; Fournier, 1979) is used to calculate the percentage of ground-water mixing. This diagram employs the bottom-hole temperatures and fluid chloride concentrations listed in Table 1 and calculated percentages of steam loss listed in Table 2. Fluid from well 54-3 (sample 5) is taken as the well fluid having the lowest percentage of ground water because it exhibits the highest enthalpy and chloride concentrations in relation to the other wells. For the purposes of these calculations, 54-3(5) is designated as zero-percent mixed. This assumption allows minimum percentages of ground-water mixing to be calculated for other well fluids using Fig. 4 (Fournier, 1979). Estimation of the percent mixing for surface seepages is complicated, however, by uncertainties in their cooling history. Assuming that surface seepages cooled entirely by steam loss to 100°C, the maximum percentages of ground water in fluids discharged from the Roosevelt seep and hot spring are calculated using Fig. 4 (Fournier, 1979).

Fluids from producing wells have undergone single-stage liquid-vapor separation in the well bore. The fraction of isoenthalpic steam separation, X_p , can

Table 1. Chemistry of Thermal Water¹

Sample No Well: Utah State	^{1,10} 14-2	^{2,11} 14-2	3 14-2	4 14-2	^{5,12} 54-3	6 72-16	7 72-16	8 52-21	9 9-1	10 Hot Spring	11 Hot Spring	12 Seep	13 Seep
Reference ² Collection Date	1 5/78	1 7/78	2 11/77	2 11/77	3 11/79	2 4/77	2 4/77	4 11/78	5 10/75	6 11/50	6 9/57	7 5/73	7 8/75
Na	2070	2340	2150	2200	2320	1800	2000	1900	1780	2080	2500	2400	1800
K	384	419	390	410	461	380	400	216	440	472	488	378	280
Ca	11	6.8	9.2	6.9	8	12.4	12.20	107	69.1	19	22	113	107
Mg	0.28	<0.24	0.6	0.08	<2	0.29	0.29	4.0	1.0	3.3	0	17	23.6
Fe	0.13	<0.02			0.03			6.3	0.370				
Al	0.31	<0.28			<0.5			<0.1			0.04		
Si			229	383	263	238	244	65	178	189	146	36	50
Sr	1.44	1.28			1.2	1.36	1.20						
Ba	0.24	<0.24			<0.5								
As	3.2	3.6	3.0	2.2	4.3								
Li	25	28			25.3	15.0	16.0				0.27		17
Be	0.004	<0.004			0.005								
B	23	25	29	28	29.9	26.4	27.2	27.0	28.2		38	37	29
Ce	<0.20	<0.20			0.27								
F			5.2	4.8	6.8	5.2	5.3	3.6		7.1	7.5	5.2	3.3
Cl			3650	3650	3860	3110	3260	2880	2860	3810	4240	3800	3200
HCO ₃					232	181	181	615.0	485	158	156	536	300
SO ₄			78	60	72	33	32	85	120	65	73	142	70
NO ₃								1.3	<0.2	1.9	11	tr.	tr.
T.D.S. ³			>6614*	>6745*	7504	6074	6444	5677	5715*	7040	7800	7506	5948
pH (collection T)			5.9	6.2	9	7.83	7.53	6.8	7.3		7.9	8.2	6.43
T (collection)			14	9						85	55	17	28
T (bottom hole) ⁴	268	268	268	268	>260 ⁵	243	243	204	225 ⁶				
Total depth (m) ⁵	1862	1862	1862	1862	878	382	382	2289	2098				
Geothermometers													
T (Na-K-Ca)(-Mg) ⁷	284	291	286	293	297	289	288	209*	278	283*	284	181*	141*
T (quartz cond) ⁸			276	302	263	254	256	156	228	234	212	123	141
T (quartz adiab) ⁸			244	268	234	227	229	149	207	211	194	121	136

¹For well locations, see Figure 1. Element concentrations are reported in mg/l and temperatures in °C. A blank indicates data not determined or information not available, and tr indicates trace amounts measured.

²References: 1 = Bamford et al. (1980), 2 = Thermal Power Co. (1978), 3 = This report, 4 = Getty Oil Co. (1978), 5 = S. D. Johnson (personal communication, 1980), 6 = Mundorff (1970), 7 = Lenzer et al. (1976).

³Total dissolved solids. Starred values were calculated in this study by summing ion concentrations (Hem, 1970).

⁴Glenn and Hulen (1979).

⁵Koenig and Gardiner (1977).

⁶Geothermal Resources Council Bulletin, 1979, P. O. Box 98, Davis California, Vol. 8, No. 8, p. 6.

⁷Calculated using the methods of Fournier and Truesdell (1973, 1974). The starred values are magnesium corrected (Fournier and Potter, 1979).

⁸Calculated using the methods of Fournier (1977).

⁹Elements analyzed for but present at concentrations less than ICPQ limits of quantitative detection (Bamford et al., 1980) include Mn, Cu, Pb, Zn, P, Ti, V, Cr, Co, Ni, Mo, Cd, Ag, Au, Sb, Bi, U, Te, Sn, W, Zr, La, and Th.

¹⁰Sample supplied by J. R. Bowman, Univ. of Utah. Silica was not preserved in this sample and therefore is not reported.

¹¹Sample supplied by A. H. Truesdell, U.S.G.S. Silica was not preserved in this sample and therefore is not reported.

¹²Chemical analyses on this sample were completed on fluid filtered to 0.45 μ in the field as follows: fluoride, chloride, and total dissolved solids were determined employing specific ion electrode, silver nitrate titration, and gravimetric methods, respectively; sulfate was determined gravimetrically on samples treated with 1% acid in the field; all other elements were determined by Inductively Coupled Plasma Quantometer on fluid diluted with 20% nitric acid in the field.

be calculated from the relation

$$X_g = (h_{f,Ti} - h_{f,Tc}) / (h_{g,Tc} - h_{f,Tc}) \quad (1)$$

where h_g and h_f are the enthalpies of saturated steam and saturated liquid, respectively, at both the initial temperature, T_i , of the deep reservoir fluid and final temperature, T_c , of the fluid at the collection site. Steam-loss fractions calculated for fluid samples from wells 14-2, 72-16 and 54-3 are listed in Table 2. Truesdell (Thermal Power Co., 1978) has calculated the presence of less than 1.5% steam in the Roosevelt reservoir, indicating that the fluid is very near liquid-vapor equilibrium. Therefore, it was not necessary to correct for excess or insufficient enthalpy

in the reservoir fluid in these steam-loss calculations.

Interpretation of geothermometer calculations allows prediction of the deep reservoir fluid temperature to be 288°C \pm 10°, compared to the maximum measured temperature of 268°C (Table 1). Calculated cation-geothermometer temperatures for producing well fluids, as listed in Table 1, range from 284° to 297°C. Cation-geothermometer temperatures, however, may be unreliable if uncorrected for the occurrence of calcite scaling (Fournier and Truesdell, 1973) in Roosevelt production wells. Sulfate-water isotopic geothermometer temperatures for samples from two Roosevelt production wells predict reservoir temperatures of 278° and 280°C (Nehring and Mariner, 1979). In addition, a minimum tem-

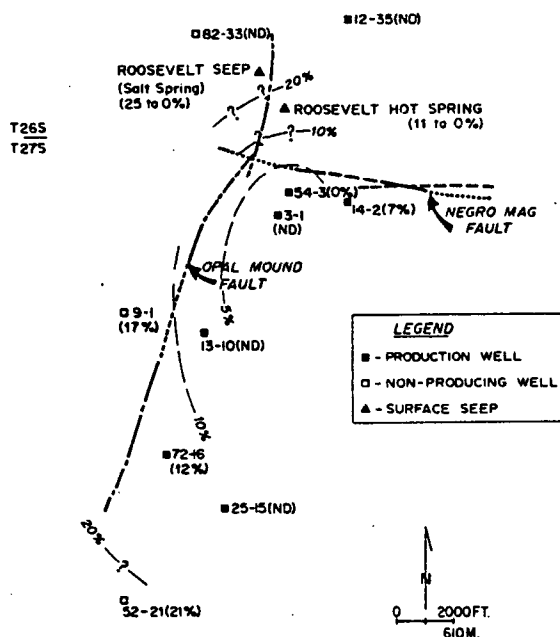


FIG. 3. Average percentage mixing of nonthermal ground water with the thermal reservoir fluid, Roosevelt Hot Springs thermal area. The percentage of mixing is included in parentheses after the well number. ND indicates not done. Refer to Fig. 1 for the location of this area.

perature for the reservoir fluid of 284° is estimated from the point of intersection of lines A and B on the enthalpy-chloride diagram (Fig. 4) (see Fournier, 1979).

CALCULATION OF DEEP RESERVOIR FLUID CHEMISTRY

The composition of the deep reservoir fluid was estimated from calculations that account for the effects of ground-water mixing, steam loss, gas release and mineral precipitation in the well bore on the pH, gas partial pressures and element concentrations of the original reservoir fluid. Fluid samples from well 14-2 are used for these calculations because they are the only samples for which all the necessary data,

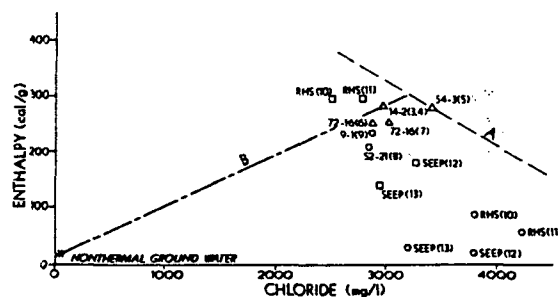


FIG. 4. Enthalpy-chloride diagram, Roosevelt Hot Springs thermal area. Data and sample numbers on this figure are taken from Tables 1 and 2. The local nonthermal ground water composition is taken from Mower and Cordova (1974). Triangles represent producing well fluid compositions corrected for steam loss, squares represent nonproducing well and surface seep samples assuming conductive cooling. Curves "A" and "B" are the upper bounding boiling and mixing curves, respectively. "RHS" denotes Roosevelt Hot Spring. This diagram was constructed employing the methods described by Fournier (1979).

including gas analyses (A. H. Truesdell, unpublished data, 1979), are available. In the absence of required data from other production wells, 14-2 well fluid was considered adequate to represent the reservoir fluid composition because, as concluded in the previous section, production well fluids all have similar compositions and are probably derived from a common source. These 14-2 samples, in particular (3) and (4), are reliable in that they were chemically preserved and filtered at the sample site. Also, chemical and isotopic data indicate that the steam and liquid have undergone nearly complete separations (Thermal Power Co., 1978).

The composition of 14-2 well fluid used in the reservoir fluid calculations (Table 3) represents the average of analyses 14-2(1) through 14-2(4). The average analysis corrected for concentration by 18% steam loss is also given in Table 3. Because the HCO₃ content of these samples was not measured, the HCO₃ concentration present in the least mixed fluid 54-3(5), corrected for 12% steam loss, is used.

An average fluid analysis corrected for both con-

Table 2. Fraction of Steam Separated from Flashed Well Fluids

Well	Sample No. ¹	Collection Pressure ² (atm)	Collection Temperature ³ (°C)	Reservoir Enthalpy (cal/g)	Reservoir Temperature ⁴ (°C)	Steam Fraction
14-2	1,2,3,4	12.83 ⁵	192	277 ⁵	265	0.18
54-3	5	23.61 ⁶	222	277 ⁷	265	0.11
72-16	6,7	20.38 ⁵	214	250 ⁵	242	0.07

¹See table 1.
²At the separator. These are absolute values excepting for 54-3 (see footnote 6).
³Determined from the collection pressure assuming liquid-vapor equilibrium (Keenan et al., 1969).
⁴Determined from the reservoir enthalpy assuming liquid-vapor equilibrium (Keenan et al., 1969).
⁵Thermal Power Co. (1978).
⁶Written communication (S. D. Johnson, 1980). This is a gauge pressure rather than absolute, therefore the calculated steam fraction is a minimum value.
⁷Data is lacking on the reservoir enthalpy at the base of well 54-3, therefore the enthalpy is assumed equivalent to that of the nearby producing well 14-2.

Table 3. Composition of Reservoir Fluids from Well 14-2

Element	Average analysis	Average analysis corrected for	
		steam loss	steam loss gas loss scaling
Na (mg/l)	2190	1800	1800
K	401	329	329
Ca	8	7	12
Mg	0.32	0.26	0.26
Fe	<0.08	<0.06	<0.06
Al	<0.30	<0.24	<0.24
Si	341	280	280
Cl	3650	2990	2990
C	206	206	1790
S	69	57	138
T.D.S. ^a	6680		9707
Geothermometers			
T(Na-K-Ca) ^b °C			277
T(SiO ₂ cond.) ^c °C			269

^aT.D.S. represents total dissolved solids calculated by the method of Hem (1970). In accord with Hem's treatment of HCO₃, H₂CO₃ is converted by a gravimetric factor (H₂CO₃ (mg/l) x 0.4837 = CO₂ (mg/l)) which assumes half of the H₂CO₃ is volatilized as CO₂. This value is used in the summation.

^bCalculated using the methods of Fournier and Truesdell (1973, 1974).

^cCalculated using the methods of Fournier (1977).

centration by 18% steam loss and dilution through 7% mixing was also determined. Both of these fluids were considered because it is not known whether mixing occurred in the well bore or reservoir. Mineral-fluid equilibrium calculations on both these calculated fluids produced very similar results. Therefore, the fluid corrected only for steam loss is discussed in this paper.

Because well 14-2 is cased to 551 m (Glenn and Hulen, 1979), sampled waters are assumed to represent a composite of fluids derived from 551 m to at least 1830 m, the total depth of the well. Well log temperatures in this depth interval vary from 210° to 268°C (Glenn and Hulen, 1979). The only significant hot-water entry occurs at 869-881 m (Bamford *et al.*, 1980), where the recorded well log temperature is 250°C.

Methodology for equilibrium calculations

The distribution of element concentrations among aqueous species is calculated using a modification of the computer program PATH (Helgeson *et al.*, 1970; Knight, 1976). The sources of thermochemical data for aqueous species considered in these calculations are Helgeson (1969), supplemented by data from Kharaka and Barnes (1973), Bladh (1978) and Rimstidt (1979). Thermochemical equilibrium constants for minerals and gases are calculated using data reported by Helgeson *et al.* (1978).

In these calculations, the standard state for H₂O and intercrystalline standard state for solids are consistent with unit activity of the pure component at

any pressure and temperature. The intracrystalline standard state for minerals calls for all activity coefficients of atoms on the lattice sites of solid solutions to approach unity as the mole fractions of the atoms on the sites approach those in the thermodynamic components of the solid at any pressure and temperature. The standard state for aqueous species, other than H₂O, is one of unit activity in a hypothetical one molal solution referenced to infinite dilution at any pressure and temperature. For gases the standard state is one of unit fugacity of the hypothetical ideal gas at one bar and any temperature.

Component activities accounting for nonstoichiometry of sericite and chlorite in rock samples from well 14-2 are calculated from electron microprobe analyses reported by Ballantyne, J. (1978, 1980) and are shown in Fig. 5. The specific expressions for calculating the activities of the components, listed in Table 4, are derived from the general equations relating site occupancy in a mineral to the activity of the thermodynamic component as presented by Helgeson *et al.* (1978, Equations (46) through (52)), and from preferential site occupancies as de-

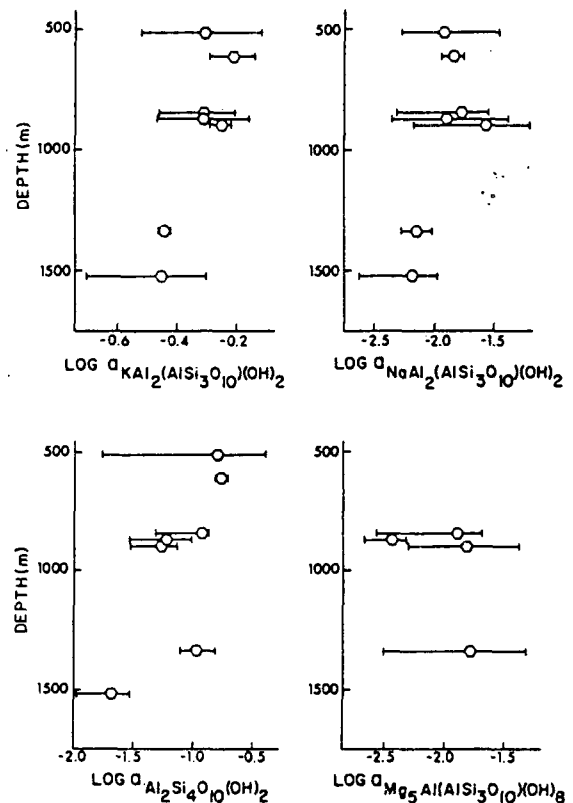


FIG. 5. Variation with depth of the activities of the $KAl_2(AlSi_3O_{10})(OH)_2$, $NaAl_2(AlSi_3O_{10})(OH)_2$ and $Al_2Si_4O_{10}(OH)_2$ components in sericite, and the $Mg_5Al(AlSi_3O_{10})(OH)_8$ component in chlorite from well 14-2. These activities are calculated using electron microprobe analyses of these minerals taken from Ballantyne, J. (1978, 1980). Hexagons indicate the average value for that depth and the bars represent the range in values. Refer to the text for the method of calculation.

Table 4. Specific Equations for Calculating Component Activities

Component	Activity ^a
KAl ₂ (AlSi ₃ O ₁₀)(OH) ₂	(X _{K⁺,A}) (X _{Al³⁺,M(2)}) ² (X _{Al³⁺,T10}) (X _{Si⁴⁺,T1m}) (X _{Si⁴⁺,T2}) ² (X _{OH⁻}) ^{2 b,c}
Al ₂ Si ₄ O ₁₀ (OH) ₂	(X _{V,A}) (X _{Al³⁺,M(2)}) ² (X _{Al³⁺,T10}) (X _{Si⁴⁺,T1m}) (X _{Si⁴⁺,T2}) ² (X _{OH⁻}) ^{2 b,c}
NaAl ₂ (AlSi ₃ O ₁₀)(OH) ₂	(X _{Na⁺,A}) (X _{Al³⁺,M(2)}) ² (X _{Al³⁺,T10}) (X _{Si⁴⁺,T1m}) (X _{Si⁴⁺,T2}) ² (X _{OH⁻}) ^{2 b,c}
Mg ₅ Al(AlSi ₃ O ₁₀)(OH) ₈	(X _{Mg²⁺,M}) ⁵ (X _{Al³⁺,M}) (X _{Al³⁺,T}) (X _{Si⁴⁺,T}) ³ (X _{OH⁻}) ^{8 b}

$a_i = k_i \prod_{j,s} x_{j,s}^{v_{s,j,i}}$ (equation (46) from Helgeson et al. (1978)), where: a_i is the activity of the i^{th} component; k_i is the proportionality constant (defined by equation (48) from Helgeson et al. (1978)) relating the intracrystalline and intercrystalline standard states; $x_{j,s}$ is the mole fraction of the j^{th} species on the s^{th} site; and $v_{s,j,i}$ is the stoichiometric number of s^{th} energetically equivalent sites occupied by the j^{th} species in one mole of the i^{th} component.

^bThese equations are consistent with random mixing and equal interactions of atoms on energetically equivalent sites.

^cThese equations are consistent with ordered standard state site distributions, equations and data reported by Helgeson et al. (1978) for muscovite, paragonite and pyrophyllite.

finied by Helgeson and Aagaard (1981). The thermodynamic components of the mineral sericite correspond to the chemical formulax units of Al₂Si₄O₁₀(OH)₂, KAl₂(AlSi₃O₁₀)(OH)₂ and NaAl₂(AlSi₃O₁₀)(OH)₂. For chlorite the activity of the component Mg₅Al(AlSi₃O₁₀)(OH)₈ is calculated.

Gas pressures

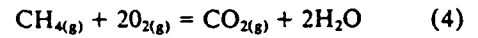
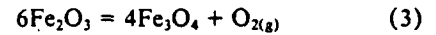
Calculated partial pressures of O₂, CO₂, H₂S and CH₄ dissolved in the reservoir fluid are shown in Fig. 6. The partial pressures of CO₂, H₂S and CH₄ are calculated using the Henry's law relation

$$f = K_T X \quad (2)$$

where f is the fugacity of the gas (at the temperatures and pressures considered in this study the fugacity is essentially equivalent to the partial pressure of a gas in atmospheres), K_T is the Henry's law constant at temperature T (Table 5), and X is the mole fraction of the gas in the reservoir fluid. Mole fractions of these gases in the reservoir fluid are calculated from concentrations measured in the steam sample. The gas content of the steam fraction collected at the same time as liquid samples (1) through (4) from well 14-2 was provided by A. H. Truesdell (unpublished data, 1979). It is assumed for these calculations that CO₂, H₂S and CH₄ separate completely into the steam fraction. This is supported by the work of Drummond (1981, Fig. 4.5) in which he calculates that with 18% steam loss as the result of isenthalpic boiling of a 250°C (3 m NaCl) fluid, less than 1% of these gases will remain in the liquid phase. This is further supported by a study of gas concentrations in geothermal discharges from the Wairakei system (Ellis, 1962) which has temperatures, pressures and fluid composition similar to those of Roosevelt Hot Springs.

The oxygen partial pressure (P_{O_2}) of the reservoir fluid is approximated using both hematite-magnetite and methane-carbon dioxide equilibria, given by

equations (3) and (4), respectively,



and from the relationship between temperature and P_{O_2} determined by D'Amore and Panichi (1980) (equation 5).

$$\log P_{O_2} = 8.20 - (23643/T(^{\circ}K)) \quad (5)$$

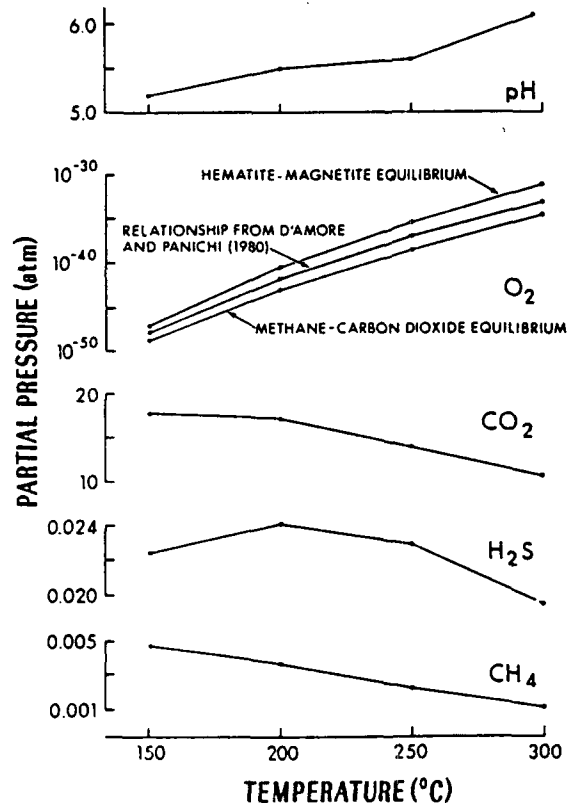


FIG. 6. The variation with temperature of pH and partial pressures of O₂, CO₂, H₂S and CH₄ in the reservoir fluid. See text for methods of calculation.

Table 5. Henry's Law Constants

Gas	K_T (atm/mole fraction)				Source ²
	150°C	200°C	250°C	300°C	
CO ₂ ¹	6750	6500	5380	4100	1
H ₂ S	1860	2000	1900	1620	2
H ₂	78387	49459	27813	13939	3
CH ₄	87952	70000	44000	22093	3

¹For 0.1 moles/l NaCl solution.

²References: 1 = Ellis and Golding (1963); 2 = Kozintseva (1964) after Ellis and Mahon (1977, p. 132); 3 = Naumov et al. (1974).

At 288°C, the P_{O_2} ranging from 10^{-32} to 10^{-35} atm, P_{CO_2} of 11 atm, P_{H_2S} of 0.020 atm, and P_{CH_4} of 0.001 atm in the Roosevelt reservoir fluid are similar in magnitude to calculated gas pressures in other high-temperature geothermal reservoirs such as Wairakei and Broadlands (Ellis, 1979; D'Amore and Panichi, 1980).

Ion concentrations corrected for gas losses and scaling

The concentrations of calcium, carbon and sulfur will decrease in the fluid by 5, 1753 and 119 mg/l, respectively, as a result of CO₂, CH₄ and H₂S gas release and calcite precipitation accompanying steam separation. The amounts of carbon and sulfur lost to the steam fraction are calculated from the concentrations of CO₂, CH₄ and H₂S released from the flashed fluid. The amounts of calcium and carbon removed from the reservoir through calcite precipitation are calculated from the change in calcite solubility as a result of boiling. The composition of the reservoir fluid corrected for these losses is given in Table 3.

As the reservoir fluid boils and thereby cools from the reported bottom-hole temperature of 265°C to the collection temperature of 192°C, the solubility of calcite decreases by 1.31×10^{-4} moles/l. This solubility decrease is largely a result of the CO₂ pressure decrease in response to the removal of CO₂ from the fluid by the gas phase. The solubility change of calcite can be determined using equation (6) (adapted from Segnit *et al.*, 1962) which gives moles of Ca⁺⁺ in a kilogram of fluid, $m_{Ca^{++}}$, in equilibrium with calcite.

$$m_{Ca^{++}}^3 = 13.9K_1K_cX_{CO_2}/K_2 \quad (6)$$

$$K_1 = a_{H^+}a_{HCO_3^-}/a_{H_2CO_3} \quad (7)$$

$$K_2 = a_{H^+}a_{CO_3^{2-}}/a_{HCO_3^-} \quad (8)$$

$$K_c = a_{Ca^{++}}a_{CO_3^{2-}}/a_{CaCO_3(s)} \quad (9)$$

K_j = equilibrium constant for the j^{th} reaction

X_{CO_2}

= mole fraction of CO₂ gas in the reservoir fluid

a_i = activity of the i^{th} species in solution

The variation in the mole fraction of CO₂ in the reservoir fluid as a result of boiling is determined using the fraction of CO₂ removed with each percentage of steam separated from the flashed 260°C reservoir fluid of the Wairakei geothermal system as reported by Ellis (1962, Fig. 3).

For the estimation of calcium and carbon loss due to calcite scaling, it is assumed the reservoir fluid is in equilibrium with calcite and that the fluid remains in equilibrium with calcite as it boils. The occurrence of calcite at depth in well 14-2 supports this assumption of equilibrium. Filtering of the sample upon collection corrects for removal of calcite precipitate that has not adhered to the piping.

Hydrogen ion concentration

The reservoir fluid pH is determined by the method of hydrogen ion mass balance (Truesdell and Singers, 1974; Bischoff and Dickson, 1975) (Fig. 6). This method of estimating pH is based on the assumption that the mass balance of hydrogen in a fluid is independent of temperature and that the hydrogen mass balance of the fluid corrected for gas separation equals that of the deep reservoir fluid. The method of hydrogen mass balance is used in this study because it is independent of mineral equilibrium relationships which the final calculated reservoir fluid will ultimately be used to predict.

The hydrogen mass balance for the fluid corrected for CO₂ and H₂S loss is 0.340 moles/l. This corresponds to a pH of 6.0 at 288°C (Fig. 6) and is similar to pH values calculated for other high-temperature geothermal fluids. For example, New Zealand geothermal fluids having temperatures of 220°C exhibit a range in calculated reservoir pH from 5.9 to 7.1 (Ellis, 1979), and Icelandic geothermal fluids with temperatures of 195° to 220°C range in pH from 5.0 to 8.3 (Arnorsson *et al.*, 1978; Ellis, 1979).

Effect of changing temperature

The effects of temperature change on the pH, gas partial pressures and distribution of aqueous species were determined at 150°, 200°, 250° and 300°C for fixed concentrations of elements in solution (Fig. 6). These calculations suggest that decreasing temperature produces a decrease in the fluid pH and P_{O_2} , an increase in P_{CO_2} and P_{CH_4} , and no consistent variation in P_{H_2S} .

DISCUSSION OF FLUID-MINERAL EQUILIBRIA

The equilibrium relationship between the alteration mineralogy and the deep reservoir fluid of the Roosevelt Hot Springs thermal system is quantita-

tively evaluated at temperatures ranging from 150° to 300°C. Species distribution calculations are used to calculate mineral equilibria in the deep reservoir fluid at 150°, 200°, 250° and 300°C. The results of these calculations are displayed on a plot of chemical affinity of each mineral in solution against temperature in Fig. 7.

The chemical affinity, A_j , (Helgeson, 1979) indicates the equilibrium condition of the mineral in the fluid and is calculated using equation 10,

$$A_j = RT \ln (K_j/Q_j) \quad (10)$$

where K_j and Q_j represent the equilibrium constant and activity product for the j^{th} reaction, T is the temperature in °K and R is the gas constant. A positive value indicates the mineral is undersaturated with respect to the fluid. The chemical affinity is zero for mineral-fluid equilibrium and negative for supersaturation. Phases that satisfy equilibrium or supersaturated conditions are shown in the lower portion of Fig. 7, with undersaturated conditions represented on the upper portion of the diagram.

Minerals included on the chemical affinity *versus* temperature diagram are those described as alteration minerals in the Roosevelt system. Thermochemical data for montmorillonite and mixed-layer clays are not supplied in the data compilation by Helgeson *et al.* (1978), nor are compositional data available to calculate component activities. Data for (Ca-) montmorillonite and illite equilibrium taken from Helgeson (1969) are, therefore, used to calculate the equilibrium trends of these minerals. Although these data are not entirely consistent with the Helgeson *et al.* (1978) data base, they will at least provide a reasonable approximation of the actual equilibrium conditions.

Microprobe analyses were available for chlorite and sericite from well 14-2 (Ballantyne, J., 1978, 1980), allowing calculation of the component activities to account for solid solution in these minerals. Using these calculated activities, the chemical affinity of the component in solution was calculated for the $KAl_2(AlSi_3O_{10})(OH)_2$ component of sericite and the $Mg_3Al(AlSi_3O_{10})(OH)_8$ component of chlorite. These component affinities are represented on Fig. 7 by the dashed lines. For comparison, the chemical affinities of the pure end members muscovite and clinocllore are also shown in Fig. 7.

The activities of the $KAl_2(AlSi_3O_{10})(OH)_2$ component of sericite used to calculate the range in chemical affinities of this component are shown in Fig. 5. The activity of the $KAl_2(AlSi_3O_{10})(OH)_2$ component of sericite tends to decrease with increased depth (Fig. 5). A similar trend is noted for the activities of the other two components of sericite (Fig. 5), $NaAl_2(AlSi_3O_{10})(OH)_2$ and $Al_2Si_4O_{10}(OH)_2$. The distribution of available compositional data with depth allows for a grouping of samples into those above 896 m and those below 1341 m in well 14-2. The average activity of $KAl_2(AlSi_3O_{10})(OH)_2$ is 0.51

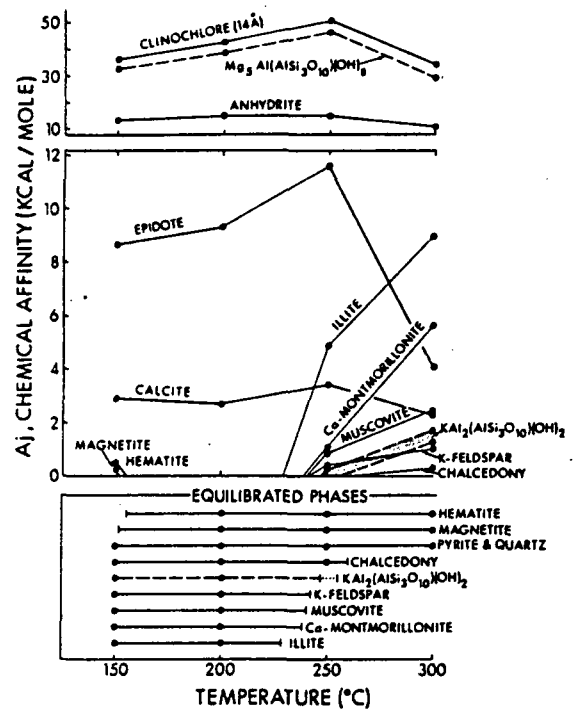


FIG. 7. Chemical affinities of minerals with respect to the Roosevelt reservoir fluid from 150° to 300°C. See text for discussion.

for the upper group and 0.36 for the lower. Measured well temperatures for these two groups is 210° to 250°C for the upper group and 255°C for the lower group (Fig. 2). The calculated equilibration temperature ($A_j = 0$) of the $KAl_2(AlSi_3O_{10})(OH)_2$ component with the reservoir fluid for the upper group is 246°C and for the lower group is 254°C (Fig. 7). This suggests that solid solution in sericite is temperature dependent and that calculation of component activities to correct for its effects on fluid-mineral equilibrium calculations is appropriate.

The activity of the $Mg_3Al(AlSi_3O_{10})(OH)_8$ component of chlorite does not appear to vary consistently within the depth range for which microprobe analyses are available (Fig. 5). Therefore, the average activity of 0.013 for all depths is used to calculate the chemical affinity of this component in solution. Chlorites in the reservoir rock contain nearly equal atomic proportions of Fe and Mg (Ballantyne, J., 1978). Thermochemical data for the Fe component of chlorite, however, are not available and therefore only the Mg component is discussed.

Comparison of mineral equilibria in the calculated reservoir fluid (Fig. 7) with alteration mineral assemblages described in producing wells (Fig. 2) indicates that the majority of these minerals could have been produced through interaction of the reservoir rocks with the present thermal fluid. Phases such as hematite, magnetite, pyrite and quartz are saturated with respect to the fluid at nearly all temperatures. These minerals are present in the production wells at all depths, except hematite which is absent from

the deeper high-temperature alteration assemblage III in well 14-2.

A select group of phases including chalcedony, the $KAl_2(AlSi_3O_{10})(OH)_2$ component of sericite, K-feldspar, (Ca-) montmorillonite and illite exhibit a crossover from undersaturated to saturated conditions in the temperature range from 229° to 260°C. Typically those phases that exhibit a crossover between 240° and 260°C occur in both the low (I and II) and high (III) temperature alteration zones of the producing wells. These phases include sericite, K-feldspar and chalcedony. A second group of minerals that equilibrate below 240°C is present only in the lower-temperature alteration zones (I and II) of the production wells and includes the clay minerals montmorillonite and illite.

Finally, there is a group of phases present as alteration minerals in production wells 72-16 and 14-2 that is undersaturated with respect to the reservoir fluid at all temperatures, suggesting that these minerals could be the result of a past thermal event. This group includes chlorite, calcite, epidote and anhydrite. Anhydrite and epidote are present in only trace amounts in producing wells, whereas chlorite and calcite are more abundant. All four of these minerals, however, are also present in the nonproducing wells, therefore their presence in the production wells could be the result of a past thermal event.

The abundance of calcite in the upper alteration zone (I) of wells 14-2 and 9-1, in contrast to the near absence of calcite in the upper 700 m of nonproducing well 52-21, however, suggests that calcite in assemblage I is a product of the present thermal event. Because calcite equilibrium is strongly dependent on those chemical characteristics of the reservoir fluid most difficult to quantify, pH, P_{CO_2} and total carbon, it is possible that the error in calculating these fluid components could indeed allow for calcite equilibrium with the fluid. On the other hand, the presence of calcite in the upper 400 m of the reservoir rock can be explained by boiling of the fluid at these shallower depths. According to data from Mahon *et al.* (1980, Fig. 1), the present Roosevelt Hot Springs reservoir fluid, with 0.64 wt % CO_2 , will be very close to, if not at, its hydrostatic boiling point in the upper portions of the reservoir (less than 400 m). Boiling of this fluid in the formation rocks can precipitate calcite, a condition analogous to steam loss in well bores in the Roosevelt Hot Springs geothermal system that produces a calcite scale.

Chlorite after plagioclase is present in both wells 72-16 and 14-2 but is lacking from nonproducing well 52-21 and found only rarely and in trace quantities in nonproducing well 9-1. Chlorite after mafics, however, is present in all wells. This suggests that chlorite after plagioclase is a product of the present thermal event, despite the apparent nonequilibrium of chlorite with the reservoir fluid. The lack of thermochemical data for the Fe component of chlorite, however, does not allow a complete evaluation of chlorite equilibrium relationships with the known

reservoir fluid. Bird and Norton (1981) in evaluating fluid-mineral equilibria in the Salton Sea geothermal system found a similar situation of nonequilibrium of the thermal fluid with chlorite which appeared related to the present thermal event.

These fluid-mineral equilibrium calculations do not take into account the effects of mineral precipitation on the composition of the fluid as it travels along its flow path in the cooling process. The possibility of mixing with nonthermal ground waters, which is undoubtedly occurring at the margins of the system, or the mineralogic consequences of boiling are also not considered in detail. It is realized, however, that in the Roosevelt thermal system the effects of these processes could be significant.

This study suggests, however, that the observed sequence of a lower to upper mineral assemblage in the production wells can be produced by the present reservoir fluid as it cools from approximately 300°C during its migration to the surface. The mineral equilibrium calculations suggest fluid temperatures of 240° to 260°C in rocks containing the lower mineral assemblage, and temperatures ranging from approximately 229° to 240°C in rocks of the upper mineral assemblage. These predicted temperatures agree within 40°C with the maximum measured temperatures of 210°C in the upper production well alteration assemblage I and 268°C in the lower production well assemblage III (Fig. 2). The highest temperature of 260°C predicted for fluid-mineral equilibrium in mineral assemblage III is remarkably close to geothermometer temperatures for the fluid. For example, geothermometer temperatures estimated from the elemental composition of the surface sample, sulfate-water isotopes and enthalpy-chloride relationships give a temperature of $288^\circ C \pm 10^\circ$. Also, the Na-K-Ca geothermometer temperature determined from the calculated composition of the deep reservoir fluid is 277°C (Table 3).

CONCLUSION

In the Roosevelt Hot Springs geothermal system, the interaction of the country rock with the present high-temperature thermal fluid will result in a complex series of dissolution and deposition reactions as the fluid and rock attempt to equilibrate. The extent to which the thermal fluid is in equilibrium with the country rock is estimated by comparing actual alteration assemblages with predicted fluid alteration products.

The composition of the high-temperature fluid at depth is estimated from well samples. The effects of nonthermal ground-water mixing, mineral precipitation in the well bore, steam loss and gas release on these surface samples are considered. The predicted composition of the deep fluid is similar in composition to fluids found in other high-temperature geothermal systems, such as Wairakei and Broadlands (Ellis, 1979).

Comparing predicted alteration mineral assem-

blages for the calculated reservoir fluid, in the temperature range from 150° to 300°C, with alteration assemblages described in drill cuttings of geothermal production wells indicates that several alteration minerals are equilibrated with the reservoir fluid. These include hematite, magnetite, pyrite and quartz which are saturated with respect to the fluid at all temperatures, and chalcedony, sericite, K-feldspar, (Ca-) montmorillonite and illite which are saturated in the fluid at temperatures less than 260° to 229°C. The calculated equilibration temperatures of the last group of minerals predicts to within 40°C the transition zone observed between shallow (lower temperature) and deep (higher temperature) alteration zones. Furthermore, the variation in temperatures of equilibration of the $KAl_2(AlSi_3O_{10})(OH)_2$ component of sericite with the reservoir fluid with depth in well 14-2 is in agreement with observed temperatures in the well. This indicates that sericite solid solution is temperature dependent and that it is necessary to correct for its effects in equilibrium calculations.

Phases that do not exhibit equilibrium with respect to the reservoir fluid, such as epidote, anhydrite, chlorite and calcite, could be remnants of an earlier event. Disequilibrium of the reservoir fluid with chlorite, however, may be the result of inadequate thermochemical data, as the presence of chlorite after plagioclase as a characteristic alteration product in production wells suggests it is a product of the present thermal event. Calcite, on the other hand, could be a product of another process inherent to geothermal activity, such as boiling.

It is suggested, therefore, that the geothermal reservoir fluid at Roosevelt Hot Springs has probably not changed character significantly in the recent past. This is supported by the similarity between the observed alteration mineralogy and fluid-mineral equilibrium calculated for the reservoir fluid and the agreement between predicted equilibration temperatures and observed temperatures.

Acknowledgements—The authors have benefited greatly from discussions and critical comments by Joe Moore, Dennis Bird, Denis Norton and Odin Christensen. Thanks are also due to Jeff Hulen, Judy Ballantyne and Bruce Sibbett for useful discussions concerning the alteration mineralogy; Dennis Bird for providing insight into the use of component activity relationships; Denis Norton for providing mineral equilibrium constants calculated from Helgeson *et al.*'s (1978) thermochemical data, and for making available the revised version of PATH; Stuart Johnson and Dick Lenzer of Phillips Petroleum for allowing the collection and release of well fluid data; and A. H. Truesdell of the U.S. Geologic Survey for providing gas analyses for well 14-2. Staff of the Earth Science Lab also contributed to this study and deserve thanks, in particular Carol Withrow for computer programming assistance. This study was funded by the U.S. Department of Energy, Division of Geothermal Energy contract number DE-AC07-80ID12079 to the Earth Science Laboratory Division of the University of Utah Research Institute.

REFERENCES

- Arnorsson S., Gronvold K. and Sigurdsson S. (1978) Aquifer chemistry of four high-temperature geothermal systems in Iceland. *Geochim. Cosmochim. Acta* 42, 523-536.
- Ballantyne G. H. (1978) Hydrothermal alteration at the Roosevelt Hot Springs thermal area, Utah: Characterization of rock types and alteration in Getty Oil Company Well Utah State 52-21. Univ. of Utah Dept. of Geology and Geophysics Topical Rep. No. 78-1701.a.1.1.4, DOE/DGE contract No. EG-78-C-07-1701, 23 p.
- Ballantyne J. M. (1978) Hydrothermal alteration at the Roosevelt Hot Springs thermal area, Utah: modal mineralogy, and geochemistry of sericite, chlorite, and feldspar from altered rocks, Thermal Power Company well Utah State 14-2. Univ. of Utah Dept. of Geology and Geophysics Rep. No. 78-1701.a.1.1.5, DOE/DGE contract No. EG-78-C-07-1701, 36 p.
- Ballantyne J. M. (1980) Geochemistry of sericite and chlorite in well 14-2 Roosevelt Hot Springs geothermal system and in mineralized hydrothermal systems. Univ. of Utah Dept. Geology and Geophysics Rep. No. 79-1701.a.1.6, DOE/DGE contract No. DE-AC07-78ET/28392, 92 p.
- Ballantyne J. M. and Parry W. T. (1978) Hydrothermal alteration at the Roosevelt Hot Springs thermal area, Utah: Petrographic characterization of the alteration at 2 kilometers depth. Univ. of Utah Dept. of Geology and Geophysics Tech. Rep. No. 78-1701.a.1.1, DOE/DGE contract No. EG-78-C-07-1701, 23 p.
- Bamford R. W., Christensen O. D. and Capuano R. M. (1980) Multielement geochemistry of solid materials in geothermal systems and its applications Part I: The hot-water system at the Roosevelt Hot Springs KGRA, Utah: Univ. of Utah Res. Inst. Earth Sci. Lab. Division Rep. No. 30, DOE/DGE contract No. DE-AC03-79ET-27002, 168 p.
- Bird D. K. and Norton D. L. (1981) Theoretical prediction of phase relations among aqueous solutions and minerals in the Salton Sea geothermal system. *Geochim. Cosmochim. Acta* 45, 1479-1493.
- Bishoff J. L. and Dickson F. W. (1975) Seawater-basalt interaction at 200°C and 500 bars: Implication for origin of seafloor heavy-metal deposits and regulation of seawater chemistry. *Earth Planet. Sci. Lett.* 25, 383-397.
- Bladh K. W. (1978) The weathering of sulfide-bearing rocks associated with porphyry-type copper deposits. Ph.D. dissertation, Univ. of Arizona, 98 p.
- D'Amore F. and Panichi C. (1980) Evaluation of deep temperatures of hydrothermal systems by a new gas geothermometer. *Geochim. Cosmochim. Acta* 44, 549-556.
- Drummond S. E. Jr. (1981) Boiling and mixing of hydrothermal fluids: chemical effects on mineral precipitation. Ph.D. dissertation, Pennsylvania State Univ., 380 p.
- Ellis A. J. (1962) Interpretation of gas analysis from the Wairakei hydrothermal area. *New Zealand J. Sci.* 5, 434-452.
- Ellis A. J. (1979) Explored geothermal systems. In *Geochemistry of Hydrothermal Ore Deposits* (ed. H. L. Barnes). John Wiley and Sons, 632-683.
- Ellis A. J. and Golding R. M. (1963) The solubility of carbon dioxide above 100°C in water and in sodium chloride solutions. *Amer. J. Sci.* 261, 47-60.
- Ellis A. J. and Mahon W. A. J. (1977) *Chemistry and Geothermal Systems*. Academic Press, 392 p.
- Forrest R. J. (1980) Historical synopsis of the Roosevelt Hot Springs geothermal field, Utah. In *Geothermal Systems in Central Utah* (ed. D. L. Nielson), Guidebook to Field Trip No. 7. Geothermal Resources Council Annual Meeting, 18-24.
- Fournier R. O. (1977) Chemical geothermometers and mixing models for geothermal systems. *Proc. International Atomic Energy Agency Advisory Group on the Application of Nuclear Techniques to Geothermal Studies*, Pisa, 1975, Geothermics, Spec. Issue 5, 41-50.
- Fournier R. O. (1979) Geochemical and hydrologic considerations and the use of enthalpy-chloride diagrams in

- the prediction of underground conditions in hot-spring systems. *J. Volcanol. Geothermal Res.* 5, 1-16.
- Fournier R. O. and Truesdell A. H. (1973) An empirical Na-K-Ca geothermometer for natural waters. *Geochim. Cosmochim. Acta* 37, 1255-1275.
- Fournier R. O. and Truesdell A. H. (1974) Geochemical indicators of subsurface temperature - part 2: estimation of temperature and fraction of hot water mixed with cold water. *J. Res. U.S. Geol. Surv.* 2, 263-270.
- Fournier R. O. and Potter R. W., II (1979) A magnesium correction to the Na-K-Ca geothermometer. *Geochim. Cosmochim. Acta* 43, 1543-1550.
- Getty Oil Co. (1978) Data for Roosevelt Hot Springs KGRA, Utah. Univ. of Utah Res. Inst. Earth Sci. Lab. Division, August 10-11, 1978, open-file release.
- Glenn W. E. and Hulen J. B. (1979) Interpretation of well log data from four drill holes at Roosevelt Hot Springs, KGRA, Utah. Univ. of Utah Res. Inst. Earth Sci. Lab. Division Rep. No. 28, DOE/DGE contract No. EG-78-C-07-1701, 74 p.
- Glenn W. E., Hulen J. B. and Nielson D. L. (1981) A comprehensive study of LASL C/T-2 Roosevelt Hot Springs KGRA, Utah and applications to geothermal well logging. Los Alamos Scientific Lab. Rep. LA-8686-MS, 175 p.
- Helgeson H. C. (1969) Thermodynamics of hydrothermal systems at elevated temperatures and pressures. *Amer. J. Sci.* 267, 729-804.
- Helgeson H. C. (1979) Mass transfer among minerals in hydrothermal solutions. In *Geochemistry of Hydrothermal Ore Deposits*, 2nd Edition (ed. H. L. Barnes), 568-610.
- Helgeson H. C., Brown T. H., Nigrini A. and Jones T. A. (1970) Calculation of mass transfer in geochemical processes involving aqueous solutions. *Geochim. Cosmochim. Acta* 34, 569-592.
- Helgeson H. C., Delany J. M., Nesbitt H. W. and Bird D. K. (1978) Summary and critique of the thermodynamic properties of rock-forming minerals. *Amer. J. Sci.* 278-A, 1-229.
- Helgeson H. C. and Aagaard P. (1981) Thermodynamic and kinetic constraints on reaction rates among minerals and aqueous solutions. I. Theoretical considerations: *Amer. J. Sci.* (in press).
- Hem J. D. (1970) Study and interpretation of the chemical characteristics of natural waters, 2nd ed. U.S. Geol. Sur. Water-Supply Paper 1473, 363 p.
- Keenan J. H., Keyes F. G., Hill P. G. and Moore J. G. (1969) *Steam Tables, Thermodynamic Properties of Water including Vapor, Liquid, and Solid Phases (SI Units)*. John Wiley and Sons, 156 p.
- Kharaka Y. K. and Barnes I. (1973) SOLMNEQ: Solution mineral equilibrium computations. U. S. Dept. Commerce, Natl. Tech. Inf. Service Rep. No. PB-215 899, 82 p.
- Knight J. (1976) A thermochemical study of alunite and copper-arsenic sulfosalt deposits. M. S. thesis, Univ. of Arizona, 142 p.
- Koenig J. B. and Gardner M. C. (1977) Geothermal potential of the lands leased by Geothermal Power Corporation in the Northern Mineral Mountains, Beaver and Millard Counties, Utah. Univ. of Utah Res. Inst. Earth Sci. Lab. Division, April 20-21, 1978, open-file release, 430 p.
- Kozintseva T. N. (1964) Solubility of hydrogen sulfide in water at elevated temperatures. *Geochim. Int.* 750-756.
- Lenzer R. C., Crosby G. W. and Berge C. W. (1976) Geothermal exploration of Roosevelt KGRA, Utah 17th U.S. Symp. Rock Mechanics, Abs., 13 p.
- Mahon W. A. J., McDowell G. D. and Finlayson J. B. (1980) Carbon dioxide: Its role in geothermal systems. *New Zealand J. Sci.* 23, 133-148.
- Mower R. W. and Cordova R. M. (1974) Water resources of the Milford area, Utah, with emphasis on ground water. Utah Dept. Nat. Resources Tech. Pub. No. 43, 99 p.
- Mundorff J. C. (1970) Major thermal springs of Utah. *Utah Geol. and Mineral Surv. Resource Bull.* No. 13, 60 p.
- Naumov G. B., Ryzhenko B. N. and Khodakovskiy I. L. (1974) *Handbook of Thermodynamic Data* (translated from the 1971 Russian original). Nat. Tech. Info. Service PB-226-722.
- Nehring N. L. and Mariner R. H. (1979) Sulfate-water isotopic equilibrium temperatures for thermal springs and wells of the Great Basin. *Geothermal Resources Council, TRANS.* 3, 485-488.
- Nielson D. L., Sibbett B. S., McKinney D. B., Hulen J. B., Moore J. N. and Samberg S. M. (1978) Geology of Roosevelt Hot Springs KGRA, Beaver County, Utah. Univ. of Utah Res. Inst. Earth Sci. Lab. Division Rep. No. 12, DOE/DGE contract No. EG-78-C-07-1701, 120 p.
- Nielson D. L. and Moore J. N. (1979) The exploration significance of low-angle faults in the Roosevelt Hot Springs and Cove Fort-Sulphurdale geothermal systems, Utah. *Geothermal Resources Council, TRANS.* 3, 503-506.
- Parry W. T. (1978) Hydrothermal alteration at the Roosevelt Hot Springs thermal area, Utah: Part I - Mineralogy of the clay fractions from cuttings, Thermal Power Company Well Utah State 14-2. Univ. of Utah Dept. of Geology and Geophysics, Tech. Rep. No. 78-1701.a.1.1.2, DOE/DGE contract No. EG-78-C-07-1701, 24 p.
- Rimstidt J. D. (1979) The kinetics of silica-water reactions. Ph. D. dissertation, Pennsylvania State Univ., 126 p.
- Rohrs D. and Parry W. T. (1978) Hydrothermal alteration at the Roosevelt Hot Springs thermal area, Utah: Thermal Power Company Well Utah State 72-16. Univ. of Utah Dept. of Geology and Geophysics Topical Rep. No. 78-1701.a.1.1.3, DOE/DGE contract no. EG-78-C-07-1701, 23 p.
- Segnit E. R., Holland H. D. and Biscardi C. J. (1962) The solubility of calcite in aqueous solutions—I. The solubility of calcite in water between 75° and 200° at CO₂ pressures up to 60 atm. *Geochim. Cosmochim. Acta* 26, 1301-1331.
- Sibbett B. S. and Nielson D. L. (1980) Geology of the Central Mineral Mountains, Beaver County, Utah. Univ. of Utah Res. Inst. Earth Sci. Lab. Division Rep. No. 33, DOE/DGE contract No. DE-AC07-78ET28392, 42 p.
- Smith R. L. and Shaw H. R. (1975) Igneous related geothermal systems. In *Assessment of Geothermal Resources of the United States-1975* (eds. D. E. White and D. L. Williams), U. S. Geol. Surv. Circ. 726, 58-83.
- Thermal Power Co. (1978) Data for Roosevelt Hot Springs KGRA, Utah. Univ. of Utah Res. Inst. Earth Sci. Lab. Division, January 23-25, 1978, open-file release.
- Truesdell A. H. and Singers W. (1974) The calculation of aquifer chemistry in hot-water geothermal systems. *J. Res. U.S. Geol. Surv.* 2, No. 3, 271-278.
- Truesdell A. H. and Fournier R. O. (1976) Calculation of deep temperatures in geothermal systems from the chemistry of boiling spring waters of mixed origin. *Proc. 2nd U.N. Symp. Dev. Use Geothermal Resour.*, San Francisco, 1975. Vol. 1, U.S. Government Printing Office, Washington, D. C., 837-844.
- Wilson W. R. and Chapman D. S. (1980) Thermal studies at Roosevelt Hot Springs, Utah. Univ. of Utah Dept. of Geology and Geophysics Technical Rep. No. DOE/ID/12079-19, DOE/DGE contract No. DE-AC07-80ID12079, 102 p.

Roosevelt Hot Springs Geothermal System, Utah—Case Study¹

HOWARD P. ROSS, DENNIS L. NIELSON, and JOSEPH N. MOORE²

ABSTRACT

The Roosevelt Hot Springs geothermal system has been undergoing intensive exploration since 1974 and has been used as a natural laboratory for the development and testing of geothermal exploration methods by research organizations. This paper summarizes the geological, geophysical, and geochemical data which have been collected since 1974, and presents a retrospective strategy describing the most effective means of exploration for the Roosevelt Hot Springs hydrothermal resource.

The bedrock geology of the area is dominated by metamorphic rocks of Precambrian age and felsic plutonic phases of the Tertiary Mineral Mountains intrusive complex. Rhyolite flows, domes, and pyroclastic rocks reflect igneous activity between 0.8 and 0.5 m.y. ago. The structural setting includes older low-angle normal faulting and east-west faulting produced by deep-seated regional zones of weakness. North to north-northeast-trending faults are the youngest structures in the area, and they control present fumarolic activity. The geothermal reservoir is controlled by intersections of the principal zones of faulting.

The geothermal fluids that discharge from the deep wells are dilute sodium chloride brines containing approximately 7,000 ppm total dissolved solids and anomalous concentrations of F, As, Li, B, and Hg. Geothermometers calculated from the predicted cation contents of the deep reservoir brine range from 520 to 531°F (271 to 277°C). Hydrothermal alteration by these fluids has produced assemblages of clays, alunite, muscovite, chlorite, pyrite, calcite, quartz, and hematite. Geochemical analyses of rocks and soils of the Roosevelt Hot Springs thermal area demonstrate that Hg, As, Mn, Cu, Sb, W, Li, Pb, Zn, Ba, and Be have been transported and redeposited by the thermal fluids.

The geothermal system is well expressed in electrical resistivity and thermal-gradient data and these methods, coupled with geologic mapping, are adequate to delineate the fluids and alteration associated with the geothermal reservoir. The dipole-dipole array seems best suited to acquire and interpret the resistivity data, although controlled source AMT (CSAMT) may be competitive for near-surface mapping. Representations

of the thermal data as temperature gradients, heat flow, and temperature are all useful in exploration of the geothermal system, because the thermal fluids themselves rise close to the surface. Self-potential, gravity, magnetic, seismic, and magnetotelluric survey data all contribute to our understanding of the system, but are not considered essential to its exploration.

INTRODUCTION

The Roosevelt Hot Springs geothermal system is located along the western side of the Mineral Mountains, approximately 12 mi (19 km) northeast of Milford, Utah (Fig. 1). The geothermal system is a high-temperature water-dominated resource, and is structurally controlled with permeability localized by faults and fractures cutting plutonic and metamorphic rocks.

The earliest exploration in the area was carried out in 1967 and 1968 by Eugene Davies of Milford who encountered boiling water in two holes on and adjacent to siliceous sinter deposits. Phillips Petroleum Co. initiated geothermal exploration at Roosevelt in 1972 and successfully bid for 18,871 acres (7,637 ha.) of the Roosevelt KGRA (Known Geothermal Resources Area) at the July 1974 competitive lease sale (Forrest, 1980). Exploratory drilling began in 1975 and the second well drilled, Roosevelt KGRA 3-1, encountered producible quantities of geothermal fluid. Additional drilling by Phillips Petroleum Co. and Thermal Power Co. has brought the total number of successful wells in the Roosevelt Hot Springs geothermal field to seven. A mobile 1.6 MWe generator has been installed in the field. Present development plans call for increasing capacity to 7 MWe in 1983 and 20 MWe by 1984. A discussion of the history of the Roosevelt Hot Springs KGRA and the exploration methods employed by Phillips Petroleum Co. is presented by Forrest (1980).

A large amount of geological, geophysical, geochemical, drilling, and reservoir data for the Roosevelt Hot Springs area has been made available in 1977-79 through the Department of Energy's Industry Coupled Program. A review of these data and earlier work helped to identify inconsistencies and weak areas in an already large geoscience data base. Additional work has helped to complete this data base. The integration of these data constitutes the present case study.

© Copyright 1982. The American Association of Petroleum Geologists. All rights reserved.

¹Manuscript received, May 26, 1981; accepted, February 24, 1982. Paper presented at the AAPG Annual Meeting EMD Geothermal Session, June 2, 1981.

²Earth Science Laboratory, University of Utah Research Institute, Salt Lake City, Utah 84108.

This work was supported by funding from the Division of Geothermal

Energy, Department of Energy under contract DE-AC07-78ET28393 and DOE-AC07-80ID12079. We thank R. C. Fox, C. E. Mackelprang, Christian Smith, and W. E. Glenn for their contribution to the geophysical interpretations, and S. H. Ward, P. M. Wright, and P. E. Wannamaker for their reviews of the manuscript. We thank G. W. Crosby for his critical review which has greatly improved our manuscript. The writers deeply appreciate the excellent support of Georgia Mitoff and Joan Pingree who typed the manuscript and of Doris Cullen and Dawnetta Bolaris who drafted the illustrations.

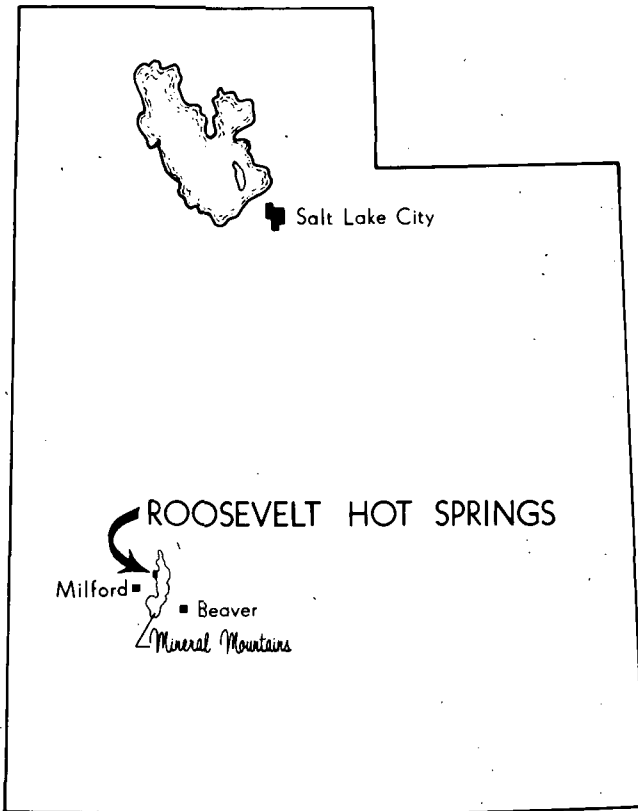


FIG. 1—Index map showing location of Roosevelt Hot Springs KGRA, Utah.

ROOSEVELT HOT SPRINGS GEOTHERMAL SYSTEM

Regional Setting

The Roosevelt Hot Springs KGRA is located on the western flank of the Mineral Mountains (Fig. 2). The Mineral Mountains are a north-trending horst bounded by Basin and Range normal faults and lie at the western edge of the transition zone between the Colorado Plateau and the Basin and Range physiographic provinces. The area is located on the western edge of the Intermountain seismic belt as defined by Smith and Sbar (1974). In addition, the Roosevelt Hot Springs KGRA lies along east-west-trending magnetic anomalies which follow the trend of the Wah Wah-Tushar mineral belt (Mabey et al, 1978). This belt has been the site of intrusive activity through the Tertiary and into Quaternary time. Associated with this igneous activity are deposits of uranium and base and precious metals.

The central part of the Mineral Mountains is a structural high relative both to adjacent ranges and also to the northern and southern parts of the range. In these northern and southern areas, sedimentary rocks of Cambrian through Cretaceous age are exposed. The southern area also contains volcanic and plutonic rocks of Tertiary age (Earll, 1957). In contrast, the central part of the Mineral Mountains contains Precambrian metasedimentary rocks and Tertiary plutonic rocks of the Mineral Mountains intrusive complex (Sibbett and Nielson, 1980). These Tertiary rocks possibly represent plutonic equivalents of the Marysville volcanic province

which is exposed to the east, south, and southwest of the Mineral Mountains.

Local Setting

The geology in the vicinity of the Roosevelt Hot Springs geothermal system has been described in detail by Nielson et al (1978). The central part of the Mineral Mountains has been mapped by Sibbett and Nielson (1980). A simplified geologic map of the Roosevelt Hot Springs area is shown in Figure 2.

The oldest unit exposed in the area of the geothermal system is a banded gneiss which was formed from regionally metamorphosed quartzo-feldspathic sediments. The rock was metamorphosed to the upper amphibolite facies during middle Proterozoic time. The banded gneiss is strongly layered with adjacent layers distinguished principally on the content of mafic minerals. The rock is compositionally heterogeneous and contains thick sequences of quartzo-feldspathic rocks. The unit also contains metaquartzite and sillimanite schist layers which have been differentiated in the more detailed geologic study (Nielson et al, 1978).

The Mineral Mountains intrusive complex is the largest intrusive body exposed in Utah. K-Ar dating and regional relationships suggest that the intrusive sequence is middle to late Tertiary in age. In the vicinity of the geothermal system, the lithologies range from diorite and granodiorite through granite and syenite in composition (Fig. 2).

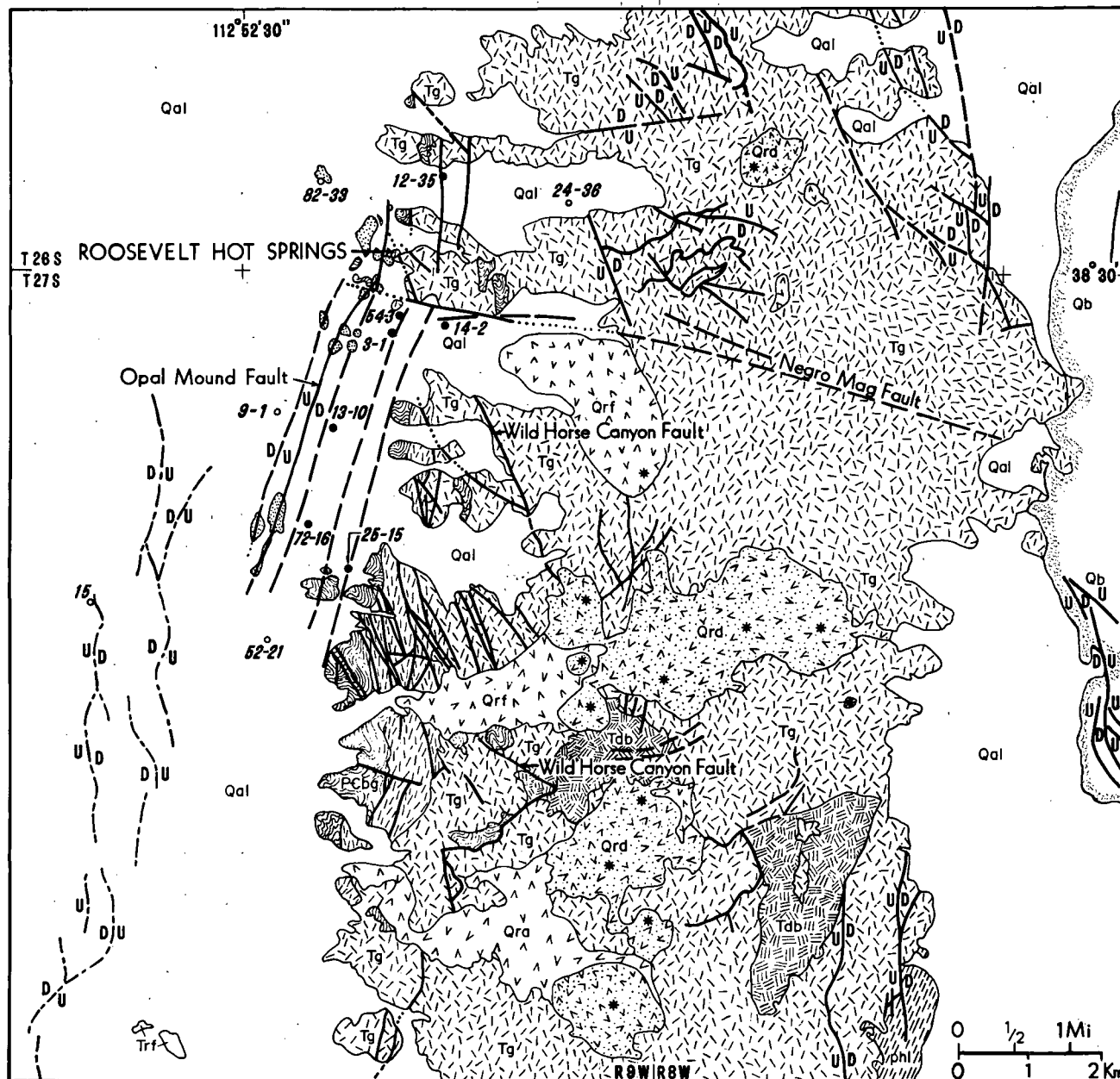
Rhyolite flows, pyroclastics, and domes were extruded along the spine of the Mineral Mountains 800,000 to 500,000 years ago (Lipman et al, 1978). The flows and domes are glassy, phenocryst-poor rhyolites. The pyroclastic rocks are represented by air-fall tuff and nonwelded ash-flow tuffs. Smith and Shaw (1975) hypothesized that young rhyolites such as these are indicative of an upper-level magma chamber which could serve as a heat source for geothermal systems.

Hot spring deposits in the vicinity of the geothermal system have been mapped as siliceous sinter, silica-cemented alluvium, hematite-cemented alluvium, and manganese-cemented alluvium. The principal areas of hot-spring deposition are along the Opal Mound fault and at the old Roosevelt Hot Springs. In both of these areas, the deposits consist of both opaline and chalcedonic sinter.

The geothermal reservoir at Roosevelt Hot Springs is structurally controlled. The controls are thought to be produced by the intersection of the faults mapped in the KGRA (Nielson et al, 1978, 1979). The structural evolution of the Roosevelt Hot Springs geothermal system is envisioned as follows. During rapid uplift of the Mineral Mountains structural block, westward-dipping low-angle normal faults formed. The most important of these is the Wild Horse Canyon fault (Fig. 2). This tectonic event produced intense zones of cataclasis both along low-angle fault planes and within the hanging wall of the principal fault block. The cataclastic zones within the hanging wall are steeply dipping zones up to 10 ft (3 m) wide which strike generally to the northwest. These zones in the hanging wall were produced by internal brecciation and interaction between rigid blocks during

the low-angle faulting. East-west-trending high-angle normal faulting, represented by the Negro Mag fault, cuts the low-angle faults. The trend is parallel with the Wah Wah-Tushar mineral belt and is probably related to movement along this deep-seated structural trend.

The Opal Mound fault and parallel structures are north-northeast-trending faults which are the youngest structures in the area. They localize siliceous hot-spring deposits and are often marked by zones of alteration and silicification of alluvium.



LEGEND

- | | | | |
|-----|------------------------------|------|--------------------------------------|
| Qal | alluvium, siliceous sinter | Trf | rhyolite flows |
| Qb | basalt | Tg | granite, quartz monzonite, & syenite |
| Qrd | rhyolite domes, with centers | Tdb | diorite |
| Qra | pyroclastic deposits | Dh | metasediments |
| Qrf | rhyolite flows | Pcbg | banded gneiss |

FIG. 2—Geologic map of Roosevelt Hot Springs KGRA and vicinity (after Sibbett and Nielson, 1980a).

Hydrothermal System

The limits of the hydrothermal system have been partially defined by deep drilling within the Roosevelt Hot Springs KGRA. The principal wells are shown on Figure 2, and important facts about the wells are presented in Table 1. The area of geothermal production is bounded on the east by the range front of the Mineral Mountains. On the west, the system is bounded by the Opal Mound fault, and on the south it terminates between Utah State 72-16, which is a producer, and Utah State 52-21, which is a hot but dry hole. The northern boundary of the system has not been determined.

The deep wells confirm that the host rocks for the hydrothermal system are the Tertiary plutonic rocks and Precambrian metamorphic rocks which have been mapped in the adjacent Mineral Mountains (Fig. 2). Thus, the rocks show little primary permeability and the system is controlled by faults and fractures (Lenzer et al, 1976; Nielson et al, 1978, 1979).

Fluid chemistry.—The hydrothermal fluids are relatively dilute sodium chloride brines which contain approximately 7,000 ppm total dissolved solids. Capuano and Cole (1982) provide the most comprehensive review of the chemistry of these fluids. Table 2 lists the composition of fluids collected from the wells and springs. These fluids are compositionally similar throughout the field, and differ mainly in their concentrations of calcium, magnesium, and bicarbonate which

may be the result of mixing with calcium-rich nonthermal ground water.

Reservoir temperatures estimated from the Na-K-Ca contents of the brines range up to 554°F (290°C), and exceed the measured maximum temperatures by as much as 36 to 54°F (20 to 30°C). Capuano and Cole (1982) suggest that temperatures calculated by geothermometers may in fact be too high, reflecting changes in the fluid chemistry produced by flashing of the brines in the well bore. Their arguments are supported by geothermometer calculations based on the composition of the deep reservoir fluid determined from the combined analyses of brine, steam, and gas. These calculations suggest a reservoir temperature of 520°F (271°C) based on the Na-K-Ca geothermometer (Fournier and Truesdell, 1973) and a temperature of 531°F (277°C) based on the SiO₂ content of the fluid and the conductively cooled quartz saturation model of Fournier (1973).

The isotopic composition of the geothermal fluids indicates that they are of meteoric origin (Rohrs, 1980). A comparison of the fluid isotopic compositions with that of water from the mountain ranges to the east suggests that the thermal fluids could be derived either from the Mineral Mountains or ranges to the east.

Hydrothermal alteration.—Hydrothermal alteration in the geothermal system and the adjacent Mineral Mountains is localized along faults and fractures. There have been several periods of alteration and it is often

Table 1. Well Summary from Roosevelt Hot Springs, Utah

Well	Location	Depth	Status	T Max	Operator	Reference
O.H.-2	SW NW Sec. 10, T27S, R9W	2,250'	Deep T-gradient	NA	Phillips	Lenzer et al, 1977
O.H.-1	SE NE Sec. 17, T27S, R9W	2,321'	Deep T-gradient	NA	Phillips	Lenzer et al, 1977 Geothermex, 1977
Roosevelt KGRA 9-1	NE NW Sec. 9, T27S, R9W	6,885'	dry	227°C	Phillips	Lenzer et al, 1977 Glenn et al, 1980
Roosevelt KGRA 3-1	SW NE Sec. 3, T27S, R9W	2,724'	producer	NA	Phillips	Lenzer et al, 1977
Roosevelt KGRA 54-3	SW NE Sec. 3, T27S, R9W	2,882'	producer	NA	Phillips	Lenzer et al, 1977
Roosevelt KGRA 12-35	NW NW Sec. 35, T26S, R9W	7,324'	producer	NA	Phillips	Lenzer et al, 1977 Geothermex, 1977
Roosevelt KGRA 13-10	SW NW Sec. 10, T27S, R9W	5,351'	producer	NA	Phillips	Lenzer et al, 1977 Geothermex, 1977
Roosevelt KGRA 82-33	NE NE Sec. 33, T26S, R9W	6,028'	dry	NA	Phillips	Lenzer et al, 1977 Geothermex, 1977
Utah State 14-2	SW NW Sec. 2, T27S, R9W	6,108'	producer	254°C	Thermal Power	Lenzer et al, 1977 Glenn and Hulen, 1979
Roosevelt HSU 25-15	NW SW Sec. 15, T27S, R9W	7,500'	producer	NA	Phillips	Lenzer et al, 1977 Geothermex, 1977
Utah State 72-16	SE NE Sec. 16, T27S, R9W	1,254'	producer	243°C	Thermal Power O'Brien	Lenzer et al, 1977 Glenn and Hulen, 1979
Utah State 24-36	SW NW Sec. 36, T27S, R9W	6,119'	dry	NA	Thermal Power	
Utah State 52-21	NW NE Sec. 21, T27S, R9W	7,500'	dry	206°C	Getty Oil Co.	Glenn and Hulen, 1979
GPC-15	SE SE Sec. 18, T27S, R9W	1,900'	Deep T-gradient	72°C	Geothermal Power Corp.	Glenn and Hulen, 1979

not possible to separate these different periods on the basis of their mineralogy and chemistry. Older periods of hydrothermal alteration are associated with the intrusion of various phases of the Mineral Mountains intrusive complex. These episodes have produced minor copper mineralization which is generally associated with xenoliths of Paleozoic and Precambrian rocks. In addition, zones of sodium metasomatism have been identified with the contact zones between some of the felsic plutonic rocks (Sibbett and Nielson, 1980). The intrusion of the various phases of the pluton have also superimposed contact metamorphic assemblages on the older rocks.

A hydrothermal event which altered the fault zones and deposited pyrite and chalcopyrite occurred with the low-angle faulting. The hydrothermal alteration produced assemblages of quartz + chlorite + epidote + hematite. Hematite is commonly found as specularite veinlets and, where genetic relationships can be observed, hematite mineralization follows sulfide mineralization.

The hydrothermal alteration assemblages associated with the present geothermal system are crudely zoned

with depth. The uppermost assemblage, occurring around the hot-spring deposits and fumeroles, is characterized by quartz, alunite, kaolinite, montmorillonite, hematite, and muscovite. Parry et al (1980) have studied the near-surface alteration and suggest that these minerals have formed above the water table by downward-percolating acid sulfate waters. Upward-convecting geothermal brines have produced, with increasing depth, alteration assemblages characterized by montmorillonite + mixed layer clays + sericite + quartz + hematite and chlorite + sericite + calcite + pyrite + quartz + anhydrite (Ballantyne, 1978). Thermochemical calculations and petrologic observations suggest that the brines are in equilibrium with the alteration assemblages produced by the upward-migrating fluids (Capuano and Cole, 1982).

Flow tests.—Most of the flow-test, production-logging, and reservoir-engineering data for the Roosevelt Hot Springs field is proprietary. However, data from Utah State 14-2 and Utah State 72-16 (Fig. 2, Table 1) are in the public domain and are summarized here.

A short flow test conducted in Utah State 72-16 on

Table 2. Chemical Analyses of Selected Thermal Waters¹

		Wells				Hot Spring
		14-2	54-3	72-16	52-21	
Na	ppm	2,150	2,320	2,000	1,900	2,500
K	ppm	390	461	400	218	488
Ca	ppm	9.2	8	12.20	114	22
Mg	ppm	0.6	<2	0.29	3.9	0
Fe	ppm		0.03		6.9	
Al	ppm		<0.5		<0.1	0.04
Si	ppm	229	263	244	67	146
Sr	ppm		1.2	1.20		
Ba	ppm		<0.5			
Mn	ppm		<0.2			
Cu	ppm		<0.1			
Pb	ppm		<0.2			
Zn	ppm		<0.1			
As	ppm	3.0	4.3			
Li	ppm		25.3	16.0		0.27
Be	ppm		0.005			
B	ppm	29	29.9	27.2	27.0	38
Ce	ppm		0.27			
F	ppm	5.2	6.8	5.3	3.4	7.5
Cl	ppm	3,650	3,860	3,260	2,885.1	4,240
HCO ₃	ppm		232	181	550.0	156
SO ₄	ppm	78	72	32	86	73
NO ₃	ppm				1.3	11
Total Dissolved Solids	ppm	>6,614	7,504	6,444	5,727	7,800
pH (at collection T)		5.9		7.53	7.3	7.9
T (at surface)	°C	14				55
T (bottom hole)	°C	268	>260	243	204	284
Geothermometer						
T (Na-K-Ca)	°C	286	297	288	210 ²	284
T (quartz cond.)	°C	276	263	256	158	212
T (quartz diab.)	°C	244	234	229	150	194
T (chalcedony)	°C	274	259	250	134	197
Total Depth	m	1,862	878	382	2,289	

¹From Capuano and Cole (1982). A blank indicates data not determined or information not available.

²Corrected for the Mg content of the fluid.

December 30, 1976, produced 454,546 kg/hr steam and hot water at a flowing wellhead pressure of 25 kg/cm² and a temperature of 432°F (222°C). A 24-hour test was conducted April 4 to 6, 1977, in 72-16. The total mass-flow rate was determined by the James method (James, 1966) as 595,000 kg/hr at a wellhead pressure of 20.7 kg/cm² psia and a temperature of 415°F (213°C). However, the mass-flow rate and wellhead pressure dropped throughout the test, indicating a longer flow test was needed to determine steady-state well production. Thermal Power Co. also concluded that the James method of determining the flow rate of a two-phase flow was unsatisfactory. On the basis of the longer test, it was calculated that Utah State 72-16 could yield 119,546 kg/hr of steam if flashed at 5.6 kg/cm². The well's electrical generating capacity was determined to be 12.5 Mw at a heat rate of 9,546 kg steam/hr/Mw.

Thermal Power Co. conducted a 48-hour flow test in geothermal well Utah State 14-2 between November 16 and 18, 1976. The last 35 hours of the test stabilized at 225,000 kg/hr and an enthalpy of 444.5 Btu/hr. Thermal Power Co. calculates that at a wellhead pressure of 4.9 kg/cm² and 17.8% flash, Utah State 14-2 has a generating capacity of 4.5 Mw. This capacity was calculated at a heat rate of 8,900 kg steam/hr/Mw. Well surges were observed during the test and their cause was attributed to temporary obstructions in the system that induced in-pipe flashing.

The Denver Research Institute (DRI) conducted several production logging tests in 1978 and 1979 (Butz and Plooster, 1979). Pressure and temperature data were logged versus depth during several constant flow-rate tests from 146,818 kg/hr to 263,636 kg/hr as measured by the James method. The flow rates are probably accurate to $\pm 15\%$. Butz and Plooster (1979) were able to match the measured borehole temperature and pressure profiles by using a program that modeled two-phase flow in the well bore and determined the flash depth in the borehole and the productivity index of the well. The best models were those that included a component of compressible gas.

EXPLORATION METHODS

The Roosevelt Hot Springs geothermal area has served as a laboratory for the development and testing of geothermal exploration methods for some time (Ward et al, 1978). Since 1978 more exploration data have become available, including detailed geologic mapping, additional deep drill holes, additional electrical resistivity surveys, a reflection seismic profile, passive seismic data, and extensive application and testing of surface and subsurface geochemical methods. These new data allow us to expand upon earlier studies. With the results of the individual exploration methods and the supreme advantage of 20/20 hindsight, the most ef-

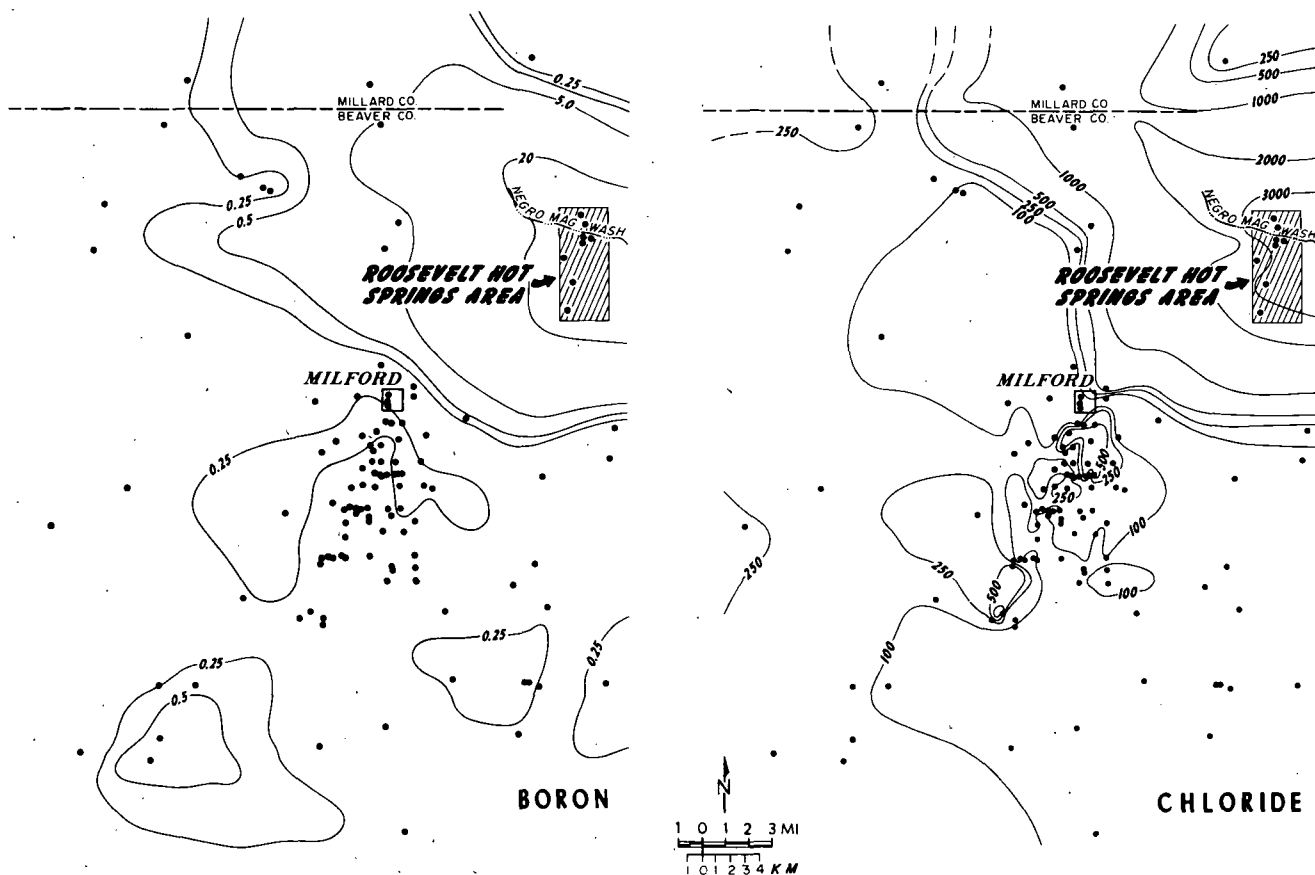


FIG. 3—Concentrations of boron and chloride in ground water in Roosevelt Hot Springs KGRA and adjacent Milford Valley. Data are from Mower and Cordova (1974) and Mower (1978) and was compiled by D. R. Cole.

efficient strategy for the exploration of the Roosevelt Hot Springs geothermal system will be presented. The results of some of the geological and geochemical exploration methods have been presented in the previous section.

Ground Water—Flow Systems and Chemistry

In contrast to the geothermal reservoir, the ground-water aquifer in the vicinity of the Roosevelt Hot Springs system is nonconfined. The study of this ground-water system is important from two aspects. First, it is probable that the present ground-water system provides the recharge to the thermal reservoir. This information bears on estimates of the longevity of the system and also whether the system will remain water-dominated during production or become vapor dominated (White et al, 1971) or possibly depleted. Second, studies of ground-water flow and chemistry are important exploration procedures which can be used to detect leakage of thermal waters into the regional ground-water systems. Hydrologic data can be inexpensively collected during thermal-gradient and heat-flow studies and for many areas are available in the ground-water literature.

Reconnaissance ground-water studies of the Milford and Beaver Valleys (Mower and Cordova, 1974; Mower, 1978) do not discuss the hydrology in the geothermal area but they do reveal the generalized ground-water configuration. The probable direction of ground-water movement within the KGRA is west-northwest toward Beaver Bottoms. The much higher elevation of the potentiometric surface in Beaver Valley than in Milford Valley—more than 984 ft (300 m) near the KGRA—prompts the speculation that if there were sufficiently transmissive fractures within the crystalline units of the Mineral Mountains, the difference in head would force ground water to flow through the range. The chances for this interbasin ground-water flow are enhanced by the cross-cutting structural zones like the Negro Mag fault zone. If ground water originating in the Beaver Valley drainage is recharging the geothermal reservoir, vast quantities of recharge may be available to the geothermal wells.

The ground-water papers by Mower and Cordova (1974) and Mower (1978) contain additional information which can be of value in exploration for the geothermal resource. Figure 3 is a map showing concentrations of chloride and boron in the vicinity of the Roosevelt Hot Springs. Lenzer et al (1976) show plots of ground water total dissolved solids which are similar to the patterns developed in Figure 3. These plots indicate that the chemical patterns produced by leakage of geothermal fluids into the ground-water system can be detected at significant distances from the geothermal system. These data are commonly available in the published literature, and its compilation and analysis can be a very efficient exploration method.

Solids Geochemistry

The geochemistry of hydrothermally altered rocks is routinely used by the minerals exploration industry as a guide to buried ore deposits. Yet despite the similarities

Table 3. Analyses of Hot Spring Deposits*

	Chalcedonic Sinter, Opal Mound	Mn-Cemented Alluvium	Altered Alluvium Over Fumarole
Na (%)	0.15	1.79	0.07
K (%)	0.14	3.12	0.26
Ca (%)	0.14	0.39	0.06
Mg (%)	0.01	0.10	0.03
Fe (%)	0.02	0.74	0.16
Al (%)	0.09	5.18	4.01
Ti (ppm)	19	560	2,040
P	—	651	336
Sr	33	386	266
Ba	—	4.9%	326
Cr	—	9	24
Mn	388	18.8%	173
Co	—	28	—
Ni	—	—	—
Cu	—	231	3
Mo	—	5	—
Pb	—	68	15
Zn	1	23	7
Cd	—	4	1
As	145	858	5
Sb	243	291	21
W	—	2,940	29
Li	11	17	8
Be	99.8	18.6	3.4
Zr	—	17	42
La	—	37	34
Ce	—	42	56
Hg (ppb)	352	2,210	49,300

*From Bamford et al (1980). Dash indicates that element was not detected.

between hydrothermal mineral deposits and active geothermal systems, the development of geochemical zoning models by the geothermal industry has been largely neglected. Recent studies (Browne, 1971; Ewers and Keayes, 1977) have suggested that trace-element zoning may be developed around the high-temperature centers of active geothermal systems. The studies at Broadlands have demonstrated that volatile and base metals are crudely zoned with depth as a result of decreasing temperature and boiling in permeable zones.

The trace- and major-element contents of surface and drill-hole samples from the Roosevelt Hot Springs thermal field were documented to determine if geochemical zoning models could be developed into an effective exploration tool (Bamford, 1978). Thirty-four elements were analyzed using an inductively coupled argon plasma spectrometer. Arsenic was determined by colorimetric methods, and mercury by a gold film detector. The analytical techniques are described by Christensen et al (1980a) and Capuano and Bamford (1978).

Geochemical analyses demonstrate that Hg, As, Sb, Mn, Cu, Co, W, Li, Pb, Zn, Be, Sr, and Ba have been transported and redistributed by the thermal fluids. These elements are strongly concentrated in hot-spring deposits (Table 3) with surface concentrations being typically more than an order of magnitude higher than

the subsurface abundances. However because of contamination during drilling, Hg, As, Sb, and Li are the only trace elements whose abundances in drill cuttings can be unambiguously related to chemical redistribution by geothermal activity.

Trace-element distributions, like the distribution of hydrothermal alteration minerals, are not pervasive but are localized along fractures and permeable alluvial horizons that have served as fluid channels. Detailed lithologic and geochemical logging has shown that at depth, arsenic is diagnostic of the hydrothermally altered rocks in the central part of the thermal field. Electron microprobe analyses and selective chemical leaching of the drill cuttings indicate that arsenic occurs primarily within pyrite and crystalline iron oxides formed from pyrite. Concentrations of arsenic as high as 4% have been detected in some pyrite crystals. In general, concentrations of arsenic are irregularly distributed within individual pyrite grains suggesting that the composition of the thermal brines has varied during the life of the system.

Mercury, in contrast to arsenic, is concentrated in the cooler parts of the thermal field, occurring in both weakly and highly altered rocks. Concentrations of mercury greater than 20 ppb define a broad envelope in the outer part of the system to depths approximately marked by the 420°F (215°C) isotherm (Fig. 4). This distribution reflects the extreme mobility of mercury at high temperatures within the thermal system.

Christensen et al (1980b) have experimentally investigated the mobility of mercury by measuring its progressive loss from drill cuttings and surface samples heated in air. These studies demonstrated that by 392°F (200°C) mercury loss had become significant, and had reached a maximum by 482°F (250°C). They concluded that mercury is present within the geothermal reservoir mainly as a native metal and suggested that its distribution reflects the present thermal configuration of the geothermal system.

At depths between 98.4 and 196.9 ft (30 and 60 m), pronounced enrichments in both arsenic and mercury occur in cuttings from thermal gradient holes located within the productive part of the thermal field. Despite the relatively small number of samples and the wide spacing between drill holes, geochemical data from shallow thermal-gradient holes nevertheless appear to be a useful means of prioritizing drilling targets that is independent of temperature measurements.

Concentrations of mercury and arsenic in soils over the thermal system are closely associated with hot-springs deposits and faults that are connected to the geothermal reservoir. The distribution of the anomalies and their shapes confirm that northeast- and west-northwest-trending (Negro Mag) structures control the near-surface hydrology of the thermal fluids.

Geophysics

Gravity Methods

Gravity methods are widely used in geothermal exploration to map structure and, in some cases, to detect directly the depositional products of hydrothermal

systems. The latter use has been demonstrated in the Imperial Valley of California (Biehler, 1971) where the precipitation of silica and carbonates in sediments above the hydrothermal systems results in an increase in density of the sediments and thus a positive gravity anomaly.

The Bouguer gravity map, for the Roosevelt Hot Springs area (Fig. 5), is dominated by two major features: a broad, closed minimum centered over Milford Valley, and a north-trending elongate high over the Mineral Mountains. The data are fully terrain corrected. The gravity relief of approximately 36 mgal reflects a density contrast of 0.3 to 0.7 between valley fill and the bedrock (Table 4) within the range. A generally planar regional gradient of approximately 1 mgal/km decreasing eastward may be estimated for the Mineral Mountains area based on regional data (Crebs and Cook, 1976).

Bouguer gravity decreases gradually from the central part of the range to the valley low. The gravity high along the northern and western parts of the Mineral Mountains can be correlated with the Paleozoic limestones, Precambrian metasediments, and Tertiary diorites. In the vicinity of the geothermal field, denser lithologies such as the Precambrian banded gneiss and Tertiary diorites have been intruded by less dense felsic phases of the Mineral Mountains intrusive complex. Local perturbations on the smooth gradient (residuals), generally less than 2 mgal, can be readily explained by density variations of 0.1 to 0.3 g/cc within the crystalline rocks, as documented in Table 4. The interpretation of structural details beneath the alluvium within and west of the geothermal field is within the range of ambiguity due to uncertainties in the regional gradient and the variable density within the bedrock. A principal result of model studies supported by well control and density data is the absence of a large (>650 ft; 200 m) displacement in the bedrock surface along any single normal fault. Instead we see a gradual dip to the west, and possibly several minor faults near the Opal Mound fault and the outcropping range front. Ward et al (1978) present a similar interpretation, and these interpretations are in agreement with reflection and refraction seismic data presented later.

Magnetic Methods

The aeromagnetic map shown in Figure 6 is part, about 100 mi² (270 km²), of a much larger 300 mi² (780 km²) survey flown in 1975 (Ward et al, 1978). Data were obtained along east-west flight lines with an average line spacing of 1,380 ft (420 m). The flight path was smoothly draped at an average 1,000 ft (305 m) above ground level.

An extensive program of magnetic susceptibility measurements was undertaken in the summer of 1979 to provide support for the magnetic interpretation. The susceptibility data (Table 5) are in-situ susceptibility measurements at more than 60 locations on smooth, unweathered outcrop surfaces. A Bison magnetic susceptibility meter Model 3100 with in-situ coil accessory was used for the measurements. The data shown in Table 5 are fully corrected for outcrop surface

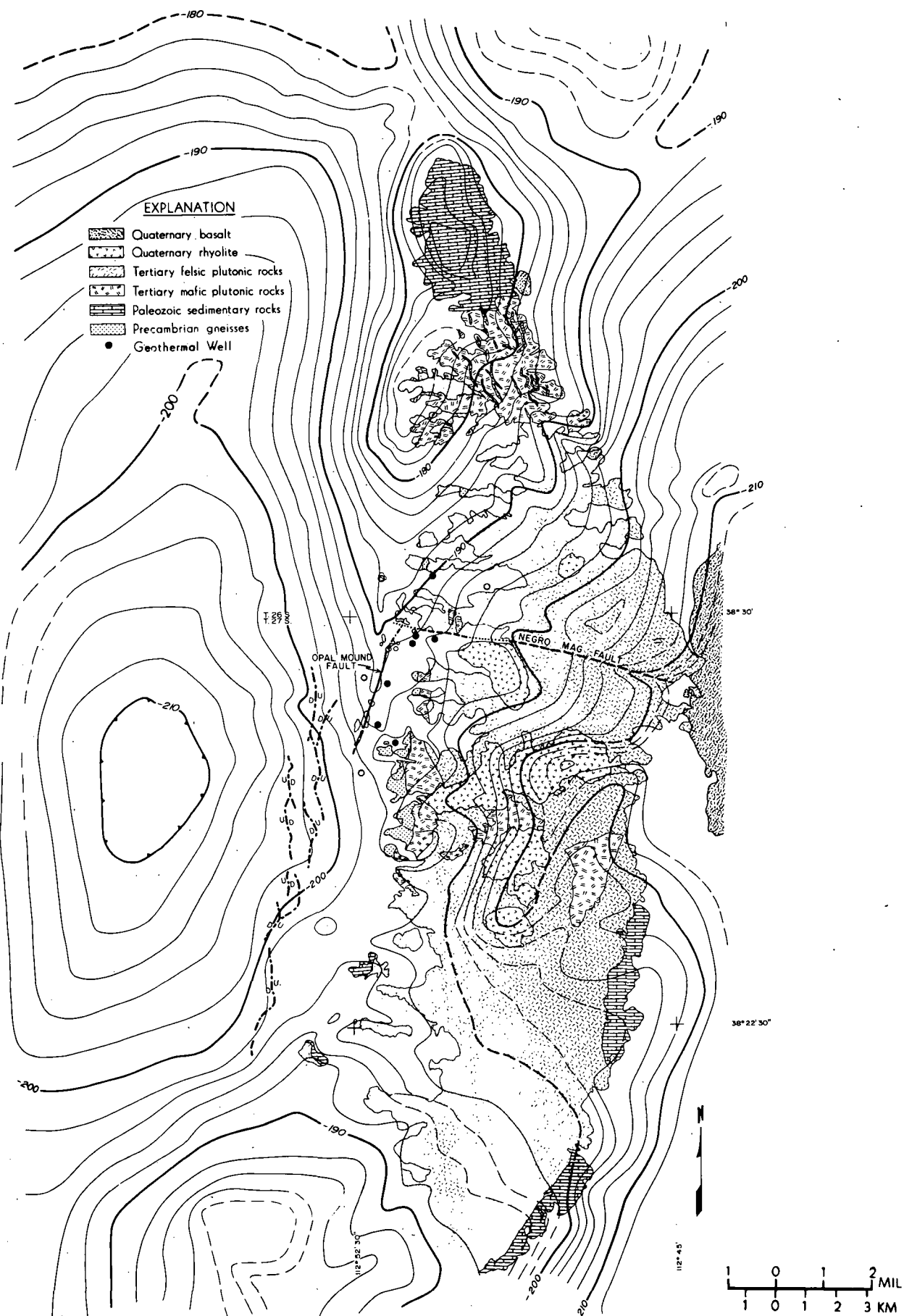


FIG. 5—Terrain-corrected Bouguer gravity map for Milford Valley and Mineral Mountains area (modified from Carter and Cook, 1978).

roughness. Additional susceptibility data determined from drill cuttings of Roosevelt KGRA 9-1 are reported by Glenn et al (1980).

A detailed inspection of the map reveals about 30 closed highs and lows over outcrop of the Mineral Mountains. The apparent complexity of the aeromagnetic map is not surprising in view of the complex igneous geology (Fig. 2) and the unavoidable variations in terrain clearance over rocks of varying magnetization. A study of the analog altimeter profiles shows actual terrain clearance values as little as 480 ft (150 m) over sharp topographic highs and as much as 1,200 ft (365 m) over canyons and between hills. This terrain clearance variation contributes to considerable

east-west elongation and irregularities in the contoured map.

An in-depth discussion of the entire magnetic map is beyond the scope of this more general paper. An interpretation has been completed with integrated spatial correlation of magnetic and geologic maps, simple depth estimates, model comparisons, and extensive magnetic susceptibility data. On this basis, most of the magnetic features over the Mineral Mountain range can be attributed to mapped rock-type and altitude variations. Table 6 summarizes the main characteristics and interpreted sources for major anomalies identified in Figure 6. Most important to the present study is the interpretation of new information that relates to the struc-

Table 4. Densities of Lithologies from Mineral Mountains

Rock Type/Unit	g/cc		No. of Samples	Reference
	ρ range	ρ (x)		
Tqm	2.43 - 2.80	2.64 ± .04	56	Glenn et al (1980)
"granitic"	2.45 - 2.71	2.59 ± .07	25	Carter and Cook (1978)
"granitic"	2.53 - 2.60	2.57 ± .02	11	Crebs and Cook (1976)
Td	2.54 - 2.90	2.76 ± .08	48	Glenn et al (1980)
Ts	2.43 - 2.63	2.55 ± .06	23	Glenn et al (1980)
Qrf/Qrd	2.16 - 2.24	2.22 ± .05	8	Crebs and Cook (1976)
Qrf/Qrd	2.22 - 2.38	2.31 ± .07	8	Carter and Cook (1978)
Obsidian	2.15 - 2.35	2.30 ± .07	8	Carter and Cook (1978)
Pebg (upper plate)	2.11 - 2.95	2.73 ± .28	136	Glenn et al (1980)
Gneiss and schist	2.63 - 2.74	2.69 ± .04	8	Crebs and Cook (1976)
Gneiss	2.63 - 2.74	2.69 ± .04	5	Carter and Cook (1978)
Limestone	2.55 - 2.97	2.71 ± .13	9	Carter and Cook (1978)
Quartzite ¹	2.50 - 2.74	2.62 ± .09	5	Carter and Cook (1978)
Alluvium		2.0 ± .1 ² 2.05 ³		Carter and Cook (1978) Glenn and Hulen (1979)

¹Samples from Star Range, Rocky Range, Beaver Lake Mountains or Beaver Dam Mountains.

²Nettleton's method.

³Well log determination above water table.

Table 5. Magnetic Susceptibilities of Lithologies, Mineral Mountains, Utah¹

Rock Type	Symbol#	No. Sites	No. Observations	Mean	Std. Dev.*	Range
						← Units of micro cgs →
Alluvium	Qal	2	8	500	86	388-640
Rhyolite flows	Qrf	3	56	179	69	41-347
Rhyolite domes	Qrd	4	43	131	84	0-372
Rhyolite dikes	Trd	1	10	406	29	363-463
Diabase dikes	Tds	1	3	474	—	466-483
Granite dikes	Tgr-d	3	14	411	129	166-650
Granite	Tg	6; tr.	63	1,353	333	623-2,053
Seyenite	Ts	5; tr.	36	1,998	272	1,546-2,056
Porphyritic granite	Tpg	6; tr.	86	1,626	282	10-2,467
Quartz monzonite	Tqm	7; tr.	58	1,918	166	1,433-2,244
Hornblende gneiss	Tgn	4	24	2,310	830	1,520-3,440
Biotite gneiss	Tn	2	6	2,644	405	2,118-3,170
Sillmanite schist	PeS	tr.	10	22	32	0-89
Banded gneiss	Pebg	6; tr.	35	1,252	1,698	38-5,421

¹Corrected in-situ susceptibilities, 6" diam. coil, Bison system.

Map symbol after Nielson et al, 1978.

*Standard deviation not always statistically significant, but indicative of susceptibility variability.

tr. = indicates observations along traverses, 500 to 2,500 ft long.

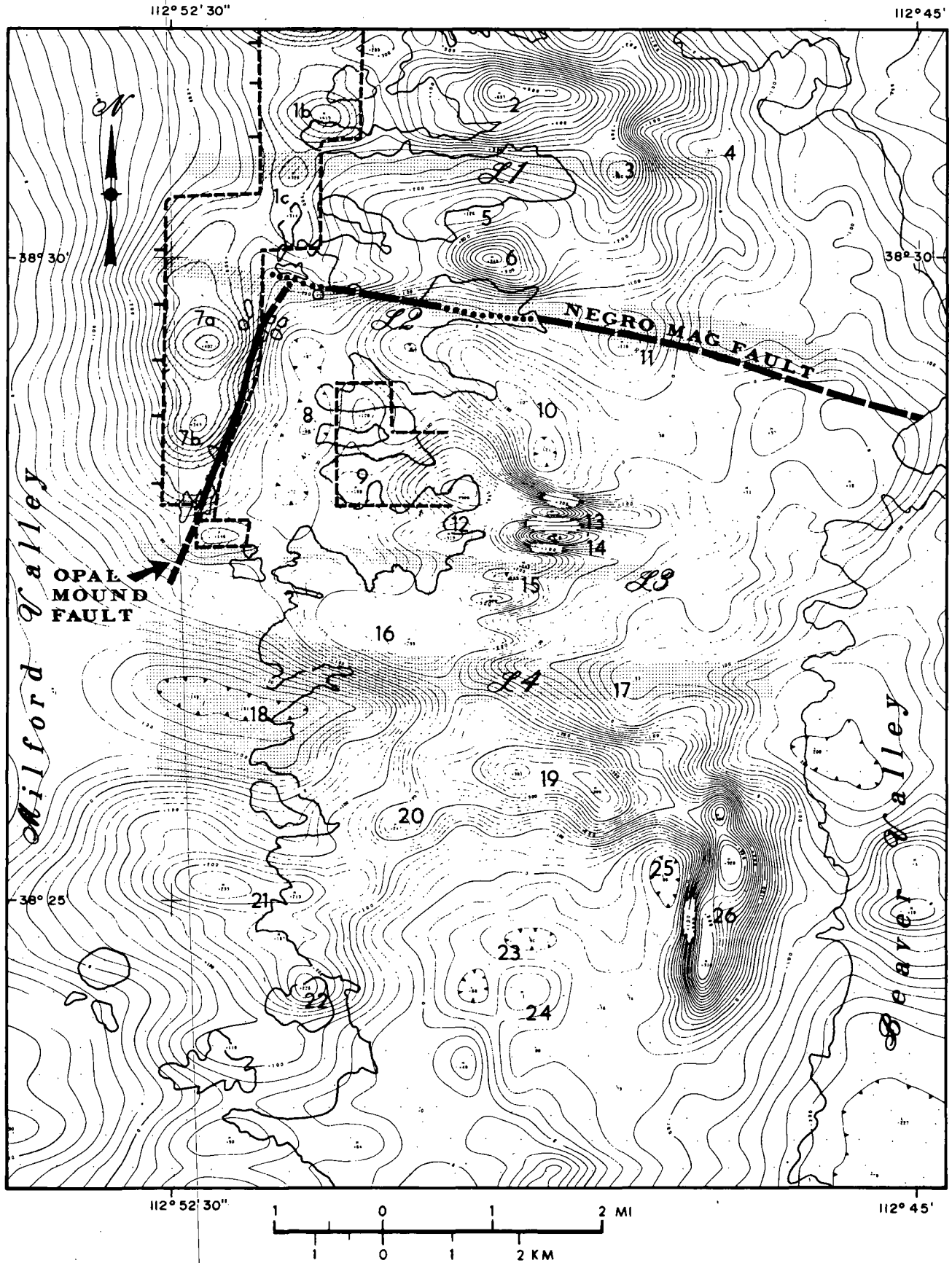


FIG. 6—Total magnetic intensity map of Roosevelt Hot Springs—Mineral Mountains area. Suballuvial magnetic sources and principal structural zones are indicated. Major anomalies are numbered for reference to text.

tural setting of the geothermal reservoir.

Several east-trending zones of low magnetic intensity cut across the Mineral Mountains (L1, L2, L3, L4). These magnetic trends are explained in part by the outcropping rock types and topographic features. The topography, geology, and magnetics are all expressions of east-west structural features. Feature L2 corresponds closely to the Negro Mag fault zone and its eastward continuation as mapped faults. It also appears to displace to the west a north-trending magnetic anomaly (7) closely associated with the Opal Mound fault. L3 terminates anomaly 7 between productive reservoir well Utah State 72-16 and the hot but dry hole, Utah State 52-21. The magnetic bodies appropriate to this magnetic field inclination are indicated on Figure 6.

The magnetic data over bedrock areas reflect the mapped geology and magnetic susceptibility. The identification of four east-trending structural zones, two of which (L1 and L3) may limit the north-south extent of the reservoir, is new information. The delineation of the alluvium-covered Opal Mound horst, bounded on the east by the reservoir-bounding Opal Mound fault, is the most important contribution to understanding the geothermal reservoir provided by the magnetic data. In view of known susceptibility values for the igneous and metamorphic rocks and the alluvium, it is not necessary to postulate an alteration low resulting from magnetite destruction to explain magnetic lows east of the Opal Mound fault (anomaly 8) and south of well Utah State 52-21 (anomaly 18).

Seismic Methods

A broad spectrum of seismic data is available at Roosevelt Hot Springs. Passive seismic data include long-term historical records of major earthquake activity, microearthquake surveys and, at a lower magnitude of naturally occurring seismic disturbance, seismic emissions or "noise" surveys. Single profiles of both refraction and CDP Vibroseis reflection data are also available for study.

In 1974 and 1975, an array of up to 12 portable high-gain seismographs was established within the Roosevelt Hot Springs and Cove Fort-Sulphurdale areas (Olson and Smith, 1976). In two survey periods totaling 49 days, 163 earthquakes of magnitude $-0.5 < M < 2.8$ were recorded. However, only four events could be associated with a 12-mi (20-km) length of the western flank of the Mineral Mountains which includes the Roosevelt Hot Springs area (Ward et al, 1978). Olson and Smith (1976) determined P-wave delays of up to 0.1 sec and detectable S-wave attenuation of ray paths across the Mineral Mountains. Ward et al (1978) interpreted the low-velocity effect and shear wave attenuation for these ray paths as possibly indicative of partial melting or major intense fracturing of crustal rocks beneath the southern part of the Mineral Mountains.

Robinson and Iyer (1981) observed P-wave residuals of up to 0.3 sec in a well-defined pattern corresponding to a region of anomalously low velocity (5 to 7%) centered under the geothermal area and extending from

Table 6. Magnetic Anomaly and Source Characteristics, Roosevelt Hot Springs Area, Utah

Anomaly	Amplitude (gammas)	Correlation ¹ ρ topo/mag	Geologic Setting ²	Probable Source ³	Susc. Contrast (micro cgs)
1 b, c	120; 100	X	Qal, Qcal, Tqm	Tqm	2,000
2	280	H	Tqm, Tgr	Tqm, Ts; r.t.c.	~ 2,000
3	120+	M	Tqm	Tqm; r.t.c.	
4	- 80	R	Qrd, Qal	Qrd, Qal; r.t.c.	~ -1,400
5	-100	M-X	Qal, Tgr, Ts, Tqm	Qal, Tgr; i.t.c.	
6	190	H	Ts, Tqm	Ts, Tqm; r.t.c.	~ 2,000
7 a, b	300; 240	X	Qal, Qcal		2,000-5,000
8	- 40	X	Qal	Qal; i.t.c.	
9	50	H	Tgn, Ts, Tpg	Tgn, Ts; r.t.c.	
10	-200	L-R	Qrt, Qal	Qrt (reversed)	~ -1,500
11	50	H	Tqm	Tqm; r.t.c.	
12	190; 200	L-X	Ts, Qal	Ts;	~ 2,000
13*	250	H	Tqm	Tqm; * r.t.c.	
14*	-180	R?	Tqm	Tqm; * i.t.c.	
15*	- 80	R	Qrd	Qrd; * r.t.c.	
16	200	H-M	Tpg, Tn, Tgn, Ts, Tg	Ts, Tpg, Tgn; r.t.c.	~ 2,000
17	-150	X-R	Qrd, Tg	Qrd; i.t.c.	
18	- 90	L-X	Qal, Pebg, Tpg	Qal; Pebg, Tg	
19	350	H	Tg, Tn, Tpg, Qra, Qrd	Tn, Tg, Tpg; r.t.c.	~ 2,500
20	250	H	Tn, Tpg, Tgn	Tn, Tpg, Tgn; r.t.c.	~ 2,000
21	250	X	Qal, Tn, Tgn, Tpg	Tpg, Tgn, Tn	~ 2,000
22	150	L	Qal, Tbg, Tgr	Tbg, Tgr	
23	- 30	L-R	Qra, Qrd	Qra; i.t.c.	
24	20	H	Qrd	Qrd; r.t.c.	
25	- 50	H-R	Tq	- r.t.c.	
26	350	H	Tdb, Tg, Tbg	Tdb; r.t.c.	~ 3,500

¹H = high, M = moderate, L = low, X = insignificant, R = reversed.

²Map symbol after Nielson et al (1978).

³r.t.c. = reduced terrain clearance; i.t.c. = increased terrain clearance; * indicates poor contour representation.

about 3 mi (5 km) depth down into the uppermost mantle. They preferred an explanation for these delays in terms of abnormally high temperatures and a small fraction of partial melt. Wechsler and Smith (1979) noted that these delays could arise from the fractured and possibly fluid-filled porosity of the western part of the Mineral Mountains pluton. Wechsler and Smith further noted the problems of accurate epicenter location and the limitations of P-wave studies in areas of complex near-surface lateral-velocity variations, such as exist at Roosevelt Hot Springs.

The relatively few earthquake locations determined for the western Mineral Mountains from this 49-day recording period and the complex near-surface velocity structure almost preclude the use of microearthquakes in delineating the Roosevelt Hot Springs geothermal system. P-wave delay studies may ultimately improve our understanding of the deep heat source at Roosevelt, but to this time have not contributed to delineation of the system.

Schaff (1981) has reported on seismic activity detected with the present nine-station seismograph array for the period October 1979 through January 1981. His results to date substantiate the earlier conclusion that seismicity in the immediate vicinity of Roosevelt Hot Springs is generally of a low level and somewhat episodic in nature. In the first 12-month period, no earthquakes were located within the anticipated production zone or along the Opal Mound fault. However, swarmlike activity was recorded east of the reservoir area in December 1980–January 1981. This trend of earthquake epicenters across the Mineral Mountains and east of the geothermal reservoir appears to lie along the eastern projection of the Negro Mag fault. More than 1,000 earthquakes of magnitude less than 1.5 have occurred in three major swarms between July and December 1981. The epicenters for these most recent events define a trend extending from the surface to 4 mi (6 km) depth parallel with the trend of the Negro Mag fault (L. McPherson and G. Zandt, personal commun.).

Seismic emissions survey.—Seismic emissions surveys have been promoted by several geophysical contractors as a geothermal exploration method in which the seismic emissions or “noise” would hopefully delineate active fault and fracture zones possibly associated with geothermal activity. The method employs an array of geophones (four or five) spaced approximately 2,000 ft (610 m) apart. In surveys at Roosevelt Hot Springs (Katz, 1977a, b) data were recorded at the array for 1 to 3 days, then moved to another station. Five such stations within a 14 to 16 mi² (36 to 41 km²) area constitute a survey. The data were edited and processed with algorithms which determine the noise source locations based on delay times computed for a half-space velocity model and the correlation of these delays with the observed data.

A reevaluation of these data has been completed by Ross et al (1982). As employed at Roosevelt Hot Springs, the seismic emissions survey may indicate areas of geothermally induced seismic noise, but it is dominated by other noise sources and is imprecise in defining geothermal conduits. The correlation procedure is severely limited by model simplicity and veloci-

ty assumptions, and generally recognizes source direction more accurately than distance to the seismic noise source. A more refined velocity model could perhaps improve the resolution of the noise source areas through a higher correlation of source-to-geophone array delay times. It is unlikely that the velocity model could be refined enough to justify inclusion of the method in geothermal exploration in complex geologic environments.

Seismic refraction.—In April 1977, a 19 mi (30-km) long seismic refraction profile was recorded across the Roosevelt Hot Springs geothermal area (Gertson and Smith, 1979). Multiple shots at seven different shot locations were used to provide multiple subsurface coverage. Although the large station spacings of nearly 820 ft (250 m) were not adequate for locating narrow structural features, Gertson and Smith were able to define a somewhat generalized velocity model for the area and also determined that the first large displacement in range front faulting occurs at least 0.6 mi (1 km) west of the Opal Mound fault. P-wave attenuation across the geothermal reservoir was much less than attenuation in other parts of the profile, and Gertson and Smith (1979) concluded that the record sections did not appear to contain any evidence for seismic waves that had penetrated and returned from “hot rock” or magma chambers even at great depth. One complicating aspect of the refraction study is that the eastern part of the refraction profile, of necessity, followed the Negro Mag fault zone from the reservoir area eastward across the Mineral Mountains.

Seismic reflection.—One profile totaling 27 mi (43 line km) of detailed reflection seismic data was available for study of the Roosevelt Hot Springs area. Line 5 and 5 OPTW of a GSI speculation survey, recorded in March and April 1978, crosses the Mineral Mountains along the same path as the refraction survey. The data cannot be reproduced, but an interpretation of the data is presented here.

The GSI profiles are high-quality 24-fold CDP Vibroseis data with a 200 ft (60 m) group interval and a 400 ft (120 m) vibrator point interval. The source consisted of 16 sweeps per VP, using a 12-sec sweep and a 12 to 60 Hz sweep band. The sample rate was 2 msec. Processing included deconvolution, velocity analysis, CDP stack, and migration.

Our interpretation of the reflection profile is presented in Figure 7. The time-to-depth conversion is supported by 14 velocity analyses along the profile. These velocities are generalized in Figure 7. The refraction survey and sonic logs of three deep wells in the geothermal system—Utah State 52-21, 72-16, and 14-2—also provide velocity control. Although similar velocities are noted for alluvium, the refraction survey and well logs indicate much higher velocities at depth than velocity analyses of CDP reflection data. To those depths where good reflection quality persists and the coherence of the velocity analysis is well supported, the reflection survey velocities are considered more valid. At greater depths (times), the velocity analyses appear to be less valid and may be as much as 40% too low.

Figure 7 shows gently dipping layers in unconsolidated sediments to depths of 4,000 ft (1,220 m) in

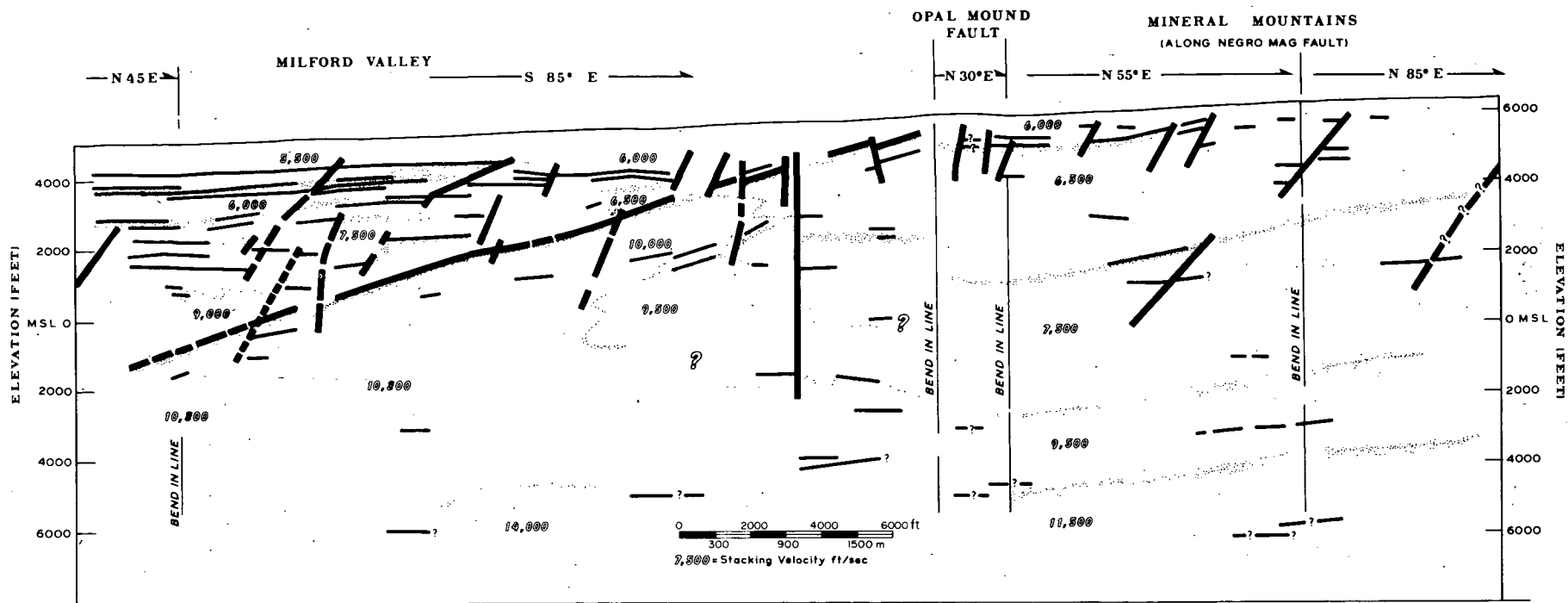


FIG. 7—Structural interpretation of Vibroseis profile GSI-5. Units as determined from velocity analysis and reflection continuity.

the Milford Valley. This sequence thins abruptly to the east as the Opal Mound fault is approached. Numerous faults cut the sedimentary sequence. A very prominent reflector which dips westward at approximately 20° from the Opal Mound fault indicates the base of the unconsolidated sediments. Few coherent reflectors are noted beneath this interface, presumably a sediment-igneous or sediment-metamorphic contrast.

The complexity of Basin and Range faulting is indicated by the reflection data. Unfortunately, the trend of the profile is along the southern edge of the horst block indicated by magnetic data, then N30°E along, and at a small angle to, the Opal Mound fault. The faulting is indicated, but less clearly than would be the case for an east-west line. East of the Opal Mound fault, the higher velocities and lack of coherent reflections indicate igneous rocks extending to depth. The interpretation of the vertical displacement along Basin and Range faults within the first 0.25 seconds is difficult because of high noise levels and probable lateral energy returns associated with the Opal Mound fault area. No single, major vertical displacement is indicated but a complex series of small displacements, of the order of 100 to 320 ft (30 to 100 m), is suggested by the data.

Electrical Studies

The recognition of Roosevelt Hot Springs as a relatively shallow geothermal resource of commercial potential has resulted in numerous electrical surveys designed to characterize the electrical resistivity distribution, and to test the effectiveness of various methods. To a large degree, Roosevelt Hot Springs has become a "test" area because of the type of resource and amount of publicly available supporting data. Included in the electrical surveys already completed are the following: magnetotelluric (MT), controlled source audio magnetotelluric (CSAMT), natural source AMT, controlled source EM, spontaneous polarization or self-potential (SP), induced polarization (IP), and electrical resistivity.

Electrical resistivity surveys.—Electrical resistivity surveys include both the dipole-dipole and bipole-dipole arrays. The bipole-dipole survey (Frangos and Ward, 1980) was undertaken with the knowledge of the resistivity distribution primarily to characterize the effectiveness of the method. The dipole-dipole survey includes at least 50 lines of various lengths, electrode separations, and depth penetrations, and constitutes one of the most complete resistivity data bases assembled. In view of this, and because all the other electrical methods are influenced by the resistivity distribution mapped by these data, a major effort was devoted to interpreting these data using two-dimensional numerical models (Ross et al, 1982).

Figure 8 shows the location of the resistivity lines which were numerically modeled and presents a summary of the intrinsic resistivity distribution for the depth interval of 330 to 500 ft (100 to 150 m). The modeled resistivity data are supplemented with a qualitative interpretation of more than 30 additional lines of data. The modeled resistivities at these depths have been transferred from the interpreted resistivity

sections shown in Figure 9.

The resistivity distribution, even as generalized by numerical modeling, is quite complex. Generally high resistivities (100 to 500 ohm-m) are observed in the range over the Precambrian gneiss and Tertiary intrusive rocks. Very low (<10 ohm-m) to low (10 to 20 ohm-m) resistivities, often modeled as thin vertical conduits, occur along the trend of the Opal Mound fault. West of the Opal Mound fault moderate to high-resistivity (30 to 400 ohm-m) layers overlie layers of moderate to very low resistivity. This appears to represent dry alluvium (above the water table) overlying areas where fresh ground waters mix with warmer, more conductive geothermal fluids migrating downdip from the Opal Mound fault and other conduits. Very low resistivities (2.5 ohm-m) observed along UU line 8100N may represent geothermal outflow, dissolved salts in Lake Bonneville sediments, or some mixture of both. South of the survey base line and Utah State 52-21, high resistivities near the surface decrease with depth but do not indicate the presence of geothermal fluids noted to the north. Figure 8 provides a better comparison with key geologic features and drill-hole locations than does the section representation (Fig. 9), and shows that the low-resistivity area of the geothermal system is bounded by high resistivities southwest, south, and east of the geothermal system at these depths. Low and moderate resistivities extend well into the range along the Negro Mag fault zone. Most of the low-resistivity areas straddle or lie east of the Opal Mound fault at these depths. Resistivities of 3 to 10 ohm-m along the fault are bounded by 10 to 20 ohm-m on all sides as a crude zoning pattern. The resistivity of the alluvium is generally 20 to 50 ohm-m to the west, and much higher (200 to 400 ohm-m) to the south. The probable continuity of resistivity zones is indicated by heavy dashed lines (Fig. 8).

Ross et al (1982) present a similar map for the depth interval 1,500 to 2,000 ft (450 to 600 m) which is less complex because only 1,000 ft (300 m) dipole data could be used for this depth and because of the resistivity averaging inherent in modeling large separation data. The high resistivities east of the Opal Mound fault extend to the west but are substantially reduced to the south (GOC lines 1, 2, 4, 5). In fact, 50 to 400 ohm-m alluvium becomes quite conductive (5 to 20 ohm-m) with the increased depth. The Negro Mag Wash area is still a moderate resistivity reentrant into the range. The alluvium west of the Opal Mound fault has become quite low in resistivity (5 to 15 ohm-m), probably due to the downdip migration of conductive thermal fluids leaking from the geothermal system. The region of the Opal Mound fault itself is modeled as 30 to 50 ohm-m except at the southernmost part of the Opal Mound itself (8 ohm-m). This is in marked contrast to the low resistivity expression at 330 to 500 ft (100 to 150 m) depth. A high resistivity (450 ohm-m) body is indicated less than 1,250 ft (380 m) south of successful well Utah State 72-16, which reached total depth at 1,256 ft (383 m). The hot but dry Getty Oil Co. well, Utah State 52-21, is located in a resistive (100 to 400 ohm-m) area. Several productive wells (Roosevelt KGRA 12-35, Roosevelt KGRA 54-3, Roosevelt KGRA 3-1, Utah State 14-2, Roosevelt KGRA 13-10, and Roosevelt HSU

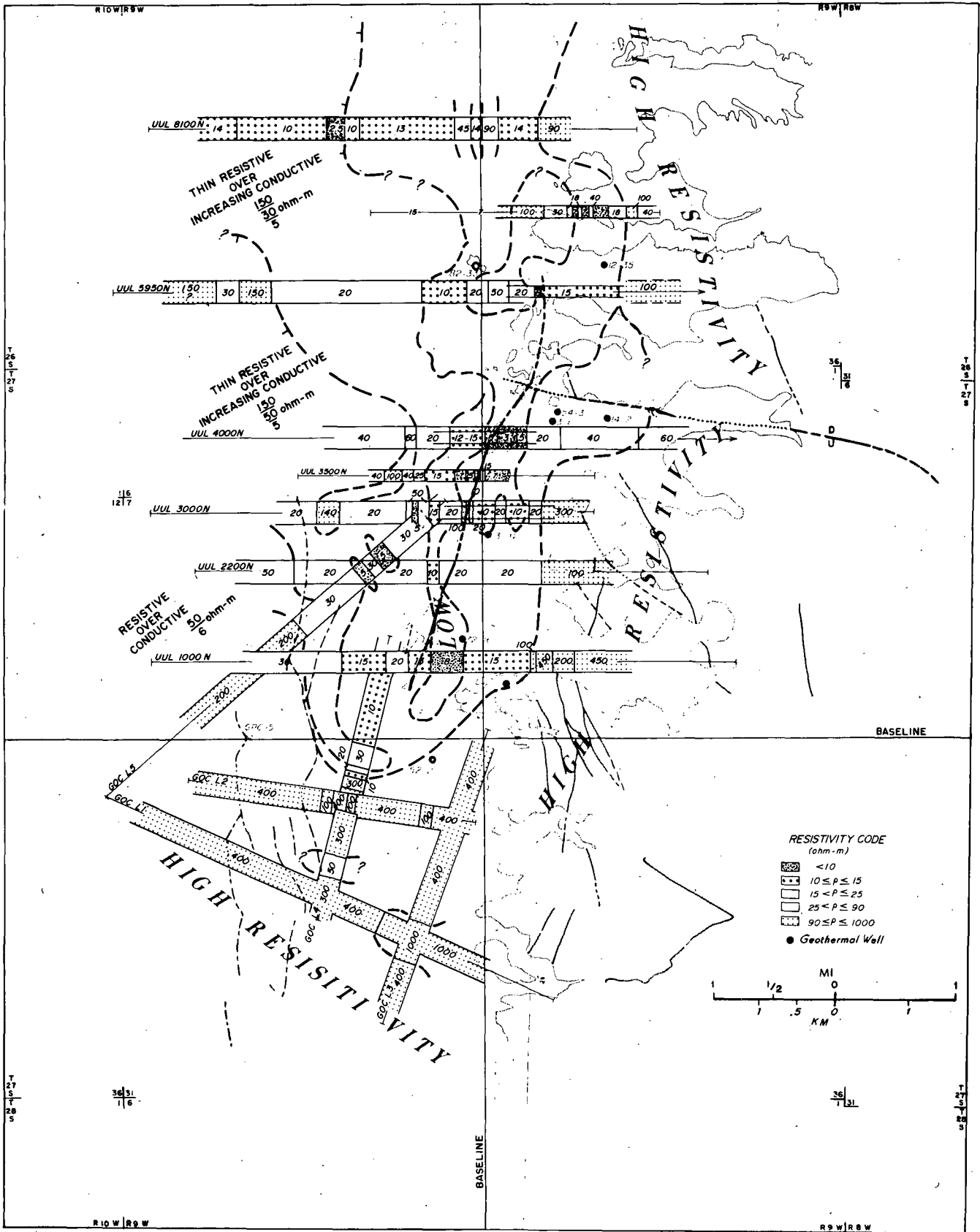


FIG. 8—Interpreted electrical resistivity distribution for depth interval 100 to 150 m, Roosevelt Hot Springs KGRA.

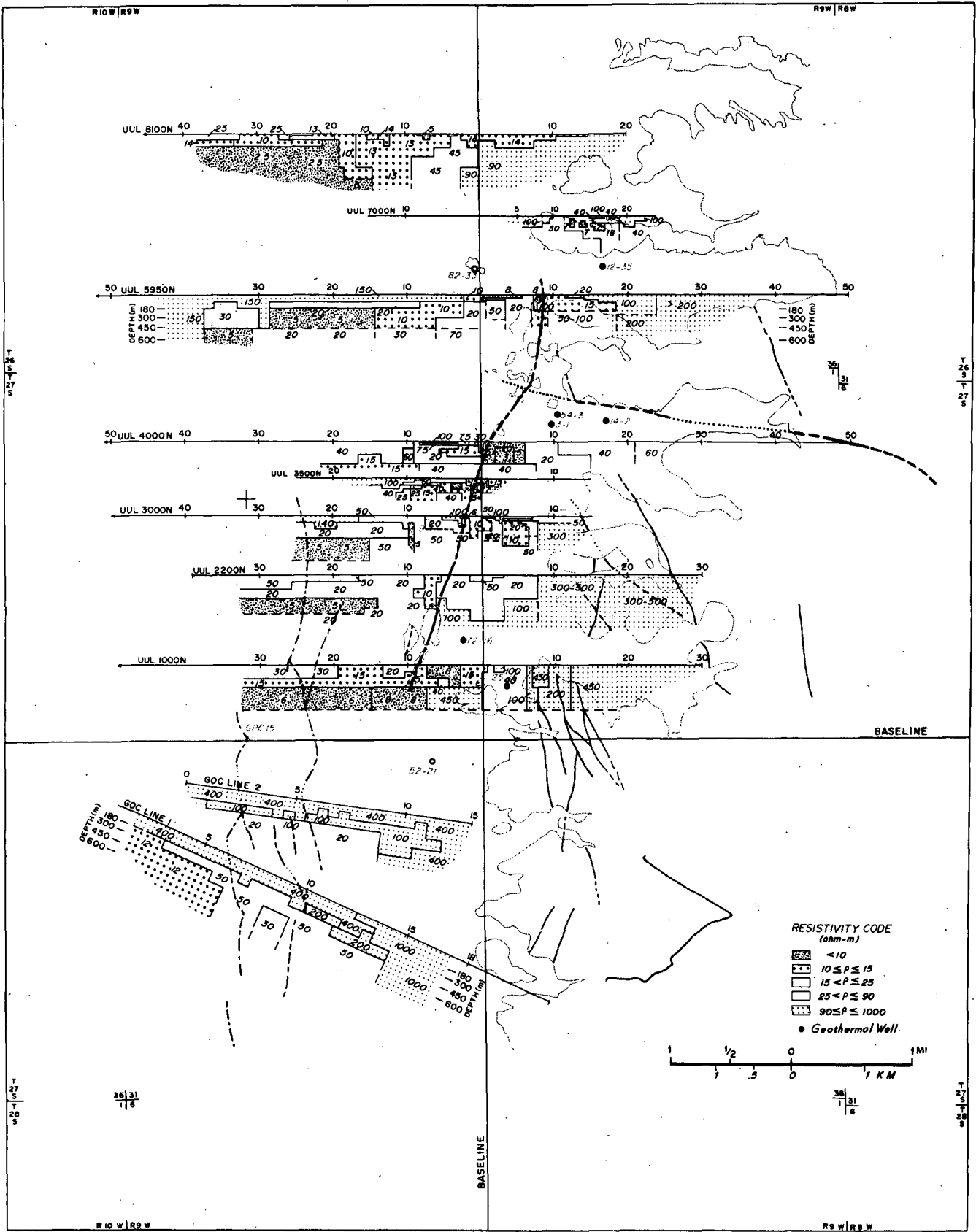


FIG. 9—Interpreted electrical resistivity sections, Roosevelt Hot Springs KGRA.

25-15) are sited in areas of moderate (15 to 40 ohm-m) resistivity which are relative lows.

The interpretations presented in Figure 9 are non-unique and are limited by the grid size which becomes coarser with depth, the validity of the two-dimensional model, the goodness of fit of computed to observed data values, and the choice of body size, position, and resistivity. Nonetheless, careful modeling of dipole-dipole resistivity data has resulted in a more accurate representation of earth resistivity distribution for a given cost than any other electrical method. The non-uniqueness is reduced by using a network of profiles, several of which intersect, and the integration of geologic data, such as the detailed (1:24,000) map of Nielson et al (1978).

Near-surface electrical methods.—Sandberg and Hohmann (1980) described a controlled source audio-magnetotelluric (CSAMT) survey at Roosevelt Hot Springs which compares well with dipole-dipole resistivity data for shallow depths (< 330 ft; 100 m). Minor disagreements in the interpretative models from these methods serve to indicate the noise and ambiguity levels for each method. Chu et al (1980) described induced polarization surveys which were unable to map clay alteration or pyritic zones related to the geothermal system.

Corwin and Hoover (1979) discussed thermoelectric coupling and electrokinetic coupling as possible mechanisms for generating self-potential anomalies observed over geothermal systems. They reported a dipolar anomaly located directly over the Opal Mound fault and concluded that it results from geothermally generated electrical activity along the fault. More detailed self-potential studies have been completed by Sill and Johng (1979). A complex "quadrapolar" anomaly of two lows (-100 mv) and two highs (+25 and +50 mv) was found to be associated with the southern part of the geothermal system. The 100-mv low which occurs over the Opal Mound fault is the most unambiguous expression of the geothermal system. Other self-potential features could arise from large resistivity contrasts, the movement of ground water from higher to lower elevation, or fluid movement along structures. Additional numerical modeling is required to obtain a more complete understanding of the SP response at Roosevelt Hot Springs, but the observed data document a complex expression of the geothermal system.

Magnetotelluric (MT) studies.—The magnetotelluric (MT) method is often used in both the reconnaissance and detailed stages of geothermal exploration. The earth's electric and magnetic fields vary as a function of frequency in response to natural electrical (telluric) currents flowing within the earth's crust. Through precise measurements of the electric and magnetic field components made at the surface, one may obtain information relating to the impedance distribution (i.e., electrical resistivity) to depths as great as 25 mi (40 km) within the earth's crust. The reader is referred to an excellent paper by Vozoff (1972) for a detailed description of the method.

In keeping with the detailed geophysical definition of the Roosevelt Hot Springs area an extensive MT network of 93 stations was established in the Milford

Valley—Mineral Mountains area (Wannamaker et al, 1978, 1980).

The reduced data for a central 14 mi (22 km) east-west profile are presented as observed apparent resistivity versus frequency for the TM (transverse magnetic) mode in Figure 10a. The best-fit model results computed for a two-dimensional model geometry TM mode (Fig. 10b) are seen to be very similar. The comparison between observed and modeled impedance phase (not shown here) is also good but has a poorer fit in the central part of the profile. The two-dimensional model that produced this best fit is shown as Figure 10c. The rather fanciful 50,000 ohm-m prism in Figure 10c was inserted in an unsuccessful attempt to match the mid-frequency (10 to 0.1 Hz) data. A frequency dependent, three-dimensional current gathering effect involving the Milford Valley to the west is now believed responsible for these particular modeling difficulties (Wannamaker et al, 1980).

Stations 78-22 through 76-2 are located over low-resistivity alluvium and valley fill. Figure 10c indicates resistivities decreasing to near 1 ohm-m at depths of 1,300 ft (400 m). Dipole-dipole resistivity data and Schlumberger soundings also indicate a thin (330 ft; 100 m) resistive (100 ohm-m) near-surface layer with resistivity decreasing to 5 ohm-m or less at depths of 1,000 ft (300 m). Station 76-3 near the center of the cross section occurs over a buried horst inferred from gravity and magnetic data and exhibits high resistivities at moderate depths. Station 76-4 was sited along the Opal Mound fault (Wannamaker et al, 1978), which has been identified earlier as a narrow, vertical conductive zone associated with ascending geothermal fluids. Silica cementation has locally decreased the porosity but fracture permeability remains.

Wannamaker et al (1978, 1980) noted great difficulty in obtaining good representations of both the TE and TM mode resistivities for any single one-dimensional or two-dimensional model. Extensive three-dimensional model studies indicate the limitations of one- and two-dimensional modeling at Roosevelt Hot Springs, and probably for most Basin and Range-type geothermal reservoir areas. A few of their more general conclusions are restated here.

1. Current gathering in the valley results in a regional distortion of the electric field affecting all stations at Roosevelt Hot Springs for lower frequencies.

2. The TM mode is most appropriate for two-dimensional interpretation, and has yielded good results for geometrically regular three-dimensional prisms.

3. Clays ($\rho = 1$ to 2 ohm-m) may exist to depths of several hundred meters in the Milford Valley. These overlie more than 0.6 mi (1 km) of semiconsolidated and unconsolidated sediments and volcanics of moderate ($\rho \approx 25$ ohm-m) resistivity.

4. A geometrically regular reservoir of conductive brine beneath the thermal anomaly seems improbable, so the search for any economic hydrothermal reservoir at Roosevelt Hot Springs using MT must be considered unsuccessful at this time. If present, it is not resolved by the two-dimensional TM algorithm. The brine-saturated reservoir zone is clearly three-dimensional and difficult to model satisfactorily with present interpretation

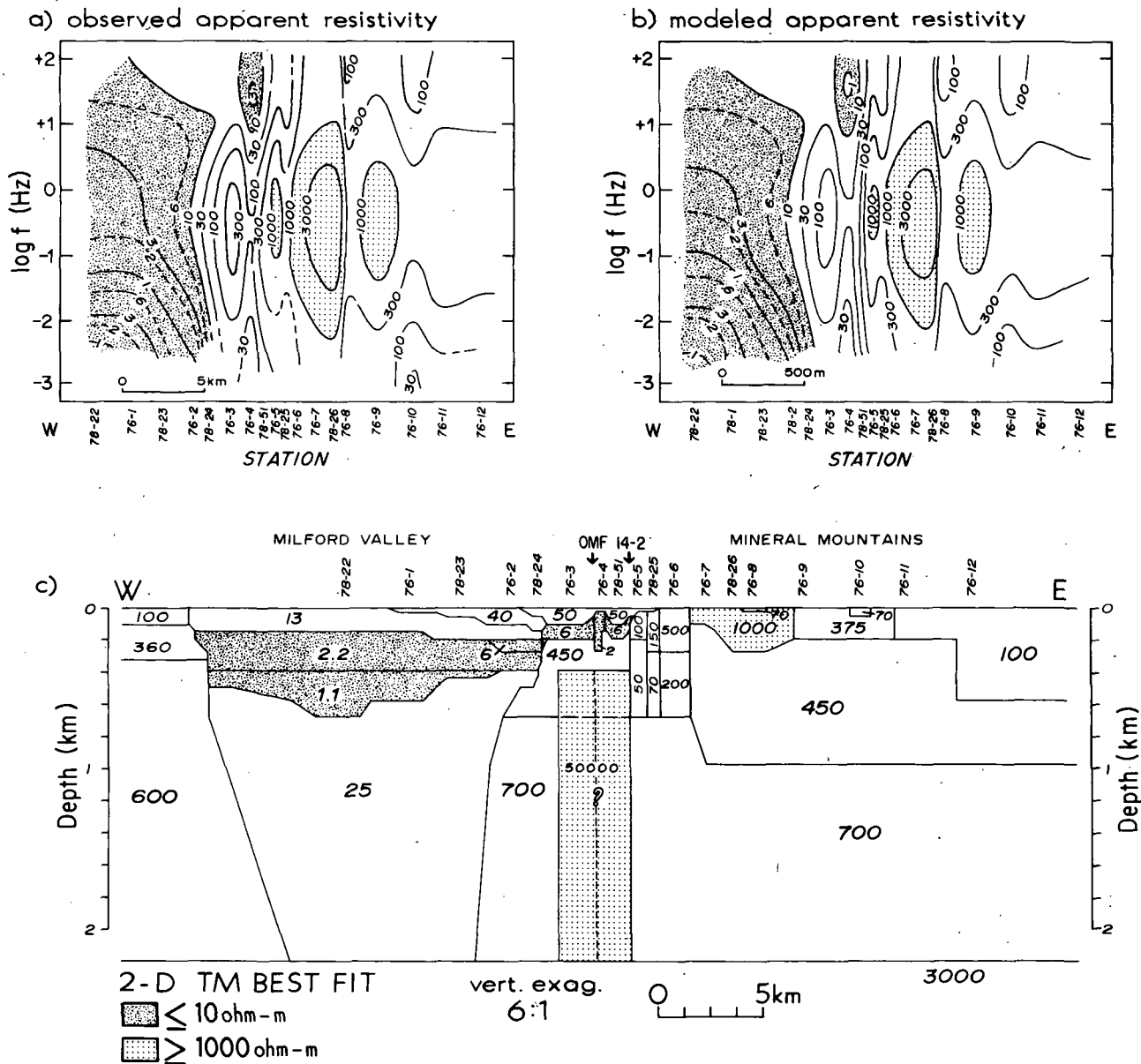


FIG. 10—Magnetotelluric profile CC': (a) observed apparent resistivity, TM mode; (b) modeled apparent resistivity, TM mode; (c) finite element model for profile CC' giving best fit between computed and observed TM mode resistivities. Intrinsic resistivity values in ohm-m; OMF = Opal Mound fault. (After Wannamaker et al, 1980.)

capabilities.

5. A deep heat source for the geothermal system also has not been discerned by MT interpretation to this time.

Thermal Studies

The thermal characteristics of the Roosevelt Hot Springs area have been defined by measurements in 53 thermal gradient, water well, and exploration drill holes (Wilson and Chapman, 1980). Most of the 53 gradient holes bottomed at depths of 200 to 360 ft (60-110 m). The observed near-surface (30 to 230 ft; 10 to 70 m depth) gradients range from 6°C/km to 3,330°C/km compared to a Great Basin average of 35 to 40°C/km.

Thermal conductivity measurements are listed in Wilson and Chapman (1980) and Glenn et al (1980).

Wilson and Chapman (1980) assign the following average conductivities (W/m/K) to principal rock types: quartz monzonite, 2.54; opaline sinter, 2.00; biotite gneiss, 2.00; alluvium, 1.64. Using the appropriate thermal conductivities and gradients for each hole, Wilson and Chapman have produced a detailed map of the near-surface heat flow associated with the geothermal system. The 400 mW/m² and 1,000 mW/m² areas determined from their study are indicated in Figure 11. The 400 mW/m² contour, approximately four times background, encloses an area of 22 mi² (57 km²), whereas the 1,000 mW/m² contour encloses an area of 6 mi² (16 km²) including the Opal Mound fault and most of the successful production drill holes. The anomalous surface heat loss for the system was calculated at 64 MW.

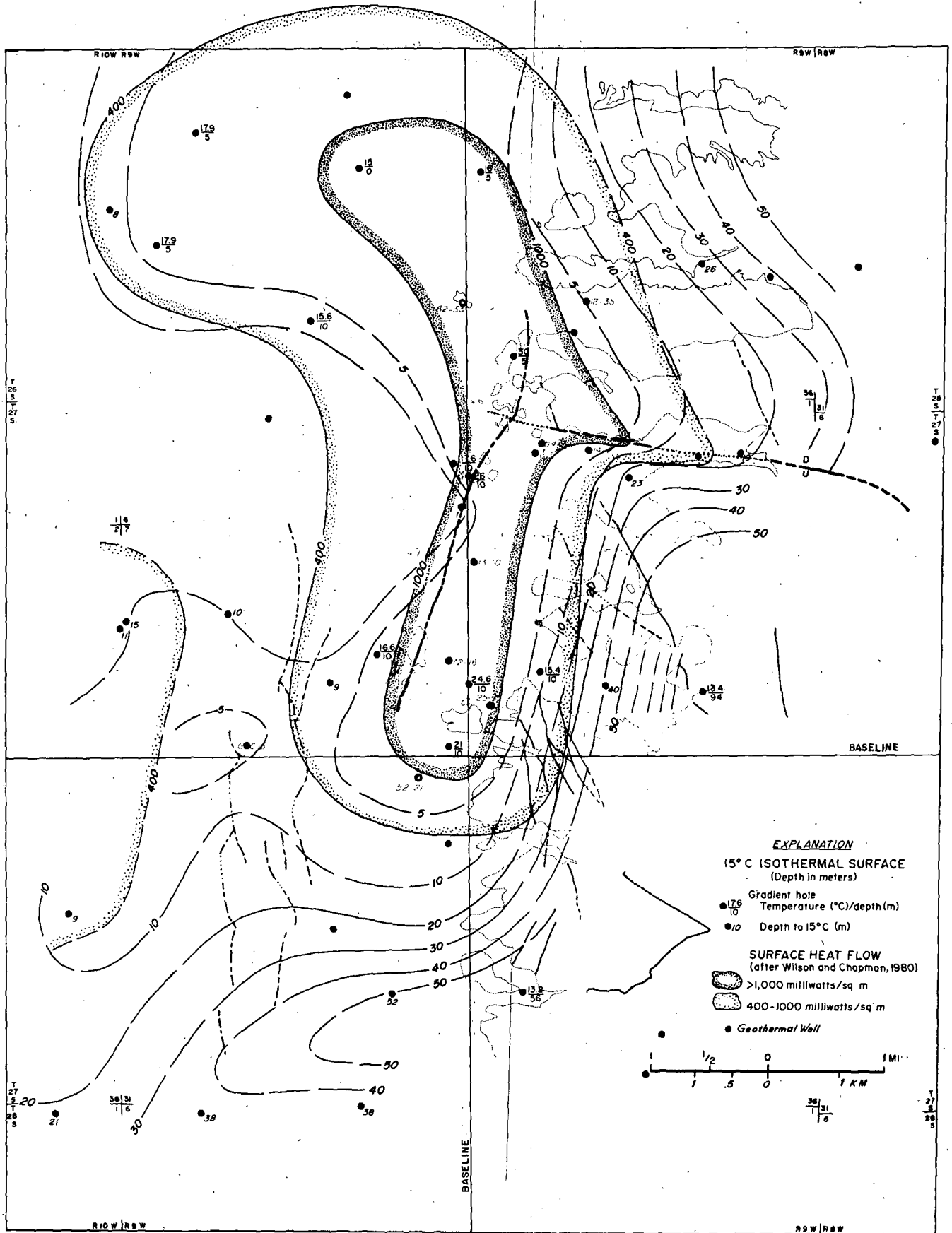


FIG. 11—Thermal studies map, Roosevelt Hot Springs KGRA.

Figure 11 compares the depth of the 15°C isothermal surface with the heat flow pattern of Wilson and Chapman (1980). Temperatures at a given depth are included for several holes. The 1,000 mW/m² area corresponds closely to the area where 15°C is mapped within 15 ft (5 m) of the surface. The steep contours along the flank of the range indicate depressed temperatures because of descending ground water, and a broad contour interval to the west and elongation to the northwest probably relate to the discharge of geothermal water within permeable strata in the alluvium. Although the contoured heat-flow map presents the thermal data in the most quantitative manner, the shallow occurrence of the high-temperature reservoir and its active discharge into the alluvium give rise to good definition of the system by contouring most thermal parameters.

RETROSPECTIVE EXPLORATION STRATEGY

The Roosevelt Hot Springs geothermal system has been used as a natural laboratory for the testing of exploration techniques. Using this relatively complete data base, it is possible to exercise 20/20 hindsight and define the most efficient strategy for the exploration of the Roosevelt Hot Springs geothermal system. Ward et al (1981) present a generalized exploration strategy which emphasizes the use of conceptual exploration models to solve specific exploration problems. The retrospective exploration strategy for Roosevelt Hot Springs involves five stages: literature study, geologic mapping, thermal gradient measurements, dipole-dipole resistivity, and drilling. The following strategy may not be applicable to other systems because the Roosevelt Hot Springs system is one of the hottest and largest hydrothermal systems in the Basin and Range province.

Phase 1.—The first stage of the strategy would be a literature search and compilation. Review of existing geologic and hydrologic reports would have demonstrated that hot springs had been active in the recent past and would have provided chemical analyses of those waters. From those analyses, geothermometers could have been calculated to give an indication of possible reservoir temperatures. In addition, the presence of siliceous sinter is considered as evidence of a water-dominated geothermal system which has a base temperature of at least 356°F (180°C) (Renner et al, 1975). The presence of Quaternary rhyolites suggests the possibility of a high-level granitic pluton which supplies heat to the geothermal system. A review of the ground-water reports would allow plotting of potentiometric surfaces and chemical trends such as shown in Figure 3.

The approximate cost of such a literature search and compilation could vary widely depending on the expertise involved and the size of the region under consideration. The costs are thought to be between \$5,000 and \$20,000. Because the surface manifestations of the Roosevelt Hot Springs system are so well developed, a decision to initiate leasing activities could be made at the end of phase I.

Phase II.—This stage would involve the geologic mapping of the project area. Nielson et al (1978) found that mapping at a scale of 1:24,000 on an air-photo base was adequate for exploration purposes. The mapping

should identify the extent of the hot-spring deposits and characterize their structural control. It would also identify the other structural systems within the geothermal area and allow a preliminary guess at the relative importance of the various fault systems in controlling the geothermal reservoir. Previous attempts at using air-photo interpretation alone to define these structural systems (Ward et al, 1978) were relatively unsuccessful.

The knowledge gained during this phase should be used to establish conceptual models of the geothermal system. In addition, the results will provide siting information for the subsequent thermal-gradient holes and electrical resistivity surveys.

The costs of the geologic mapping will probably be \$15,000 to \$25,000, one of the most cost-effective exploration options available.

Phase III.—The principal activities of phase III would be the delineation of the near-surface thermal anomaly and mapping of deeper resistivity structure. An area of 8 mi (12 km) north-south by 4 mi (6 km) east-west would be sampled by 25 to 30 shallow thermal-gradient holes drilled to depths of 300 to 600 ft (100 to 200 m). The deeper holes would logically be sited west of the Opal Mound fault where alluvium is predictably deeper and problems of near-surface water flow could be anticipated. This program would have detected temperature gradients in excess of 44°F/100 ft (800°C/km), and localized a high-temperature anomaly within 1.2 mi (2 km) of the Opal Mound fault. The cost of the survey, at 1980 prices, would have been between \$130,000 and \$160,000.

A slightly larger area, 10 by 5 mi (15 by 8 km), would have been selected for a dipole-dipole electrical resistivity survey. Cost-effective survey design, based on geologic mapping and in-progress temperature-gradient studies, would dictate perhaps 10 dipole-dipole lines of 1.8 to 3 mi (3 to 5 km) lengths, with perhaps 7 lines of 984-ft (300-m) dipole length and 3 lines of 492-ft (150-m) dipole length. The survey costs are estimated at \$40,000 to \$50,000, with selected numerical modeling estimated at an additional \$10,000.

Without the prior knowledge of the valley-range transition, it would have been logical to plan several detailed gravity profiles in an attempt to define a range-front fault with major vertical offset. Such an effort would have cost \$3,000 to \$5,000, and would have contributed little to target definition.

It would be prudent to collect fluid samples from the gradient holes and to complete chemical analysis and geothermometric calculations on these samples. These costs would have added \$1,000 to \$2,000 to the exploration bill and provided valuable information on water type, mixing, and preliminary estimates of reservoir temperatures.

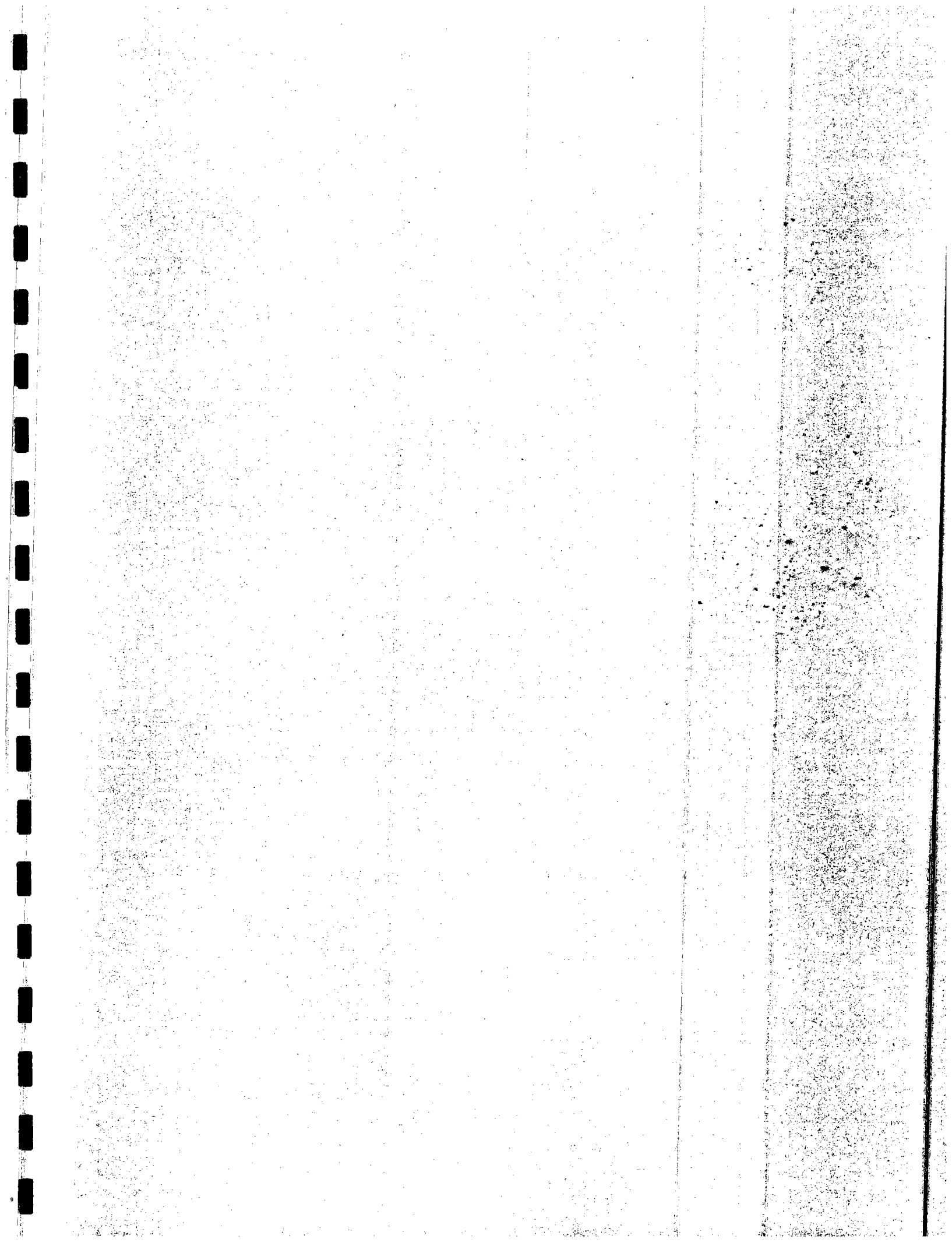
Phase IV.—After careful consideration of the geologic, thermal, and electrical data bases, the prudent exploration program would have sited two to four deep thermal-gradient holes, to depths of 1,000 to 2,000 ft (300 to 600 m). These could be expected to cost \$15 to \$18 per foot (\$50 to \$60 per meter). At Roosevelt Hot Springs these holes, if well chosen, might have intersected a major fracture at shallow depth (as in Utah State 72-16), or would at least indicate temperatures ap-

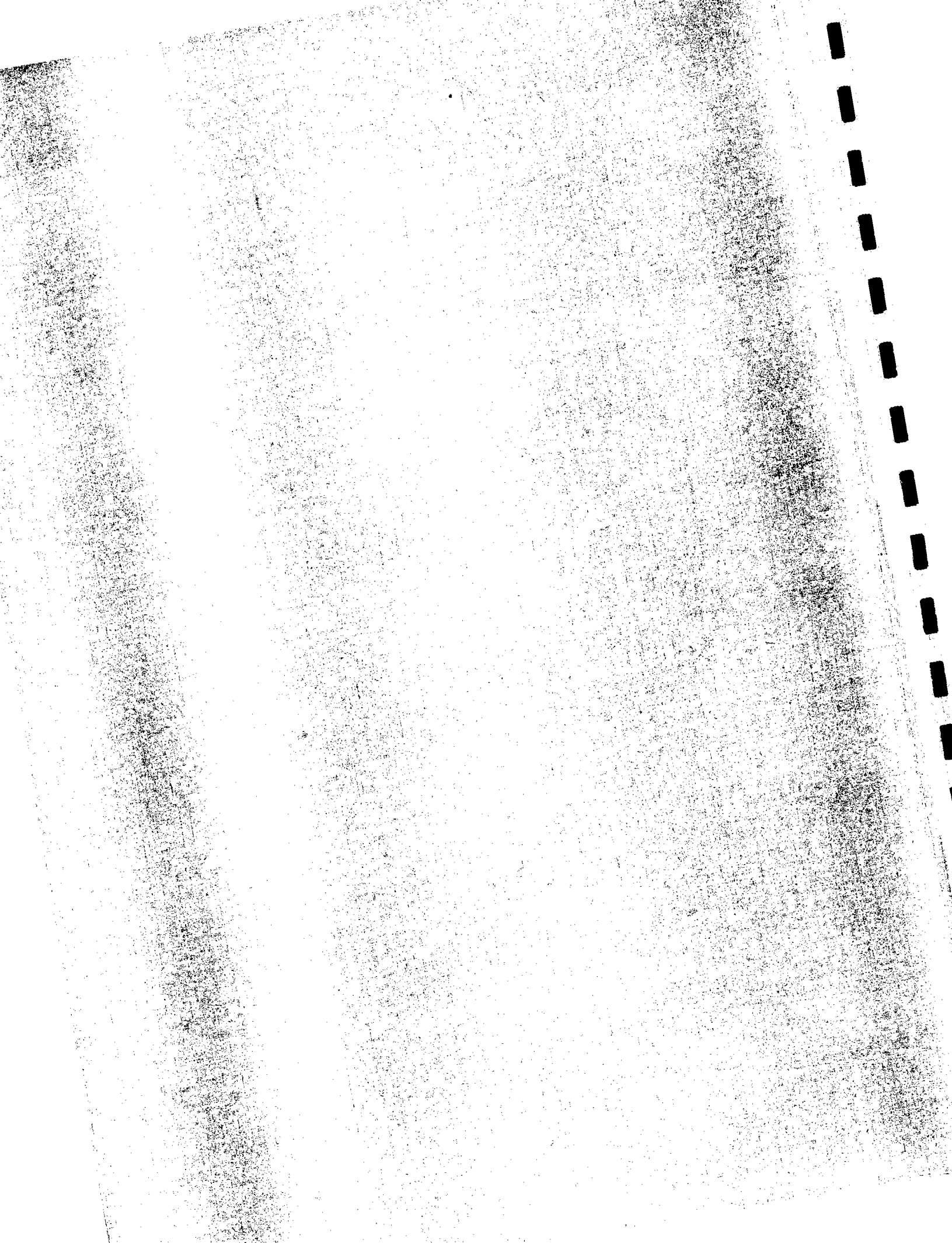
proaching 300°F (150°C) within 2,000 ft (600 m) depth. The program cost, with fluid collection and lithologic studies, is estimated at \$100,000 to \$200,000. A substantial effort in data interpretation and data integration would follow as a result of the strong encouragement for a high-temperature system. On the basis of this data analysis, production holes would be drilled.

REFERENCES CITED

- Ballantyne, J. M., 1978, Hydrothermal alteration at the Roosevelt Hot Springs thermal area, Utah; modal mineralogy and geochemistry of sericite, chlorite, and feldspar from altered rocks, Thermal Power Company well Utah State 14-2: Univ. Utah, Dept. Geology and Geophysics, 42 p.
- Bamford, R. W., 1978, Geochemistry of solid materials from two U.S. geothermal systems and its application to exploration: Univ. Utah Research Inst., Earth Science Lab. Rept. 6, 196 p.
- _____, O. D. Christensen, and R. M. Capuano, 1980, Multielement geochemistry of solid materials in geothermal systems and its applications. Part 1: The hot water system at the Roosevelt Hot Springs KGRA, Utah: Univ. Utah Research Inst., Earth Science Lab. Rept. 30, 168 p.
- Biehler, S., 1971, Gravity studies in the Imperial Valley, in Cooperative geological-geophysical-geochemical investigations of geothermal resources in the Imperial Valley area of California: Univ. California, Riverside, Education Research Service, p. 29-41.
- Browne, P. R. L., 1971, Mineralization in the Broadlands geothermal field, Taupo volcanic zone, New Zealand: Japan Soc. Mining Geol., Spec. Issue 2, p. 64-75.
- Butz, J., and M. Plooster, 1979, Final report subsurface investigations at the Roosevelt KGRA, Utah: Denver Research Inst. Rept. Open-File Data, Univ. Utah Research Inst. Earth Science Lab., 72 p.
- Capuano, R. M., and R. Bamford, 1978, Initial investigation of soil mercury geochemistry as an aid to drill site selection in geothermal systems: Univ. Utah Research Inst., Earth Science Lab. Rept. 13, 32 p.
- _____, and D. Cole, 1982, Fluid-mineral equilibria in high temperature geothermal systems; the Roosevelt Hot Springs geothermal system, Utah: *Geochim. et Cosmochim. Acta*, v. 46, in press.
- Carter, J. A., and K. L. Cook, 1978, Regional gravity and aeromagnetic surveys of the Mineral Mountains and vicinity, Millard and Beaver Counties, Utah: Univ. Utah, Dept. Geology and Geophysics, 178 p.
- Christensen, O. D., R. L. Kroneman, and R. M. Capuano, 1980a, Multielement analysis of geologic materials by inductivity coupled plasma-atomic emission spectroscopy: Univ. Utah Research Inst., Earth Science Lab. Rept. 32, 32 p.
- _____, J. N. Moore, and R. M. Capuano, 1980b, Trace element geochemical zoning in the Roosevelt Hot Springs thermal area, Utah: Geothermal Resources Council Trans., v. 4, p. 149-152.
- Chu, J. J., W. R. Sill, and S. H. Ward, 1980, Induced polarization measurements at Roosevelt Hot Springs thermal area, Utah (abs.): *Geophysics*, v. 45, no. 3, p. 587.
- Corwin, R. F., and D. B. Hoover, 1979, The self-potential method in geothermal exploration: *Geophysics*, v. 44, p. 226-245.
- Crebs, T. L., and K. L. Cook, 1976, Gravity and ground magnetic surveys of the central Mineral Mountains, Utah: Univ. Utah, Dept. Geology and Geophysics Final Rept., v. 6, 129 p.
- Earll, F. N., 1957, Geology of the central Mineral Range, Beaver Co., Utah: PhD thesis, Univ. Utah, 112 p.
- Ewers, G. R., and P. R. Keays, 1977, Volatile and precious metal zoning in the Broadlands geothermal field, New Zealand: *Econ. Geology*, v. 72, p. 1337-1354.
- Forrest, R. J., 1980, Historical synopsis of the Roosevelt Hot Springs geothermal field, Utah, in D. L. Nielson, ed., Geothermal systems in central Utah: Geothermal Resources Council Field Trip 7, p. 18-24.
- Fournier, R. O., 1973, Silica in thermal water; laboratory and field investigations: Internat. Symp. on Hydrogeochemistry and Biogeochemistry Proc., Japan, 1970, Washington, D.C., Clark Publishing Co., p. 122-139.
- _____, and A. H. Truesdell, 1973, An empirical Na-Ca-K geothermometer for natural waters: *Geochim. et Cosmochim. Acta*, v. 37, p. 1255-1275.
- Frangos, W., and S. H. Ward, 1980, Bipole-dipole survey at Roosevelt Hot Springs KGRA, Beaver County, Utah: Univ. Utah Research Inst., Earth Science Lab. Rept. 43, 41 p.
- Geothermex, 1977, Geothermal potential of the lands leased by Geothermal Power Corporation in the Northern Mineral Mountains, Beaver and Millard Counties, Utah: Open File Rept., Univ. Utah Research Inst., Earth Science Lab., 43 p.
- Gertson, R. C., and R. B. Smith, 1979, Interpretation of a seismic refraction profile across the Roosevelt Hot Springs, Utah and vicinity: Univ. Utah, Dept. Geology and Geophysics Rept., 109 p.
- Glenn, W. E., and J. B. Hulen, 1979, Interpretation of well log data from four drill holes at Roosevelt Hot Springs KGRA: Univ. Utah Research Inst., Earth Science Lab. Rept. 28, 74 p.
- _____, J. B. Hulen, and D. L. Nielson, 1980, A comprehensive study of LASL well C/T-2 (Phillips 9-1) Roosevelt Hot Springs KGRA, Utah, with applications to geothermal well logging: Los Alamos Scientific Lab. Rept. LA-8686-MS, 175 p.
- James, R., 1966, Metering of steam-water two-phase flow by sharp-edged orifices: *Inst. Mech. Engineers Proc.*, v. 180, pt. 1, no. 23, p. 548-572.
- Katz, L., 1977a, Seismic emissions study, Roosevelt Hot Springs, Milford, Utah (for Getty Oil Co.): Open-File Rept., Univ. Utah Research Inst., Earth Science Lab., 7 p.
- _____, 1977b, Seismic emission study, Roosevelt Hot Springs, Milford, Utah (for Union Oil Co.): Open-File Rept., Univ. Utah Research Inst., Earth Science Lab., 7 p.
- Lenzer, R. C., G. W. Crosby, and C. W. Berge, 1976, Geothermal exploration of Roosevelt KGRA, Utah: 17th U.S. Symposium on Rock Mechanics, Site Characterization Volume, Univ. Utah Engineering Experimental Station, p. 3B1-1.
- _____, 1977, Recent developments at the Roosevelt Hot Springs, KGRA: Trans. Am. Nuclear Soc. Topical Mtg., Golden, Colo., April 12-14.
- Lipman, P. W., et al, 1978, Pleistocene rhyolite of the Mineral Mountains, Utah geothermal and archeological significance: *U.S. Geol. Survey Jour. Research*, v. 6, p. 133-147.
- Mabey, D. R., et al, 1978, Regional magnetic patterns in part of the Cordillera in the western United States, in R. B. Smith and G. P. Eaton, eds., Cenozoic tectonics and regional geophysics of the western Cordillera: *Geol. Soc. America Mem.* 152, p. 313-340.
- Mower, R. W., 1978, Hydrology of the Beaver Valley area, Beaver County, Utah, with emphasis on ground water: Utah Dept. Natural Resources Tech. Pub. 63, 90 p.
- _____, and R. M. Cordova, 1974, Water resources of the Milford area, Utah, with an emphasis on ground water: Utah Dept. Natural Resources Tech. Pub. 43, 106 p.
- Nielson, D. L., B. S. Sibbett, and D. B. McKinney, 1979, Geology and structural control of the geothermal system at Roosevelt Hot Springs, Beaver County, Utah (abs.): *AAPG Bull.*, v. 63, p. 836.
- _____, et al, 1978, Geology of Roosevelt Hot Springs KGRA, Beaver County, Utah: Univ. Utah Research Inst., Earth Science Lab. Rept. 12, 121 p.
- Olson, T. L., and R. B. Smith, 1976, Earthquake surveys of the Roosevelt Hot Springs and the Cove Fort areas, Utah: Final Rept. to Natl. Sci. Foundation, Univ. Utah, Dept. Geology and Geophysics, 82 p.
- Parry, W. T., et al, 1980, Geochemistry of hydrothermal alteration at the Roosevelt Hot Springs thermal area, Utah: *Geochim. et Cosmochim. Acta*, v. 44, p. 95-102.
- Renner, J. L., D. E. White, and D. L. Williams, 1975, Hydrothermal convection systems, in D. E. White and D. L. Williams, eds., Assessment of geothermal resources of the United States—1975: *U.S. Geol. Survey Circ.* 726, p. 5-57.
- Robinson, R., and H. M. Iyer, 1981, Delineation of a low-velocity body under the Roosevelt Hot Springs geothermal area, Utah, using teleseismic P-wave data: *Geophysics*, v. 46, p. 1456-1466.
- Rohrs, D. T., 1980, A light stable isotope study of the Roosevelt Hot Springs thermal area, southwestern Utah: Master's thesis, Univ. Utah, 94 p.
- Ross, H. P., et al, 1982, Interpretation of electrical resistivity, gravity and seismic emissions data from Roosevelt Hot Springs, Utah: Univ. Utah Research Inst., Earth Science Lab. Rept. (in prep.).
- Sandberg, S. K., and G. W. Hohmann, 1980, Controlled-source audiomagnetotellurics in geothermal exploration: Univ. Utah,

- Dept. Geology and Geophysics Rept. DOE/ID/12079-5, 85 p.
- Schaff, C., 1981, Seismic monitoring and potential for induced seismicity at Roosevelt Hot Springs, Utah and Raft River, Idaho: 1981 Ann. Mtg., Seismological Soc. America.
- Sibbett, B. S., and D. L. Nielson, 1980, Geology of the central Mineral Mountains, Beaver Co., Utah: Univ. Utah Research Inst., Earth Science Lab. Rept. 33, 42 p.
- Sill, W. R., and D. S. Johng, 1979, Self-potential survey, Roosevelt Hot Springs, Utah: Univ. Utah Dept. Geology and Geophysics Tech. Rept. DOE/ET/28393-21, 40 p.
- Smith, R. B., and M. Sbar, 1974, Contemporary tectonics and seismicity of the western states with emphasis on the Intermountain seismic belt: Geol. Soc. America Bull., v. 85, p. 1205-1218.
- Smith, R. L., and H. R. Shaw, 1975, Igneous-related geothermal systems, in D. E. White and D. L. Williams, eds., Assessment of geothermal resources of the United States: U.S. Geol. Survey Circ. 726, p. 58-83.
- Vozoff, K., 1972, The magnetotelluric method in the exploration of sedimentary basins: Geophysics, v. 37, p. 98-141.
- Wannamaker, P. E., W. R. Sill, and S. H. Ward, 1978, Magnetotelluric observations at the Roosevelt Hot Springs KGRA and Mineral Mountains, Utah: Geothermal Resources Council Trans., v. 2, p. 697-700.
- _____ et al, 1980, Magnetotelluric models of the Roosevelt Hot Springs thermal area, Utah: Univ. Utah, Dept. Geology and Geophysics Rept. DOE/ET/27002-8, 213 p.
- Ward, S. H., H. P. Ross, and D. L. Nielson, 1981, Exploration strategy for high-temperature hydrothermal systems in the Basin and Range province: AAPG Bull., v. 65, p. 86-102.
- _____ et al, 1978, A summary of the geology, geochemistry, and geophysics of the Roosevelt Hot Springs thermal area, Utah: Geophysics, v. 43, p. 1515-1542.
- Wechsler, D. J., and R. B. Smith, 1979, An evaluation of hypocenter location techniques with application to southern Utah; regional earthquake distributions and seismicity of geothermal areas: Univ. Utah, Dept. Geology and Geophysics Rept. 78-28392.a.12, 131 p.
- White, D. E., L. J. P. Muffler, and A. H. Truesdell, 1971, Vapor-dominated hydrothermal systems compared with hot-water systems: Econ. Geology, v. 66, p. 75-97.
- Wilson, W. R., and D. S. Chapman, 1980, Thermal studies at Roosevelt Hot Springs, Utah: Univ. Utah, Dept. Geology and Geophysics Rept. DOE/ID/12079-19, 144 p.





HYDROTHERMAL FLUIDS

INTRODUCTION

SOLUTION CHEMISTRY REVIEW

WATER SAMPLING

WATER CLASSIFICATION

SOURCE OF WATER

AGE OF WATER

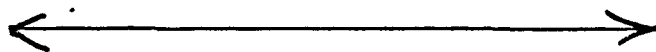
SUBSURFACE TEMPERATURE

GEOCHEMICAL FLUID STUDIES

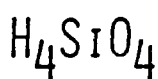
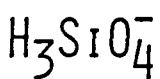
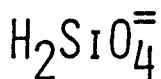
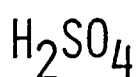
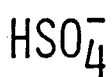
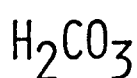
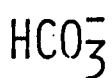
- COMPOSITIONAL RANGE AND HOMOGENEITY OF HOT FLUIDS
IN OVERALL SYSTEM
- SUBSURFACE TEMPERATURE AND PRESSURE
- VAPOR VS. LIQUID DOMINATED
- SUBSURFACE ALTERATION ASSOCIATED WITH THE FLUIDS
- ORIGIN OF HOT FLUIDS
- DIRECTION OF FLUID FLOW
- TURNOVER TIME OF THE FLUID
- PERMEABILITY
- POTENTIAL FOR MINERAL DEPOSITION(SCALING PROBLEMS)
- FLUID CONSTITUENTS WHICH COULD HAVE ECONOMIC VALUE
- FEASIBILITY OF REINJECTION

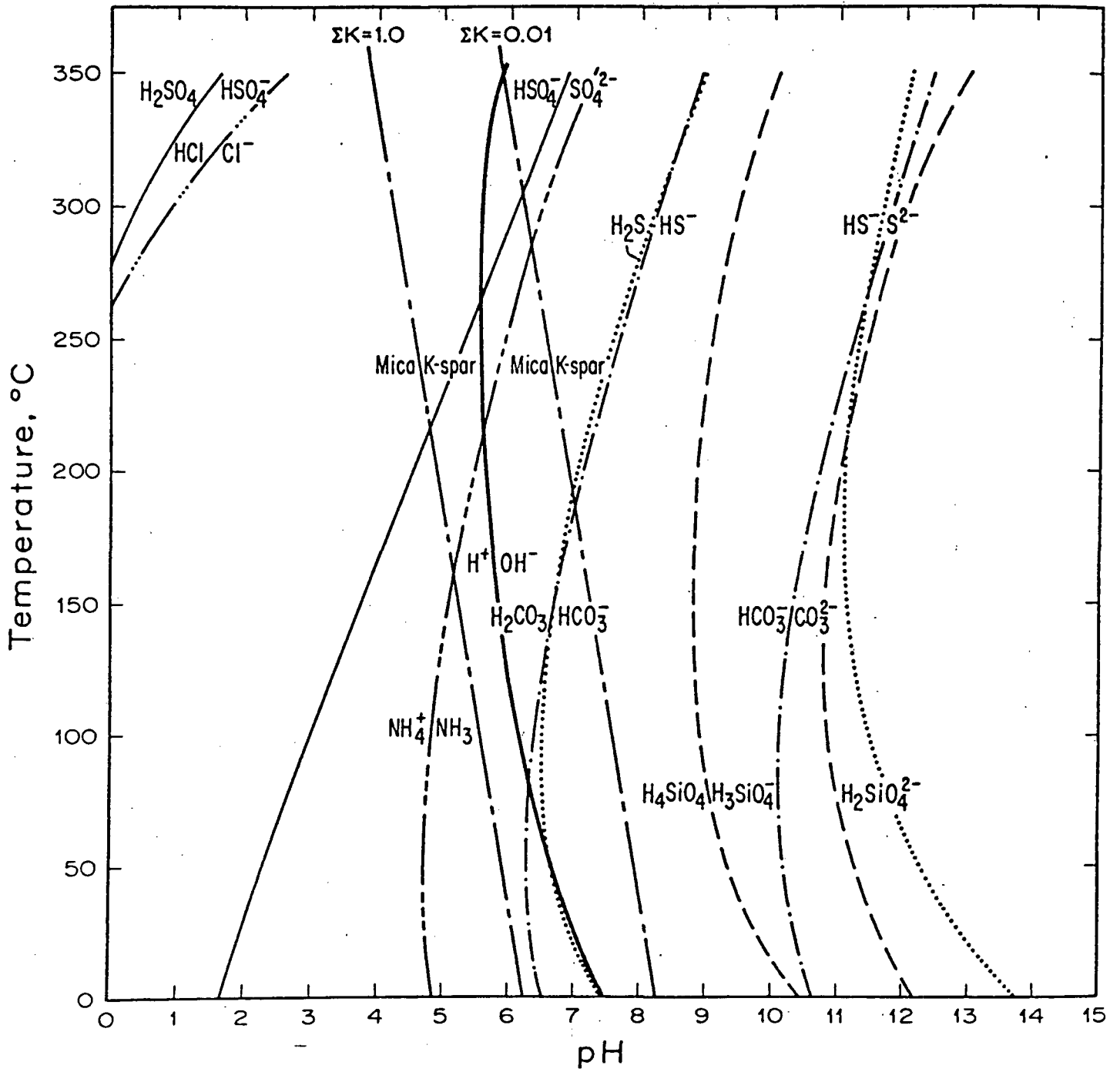
DOMINANT IONIC COMPLEXES

BASIC



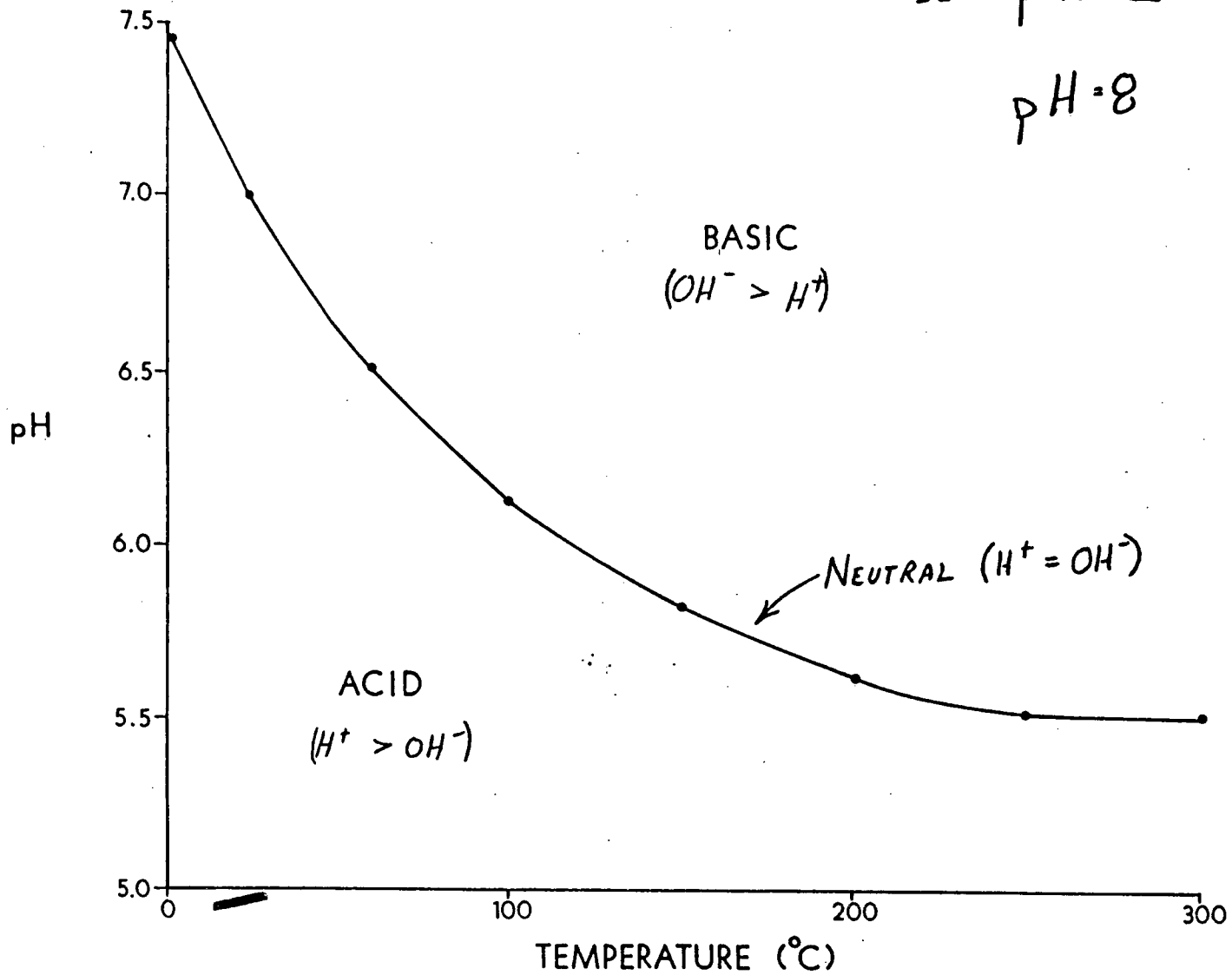
ACID





$$\text{pH} = -\log a_{\text{H}^+}$$

so: $\text{pH} = 2$ $a_{\text{H}^+} = 10^{-2}$
 $\text{pH} = 8$ $a_{\text{H}^+} = 10^{-8}$



CONCENTRATION: AMOUNT OF ELEMENT DETERMINED BY
QUANTITATIVE ANALYSIS

-SUM OF THE MOLALITIES OF ALL SPECIES CONTAINING
THAT ELEMENT

ACTIVITY: EFFECTIVE CONCENTRATION OF A SPECIES
IN SOLUTION

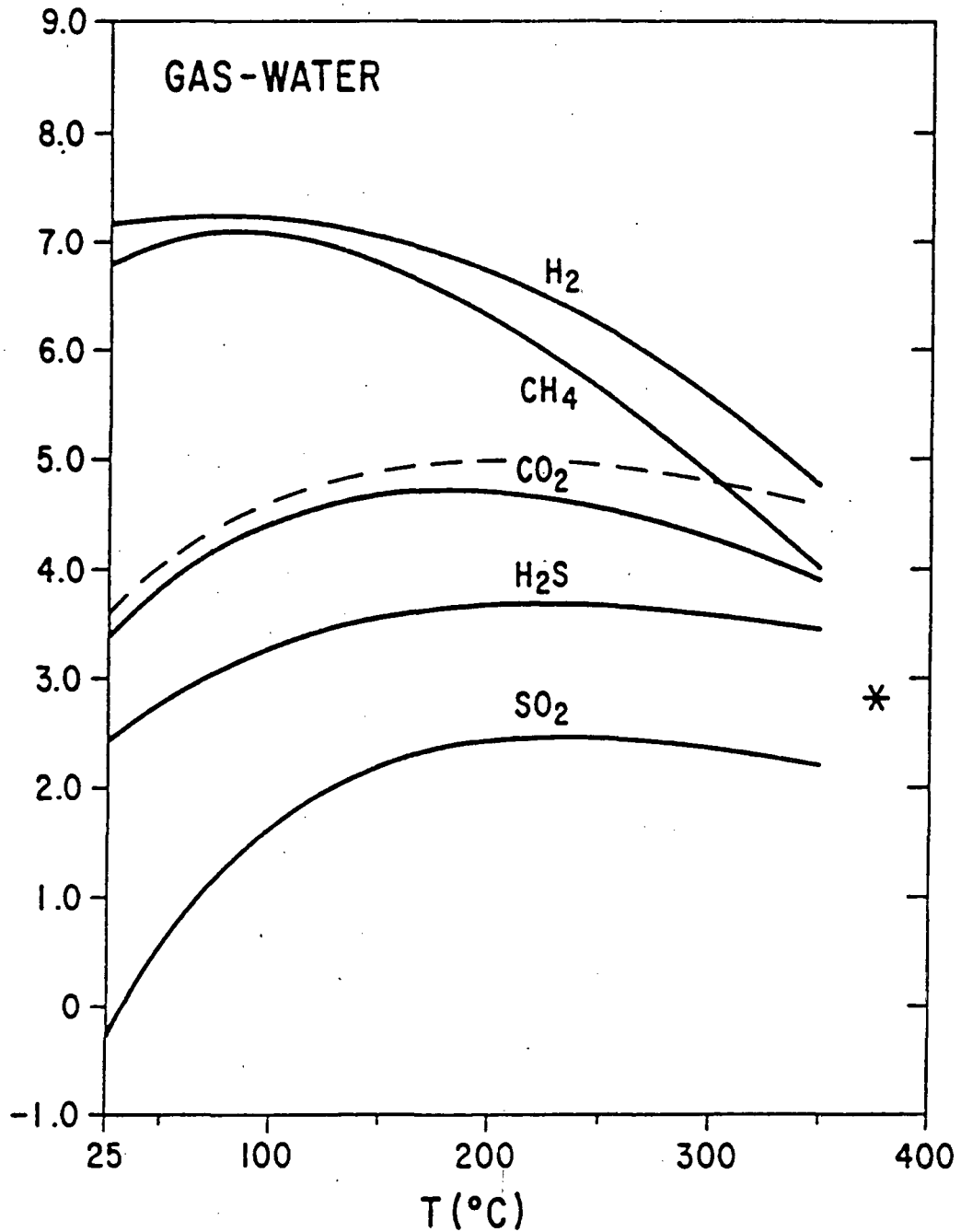
$$a = \gamma m$$

-ACCOUNTS FOR ELECTROSTATIC FORCES BETWEEN
MOLECULES

DECREASED SOLUBILITY

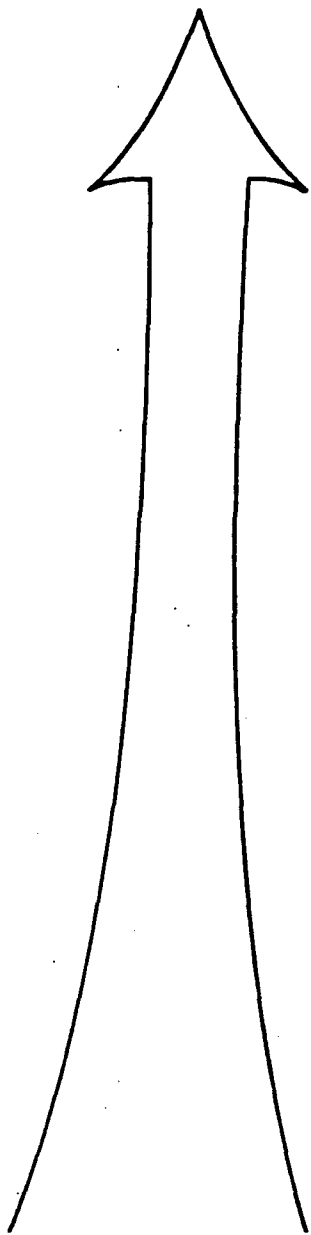


--- 1m NaCl (CO₂)
 — pure H₂O



Values of Henry's Constants (units = fugacity (atm)/molality) Corresponding (via Equation 3.7) to the Volatility Ratios in Figure 3.10 for the Gases H₂, CH₄, CO₂, H₂S, and SO₂ in Water. The theoretical critical point solubility is indicated by (*).

SURFACE SAMPLE



TEMPERATURE DECREASE

STEAM LOSS + GAS

[CO₂, H₂S, CH₄, NH₄, H₂, etc.]

MIXING WITH

NONTHERMAL GROUNDWATER

SCALE PRODUCTION

RESERVOIR FLUID

Roosevelt Hot Springs Fluid Analyses

WELL 14-2

	<u>Brine Sampled at the Surface</u> (ppm)	<u>Calculated Deep Reservoir Fluid</u> (ppm)
Na	2190	1796
K	401	329
Ca	8	12
Si	341	280
Cl	3650	2993
C	206	1793
S	69	138
T.D.S.	6680	9707
pH	6.1	5.8
Na-K-Ca (°C)	289	277
Quartz cond. (°C)	289	269



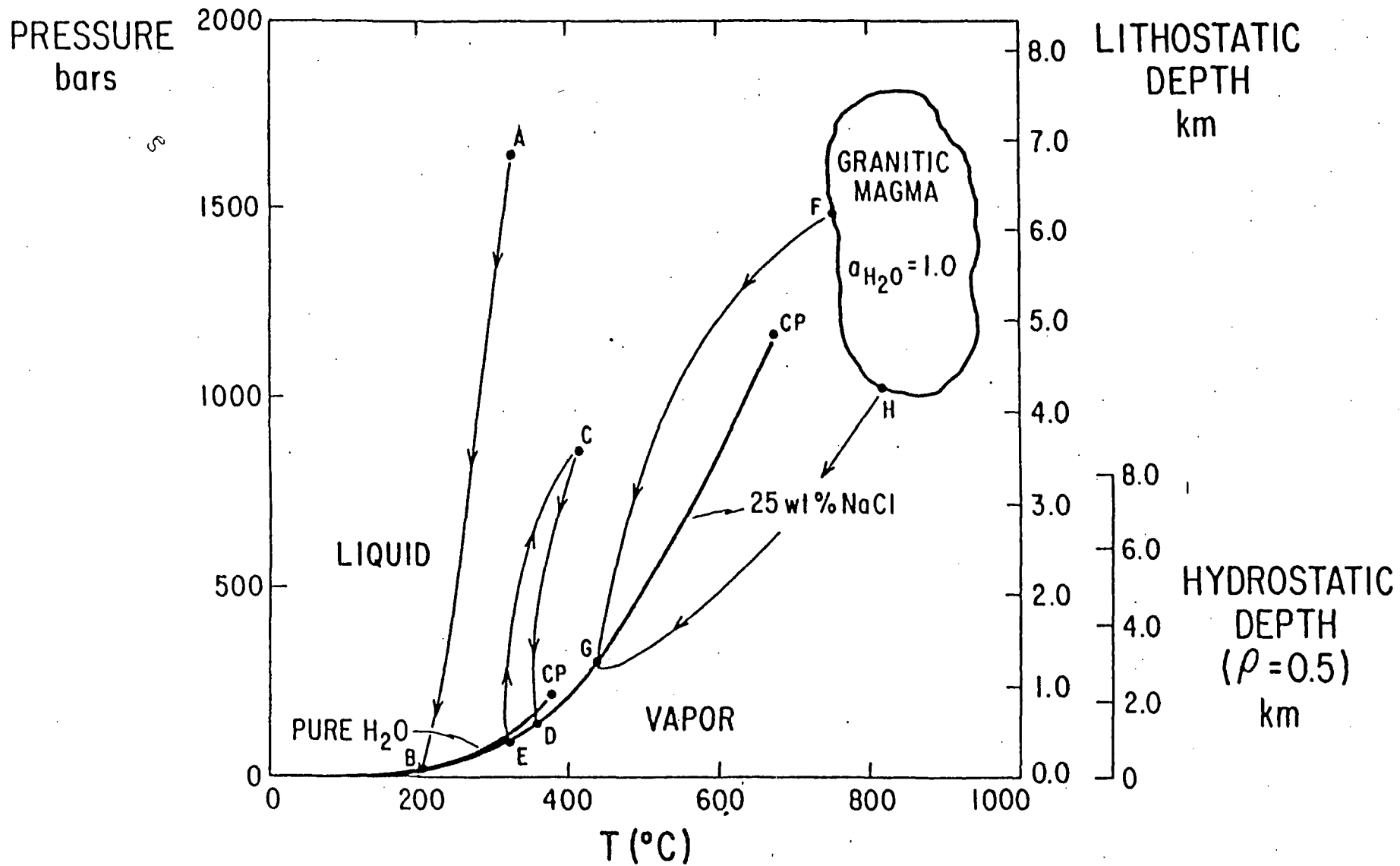


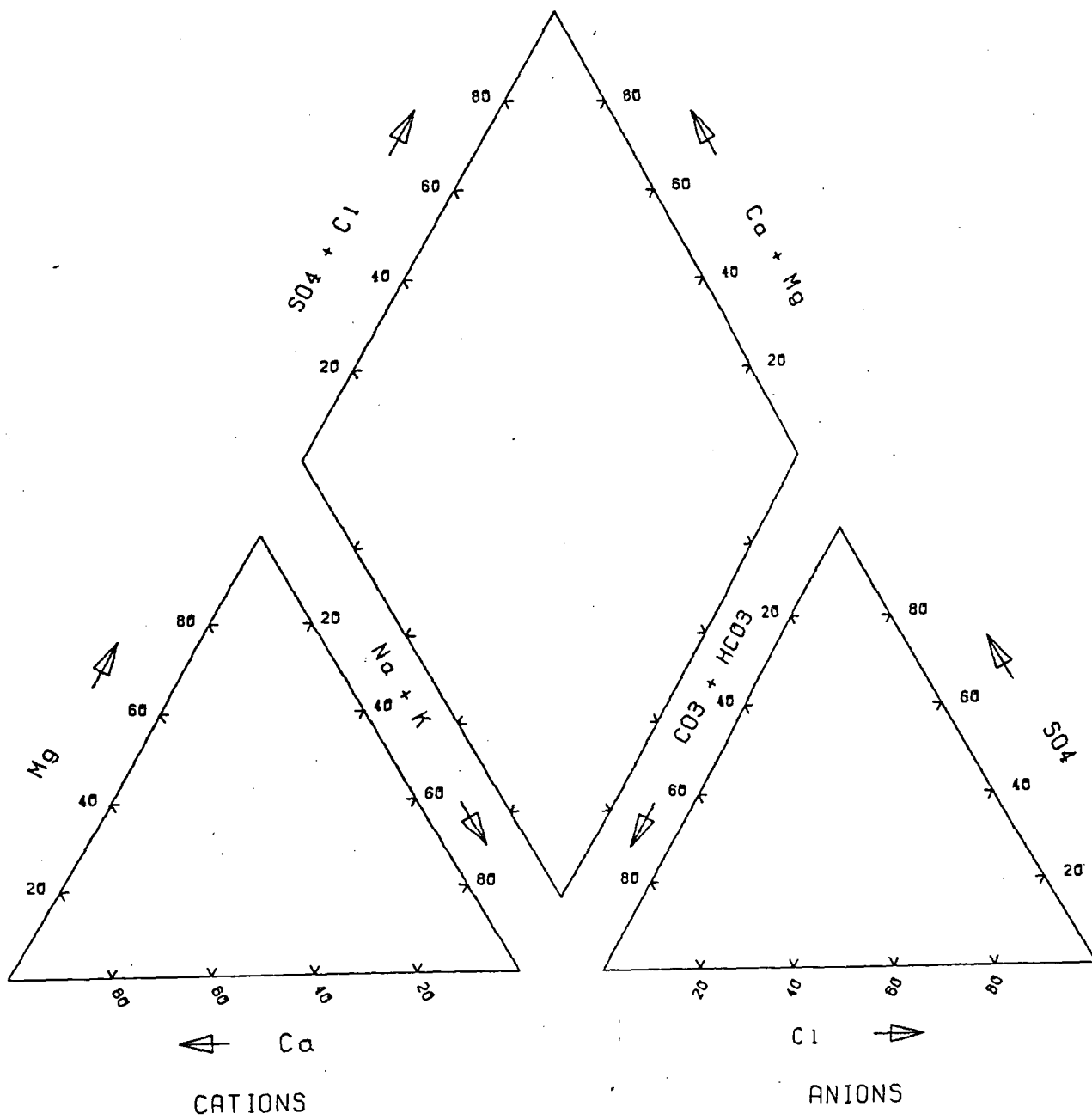
Figure 4.1. Several Schematic Pressure-Temperature Paths for Liquid-Vapor Hydrothermal Systems. Refer to text for an explanation of the P-T paths (A-B, C-D, E-C, F-G, H-G).

SAMPLING PHILOSOPHY

- THE PURPOSE OF SAMPLING AND ANALYSIS OF A NATURAL FLUID IS TO DETERMINE THE PROPERTIES OF THE FLUID IN THE NATURAL STATE
- SOME CONSTITUENTS IN NATURAL FLUIDS ARE UNSTABLE AND CHANGE SIGNIFICANTLY WITH TIME
- DEPENDING ON THE PURPOSE AND NATURE OF THE STUDY, CHANGES IN CONSTITUENTS UPON COLLECTION AND STORAGE MAY OR MAY NOT BE A PROBLEM
- NO ONE SAMPLE COLLECTION PROCEDURE WILL BE SATISFACTORY FOR ALL PURPOSES
- THE INFORMATION NEEDED FOR A PARTICULAR STUDY AND THE DESIRED ACCURACY SHOULD BE ESTABLISHED FIRST; THEN APPROPRIATE SAMPLING TECHNIQUES SHOULD BE SELECTED

ACCURACY CHECKS

- I. CALCULATE THE CATION - ANION BALANCE
- II. TOTAL CATIONS EQUALS TOTAL ANIONS IN MEQ/ L
- III. ASSUME THAT THE WATER DOES NOT CONTAIN UNDETERMINE SPECIES WHICH CAN PARTICIPATE IN THE BALANCE, AND THAT THE FORMULA AND CHARGE OF ALL ANIONS AND CATIONS ARE KNOWN.
- IV. FOR MOD. CONCENTRATIONS (250 - 1000 mg/l) ERROR = 1 to 2%
FOR CONCENTRATIONS LESS THAN 250 OR GREATER THAN 1000 mg/l,
ERROR = 2 to 10%.
- V. CAN ALSO COMPARE TDS(CALCULATED) WITH THE TDS(MEASURED), THEY SHOULD AGREE TO WITHIN A FEW MG/L.



PERCENT OF TOTAL
MILLIEQUIVALENTS PER LITER

CONVERSIONS

PPM = MG/KG \approx MG/LITER (FOR TDS < 7000 MG/LITER)

MILLIEQUIVALENTS - CONSIDER CHARGE AND MOLECULAR
WEIGHT (COMBINING WEIGHT)

$$\frac{\text{MILLIGRAM EQUIVALENTS}}{\text{LITER}} = \frac{\text{MG/LITER} \times \text{CHARGE}}{\text{GRAM FORMULA WEIGHT} \times 10^{-3}}$$

TABLE 9.—Conversion factors: Milligrams per liter $\times F_1$ = milliequivalents per liter; milligrams per liter $\times F_2$ = millimoles per liter (based on 1961 atomic weights, referred to carbon-12)

Element and reported species	F_1	F_2
Aluminum (Al^{+3})	0.11119	0.03715
Ammonium (NH_4^+)	.05544	.05544
Barium (Ba^{+2})	.01456	.00728
Beryllium (Be^{+3})	.33288	.11096
Bicarbonate (HCO_3^-)	.01639	.01639
Boron (B)		.09250
Bromide (Br^-)	.01251	.01251
Cadmium (Cd^{+2})	.01779	.00890
Calcium (Ca^{+2})	.04990	.02495
Carbonate (CO_3^{-2})	.03333	.01666
Chloride (Cl^-)	.02821	.02821
Chromium (Cr)		.01923
Cobalt (Co^{+2})	.03394	.01697
Copper (Cu^{+2})	.03148	.01574
Fluoride (F^-)	.05264	.05264
Germanium (Ge)		.01378
Gallium (Ga)		.01434
Gold (Au)		.00511
Hydrogen (H^+)	.99209	.99209
Hydroxide (OH^-)	.05880	.05880
Iodide (I^-)	.00788	.00788
Iron (Fe^{+2})	.03581	.01791
Iron (Fe^{+3})	.05372	.01791
Lead (Pb)		.00483
Lithium (Li^+)	.14411	.14411
Magnesium (Mg^{+2})	.08226	.04113
Manganese (Mn^{+2})	.03640	.01820
Molybdenum (Mo)		.01042
Nickel (Ni)		.01703
Nitrate (NO_3^-)	.01613	.01613
Nitrite (NO_2^-)	.02174	.02174
Phosphate (PO_4^{-3})	.03159	.01053
Phosphate (HPO_4^{-2})	.02084	.01042
Phosphate ($H_2PO_4^-$)	.01031	.01031
Potassium (K^+)	.02557	.02557
Rubidium (Rb^+)	.01170	.01170
Silica (SiO_2)		.01664
Silver (Ag)		.00927
Sodium (Na^+)	.04350	.04350
Strontium (Sr^{+2})	.02283	.01141
Sulfate (SO_4^{-2})	.02082	.01041
Sulfide (S^{-2})	.06238	.03119
Titanium (Ti)		.02088
Uranium (U)		.00420
Zinc (Zn^{+2})	.03060	.01530

(HEM, 1970)

GEOHERMAL WATER CLASSIFICATION

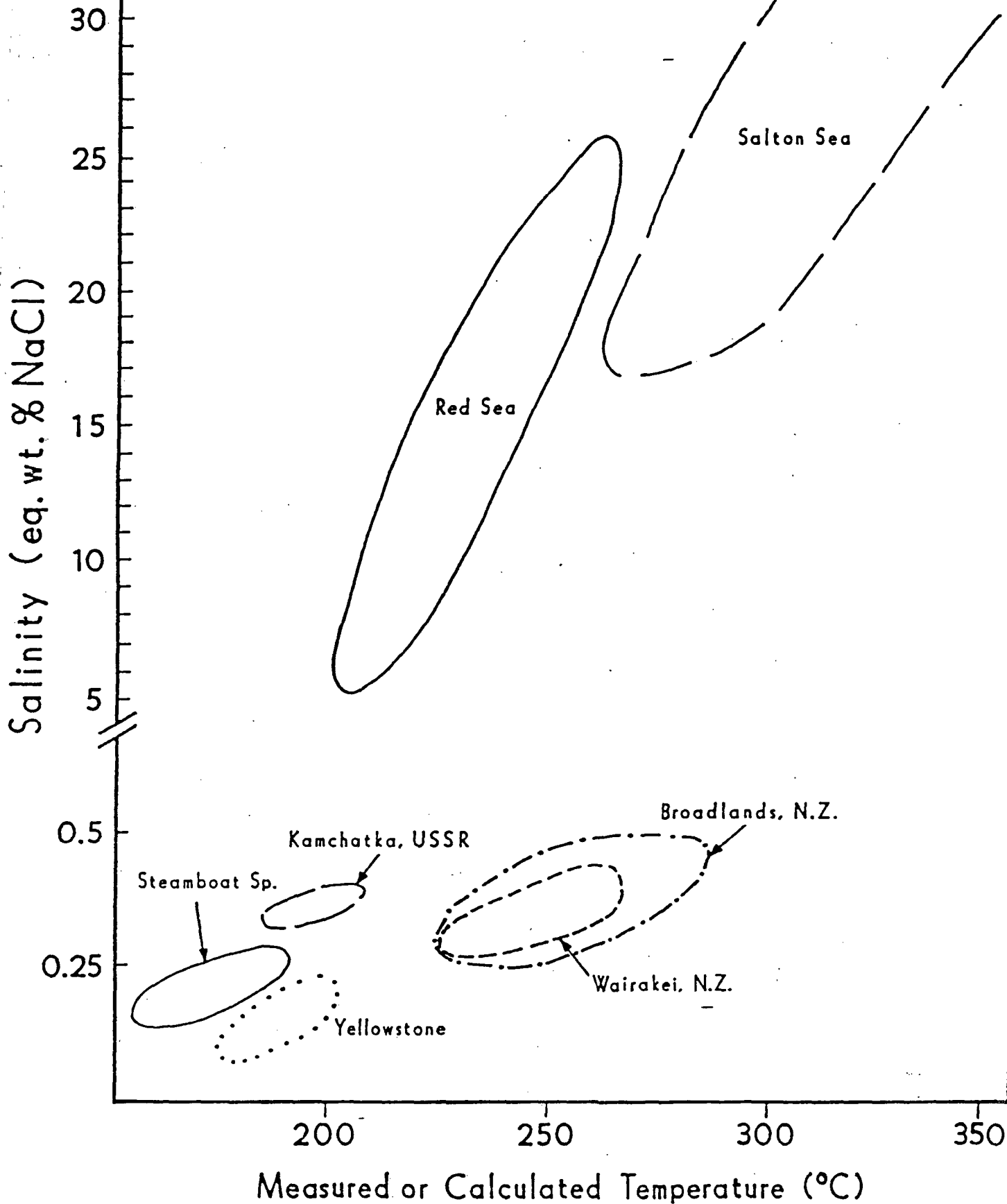
TYPE	ORIGIN	CHARACTER	OCCURRENCE
NEAR-NEUTRAL SODIUM CHLORIDE	REACTION OF HYDROTHERMAL FLUIDS WITH ROCKS	HIGH DISSOLVED SOLIDS GENERALLY 1,000 TO 30,000. ENRICHED IN: Na, K, Ca, Cl, SO ₄ , HCO ₃ , Si. DISSOLVED GASES: CO ₂ , H ₂ S, PREDOMINATE.	COMMON DEEP HIGH TEMP. RESERVOIR FLUID. WHERE THIS FLUID COMES TO SURFACE IT FORMS HOT SPRINGS.
ACID SULFATE	STEAM RISES FROM HIGH TEMP. WATER AND CONDENSES IN NEAR SURFACE OXIDIZING ENVIRONMENT	VERY DILUTE, ENRICHED IN SO ₄ FROM STEAM. OTHER ELEMENTS DERIVED FROM ACID LEACHING OF COUNTRY ROCK. $(H_2S(g) + 2O_2(g) \rightarrow 2H^+ + SO_4^-)$	NEAR SURFACE, GENERALLY ABOVE THE WATER TABLE
ACID SULFATE- CHLORIDE	(1) MIXING OF SODIUM CHLORIDE AND ACID SULFATE WATERS (2) HIGH TEMP. VOLCANIC STEAM RICH IN F, Cl, AND S, RISES AND CONDENSES IN NEAR SURFACE (OXIDIZED) WATER	(1) COMPOSITION CAN VARY WIDELY (2) ENRICHED IN: Cl, SO ₄ , F	NEAR SURFACE
NEAR-NEUTRAL SODIUM BICARBONATE- SULFATE	-VOLCANIC OR THERMAL STEAM RISES AND CONDENSES IN REDUCED GROUNDWATER -REACTION OF ACID SULFATE WATER WITH COUNTRY ROCK TO NEUTRALIZE	LOW DISSOLVED SOLIDS ENRICHED IN HCO ₃ , VARIABLE AMOUNTS OF SO ₄ .	ON PERIPHERY OR ABOVE THE HIGH TEMP. RESERVOIR

(AFTER ELLIS AND MAHON, 1977)

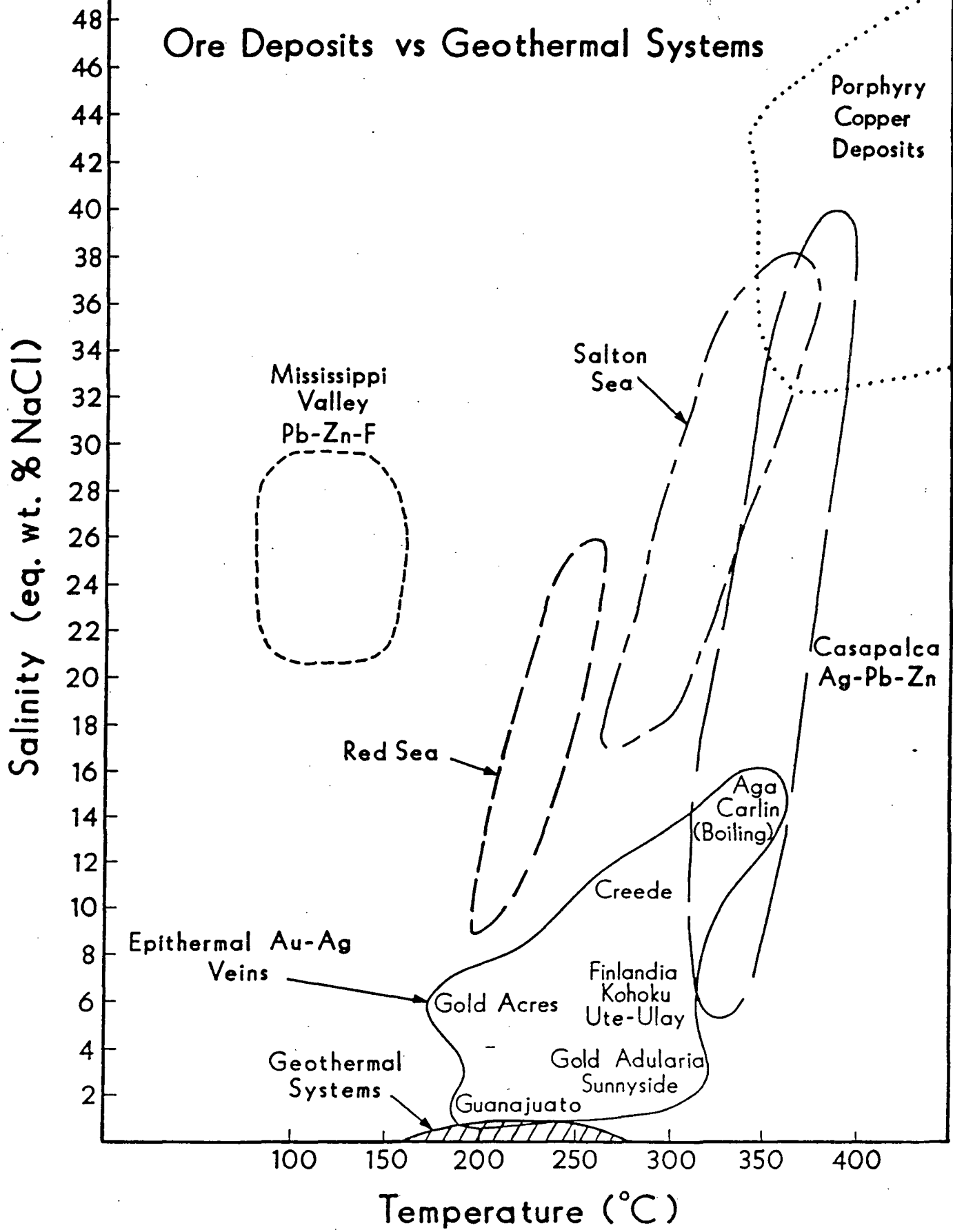
EXAMPLES OF GEOTHERMAL WATER TYPES

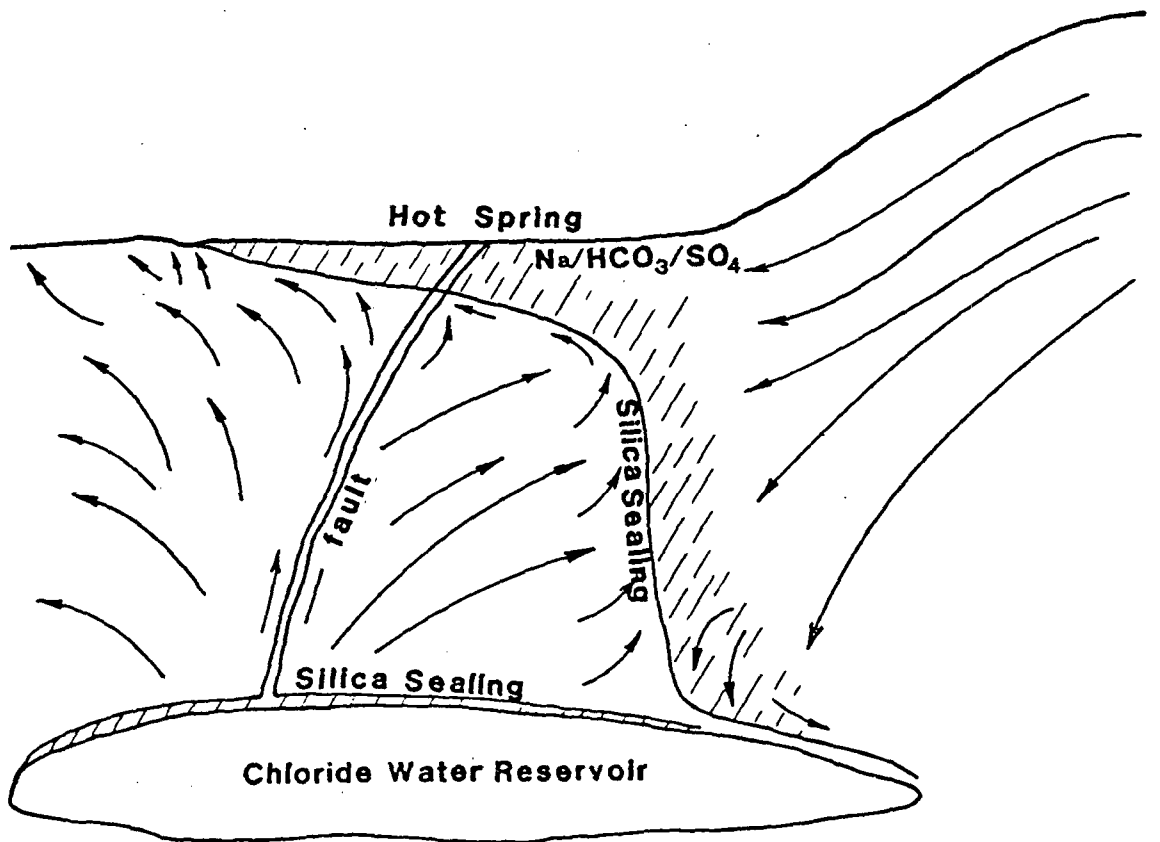
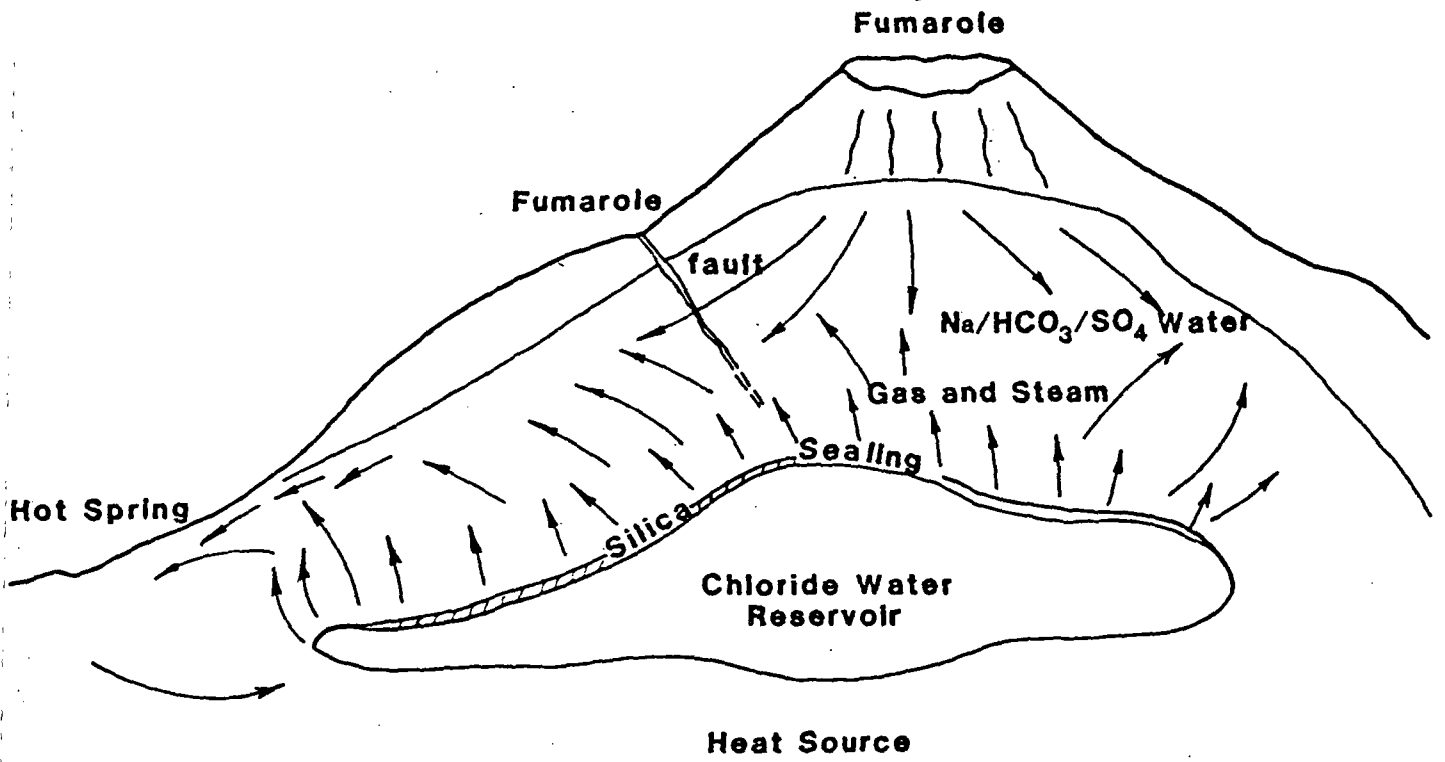
TYPE	EXAMPLE	pH	Na	K	Ca	Mg	Fe	Cl	SO ₄	HCO ₃	SiO ₂	F	Mn	B	Li
SODIUM CHLORIDE	GEYSER— EL TATIO, CHILE	7.3	4340	520	272	.5	.1	7922	30	46	260	3.1	.4	178	45
ACID SULFATE	GEYSER— TOKAANU, N.Z.	2.8	43	11	27	3.5	8.2	32	347	0	280	—	—	2.5	—
ACID SULFATE- CHLORIDE	HOT SPRING— WAIOTAPU, N.Z.	2.8	405	74	40	7.5	5.0	612	666	0	370	—	—	10.1	—
	CRATER LAKE— RUAPEHA, N.Z.	1.2	740	79	1200	1030	900	9450	10950	0	852	260	34	13.8	1.6
BICARBONATE- SULFATE	WELL— (500 m) KAWAH KAMOJANG, INDONESIA	8.0	148	6.7	11.6	.1	.15	10	120	207	375	—	—	10	.35

Geothermal Systems



Ore Deposits vs Geothermal Systems





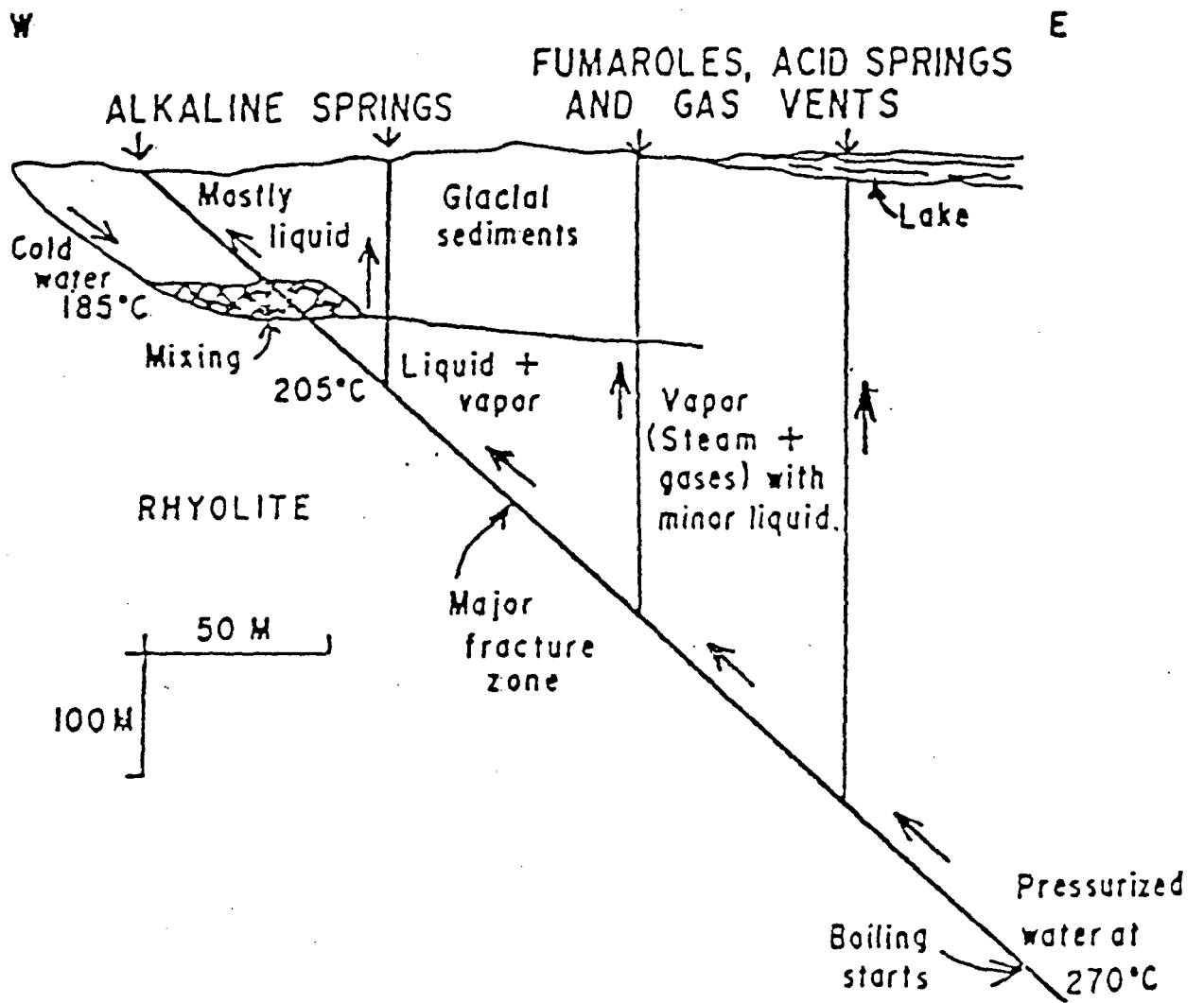


Fig. 8. Hypothetical east-west cross section of part of the Shoshone geothermal system

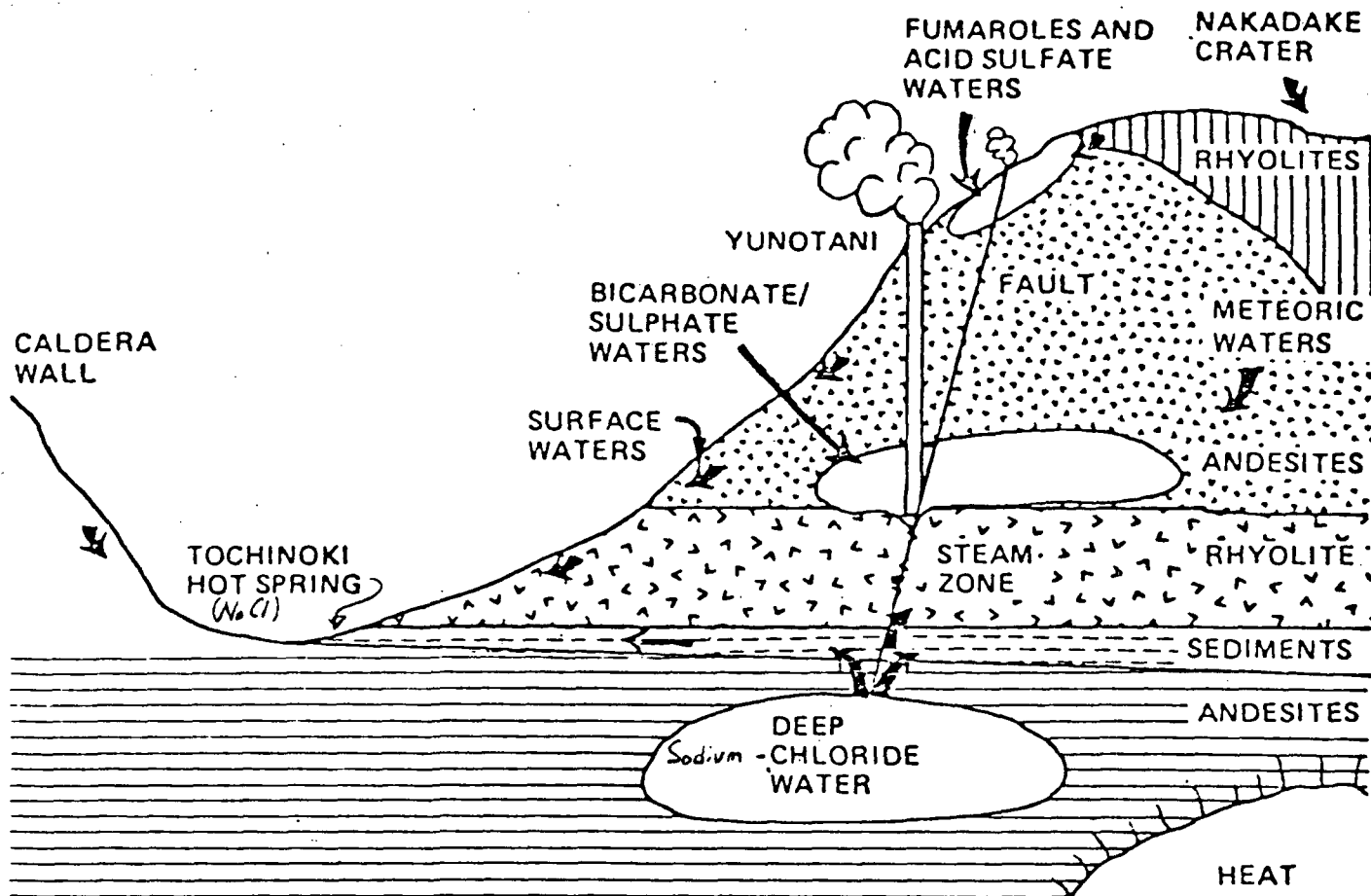
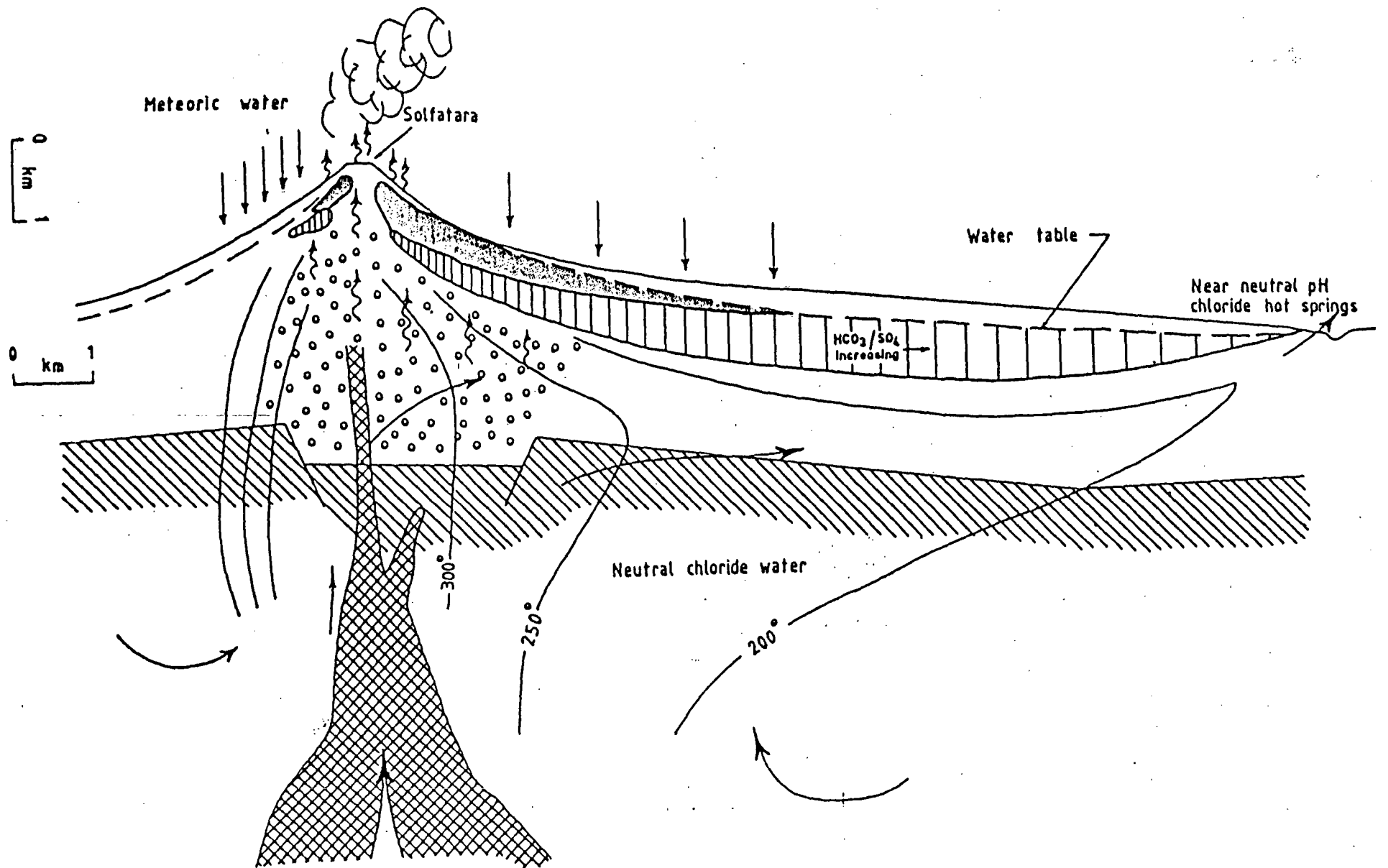
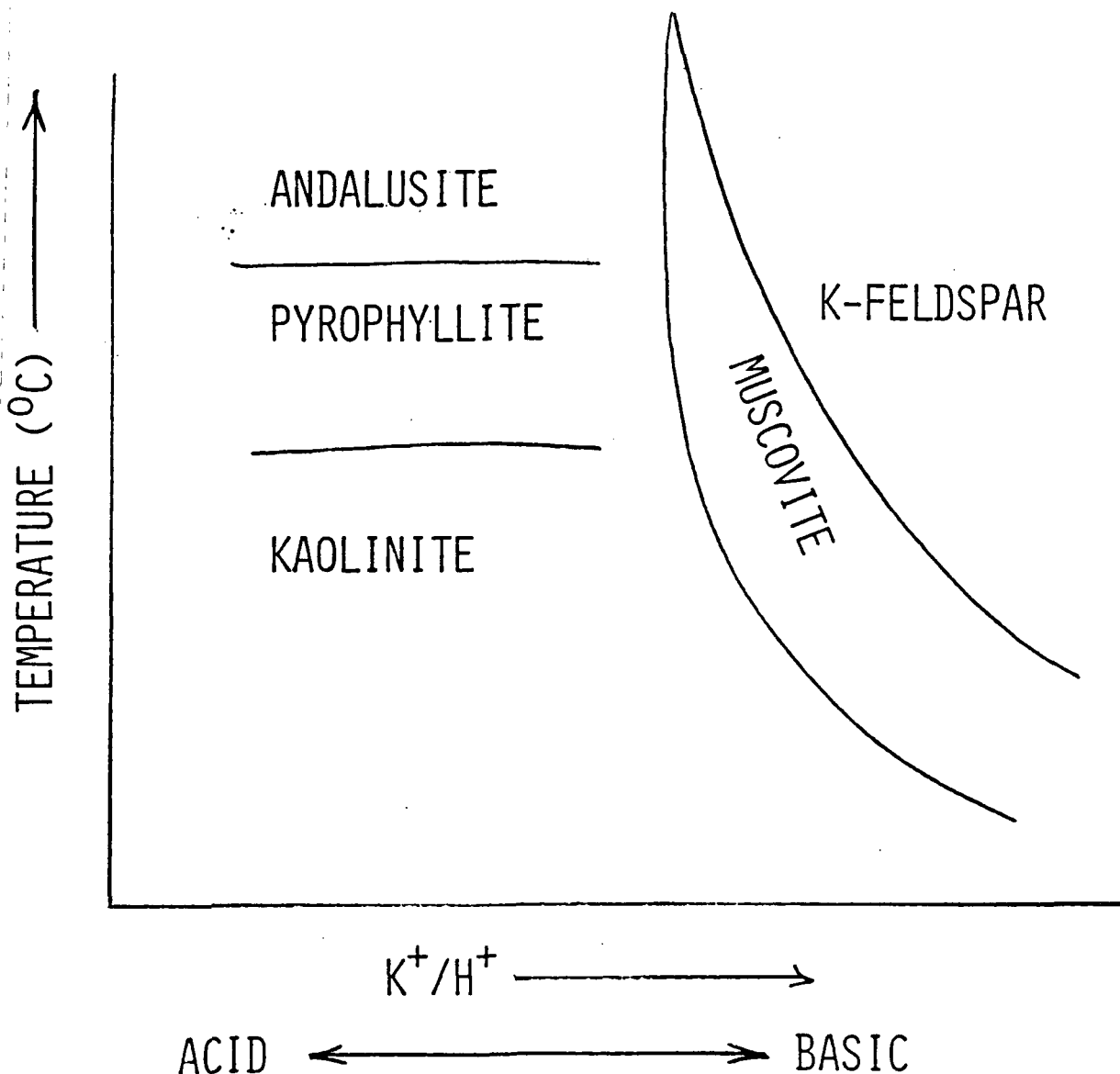
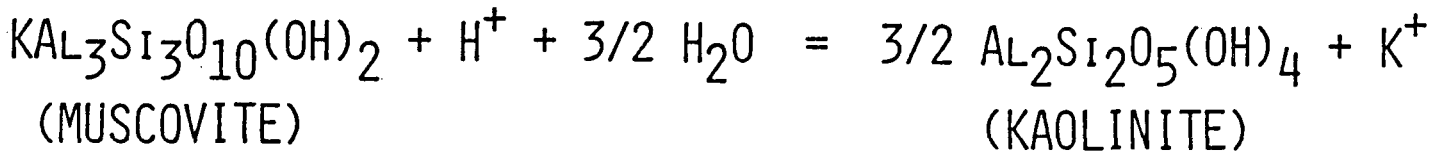
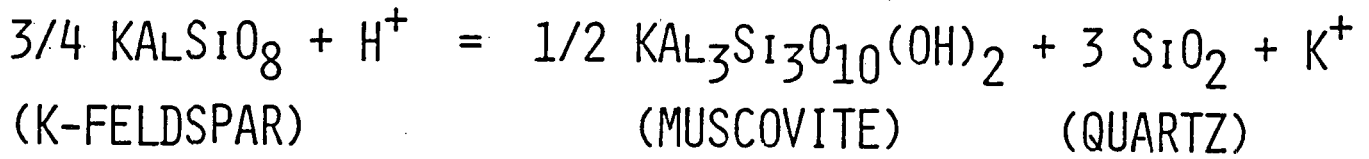
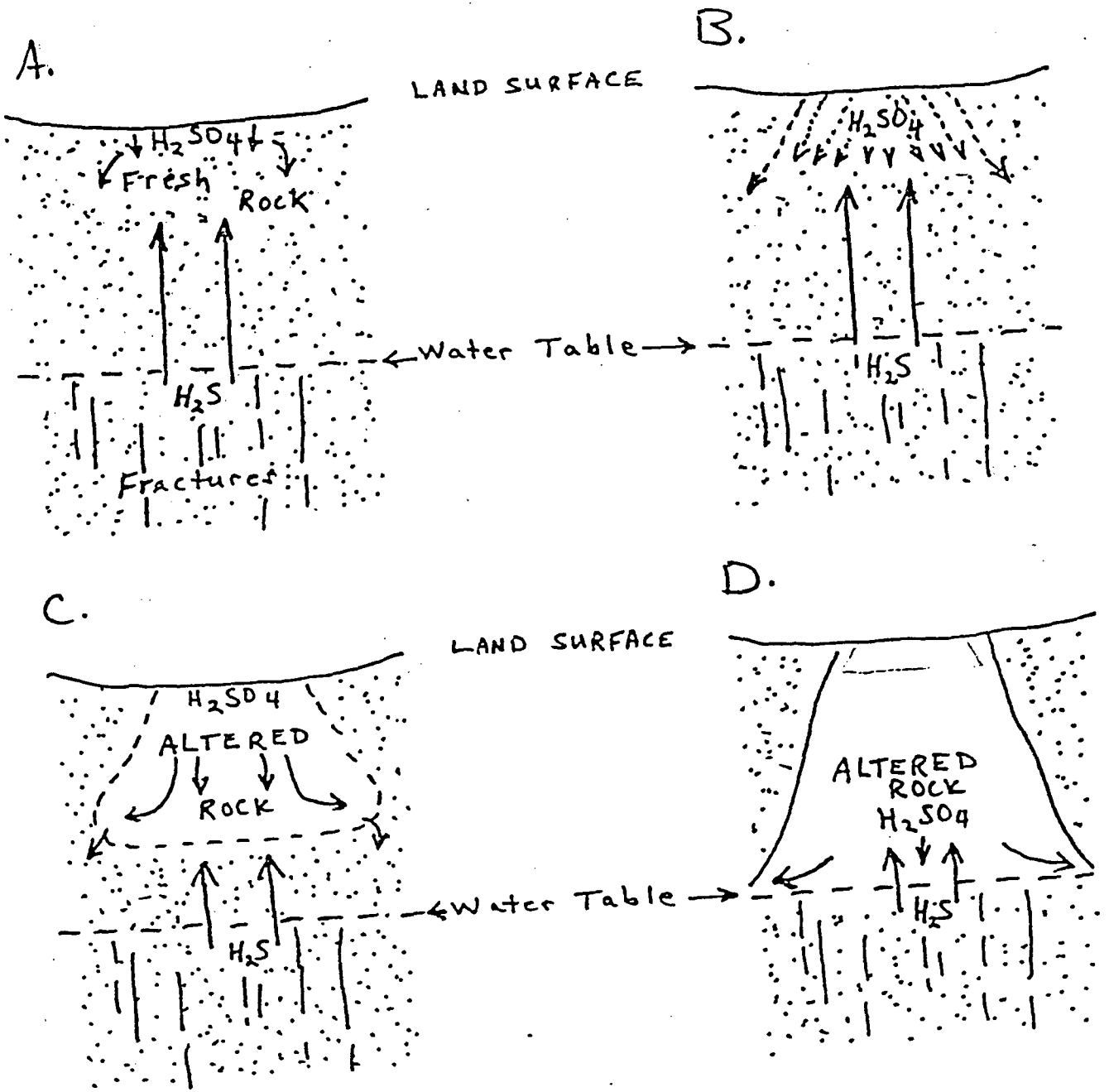


FIGURE 2: MODEL OF THE YUNOTANI GEOTHERMAL SYSTEM.
 GEOLOGIC LEGEND: SEE FIG. 1. SEE TEXT FOR
 EXPLANATIONS. (SCHEMATIC FIGURE NOT TO SCALE.)



(HENLEY AND ELLIS, 1982)





Hypothetical Four-stage Development of Acid-Altered Area

(SCHOEN et al., 1974)

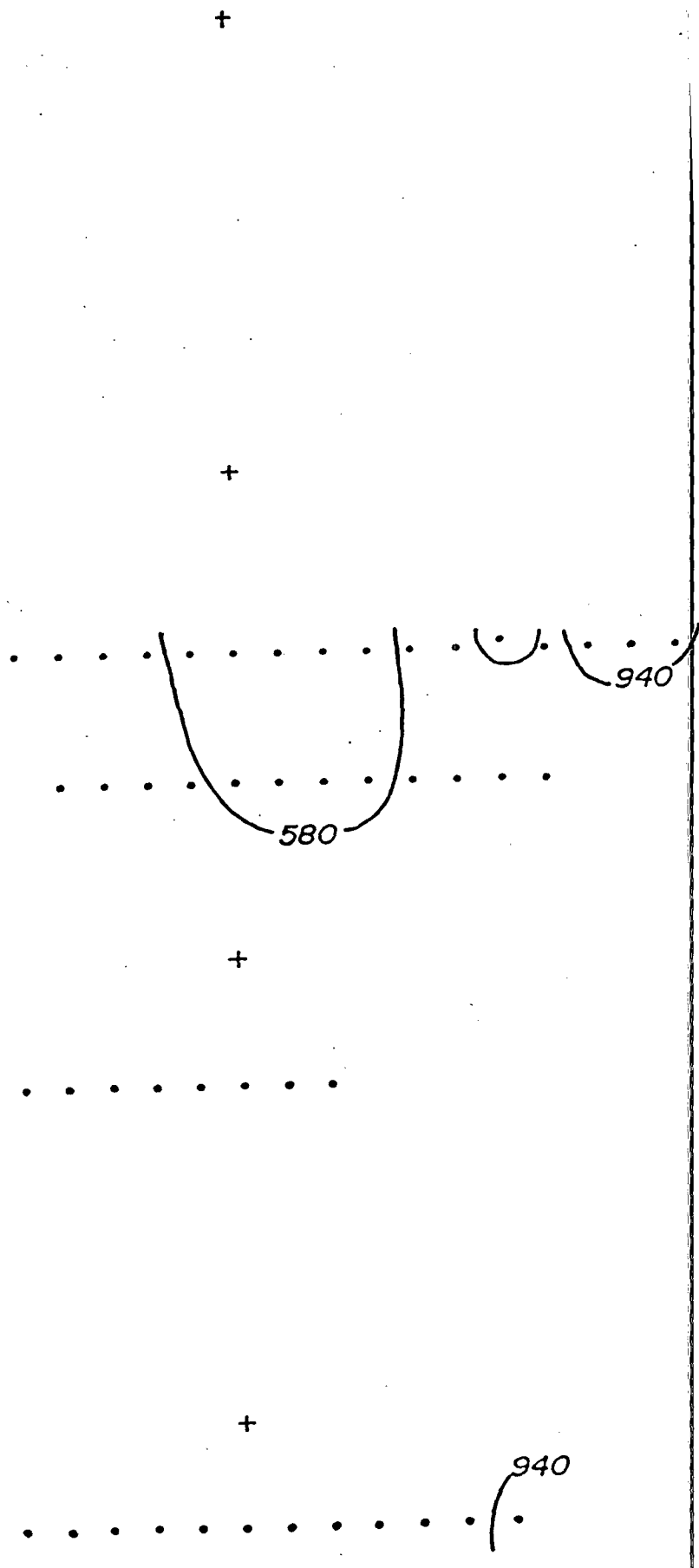
**SPEARMAN RANK CORRELATION
-80 MESH SOILS *
ROOSEVELT H.S. KRGA, UTAH**

	Hg			
Mn	-.4	Mn		
Cu	-.4	.6	Cu	
Zn	-.2	.6	.5	Zn
Li	-.3	.5	.6	.4

* 178 SAMPLES

MANGANESE IN -80 MESH SOIL

- > 940 ppm Mn
- 940 TO 580 ppm Mn
- < 580 ppm Mn



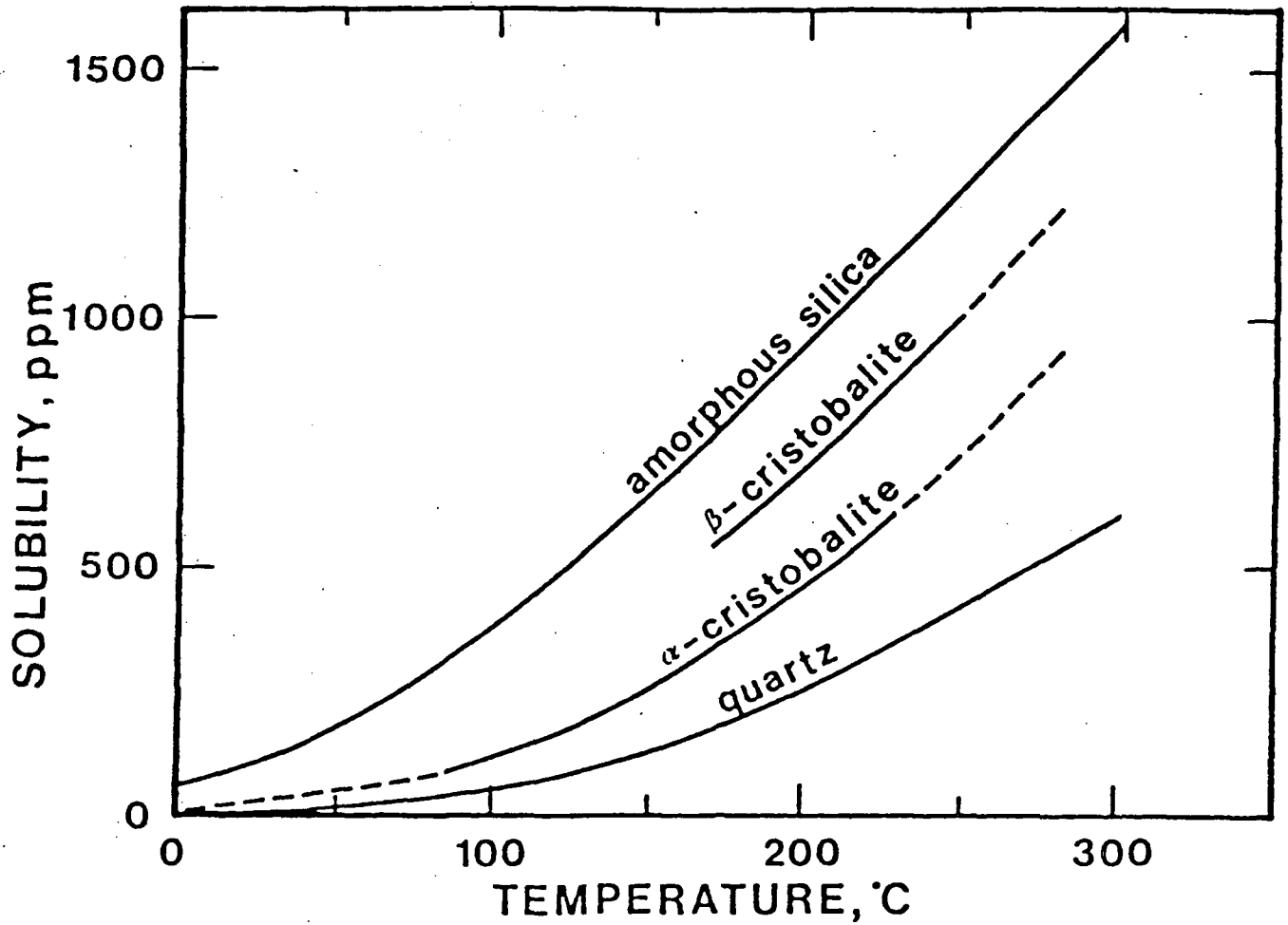
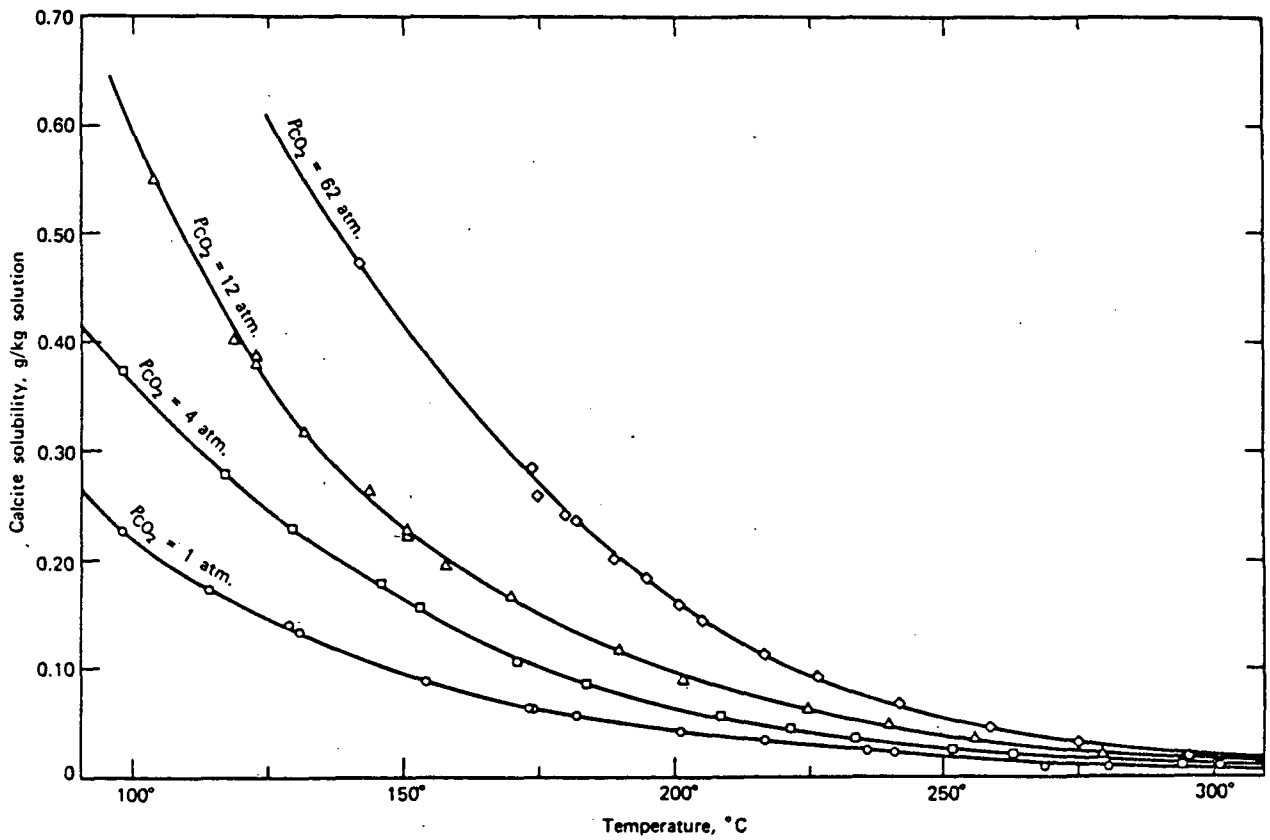


Figure 8. Solubilities of silica phases calculated from the temperature functions listed in Table 4.

(Drummond, 1981)



The solubility of calcite in water up to 300°C at various partial pressures of carbon dioxide. (From Ellis, 1959, *Am. J. Sci.*, 257, 354-365.) The solubility values have been revised downward slightly by Ellis (1963).

HOLLAND AND MALININ (1979)

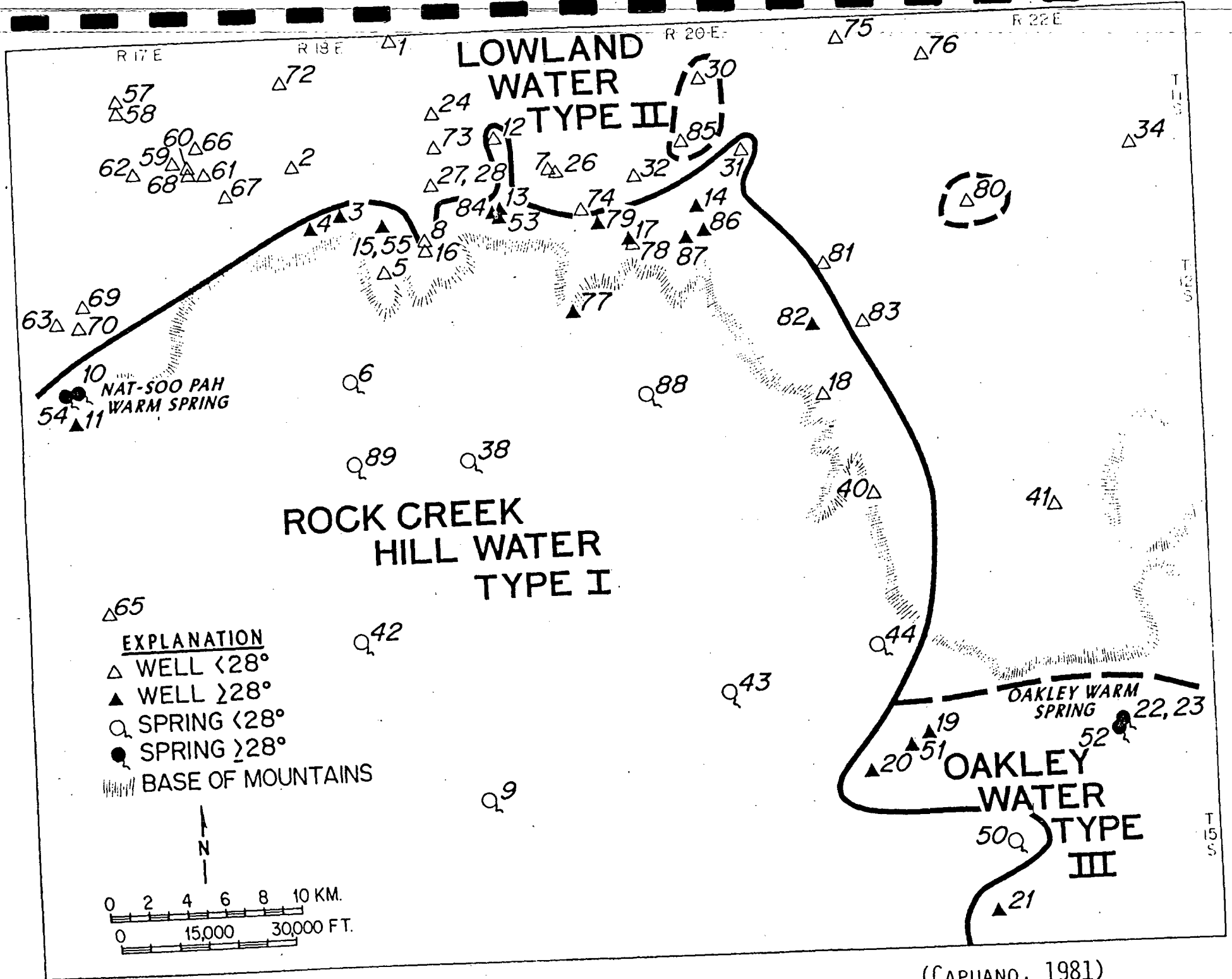
SOURCE OF WATER

-WATER-ROCK REACTIONS:

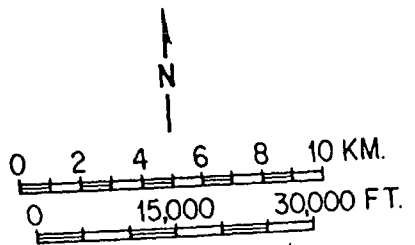
COMPOSITION OF FLUID AFFECTED BY COMPOSITION OF
ROCKS ALONG ITS FLOW PATH, AND TEMPERATURE AND
PRESSURE OF REACTION

-ISOTOPIC CHARACTER:

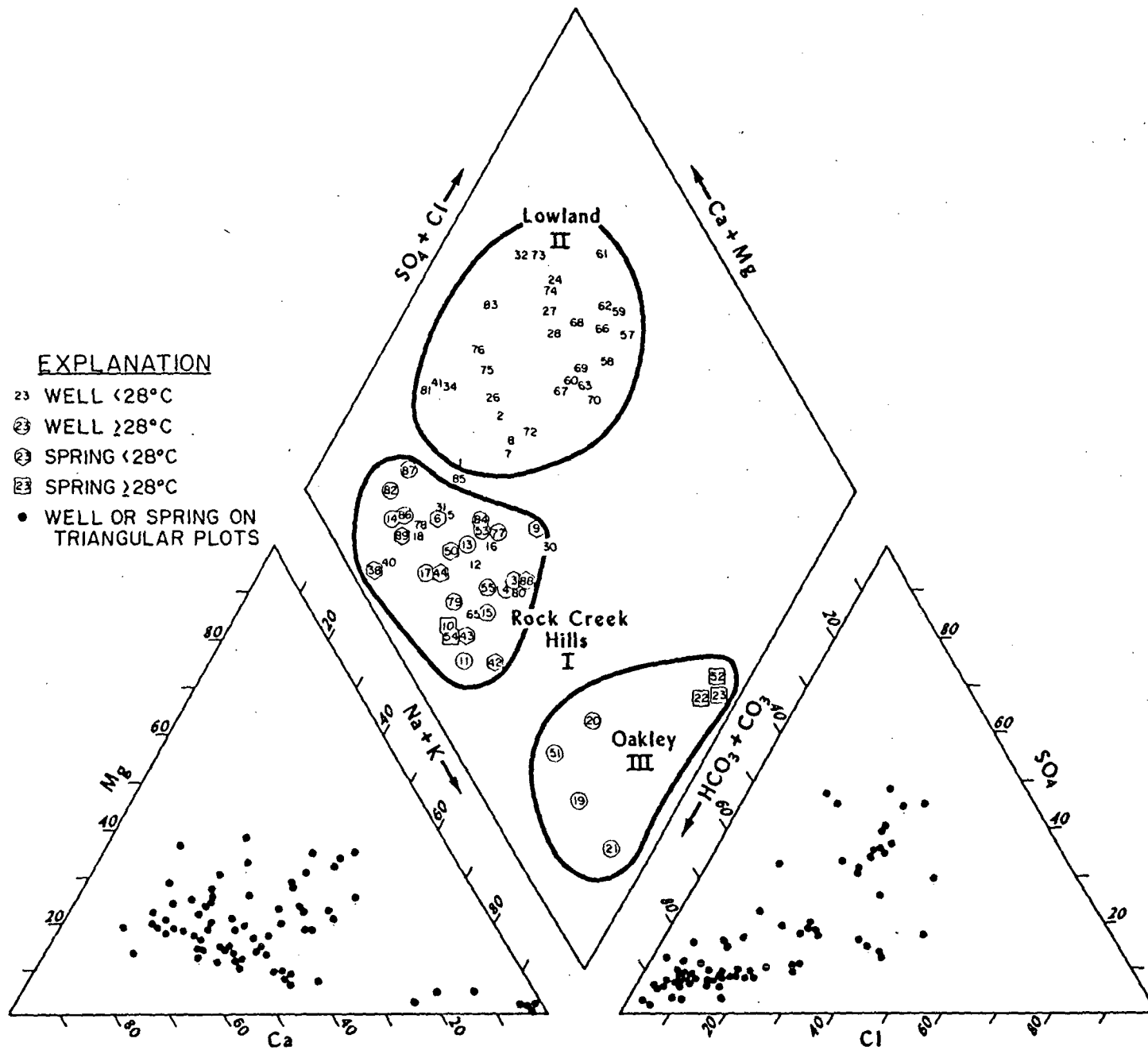
OXYGEN-DEUTERIUM



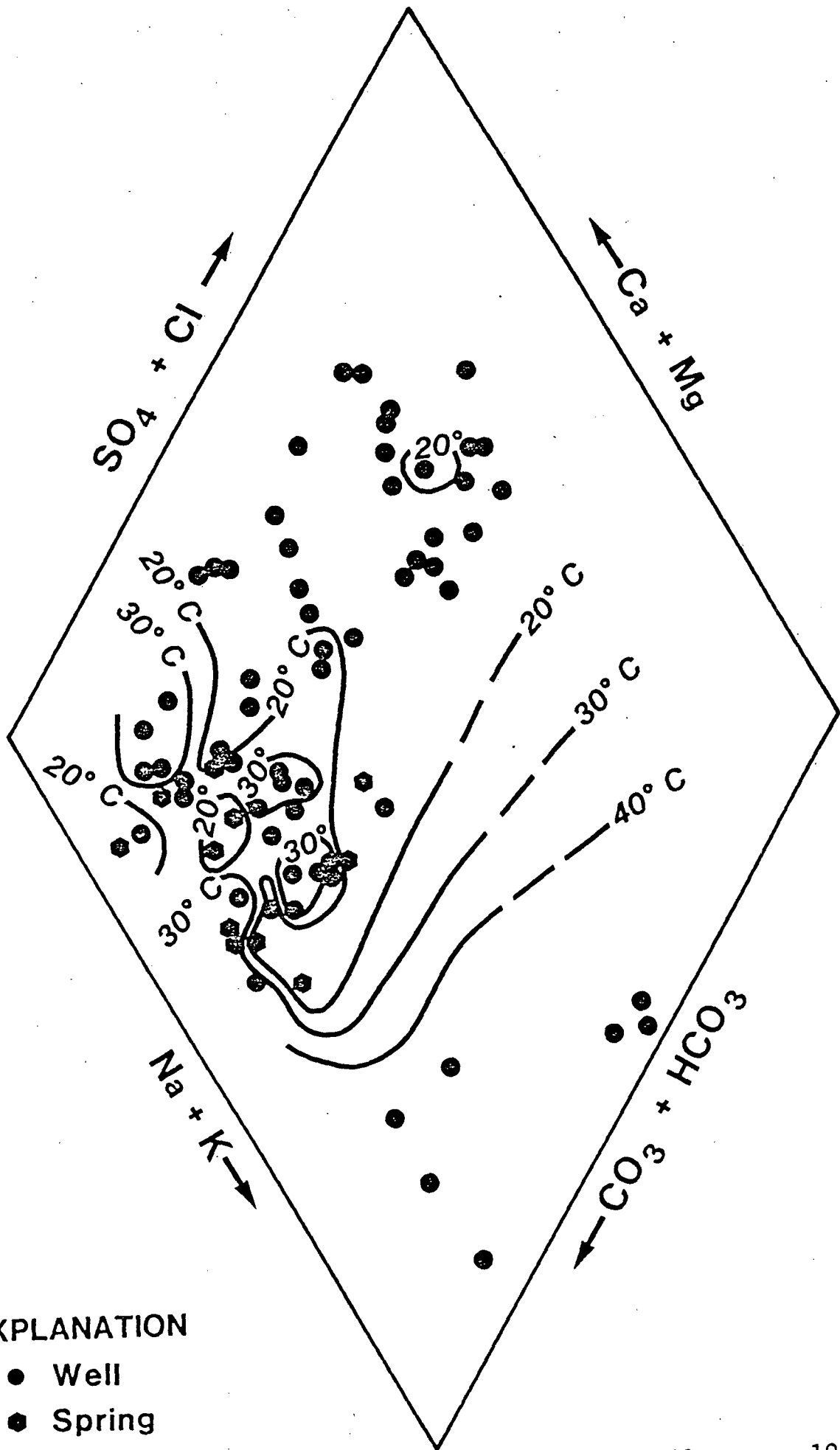
EXPLANATION
 △ WELL <28°
 ▲ WELL ≥28°
 ○ SPRING <28°
 ● SPRING ≥28°
 ▨ BASE OF MOUNTAINS



(CAPUANO, 1981)



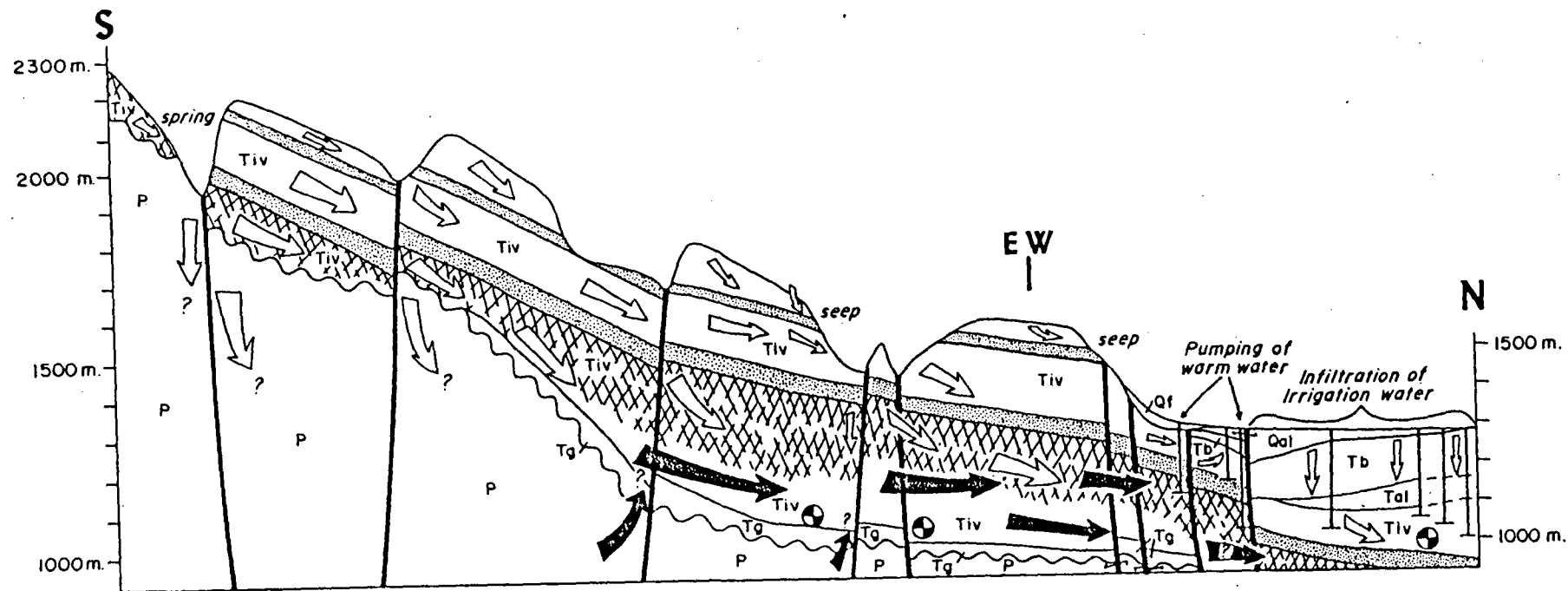
(CAPUANO, 1981)



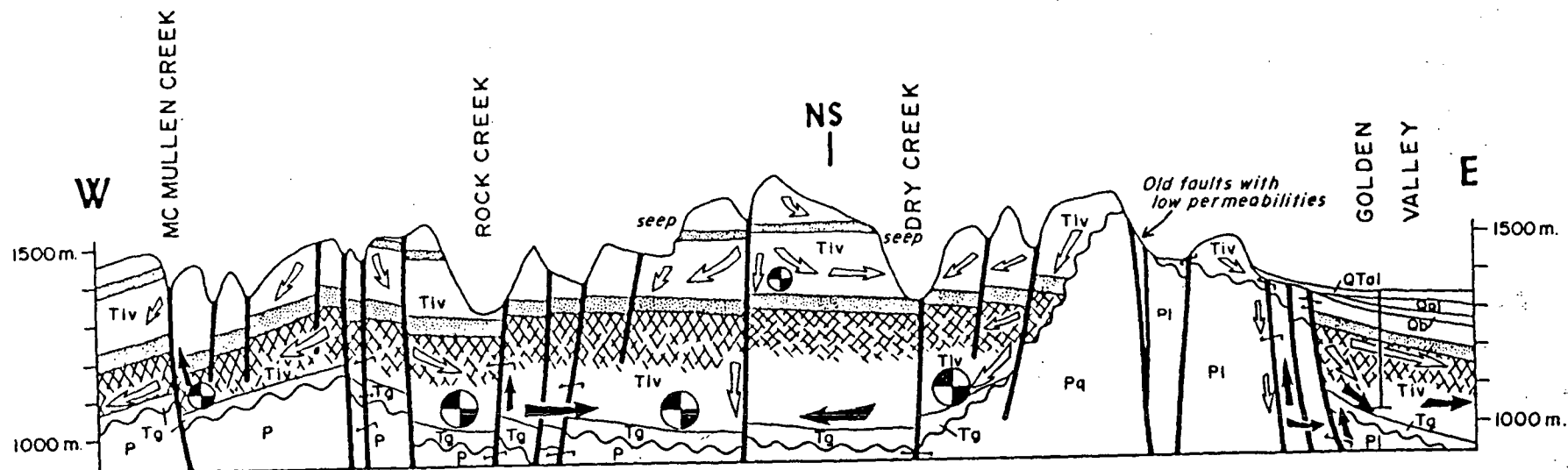
EXPLANATION

- Well
- Spring

(CAPUANO, 1981)



(A)



(B)

↑ warm. water ↓ cold water ⊕ horizontal ground water flow into plane of page — confining tuffaceous sediment xxx permeable jointed welded tuff or flow

OXYGEN

$$^{16}\text{O} = 99.756\%$$

$$^{17}\text{O} = 0.039\%$$

$$^{18}\text{O} = 0.205\%$$

HYDROGEN

$$^1\text{H} = 99.985\%$$

$$^2\text{H} = \text{D} = 0.015\%$$

$$^3\text{H} = T_{1/2} = 12.26\text{y}$$

DC/Iso Gen-004

PROCESSES THAT PRODUCE STABLE ISOTOPIC VARIATIONS IN WATERS

Separation of $\text{H}_2\text{O}(\text{vap.})$; boiling

Mixing of different fluids

Shale-membrane filtration

Changes in redox state

Interaction of water with rock

STABLE ISOTOPE NOTATION

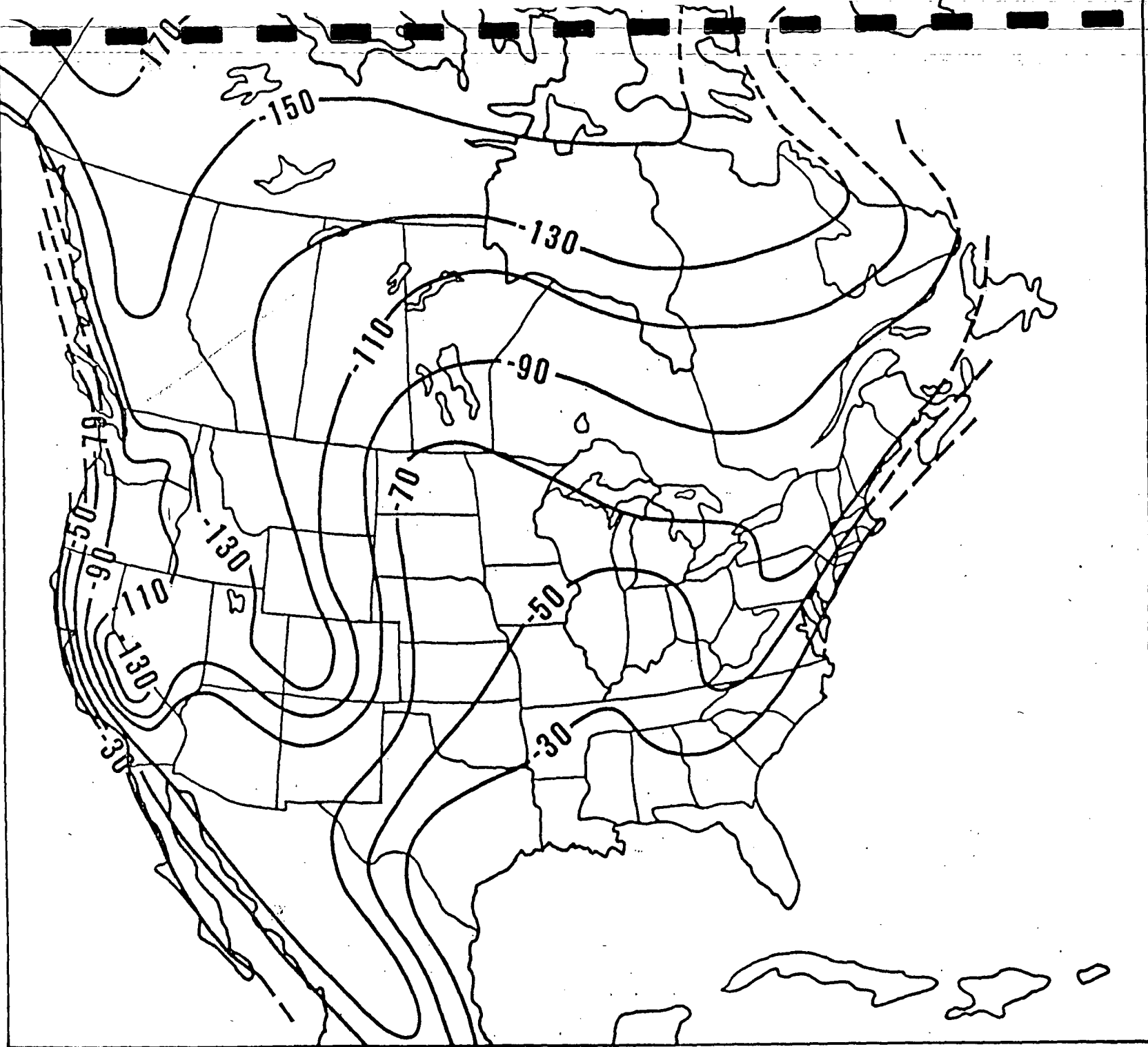
$$\delta (\text{‰}) = \left(\frac{R_x - R_{\text{std}}}{R_{\text{std}}} \right) 10^3$$

Where $R_x = (D/H)_x, ({}^{13}\text{C}/{}^{12}\text{C})_x, ({}^{18}\text{O}/{}^{16}\text{O})_x, ({}^{34}\text{S}/{}^{32}\text{S})_x$

and R_{std} is the corresponding ratio in a standard



SD

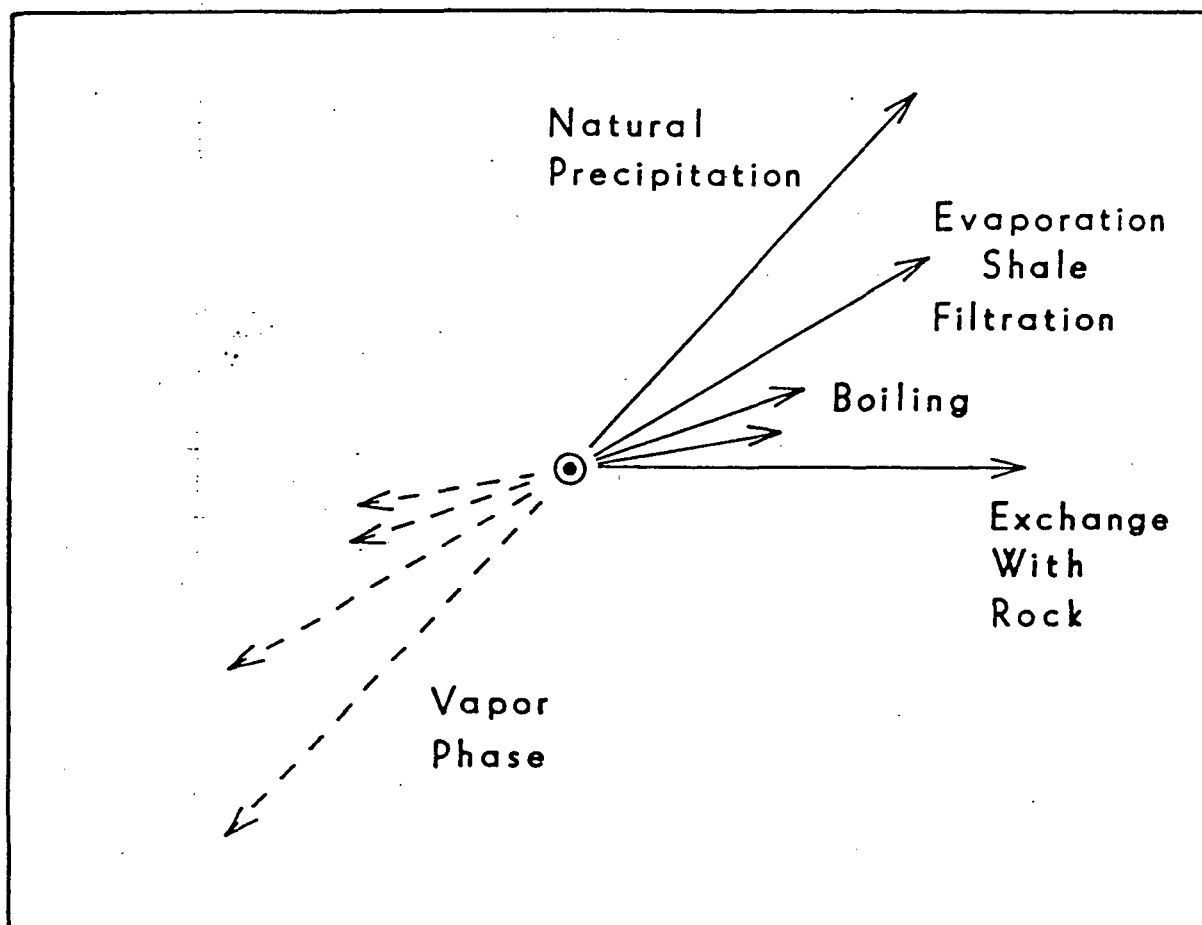


(Taylor, 1974)

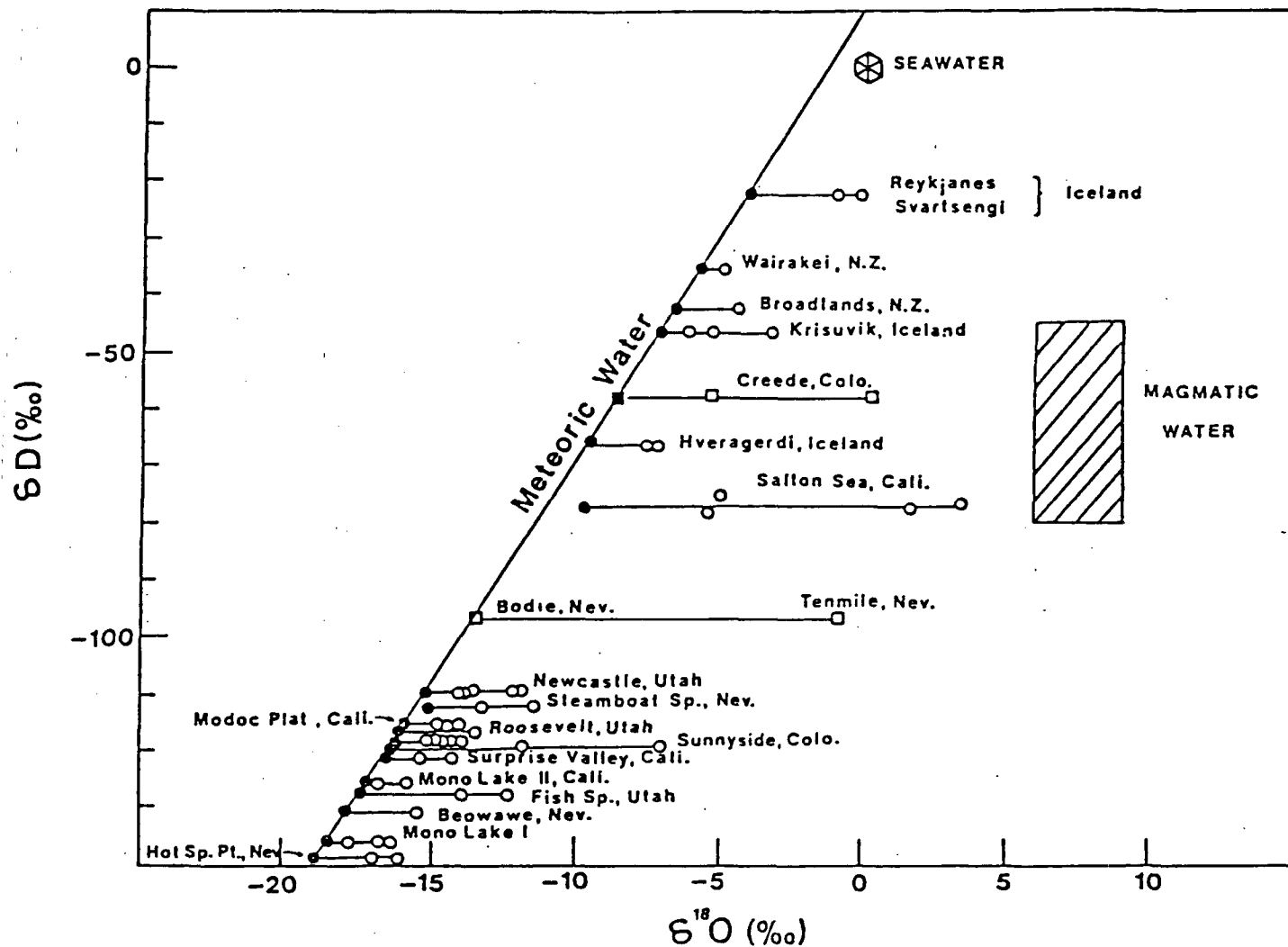
DC/lao Gen-001

COMMON ISOTOPIC FRACTIONATION MECHANISMS FOR WATER

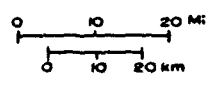
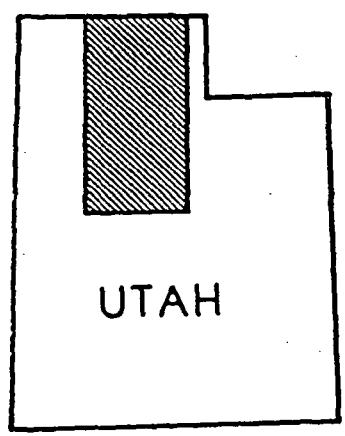
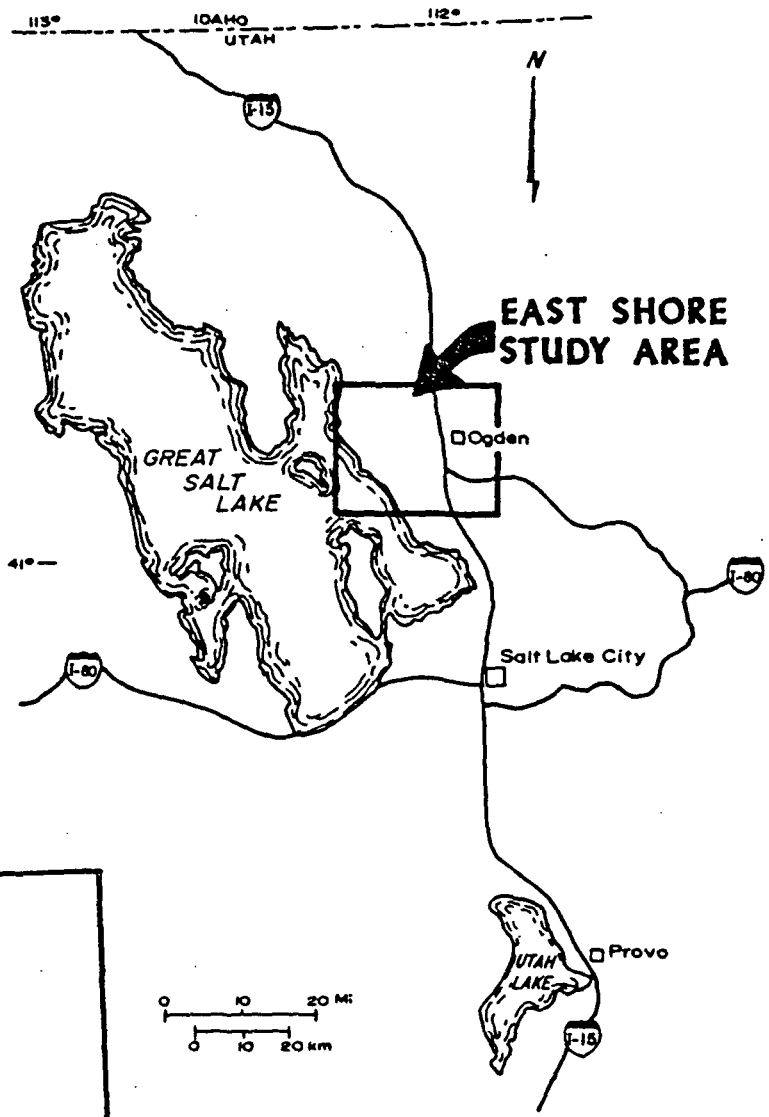
↑
 δD
x 10



$\delta^{18}O \rightarrow$

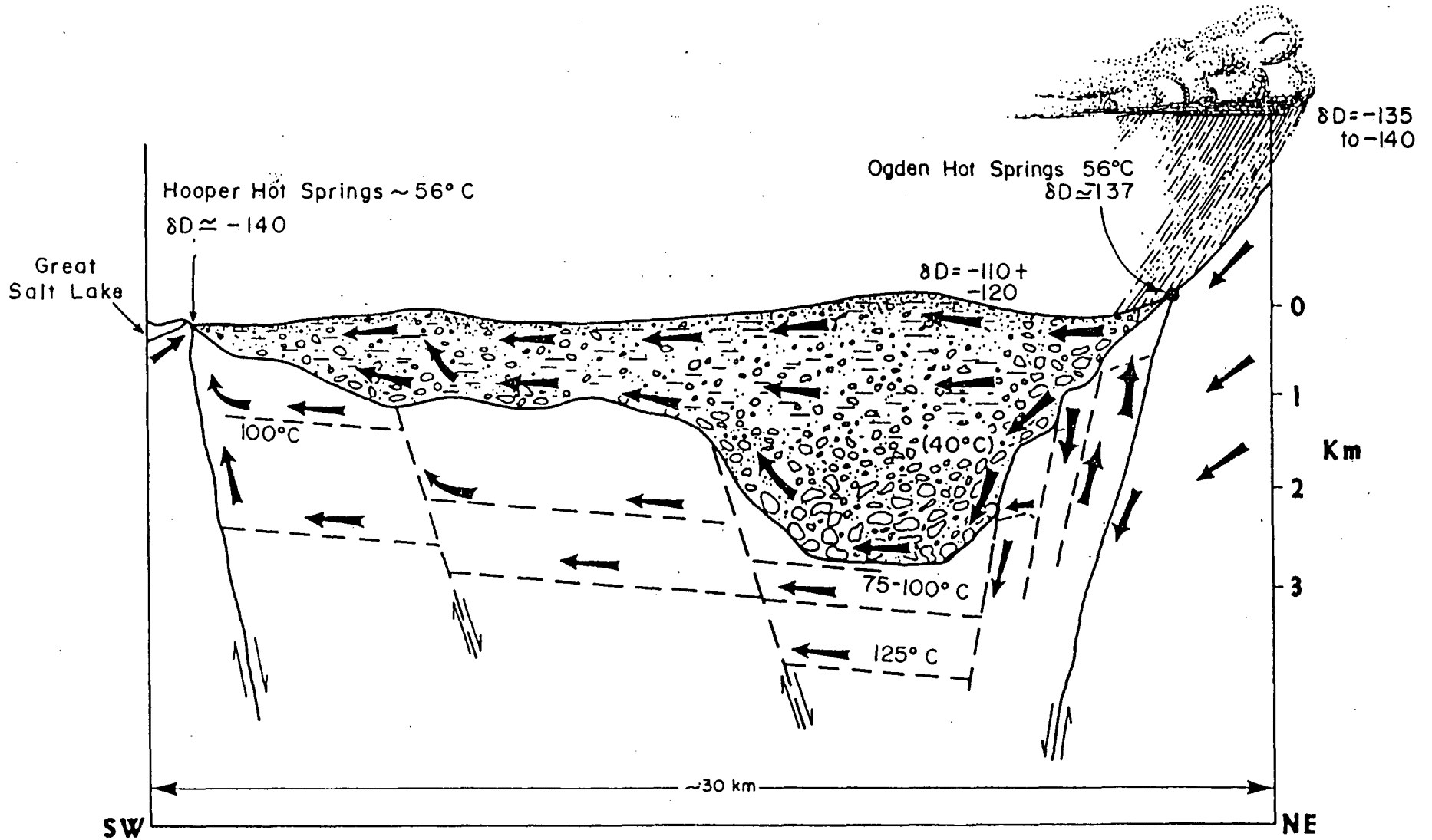


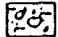
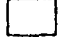



Oxygen and deuterium isotopes for selected hydrothermal systems (Cole, 1980).



GROUND WATER MODEL

← Increases Shallow well temperature
 ← Increases Chloride/bicarbonate
 (Gradual)



-  alluvium
-  bedrock
-  thrust fault or fractures in bedrock
-  normal faults (arrows indicate movement)
-  direction of ground water movement

-GIVEN SOURCE AND POSSIBLE FLOW PATHS ESTIMATE
FLOW RATES

-TRITIUM (^3H)

BEFORE 1953: T.U. < 10

1953 TO 1963: T.U. UP TO 7000

1963 TO RECENT: DECREASING

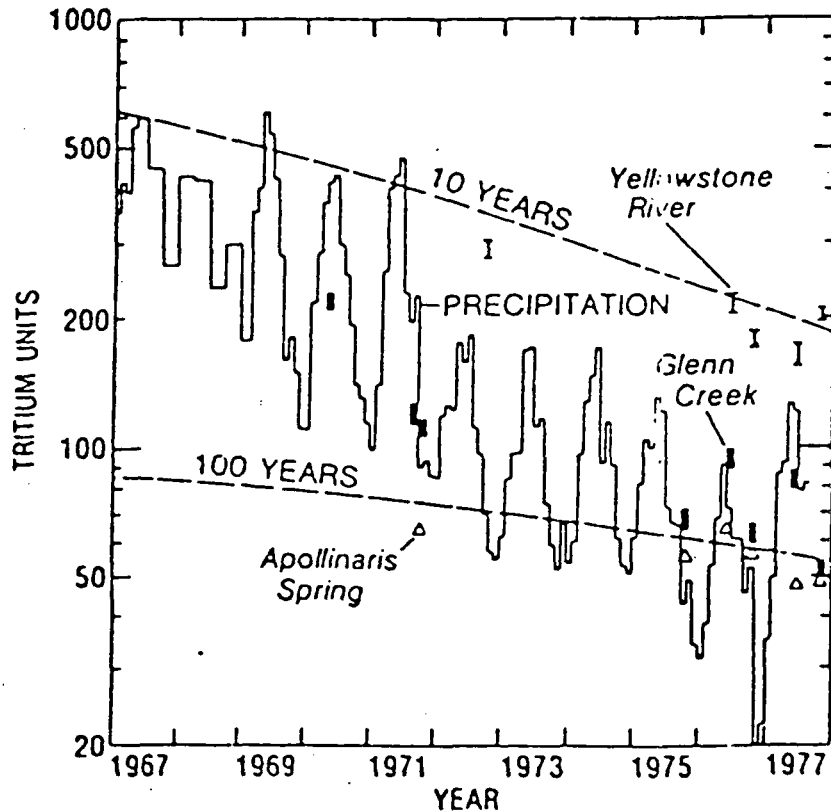


Figure 2.--Tritium in precipitation, mixed reservoirs, and cold waters of Yellowstone Park.

PEARSON AND TRUESDELL, 1978

Table 1.--Equations expressing the temperature dependence of selected geothermometers. C is the concentration of dissolved silica. All concentrations are in mg/kg.

GEO THERMOMETER	EQUATION	RESTRICTIONS
a. Quartz-no steam loss	$t^{\circ}\text{C} = \frac{1309}{5.19 - \log C} - 273.15$	$t = 0^{\circ}\text{C}-250^{\circ}\text{C}$
b. Quartz-maximum steam loss	$t^{\circ}\text{C} = \frac{1522}{5.75 - \log C} - 273.15$	$t = 0^{\circ}\text{C}-250^{\circ}\text{C}$
c. Chalcedony	$t^{\circ}\text{C} = \frac{1032}{4.69 - \log C} - 273.15$	$t = 0^{\circ}\text{C}-250^{\circ}\text{C}$
d. α -Cristobalite	$t^{\circ}\text{C} = \frac{1000}{4.78 - \log C} - 273.15$	$t = 0^{\circ}\text{C}-250^{\circ}\text{C}$
e. β -Cristobalite	$t^{\circ}\text{C} = \frac{781}{4.51 - \log C} - 273.15$	$t = 0^{\circ}\text{C}-250^{\circ}\text{C}$
f. Amorphous silica	$t^{\circ}\text{C} = \frac{731}{4.52 - \log C} - 273.15$	$t = 0^{\circ}\text{C}-250^{\circ}\text{C}$
g. Na/K (Fournier)	$t^{\circ}\text{C} = \frac{1217}{\log (\text{Na/K}) + 1.483} - 273.15$	$t > 150^{\circ}\text{C}$
h. Na/K (Truesdell)	$t^{\circ}\text{C} = \frac{855.6}{\log (\text{Na/K}) + 0.8573} - 273.15$	$t > 150^{\circ}\text{C}$
i. Na-K-Ca	$t^{\circ}\text{C} = \frac{1647}{\log (\text{Na/K}) + \beta [\log (\sqrt{\text{Ca/Na}}) + 2.06] + 2.47} - 273.15$	$t < 100^{\circ}\text{C}, \beta = 4/3$ $t > 100^{\circ}\text{C}, \beta = 1/3$
j. $\Delta^{18}\text{O}(\text{SO}_4^{2-}-\text{H}_2\text{O})$	$1000 \ln \alpha = 2.88(10^6 T^{-2}) - 4.1$ $\alpha = \frac{1000 + \delta^{18}\text{O}(\text{HSO}_4^{-})}{1000 + \delta^{18}\text{O}(\text{H}_2\text{O})}$ and $T = ^{\circ}\text{K}$	

Mg-CORRECTION FOR Na-K-Ca GEOTHERMOMETER^a

To be used when calculated temperature > 70°C, for Mg-rich fluids where $R = (Mg/Mg+Ca+K) \times 100$ is between 0.5-50 (eq.)

(1) R=0.5-5

$$\Delta T_{mg} = -1.03 + 59.971(\log R) + 145.05(\log R)^2 - \frac{367111}{T} (\log R)^2 - 1.67 \times \frac{10^7 (\log R)}{T^2}$$

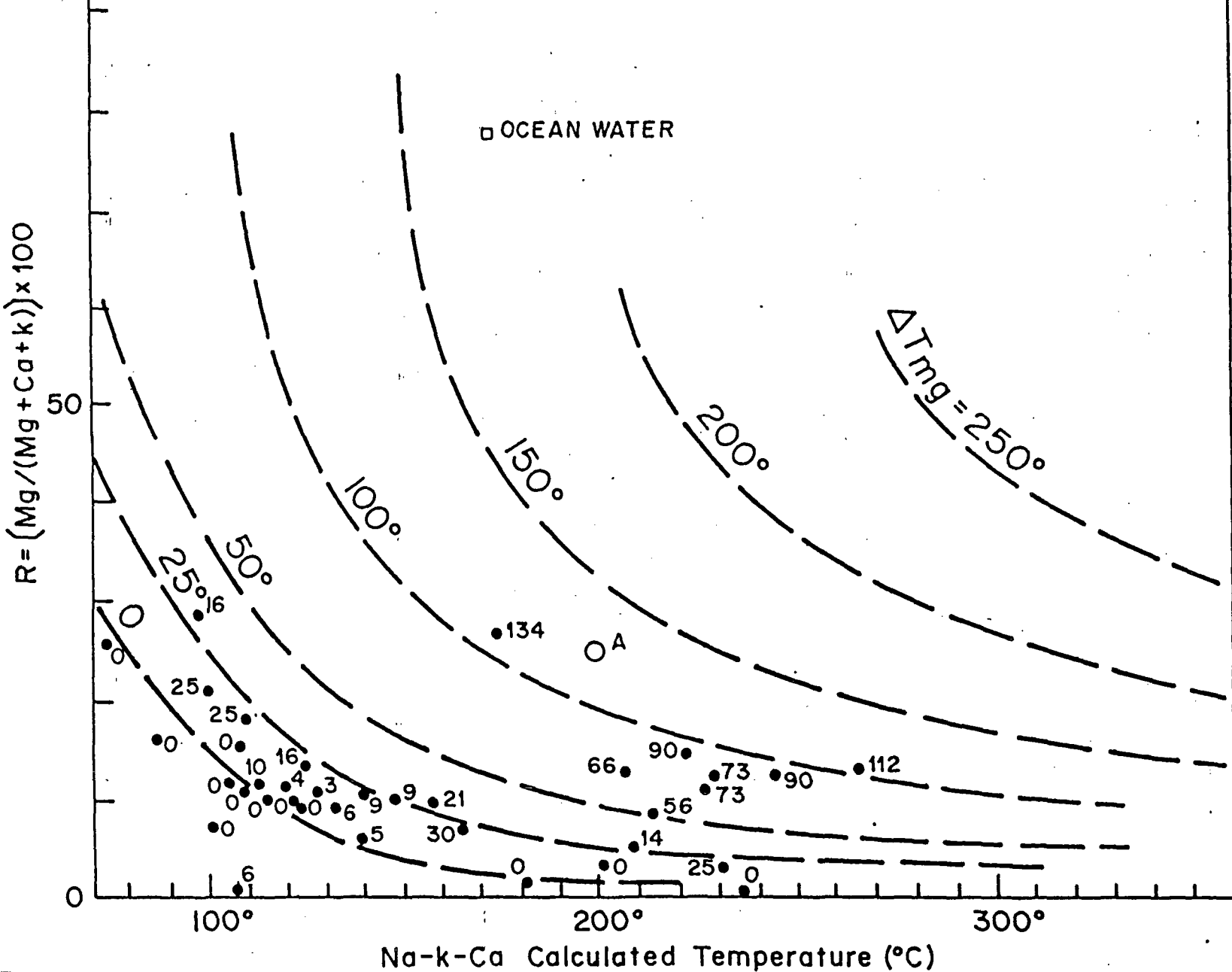
(2) R=5-50

$$\Delta T_{mg} = 10.66 - 4.7415 R + 325.87(\log R)^2 - 1.032 \times \frac{10^5 (\log R)^2}{T} - 1.968 \times \frac{10^7 (\log R)^2}{T^2} + 1.605 \times \frac{10^7 (\log R)^3}{T^2}$$

(3) R > 50: Measured Temp. \approx Underground Temp., disregard the Na-K-Ca Temp.



Mg - Correction



CO₂ - CORRECTED Na - K - Ca GEOTHERMOMETER

Paces, 1975

$$T(^\circ\text{C}) = \frac{1647}{\log(\text{Na}/\text{K}) - \beta \log(\sqrt{\text{Ca}}/\text{Na}) + 2.24 - I} - 273.15$$

WHERE: $I = -1.36 - 0.253 \log P_{\text{CO}_2}$ FOR $P_{\text{CO}_2} \geq 10^{-4}$ atm.

$$-\log P_{\text{CO}_2} = -\log a_{\text{H}^+} - \log a_{\text{HCO}_3^-} + 7.689 + 4.72 \times 10^{-3} T + 3.54 \times 10^{-5} T^2$$

(T = Surface T $^\circ\text{C}$)

USE FOR $T < 75^\circ\text{C}$

NA/LI GEOTHERMOMETER

$$\text{LOG (NA/LI)} = 1000/T - 0.38 \quad \text{FOR } C_L < 7000\text{PPM}$$

$$\text{LOG (NA/LI)} = 1195/T + 0.13 \quad \text{FOR } C_L > 10000\text{PPM}$$

FOUILLAC AND MICHARD (1981)

PRESSURE CORRECTION - SILICA GEOTHERMOMETER

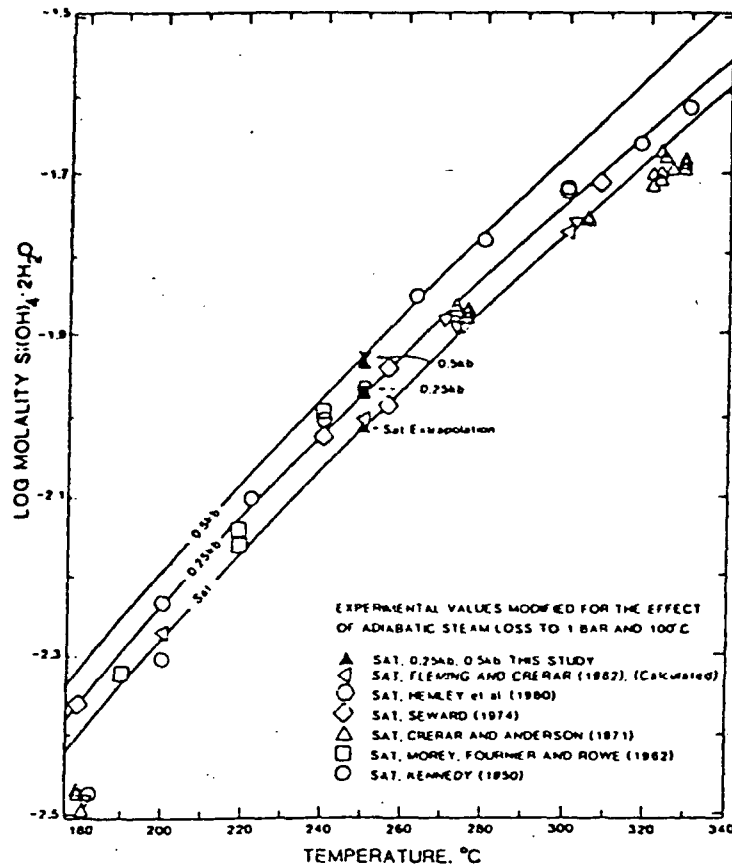


FIG. 5. Symbols indicate log molality of $\text{Si(OH)}_4 \cdot 2\text{H}_2\text{O}$ determined in quartz solubility experiments as a function of temperature, after modification due to the effect of adiabatic steam loss on decompression and cooling to 1 bar and 100°C. The solid lines are those computed in this study from Eqn. (5).

$$T(^{\circ}\text{C}) = 874 - \frac{0.156 P}{(\text{LOG } M_{\text{SiO}_2})^2} + 411 \text{ LOG } M_{\text{SiO}_2} + 51(\text{LOG } M_{\text{SiO}_2})^2$$

APPLICABLE TO: 500 BARS
180° TO 340°C

pH EFFECT ON SILICA SOLUBILITY

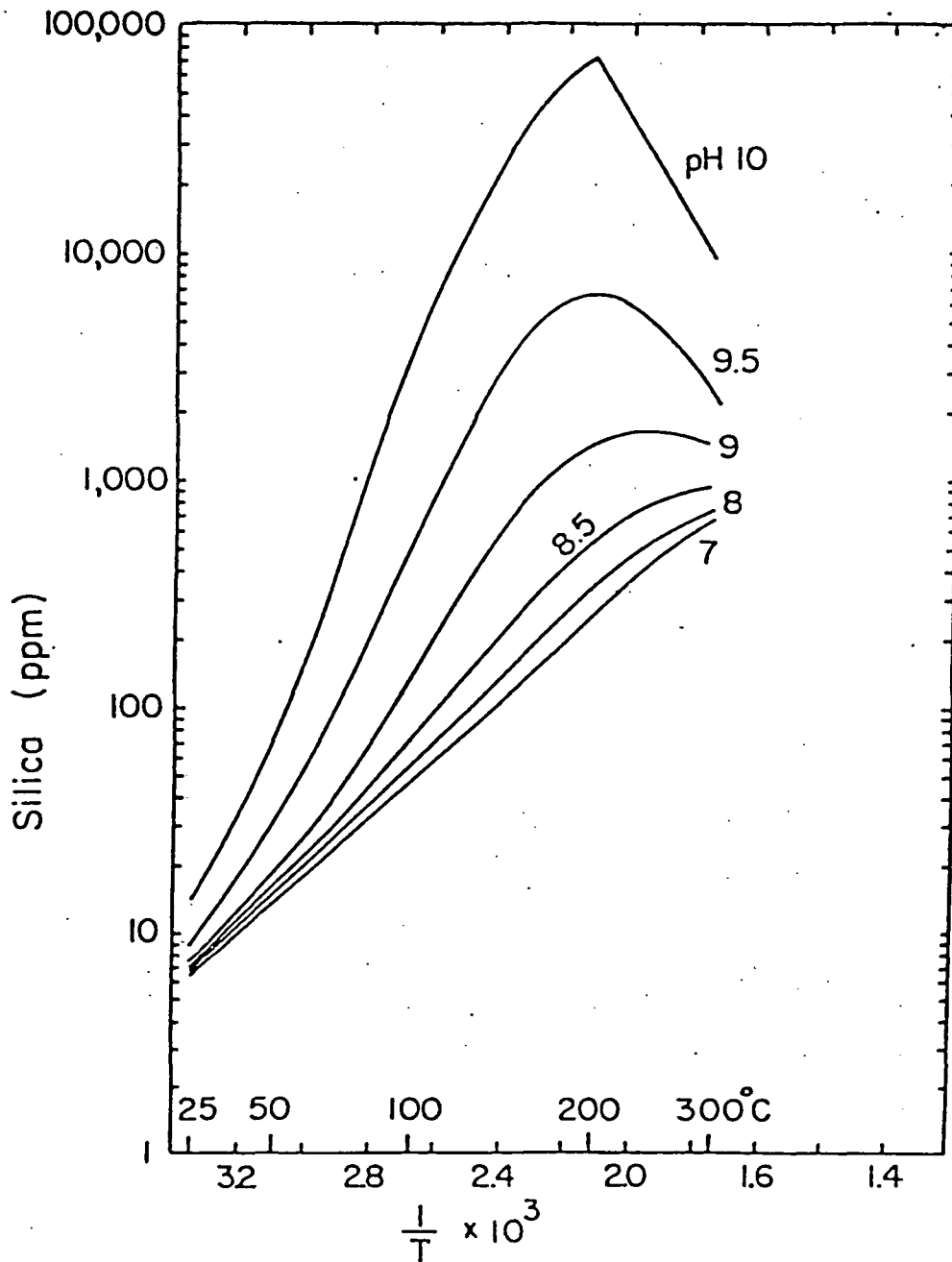
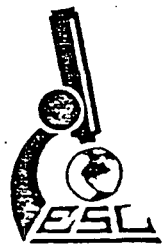


Figure 3. Solubility of quartz vs. temperature at various pH values, calculated using dissociation constants reported by Ryzhenko (1967).

QUANTITATIVE GEOTHERMOMETERS

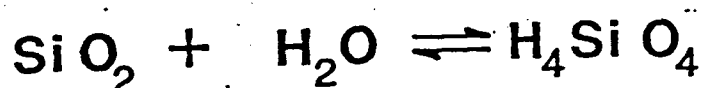
Assumptions:

- (1) Temperature-dependent reactions involving rock and water fix the amount or amounts of dissolved "indicator" constituents in water.
- (2) There is an adequate supply of all reactants.
- (3) There is equilibrium in the reservoir or aquifer in respect to the indicator reaction.
- (4) No reequilibration of the "indicator" constituents occur after the water leaves the reservoir.
- (5) Either no mixing of different waters occurs during movement to the surface or evaluation of the results of such mixing is possible.

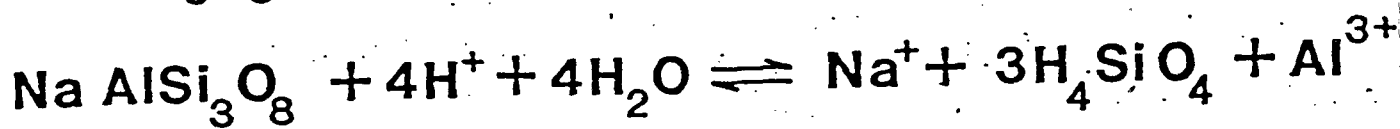
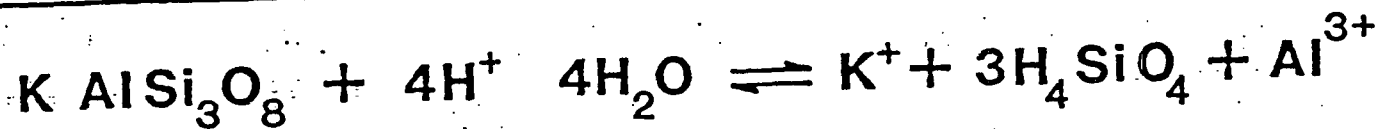


CHEMICAL REACTIONS USED IN GEO THERMOMETRY

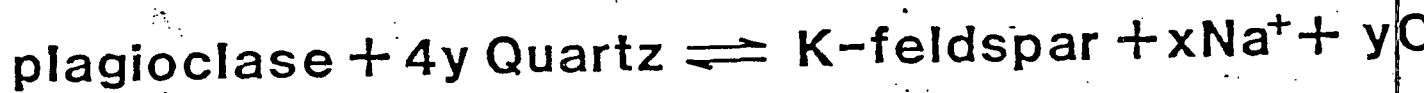
Quartz Dissolution:

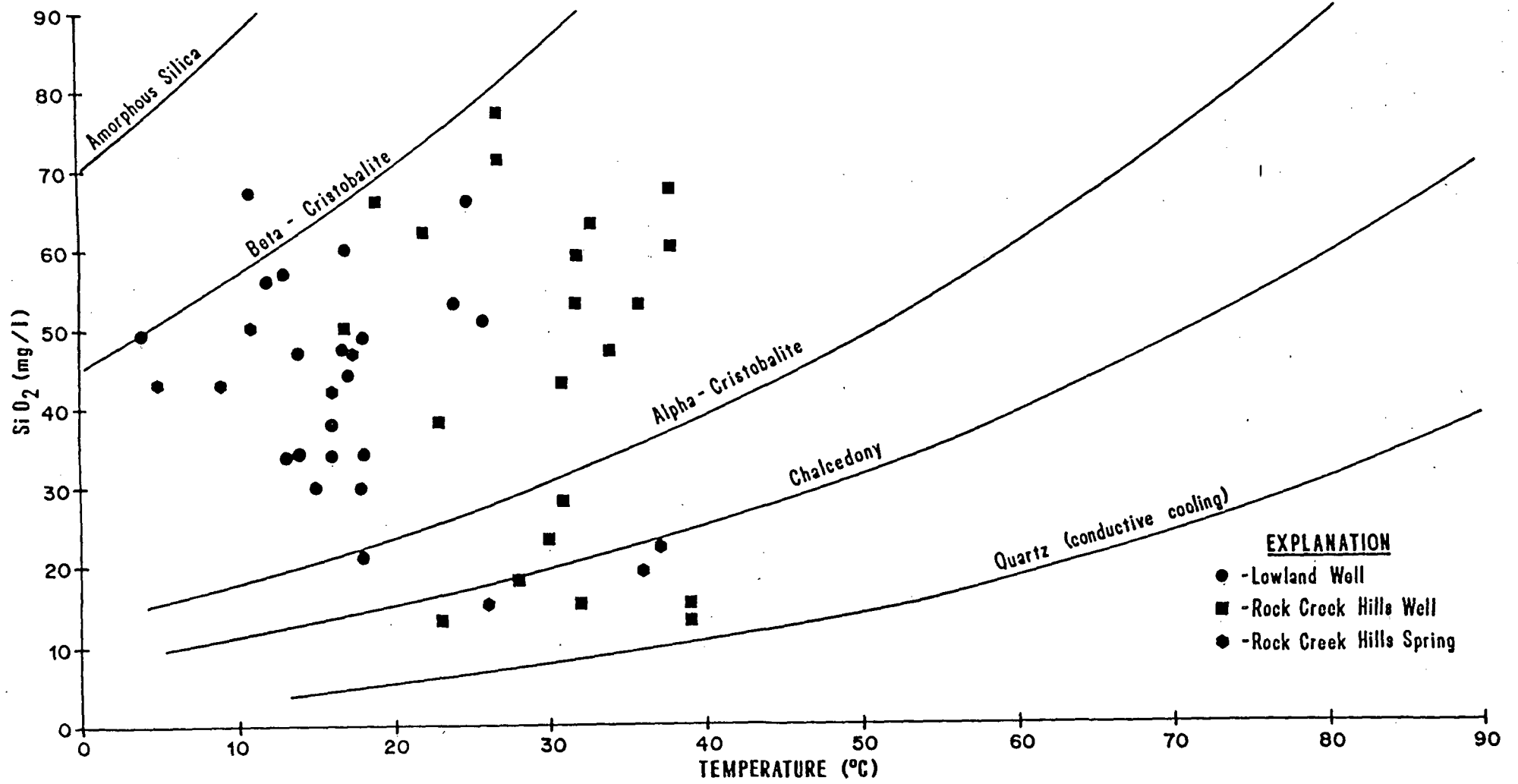


Feldspar Dissolution:



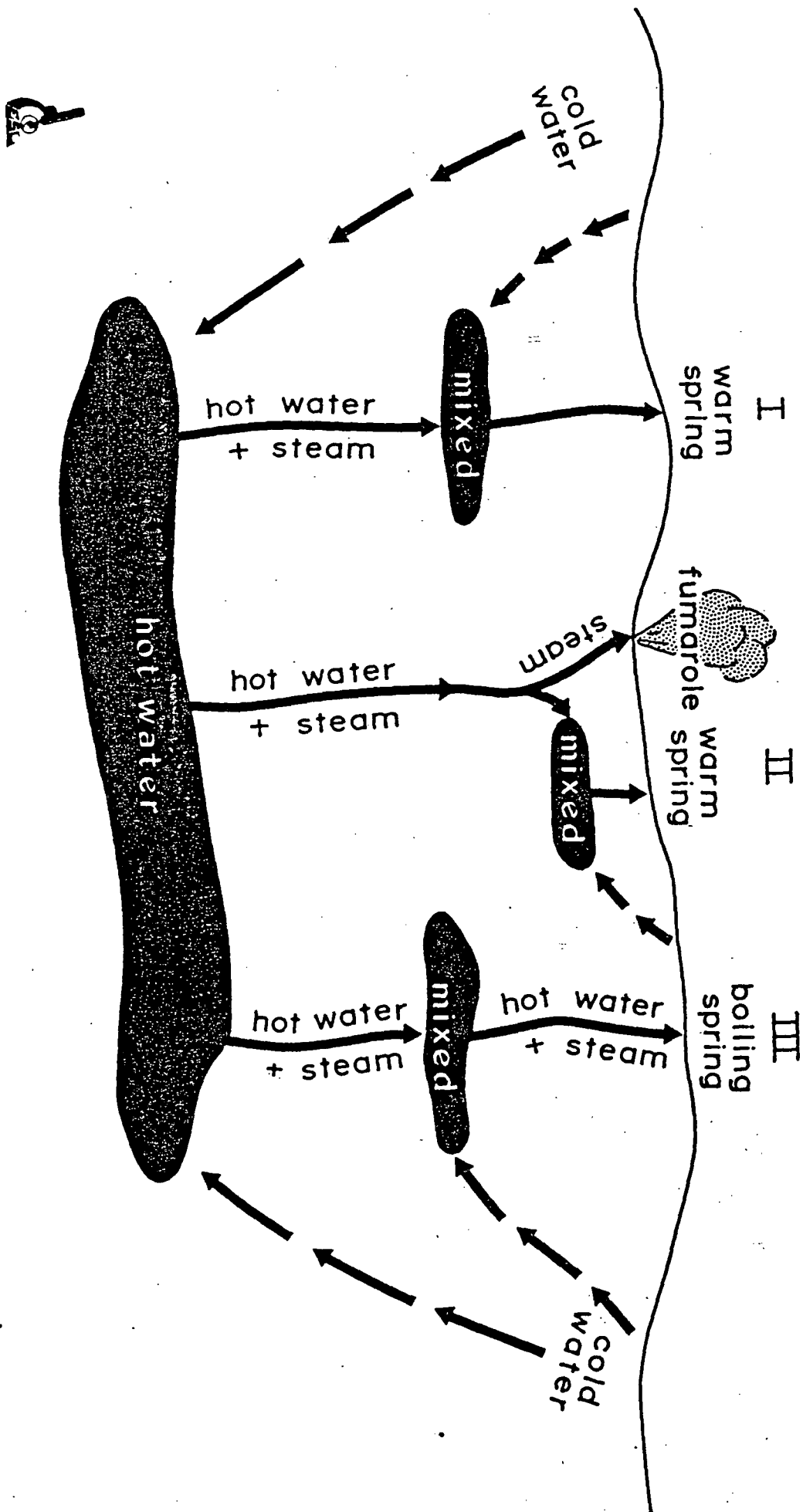
Cation Exchange:



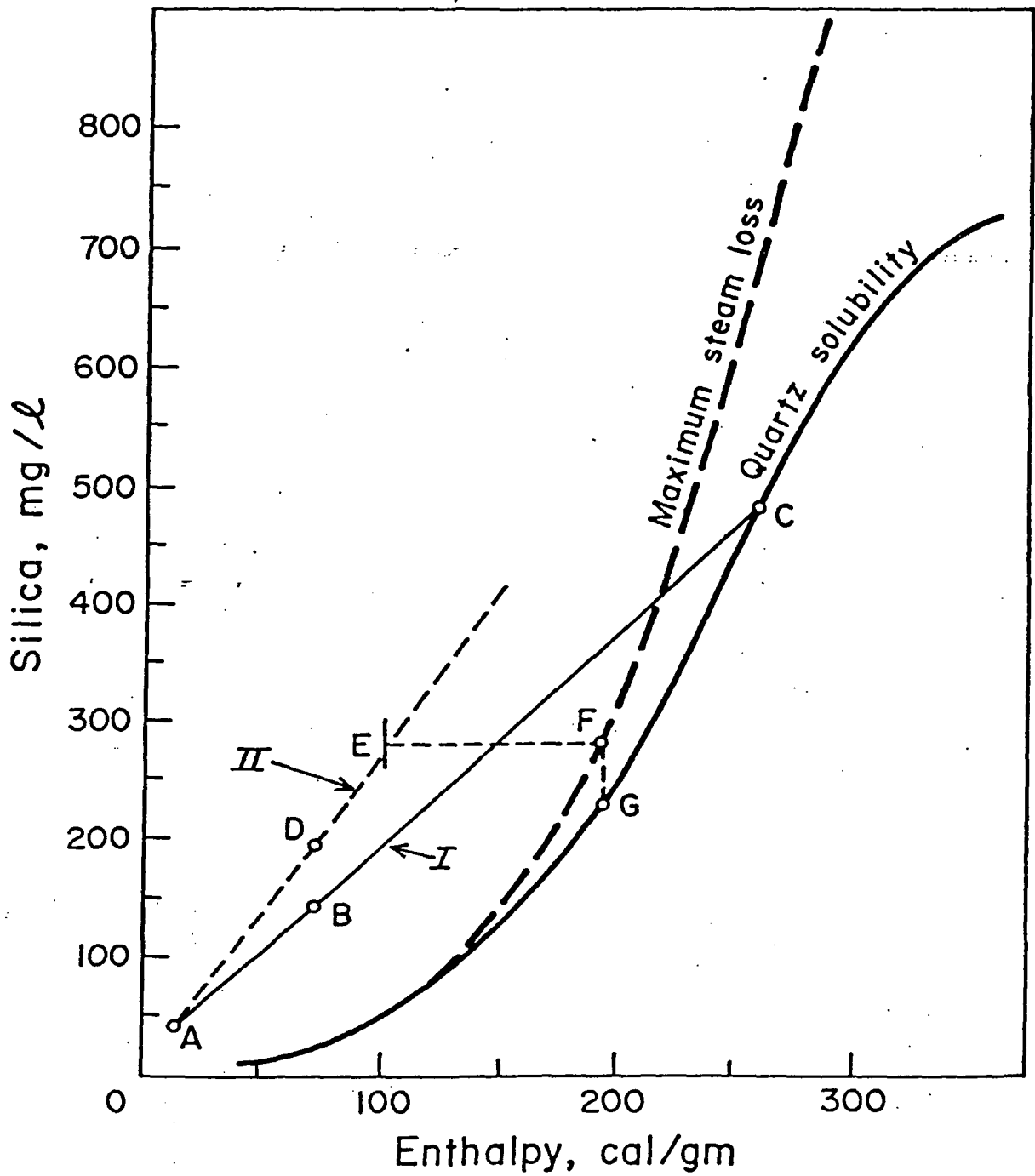


(CAPUANO, 1981)

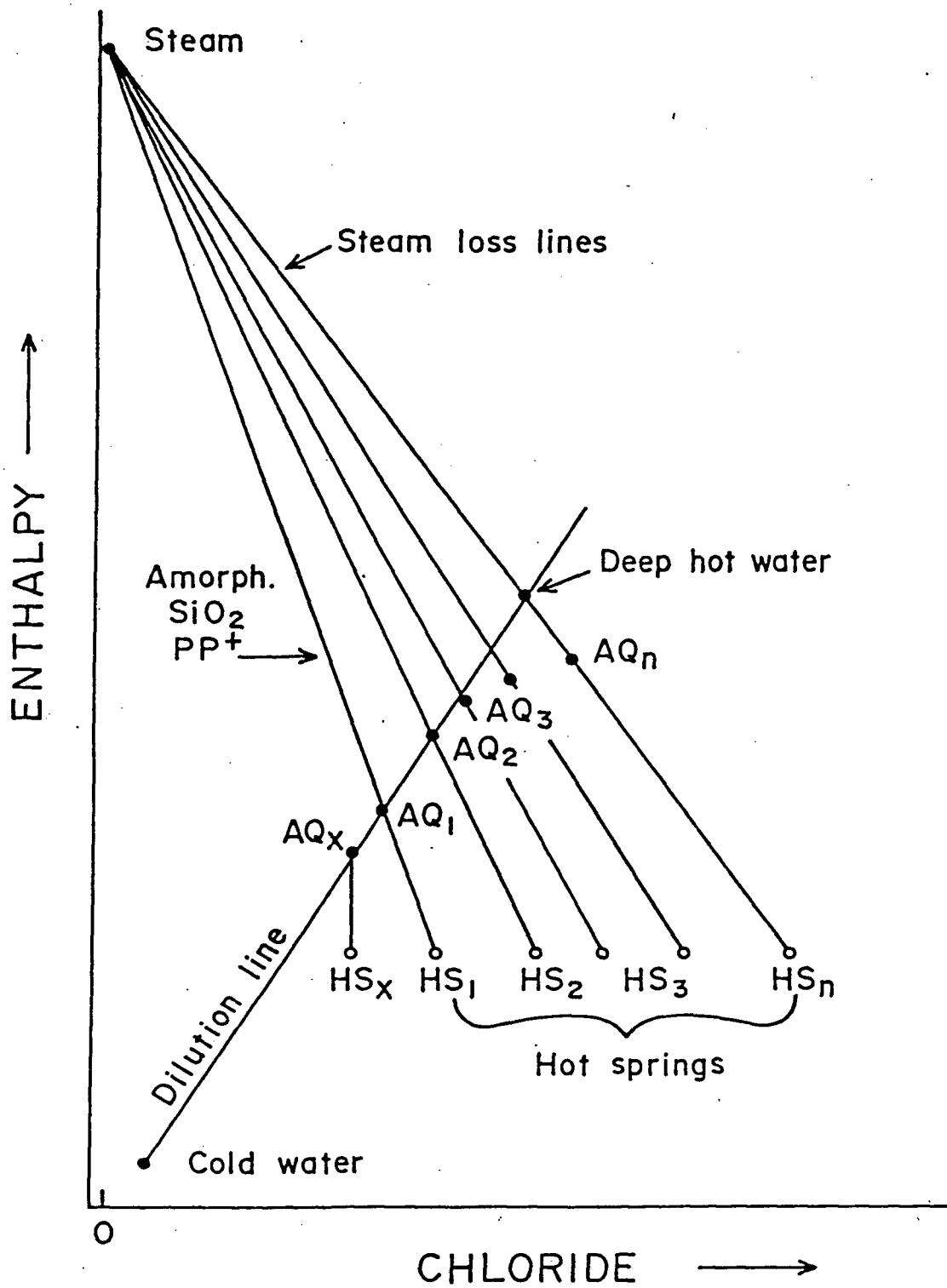
MIXING MODELS

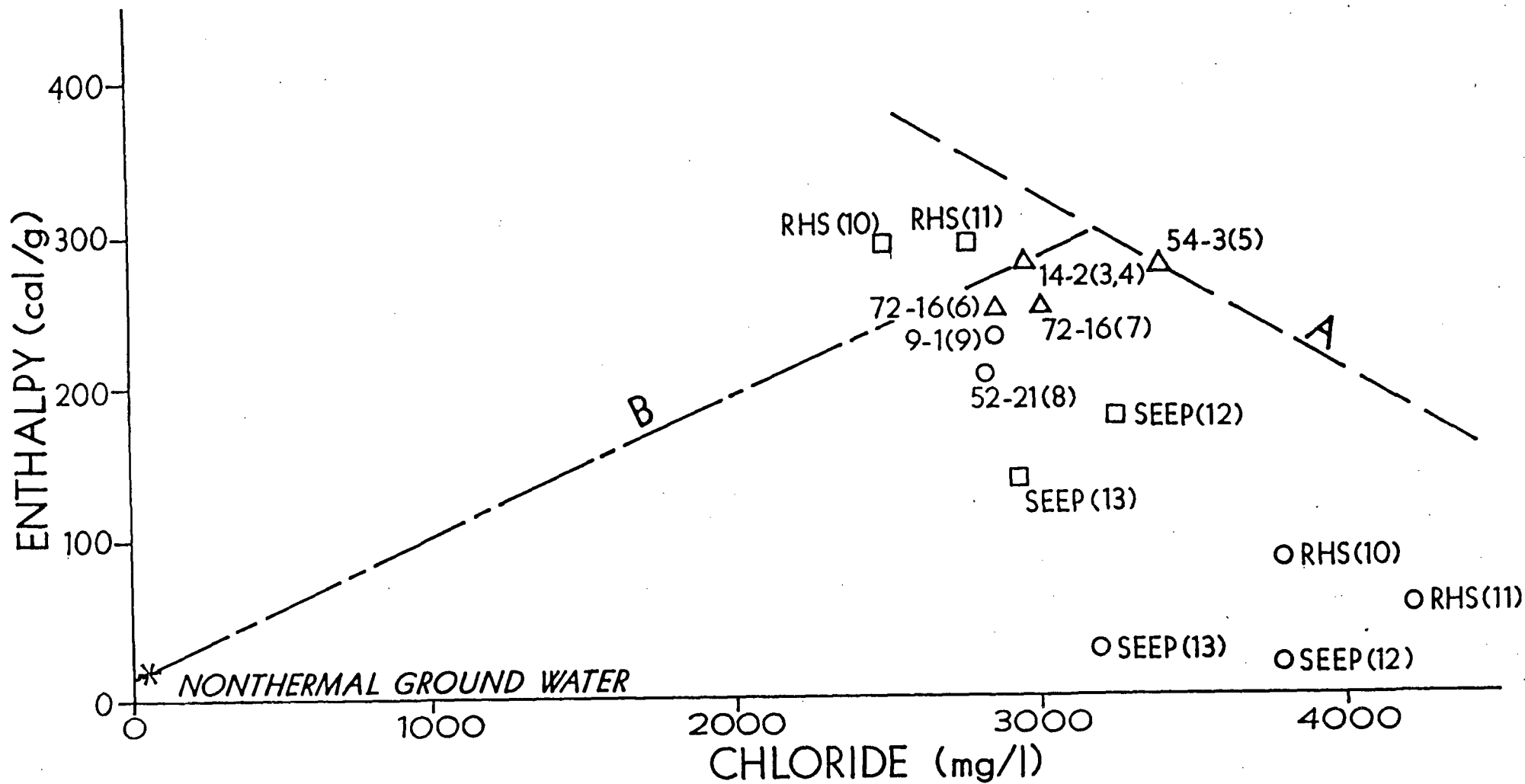


MIXING MODELS FOR WARM SPRINGS

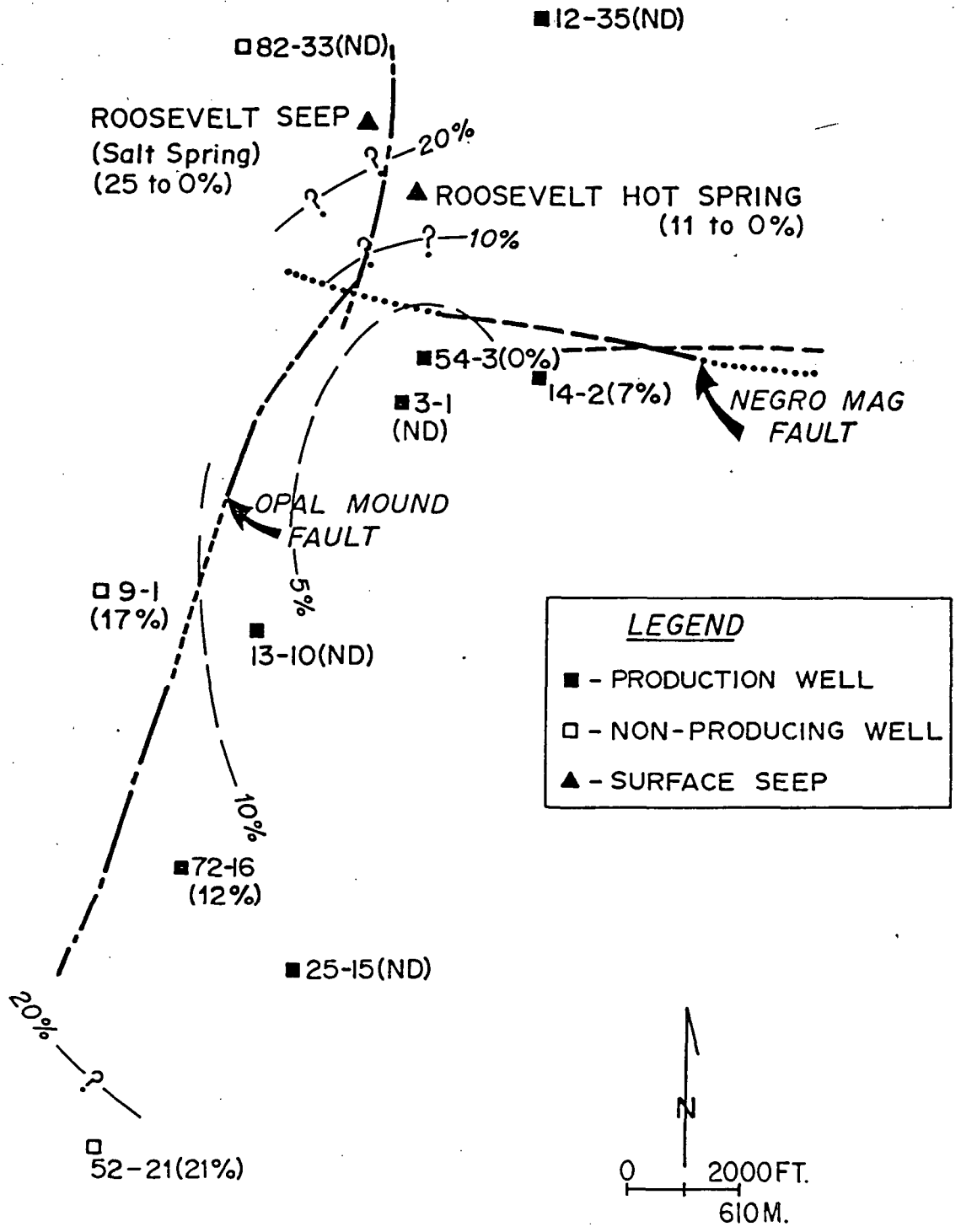


III Mixing model for boiling hot springs.



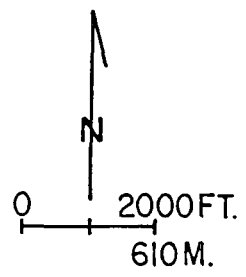


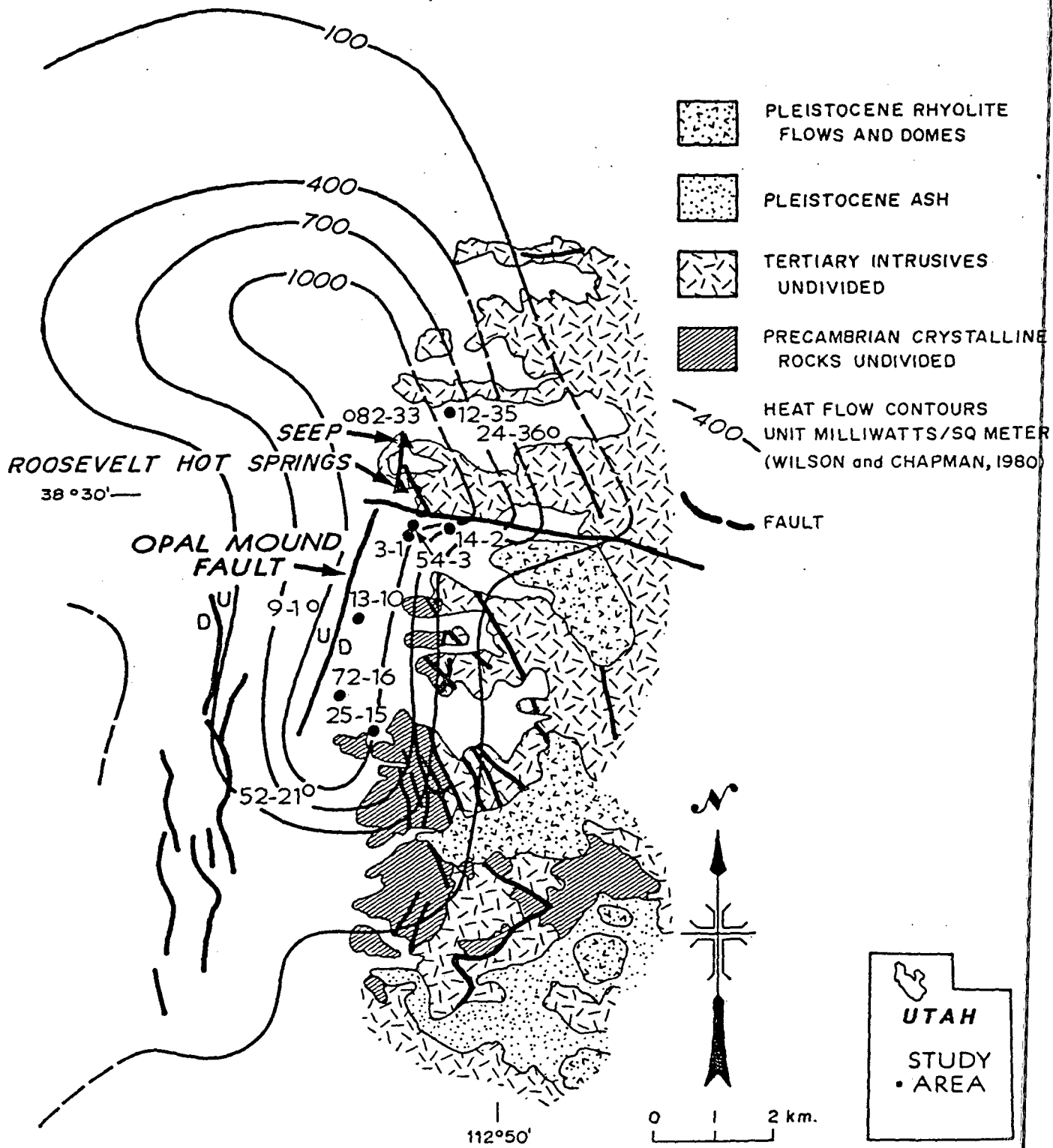
T26S
T27S



LEGEND

- - PRODUCTION WELL
- - NON-PRODUCING WELL
- ▲ - SURFACE SEEP





CAPUANO AND COLE, 1982

- Barnes, H. L., 1979, Solubility of Ore Minerals, in H. L. Barnes ed., Geochemistry of Hydrothermal Ore Deposits, John Wiley and Sons, N.Y., p. 404-460.
- Capuano, R. M., 1982, Depositional environments of trace elements in soils over an active hydrothermal system, Roosevelt Hot Springs, Utah: Geol. Soc. Am. Annual Meeting Abs., v. 14, no. 7, p. 459.
- Capuano, R. M., 1982, Fluid-mineral equilibria in a hydrothermal system, Roosevelt Hot Springs, Utah: Geochim. Cosmochim. Acta.
- Capuano, R. M., 1981, Water chemistry as an aid in reconnaissance exploration for a low-temperature geothermal system, Artesian City Area, Idaho: Geothermal Resources Council Transactions, v. 5, p. 59-62.
- Capuano, R. M., and Cole, D. R., 1982, Fluid-mineral equilibria in a hydrothermal system, Roosevelt Hot Springs, Utah: Geochim. Cosmochim. Acta, v. 46, no. 8, p. 1353-1364.
- Cole, D. R., 1982, Tracing fluid sources in a complex geothermal-groundwater regime: application of stable isotopes to the East Shore Area, Utah: Ground Water J., v. 20, p. 586-593.
- Cole, D. R., 1980, Mechanisms and rates of stable isotopic exchange in hydrothermal rock-water systems: Ph.D. Thesis, the Pennsylvania State University, 255 p.
- D'Amore, F. and Panichi, C., 1980, Evaluation of deep temperatures of hydrothermal systems by a new gas geothermometer: Geochim. Cosmochim. Acta, v. 44, p. 549-556.
- Drummond, S. E., Jr., 1981, Boiling and mixing of hydrothermal fluids: Chemical effects on mineral precipitation: Ph.D. dissertation, Dept. of Geosciences, Pennsylvania State University, 380 p.
- Ellis, A. J., 1979, Explored geothermal systems, in H. L. Barnes ed., Geochemistry of Hydrothermal Ore Deposits, John Wiley and Sons, N.Y., p. 632-683.
- Ellis, A. J., and Mahon, W. A. J., 1977, Chemistry and Geothermal Systems: Academic Press, N.Y., 392 p.
- Fouillac, C., and Michard, G., 1981, Sodium/lithium ratio in water applied to geothermometry of geothermal reservoirs: Geothermics, v. 10, p. 55-70.
- Fournier, R. O., 1981, Application of water chemistry to geothermal exploration and reservoir engineering, in L. Rybach and L. J. P. Muffler: Geothermal Systems: Principles and Case Histories, John Wiley and Sons, N.Y., p. 109-144.
- Fournier, R. O., and Potter, R. W., II, 1979, Magnesium correction to the Na-K-Ca chemical geothermometer: Geochim. Cosmochim. Acta, v. 43, p. 1543-1550.

- Fournier, R. O., and Truesdell, A. H., 1970, Chemical indicators of subsurface temperature applied to hot waters of Yellowstone National Park, Wyoming, USA, Geothermics, Spec. Issue Δ2, 529-535.
- Garrels, R. M., and Christ, C. L., 1965, Solutions, Minerals and Equilibria: Freeman Cooper Co., San Francisco, Calif., 450 p.
- Haas, J. L., 1971, The effect of salinity on the maximum thermal gradient of a hydrothermal system at hydrostatic pressure: Econ. Geol., v. 66, p. 940-946.
- Hem, J. D., 1970, Study and interpretation of the chemical characteristics of natural water, 2nd edition: U.S. Geol. Surv. Water-Supply Paper 1473, p. 363.
- Henley, R. W., and Ellis, A. J., 1982, Geothermal systems ancient and modern: a geochemical review: Earth Science Review, in press, 50 p.
- Hoefs, J., 1981, Stable Isotope Geochemistry, Springer Verlag.
- Holland, H. D., and Malinin, S. D., 1979, The solubility and occurrence of non-ore minerals, in H. L. Barnes ed., Geochemistry of Hydrothermal Ore Deposits, John Wiley and Sons, N.Y., p. 461-508.
- Knight, J. E., 1977, A thermochemical study of alunite, enargite, luzonite and tennantite deposits: Econ. Geol., v. 72, p. 1321-1336.
- Mahon, W. A. J., Klyen, L. E., and Rhode, M., 1980, Neutral sodium/bicarbonate/sulphate hot waters in geothermal systems: J. Japan Geothermal Energy Assoc., vol. 17, no. 1, p. 11-24.
- Mahon, W. A. J., McDowell, G. D., and Finlayson, J. B., 1980, Carbon dioxide: its role in geothermal systems: N.Z.J. Sci., v. 23, p. 133-148.
- Nehring, N. L., and Truesdell, A. H., 1978, Collection of chemical, isotope and gas samples from geothermal wells: Proceedings, Second Workshop on Sampling Geothermal Effluents, Las Vegas, 1977, Environmental Protection Agency Rept., EPA-60017-78-121, p. 130-140.
- Paces, T., 1975, A systematic deviation from Na-K-Ca geothermometer below 75°C and above 10^{-4} atm p_{CO_2} : Geochim. Cosmochim. Acta, v. 39, p. 54-544.
- Paramentier, P. P., and Hayashi, M., 1981, Geologic model of the "vapor-dominated" reservoir in Yunotani geothermal field, Kyushu, Japan: Geothermal Resources Council, Transactions, v. 5, p. 201-4.
- Pearson, F. J., Jr., and Truesdell, A. H., 1978, Tritium in the waters of Yellowstone National Park: R. E. Zartman, ed., Fourth Int. Conf. Geochronology, Cosmochronology and Isotope Geology, 1978, U.S.G.S. Open File Report 78-701, p. 327-329.
- Piper, A. M., 1944, A graphic procedure in the geochemical interpretation of water-analyses: Transactions, Am. Geophysical Union, v. 25, p. 914-923.

- Ragnarsdottir, K. V., and Walther, J. V., 1983, Pressure sensitive "silica geothermometer" determined from quartz solubility experiments at 250°C: *Geochim. Cosmochim. Acta*, v. 47, p. 941-946.
- Robertson, D. E., Fruchter, J. S., Ludwick, J. D., Wilkerson, C. L., Crecelius, E. A., and Evans, J. C., 1978, Chemical characterization of gases and volatile heavy metals in geothermal effluents: *Geoth. Res. Council, TRANS.*, v. 2, p. 579-582.
- Rose, A. W., and Burt, D. M., 1979, Hydrothermal alteration, in H. L. Barnes ed., *Geochemistry of Hydrothermal Ore Deposits*, John Wiley and Sons, N.Y., p. 173-235.
- Schoen, R., White, D. E., and Hemley, J. J., 1974, Argillization by descending acid at Steamboat Springs, Nevada: *Clays and Clay Min.*, v. 22, p. 1-22.
- Shanks, W. C., and Bischoff, J. L., 1977, Ore transport and deposition in the Red Sea geothermal system: a geochemical model: *Geochim. Cosmochim. Acta.*, v. 41, p. 1507-1519.
- Struhsacker, E. M., Smith, C., and Capuano, R. M., 1983, An evaluation of exploration methods for low-temperature geothermal systems in the Artesian City area, Idaho: *Geol. Soc. Am. Bull.*, v. 94, p. 58-79.
- Taylor, H. P., 1974, The application of oxygen and hydrogen isotope studies to problems of hydrothermal alteration and ore deposition: *Econ. Geol.*, v. 69, p. 843-883.
- Truesdell, A. H., 1974, Chemical evidence of subsurface structure and fluid flow in geothermal systems: in *First Symposium on Water-Rock Interaction*, Prague, Czech., p. 250-259.
- Truesdell, A. H., and Fournier, R. O., 1976, Calculation of deep temperatures in geothermal systems from the chemistry of boiling spring waters of mixed origin: *2nd U.N. Symposium on the development and utilization of geothermal resources*, San Francisco, 1975, vol. 1, p. 837-844.

GUIDE TO WATER SAMPLING

by

Ruth L. Kroneman

January, 1981

Earth Science Laboratory
University of Utah Research Institute
420 Chipeta Way, Suite 120
Salt Lake City, Utah 84108

Guide to Water Sampling

Introduction

The stability of natural water with respect to dissolved species has been the source of many publications and much study. No one method of sampling or sample handling is ideal for all types of water or analytical schemes. This guide is written with a two-fold purpose: one is to give a general understanding of the problems involved in collecting and preserving water samples; the second is to specify the treatment of samples necessary for analysis by the Earth Science Laboratory. Because of our instrument capability (an Inductively Coupled Plasma Emission Spectrograph with a 37 element array), our requirements are somewhat different from laboratories with only atomic absorption and UV-visible spectrophotometers.

Many factors affect solubility. Perhaps the two most important factors influencing gas solubility are temperature and pressure. Since it is difficult to maintain either of these conditions after the samples are collected, it is imperative to analyze for dissolved gasses at the time of collection. Mineral solubilities are affected primarily by pH, temperature, and concentrations of other dissolved species. Some of the dissolved elements and ions can be stabilized after filtration. The addition of acid is commonly used to prevent precipitation of sulfate and metals.

Collection and Sample Preservation

Cleanliness of equipment and storage bottles is very important. In the field, equipment that must be reused should be rinsed immediately after use with demineralized or distilled water. If sample water dries on the equipment or containers, they must be acid washed prior to reuse. Sample bottles (polyethylene or polypropylene) must be soaked for at least 2 hours, preferably overnight, in 20% HNO_3 then rinsed 3 times with demineralized water. After draining (dry or nearly dry), bottles should be capped tightly to prevent recontamination. This procedure must be followed for new as well as reused bottles. Polyseal caps, which provide a good airtight seal, cannot be soaked in acid but should be washed briefly in an acid bath and immediately rinsed several times with demineralized water. Molded polypropylene caps may be used if they give an airtight seal; this can be checked by capping an empty bottle and squeezing to check for air leakage. Polypropylene caps should be cleaned in the same manner as bottles. Contamination, particularly with Na, K, Ca or trace metals may occur if this procedure is not followed. Contamination may result as well if any sample collection or handling equipment is made of metal.

It should be decided prior to sample collection what analyses are needed. If these analyses include some which must be done immediately, field procedures or test kits should be acquired. These should always be tried in a laboratory prior to field use. Hach Chemical Co., Ames, Iowa makes a number of field kits, most of which are adequate. However, it is wise to try all kits or procedures on accurately prepared standards or known water samples. The expected range of sample concentrations should be tested. As an example,

the Hach alkalinity test kit gives instructions for two ranges. The kit instructions do not give an alkalinity figure at which the low-range test should be used. Assuming a possible error of one drop, it becomes apparent that a 10% error (1 grain/gallon) is likely at 10 grains/gallon, with the error increasing as alkalinity decreases. To minimize this error the low range (15 ml) procedure should be used for 10 grains/gallon or less. A one-drop error is then reduced to 0.4 grains/gallon. It is also wise to check the accuracy of volumes used in measuring devices.

If accurate temperature measurement is important, be certain the thermometer is accurate by checking all thermometers in the laboratory. Even mercury thermometers are not necessarily accurate. Do not use a "total immersion" thermometer for "partial immersion" application. If hot waters are to be sampled, a maximum indicating thermometer is usually necessary. A digital thermometer may be a good investment.

Accurate pH measurement is often difficult to obtain. An adequate understanding of your pH meter requires reading the manufacturer's instructions. A meter and electrode in good condition should not change (need calibration adjustment) by more than a few hundredths of a pH unit if checked over several days. Calibration should be done with 2 buffers. Nearly all meters have a calibration adjustment and a slope adjustment. Always use pH 7 buffer to adjust the calibration knob. Slope adjustment is done with a second pH standard, usually pH 4 or 10. Notice the drift before a stable pH is reached with the buffer solution. This drift is usually more lengthy in natural waters. The electrode should be rinsed with demineralized water and blotted dry before immersing in the buffer. A hydrous silica layer on the

glass sensing tip is necessary for proper operation and it can be damaged or destroyed by dry storage. Always fill the electrode end cap before putting it on the electrode. Water, KCl solution or pH 7 buffer may be used.

Filtration of water samples is normally done with 0.45 micron pore size filter. This may be very difficult if the water contains a considerable volume of suspended solids. Prefiltration with a coarser filter (5 or 1 micron) may be necessary. Filtration can be done with either vacuum or pressure. Vacuum filtration will usually degas the sample and may (especially if the sample is hot or muddy) concentrate the dissolved minerals due to evaporation. Pressure filtration may introduce O_2 or CO_2 from the air but is less likely to change the sample composition appreciably. Pressure filtration is therefore recommended, especially for alkalinity determination. The simplest apparatus is a large (50 to 100 cc) plastic syringe with a swinnex filter holder, available from most laboratory supply houses. Larger plexiglass pressure filters can be machined or purchased. These can use a valved rubber bulb, a tire pump, cylinder gas (N_2 or Ar) or a peristaltic pump for pressure.

Since there is some degree of uncertainty in all analytical procedures, it is a good practice to submit an occasional blind duplicate sample (same sample with different number or name designation). This gives a good indication of the quality of analytical work you are getting. Field procedures should also be repeated to test their repeatability.

Sampling Procedure

Instruction	Reason
1. Assemble filtering apparatus, test equipment, sampling container, storage bottles, etc. Calibrate pH meter. If water is pumped, allow time for the pump to flush before sampling.	Rapid handling & testing of water sample minimizes changes in composition.
2. If possible, measure pH and temperature in the spring, stream or other water source.	Changes caused by sampling are avoided.
3. Fill sample collection container with water sample, then discard.	To prevent contamination (from previous sample or any foreign material which might have gotten in the container) or dilution with residual distilled water.
4. To remove particulate matter, filter (pressure if possible) sufficient sample to fill necessary sample bottles, filling & capping bottles as quickly as possible. <u>SAMPLES MUST BE VISIBLY CLEAR</u> ; if not, check filter membrane and apparatus. Unclear samples must be refiltered <u>prior</u> to acidification. The following splits should be taken depending upon the analyses required.	Acidification of unfiltered water may dissolve particulate material. This would change water composition. Particulates also interfere with analyses (ICP, SO ₄ , TDS).
a) 60 ml (2 oz) acidified to 20% with reagent grade HNO ₃ <u>for ICP analysis</u> . This includes <u>37 elements</u> . See appendix A. This is most easily done by measuring the true volume of the bottle in the lab and adding the measured amount of acid to the clean bottle. The bottle is then filled with filtered water at the sample location - full, but not overflowing.	This acid concentration has a two-fold purpose. (1) Both major cations including SiO ₂ and trace metals remain in solution with no apparent degradation of sample for a month or more. (2) This matrix matches the matrix of calibration solutions for the ICP and is necessary for accurate analysis.
We strongly recommend the use of variable volume dispenser bottles for acid addition. This is fast & repeatable. Please submit a sample of the HNO ₃ for blank determination (60 ml conc.). If acid in bottle is discolored, discard.	

b) 500 ml (8 oz) acidified to 1% with concentrated HCL. This split is used for SO₄ analysis. Acid can be added to bottles in the lab as done for split a. This bottle is also filled full but not overflowing with filtered H₂O.

1% HCL prevents SO₄ precipitation and is useful for gravimetric determination.

c) 500 ml (8 oz) filtered with no additive. This split is used for TDS, Cl, and F determinations.

Any additives would interfere with analysis.

This split may not be stable. If possible, it should be kept close to the temperature of the water at its source and delivered to ESL as soon as possible.

Since solubilities are affected by temperature, cold waters should be kept cold (an ice chest) but hot waters should not be refrigerated.

5. If isotope determination is required, a glass bottle of unfiltered, untreated sample should be collected.

Filtering may reduce isotope fractionation across the paper.

6. Collect additional sample for any field analyses necessary, i.e., alkalinity (pressure filtered only), dissolved O₂, H₂S, etc.

Carbonate mineral particles may react with alkalinity titration acid. CO₂ may be lost during vacuum filtration.

These analyses should be done as quickly as possible.

Samples may degas very rapidly.

7. Rinse all equipment in demineralized H₂O. A minimum of a squeeze bottle can be carried to sample location.

This prevents sample drying on equipment. Dried water residue may contaminate the next sample.

8. Check to be sure field notes and sample labels are accurate. Site location on topographic map or areal photo is best. Be sure acidified samples are labeled.

Acknowledgements

Critical reviews of this manuscript by Dave Cole, Odin Christensen, Joe Moore and Riki Darling are appreciated.

Funding for this project is from Department of Energy, Division of Geothermal Energy under contract number DE-AC07-80ID12079.

APPENDIX A

ELEMENTS AND DETECTION LIMITS

ELEMENT	CONCENTRATION (PPM)
Na	1.25
K	2.5
Ca	0.25
Mg	0.5
Fe	0.025
Al	0.625
Si	0.25
Ti	0.125
P	0.625
Sr	0.013
Ba	0.625
V	1.25
Cr	0.05
Mn	0.25
Co	0.025
Ni	0.125
Cu	0.063
Mo	1.25
Pb	0.25
Zn	0.125
Cd	0.063
Ag	0.05
Au	0.1
As	0.625
Sb	0.75
Bi	2.5
U	6.25
Te	1.25
Sn	0.125
W	0.125
Li	0.05
Be	0.005
B	0.125
Zr	0.125
La	0.125
Ce	0.25
Th	2.5

APPENDIX B

POSSIBLE INFORMATION SUPPLIED BY GEOCHEMICAL FLUID STUDIES

- I Range in composition and homogeneity of hot fluids in overall system.
- II Subsurface temperatures and pressure.
- III Type of system: vapor vs. liquid dominated.
- IV Subsurface alteration associated with the fluids.
- V Origin of hot fluids, direction of fluid flow, turnover time of the fluid, and permeability.
- VI Mineral deposition potential of the fluid (scaling problems likely to be encountered).
- VII Natural heat flow.
- VIII Zones of upflow permeability.
- IX Fluid constituents which could have economic value (metal recovery).
- X Feasibility of reinjecting the fluid back into the system to eliminate local thermal and chemical pollution.

APPENDIX C

ACCURACY CHECKS

- I. CALCULATE THE CATION - ANION BALANCE.

TOTAL CATIONS EQUALS TOTAL ANIONS IN MEQ/ L

- II. ASSUME THAT THE WATER DOES NOT CONTAIN UNDETERMINED SPECIES WHICH CAN PARTICIPATE IN THE BALANCE, AND THAT THE FORMULA AND CHARGE OF ALL ANIONS AND CATIONS ARE KNOWN.

FOR MODERATE CONCENTRATIONS (250 - 1000 mg/l) ERROR = 1 to 2%
FOR CONCENTRATIONS LESS THAN 250 OR GREATER THAN 1000 mg/l,
ERROR = 2 to 10%.

- III. COMPARE TDS (CALCULATED) WITH THE TDS (MEASURED), THEY SHOULD AGREE TO WITHIN A FEW MG/L.

HYDROTHERMAL ALTERATION

8.0 ALTERATION AND METAMORPHISM

8.1 Introduction

The mineralogy and often the bulk composition of rocks changes in response to pressure and temperature as well as the catalyzing effects of fluids. These changes are attempts of the rocks to re-equilibrate under sets of conditions which are different than those under which they formed. Although most silicate phases show broad ranges of stabilities when they are by themselves, the presence of an additional phase or the presence of a fluid will cause them to react under much lower temperatures. The kinetics of mineral reactions are such that prograde reactions are more rapid and complete than retrograde reactions.

Alteration reactions are presently taking place in most active geothermal systems. These reactions are not only of interest from the scientific standpoint, they may be of great importance from the commercial aspects of production and evaluation. For instance, mineral phases which are indicative of temperature can be used to cross-check temperature readings from well logs. Production, and particularly injection, may cause mineral assemblages and permeability to change affecting field production. The oil and gas industry has recently been very interested in using mineral indicators of temperature to document the maturation history of potential petroleum source beds. The metals exploration industry has long recognized the importance of alteration assemblages as guides to mineralization.

In this work we will be interested in a broad spectrum of alteration and metamorphism, extending from contact metamorphism in the vicinity of shallow igneous bodies, through the reactions characterized by rock and hot fluids in

both active and fossil hydrothermal systems, to acid alteration above the water table in the vicinity of both active and fossil hydrothermal systems. We will also give some additional consideration to the alteration of volcanic glass in low-temperature groundwater and surface water environments.

Metamorphism in the vicinity of plutons is often relatively simple, involving only small volumes of fluids. The reactions are mineral transformations induced by the temperature gradient surrounding the intrusive. When fluids are present in only small amounts, the reaction can often be considered isochemical in that the minerals present in the rock change but the bulk composition remains essentially the same.

8.4 Processes in Active Hydrothermal Systems

8.4.1 Clay Minerals

Clay minerals are very sensitive indications of conditions of maximum temperature in younger (Tertiary) rock sequences. Clays can be divided into a number of groups, the most important of which are kandites (kaolinite) illites, smectites, and vermiculites. These groups have characteristic basal spacings of 7\AA , 10\AA , 15\AA , and 14.5\AA respectively.

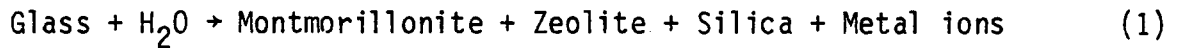
The kandites or kaolinite group has the chemical composition $\text{Al}_2\text{Si}_2\text{O}_5(\text{OH})_4$ with some variation in the replacement of aluminum by ferric iron (Brindley, 1981). The members of this group include kaolinite, dickite, nacrite, halloysite and meta-halloysite. Clays of this group are generally formed by the alteration of alumino-silicates either by hydrothermal or weathering processes. In active hydrothermal systems, the minerals are characteristic of highly acid conditions associated with alteration above a boiling geothermal system.

The illite group is composed of the minerals illite, phengite, glauconite, and celadonite. Illites have a structure which is very similar to micas and the term illite is often applied to all clay-grade micas. Deer et al (1966) give the chemical formula of illite as $K_{1-1.5}Al_4[Si_{7-6.5}Al]_{1-1.5}O_{20}(OH)_4$. However, as we will discuss shortly, natural illites are often interstratified with smectite. Illites are the dominant clay minerals in sediments and increase in abundance with the age of the sedimentary sequence and with increase in grade of metamorphism. They are also common products of hydrothermal alteration.

Glauconite is generally confined to sedimentary sequences, and, at times, makes up a large percentage of the rock type. Celadonite $(K(MgFe^{3+})Si_4O_{10}(OH)_2$ is commonly formed from the alteration of volcanic rocks. The color is not unlike that of malachite with which it is often confused.

Smectites are a group which includes montmorillonite, nontronite, hectorite, saponite, and sanconite. These are "swelling clays" which are able to absorb water or organic material between their structural layers. They are also well known for their cation exchange capacity.

Smectites are very common alteration products of volcanic rocks. The alteration does not necessarily involve high temperature fluids as evidenced by the widespread distribution of bentonites. These rocks contain significant amounts of montmorillonites and are generally believed to have been formed by the alteration of volcanic ash. Slaughter and Earley (1965) have proposed that the reaction for the formation of montmorillonite from volcanic glass could be summarized as follows



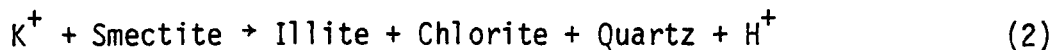
They feel that the critical step in the breakdown of glass is the extraction of cations. The pH of the water in the above reaction is important because it will cause the breakdown of the glass and govern the removal of Mg^{++} from the glass for the formation of montmorillonite. If the pH is low, the reaction will go to the right. Under alkaline conditions montmorillonite can form using Mg^{+2} from other sources such as sea water or alkaline lakes. Note that the above reaction also frees metals from the glass structure. This has often been cited as the source of uranium which later forms sandstone (role-front) uranium ore bodies.

Smectites are also found in the lower temperature ranges of hydrothermal activity. The upper portion of their stability range is somewhat variable, but can extend from 70°C (Heling, 1974) to 150°C (Elders et al, 1978). Eberl et al (1978) have suggested that although montmorillonite will form mixed layer clays with depth, trioctahedral smectites may be stable into much higher temperature ranges.

Vermiculite has the general composition of $(\text{Mg}, \text{Ca})_{.7}(\text{Mg}, \text{Fe}^{+3}, \text{Al})_6[(\text{Al}, \text{Si})_8\text{O}_{20}](\text{OH})_4 \cdot 8\text{H}_2\text{O}$. It is often found as a weathering or hydrothermal alteration product of biotite. It has been found in some of the higher temperature portions of geothermal fields.

Many clays have the characteristic of forming mixed-layer aggregates. One of the most common and widely researched is the illite-smectite (I/S) mixed layer clay (Reynolds and Hower, 1970). This mineral changes its composition and also ordering as a function of temperature and pressure and is thus widely used in the petroleum industry as an indication of the maturity of

potential petroleum source rocks. With an increase in temperature the percentage of illite layers in the I/S clay increases. The precise reactions responsible for this transformation are still conjectural but probably a good simplification is.



(Boles and Franks, 1979). Hower (1981) gives evidence that in shale sequences the K^+ is derived from the breakdown of K-feldspar. In addition to an increase in the amount of illite with temperature, ordering also increases. Hower (1981a) presents Table 8-1 which shows how ordering changes with increase in temperatures and also increase in the percent illite in the mixed layer clay. The thermal stability range of I/S and some other minerals from shale sequences are shown in Fig. 8-1.

8.4.2 Mineral Precipitation

One important characteristic of liquid-dominated hydrothermal systems is their ability to precipitate solids. This is commonly seen at the surface as deposits of sinter which may be either carbonate (travertine) or siliceous. It is also important at depth where the precipitation of solids from solution decreases the permeability of fluid pathways. This process is commonly referred to as 'self sealing', and many workers conceptualize liquid-dominated systems as possessing a 'sealing cap' or 'self-sealed zone' (Facca and Tonani, 1967; White et al, 1975; Elders and Bird, 1976).

In the self-sealing process, as well as the precipitation of sinters on the surface, silica and calcium carbonate are the principal phases involved. Figure 8-2 shows the solubility of SiO_2 species in water as a function of temperature. The solubility of SiO_2 increases with an increase in

Table 8-1 Compositional dependence of manner of interstratification of illite/smectite (Hower, 1981b)

	I/S Composition	Number of illite layers between each smectite	I/S Type
Low T	0~60% illite	≥ 0	random I/S
	~65-70~85% illite	≥ 1	"allevardite ordered" I/S
+			
High T	~85~100% illite	≥ 3 or more	"Kalkberg ordered" I/S

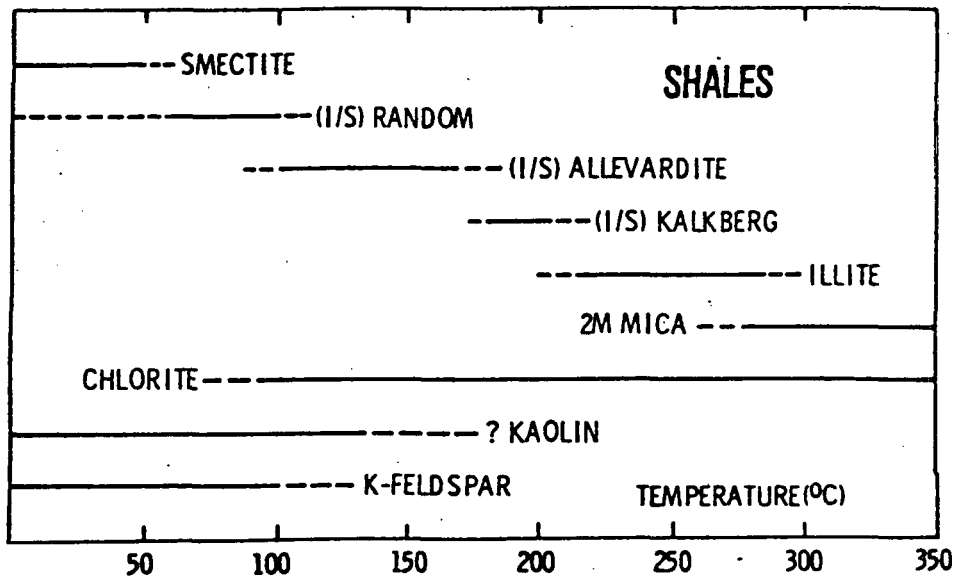


Fig. 8-1 Mineral diagenetic sequence in shales (Hower, 1981b).

temperature. Pressure has very little effect on this solubility relationship.

It has been determined empirically that hot springs which are depositing silica have base temperatures which are greater than 180°C (Renner et al, 1975). Keith et al (1978) have documented that fresh sinter is precipitated as amorphous opal. This can grade into beta-cristobalite without solution and redeposition. There is probably also continuous ordering to alpha-cristobalite but this phase is often not present. The conversion of cristobalite to chalcedony or quartz probably requires solution and redeposition. This was also the conclusion of Murata and Larson (1975) from their studies on the diagenesis of siliceous shales.

Figure 8-2 would suggest that hot springs should precipitate quartz or cristobalite in preference to the more soluble amorphous silica. Both White et al (1956) and Murata and Larson (1975) have concluded that water only slightly supersaturated with respect to a particular silica phase will precipitate that phase to the exclusion of less soluble phases. Additional data on the nomenclature and identification of silica phases can be found in Jones and Segnit (1971) and Murata and Norman (1976).

Figure 8-3 is a solubility diagram for calcite in water as a function of temperature and P_{CO_2} . Calcite has a retrograde solubility, i.e., it is more soluble at low temperatures than at high temperatures. However, the solubility does increase rapidly with an increase in the partial pressure of carbon dioxide. Thus, as fluids which are saturated with calcium carbonate approach the surface $CaCO_3$ is deposited as a result of the loss of CO_2 rather than from cooling. Other carbonate species such as witherite ($BaCO_3$) and dolomite ($MgCO_3$), as well as sulfates such as anhydrite ($CaSO_4$), show solubility relationships similar to those of calcite (Holland and Malinin,

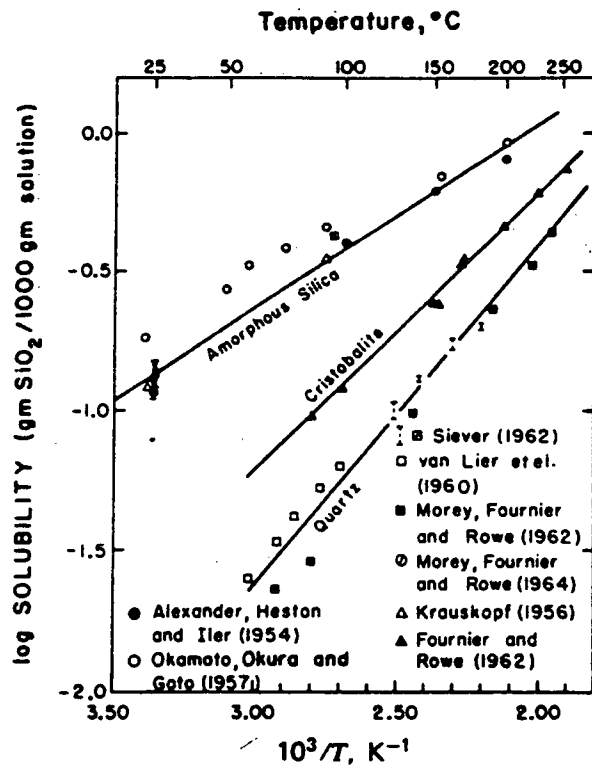


Fig. 8-2 Solubility of silica species in water as a function of temperature (Holland and Malinin, 1979).

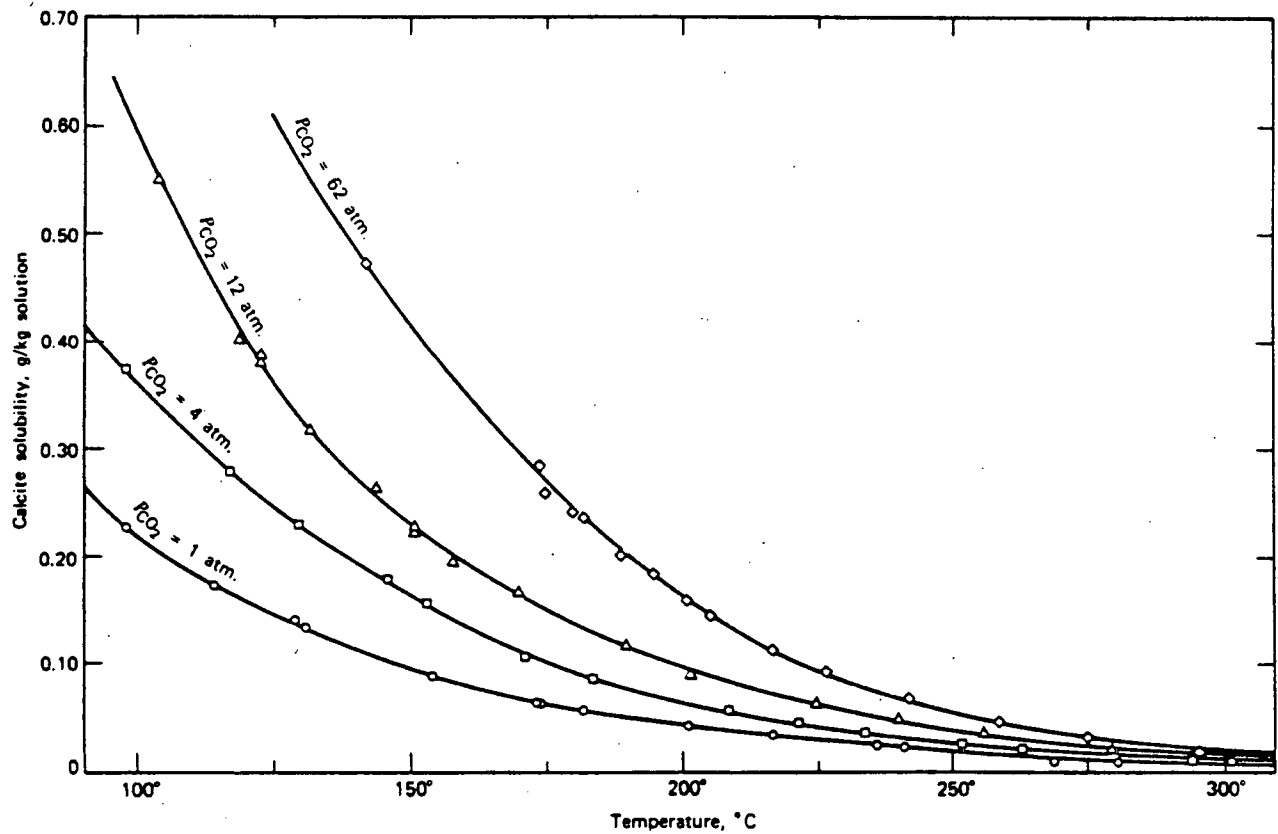


Fig. 8-3 Solubility of calcite in water as a function of temperature and P_{CO_2} (Holland and Malinin, 1979).

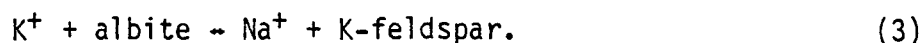
1979).

Other factors may, however, also affect the deposition of carbonates and sulfate minerals, such as variations in pH, total pressure and partial pressure of oxygen.

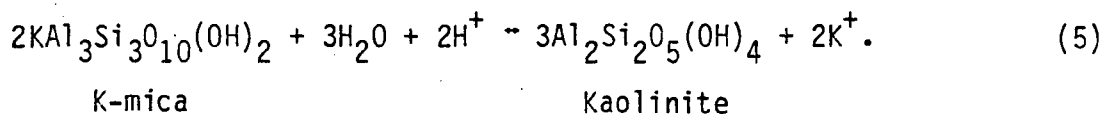
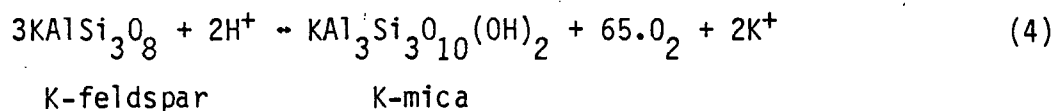
8.4.3 Water-Rock Reactions

As meteoric waters become heated in the earth, they begin to interact with the surrounding rock. As a result, both the chemistry of the water and the chemistry and mineralogy of the rock are changed. This chemical exchange is the basis of the chemical geothermometers which will be discussed elsewhere. We will largely be concerned here with the changes which take place within the wall rocks. Thermodynamic modeling of these alteration reactions has reached a high level of sophistication, and the reader is directed to Helgeson (1979) for a review.

When fluids react with their wall rocks, a large number of reactions take place simultaneously. In order to understand the changes taking place, we must consider systems which are somewhat limited, such as cation exchange reactions like



In addition, many alteration reactions involve hydration of silicate phase:



The above reactions define the probable mechanism for the formation of kaolinite under acid conditions. The rate controlling step in reactions of this type is often related to diffusional transfer of reactants through intermediate or final reaction products. Thus the factor of permeability and water-rock ratios enters the picture and will be discussed later in this chapter.

The above reactions can be generalized as follows



The path of the reaction is determined by an equilibrium constant

$$K = \frac{(X)^x (Y)^y}{(A)^a (B)^b} \quad (7)$$

where the parentheses represents the concentration of compounds in dilute quantities and activity in more concentrated form. Activity (a) represents the effective concentration of a species,

$$a = m\gamma \quad (8)$$

where m is the molality and γ is an activity coefficient which changes as a function of temperature. The concentration of a solid is 1, and thus for the reaction expressed in (3)

$$K = \frac{a_{Na^+}}{a_{K^+}} \quad (9)$$

The above relationships can be used to construct activity diagrams. The reader is directed toward work by Helgeson (1967) and Helgeson et al (1969) for a more detailed discussion of the construction of the diagrams. Figure

8-4 is an activity - activity diagram which shows that the system is in equilibrium with K-mica at temperatures of 260°C. With steam loss, the water composition changes along the indicated path through the K-feldspar stability field to albite. The change in the position of the Albite - K-feldspar - K-mica stability field with a change in temperature to 230°C is also shown.

8.4.4 Acid Sulfate Alteration

Rock alteration by descending acid sulfate solutions is common around both fossil and active hydrothermal systems. In fossil systems, this alteration is termed supergene and relies on the oxidation of sulfide species above the water table. The acid solutions derived through this process alter the enclosing rock on their descent to the water table, producing many of the same phases as does acid sulfate alteration above an active hydrothermal system.

Details of acid sulfate alteration above an active hydrothermal system have been presented by Schoen et al (1974) and the following is taken largely from their work. Acid is produced largely from hydrogen sulfide which is boiling off hydrothermal fluids. White et al (1974) state that the overall reaction is



An important factor in catalyzing this reaction is the presence of bacteria of the genus Thiobacillus.

In the alteration process, pH is the dominant controlling factor, followed by temperature and fluid composition. The acid component can contain carbonic, hydrochloric, and hydrofluoric acid, particularly in an active hydrothermal environment.

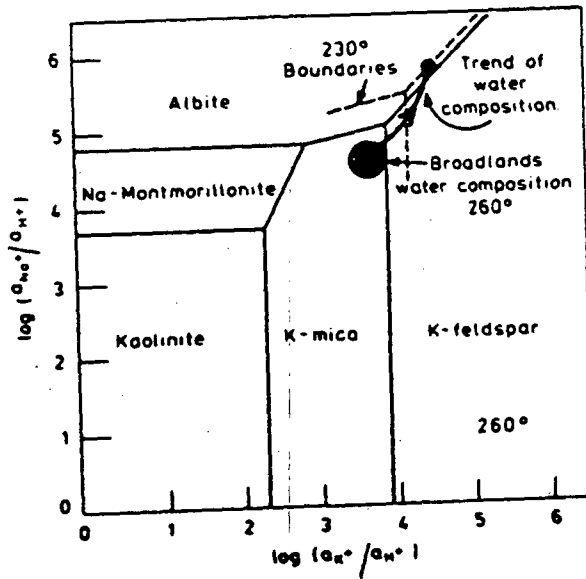


Fig. 8-4 Stability diagram for sodium and potassium minerals at 260°C in solid lines, and 230°C in broken lines (Browne and Ellis, 1970).

Rock permeability is also important in determining the location of the alteration process which is often initiated along fracture zones. In addition, the products of the acid alteration can create permeability barriers which can channel solutions laterally, and the local groundwater flow will exercise obvious controls on the distribution of the alteration zonation.

The ultimate product of acid alteration is a porous siliceous residue. This is generally a porous siliceous aggregate and should not be confused with siliceous sinters which would be deposited by hot springs from a high-temperature water-dominated geothermal system. The downward zonation would include kaolinite and alunite ($KAl_3(OH)_6(SO_4)_2$), montmorillonite, and then fresh rock as the acid is neutralized through its reaction with the rock. During the alteration process calcium, iron, and sodium tend to be released early from the rock and carried away in solution. These elements are followed by potassium and eventually aluminum. Sodium and iron have been found to have been completely removed from the rock by the time alunite forms.

8.5 Mineral Zonation in Active Thermal Systems

In recent years, a number of workers have published detailed studies of alteration in active geothermal systems. Browne (1978) has reviewed many of these studies and has summarized the occurrence of many of the reported hydrothermal phases (Table 8-2). Ellis (1979) also presents a brief discussion of hydrothermal alteration in a large number of geothermal systems.

This section presents discussions of some of the zonations which have been documented in active hydrothermal systems. In addition, clay mineral zonation which has been found in some deep wells in sedimentary sequences will also be discussed. This deep work is largely from oil and gas exploration and

Table 8-2 Some hydrothermal minerals in selected geothermal fields ¹

	Imperial Valley, California ^a	Yellowstone, Wyoming	The Geysers, California	Pauzhetsk, Kamchatka	Matsukawa, Japan	Otake, Japan	Tongonan, Philippines	Kawah Kamojang, Java	N.Z. Volcanic Zone	El Tatio, Chile	Low temp Iceland	High temp. Iceland	Larderello, Italy
Allophane				x									
Quartz	x	x	x	x	x	x	x	x	x	x	r?	x	x
Cristobalite		x		x	x	x	x	x	x	x			
Kaolin group	d	x	x	x	x	x	x	x	x	x			
Montmorillonite	d	x		x	x	x	x	x	x	x	x	x	
Interlayered illite-mont.	x			x	x	x	x	x	x		x	x	
Illite	x	x	x	x	x	x	x	x	x	x			
Biotite	x			x					x				
Chlorite	x	x	x	x	x	x	x	x	x	x	?	x	x
Celadonite		x		x						x	x		
Alunite			x	x	x	x	x		x				
Anhydrite	x		x	x	x	x	x	x	x	x		x	x
Sulfur			x	x	x		x		x				
Pryrophyllite					r	x	r	r					
Talc	x						x						
Diaspore					x	x		x					
Calcite	x	x	x	x	x	x	x	x	x	x	x	x	x
Aragonite	x ^b						x ^b		x ^b				
Siderite			x	x			x		x	x			
Ankerite	x			x								x	
Dolomite	d												
Analcime		x		x					x		x	x	
Wairakite	x		x	x		x	x	x	x			x	x
Gmelinite											x		
Gismondine											x		
Erionite		x											
Laumontite		x		x	x	x			x	x	x	x	
Phillipsite				x									
Scolecite				x							x		
Chabazite				x							x		
Thomsonite				x							x		
Clinoptilolite		x					x						
Heulandite		x		x		x	x		x		x	x	
Stilbite											x	x	
Mordenite		x		x					x		x	x	
Prehnite	x			x					x		r?	x	
Amphibole	x			x			x					x	
Garnet	x			?								r	
Epidote	x			x		x	x	x	x		r	x	x
Clinozoisite									x				
Pectolite		x							x ^b				
Sphene	x			x			x	x	x				
Adularia	x	x	x	x		x	x	x	x	x			x
Albite	x			x		x	x	x	x			x	
Rutile				x	x	x							
Leucoxene			x	x	x		x		x				
Magnetite							x						
Hematite	x	x		x			x	x	x	x	x		
Pyrite	x	x	x	x	x	x	x	x	x	x	x	x	x
Pyrrhotite	x						x		x				x
Marcasite							x		x				
Base-metal sulfides	x						x		x				x
Fluorite		x						x					

(1) From Browne, 1978

Note: d = detrital, r = relict.

^a includes Cerro Prieto, Baja California, Mexico.

^b deposited in discharge pipes and channels.

develops some of the most detailed knowledge of clay mineralogy which has been generated to this time.

8.5.1 Yellowstone National Park

Work by the U.S. Geological Survey, and the Carnegie Institute before them, has documented extensive hydrothermal alteration in the near-surface environment of this very active hydrothermal area. Most of this work has centered around the interpretation of a large number of shallow holes which have been drilled for the express purpose of scientific investigation. In 1929 and 1930, the Carnegie Institute drilled three holes which are located in Figure 8-5 and described by Fenner (1936). In 1967 and 1968 the USGS drilled thirteen holes (Fig. 8-5) which have been documented in numerous reports. White et al (1975) have discussed the drilling and the temperature and pressure data from all of the USGS holes. Data on hydrothermal alteration in these holes has been presented by the following authors; Y-1 by Honda and Muffler (1970), Y-2 by Bargar and Beeson (1981), Y-3 by Bargar et al (1973), Y-5 by Keith and Muffler (1978), Y-7 and 8 by Keith et al (1978, 1983), Y-10 by Bargar (1978), and Y-11 by White et al (1971) and Bargar and Muffler (1982).

These studies provide an excellent description of the alteration processes affecting high-silica environments with much of the altered material being obsidian initially. Volcanic glasses are extremely reactive although permeability and fluid access are very important. At temperatures below about 280°C rock type has a significant effect on the products of hydrothermal alteration (Browne, 1978) and the Yellowstone studies present important contributions from a high-silica environment.

The down-hole distribution of alteration phases in drill hole Y-8 are

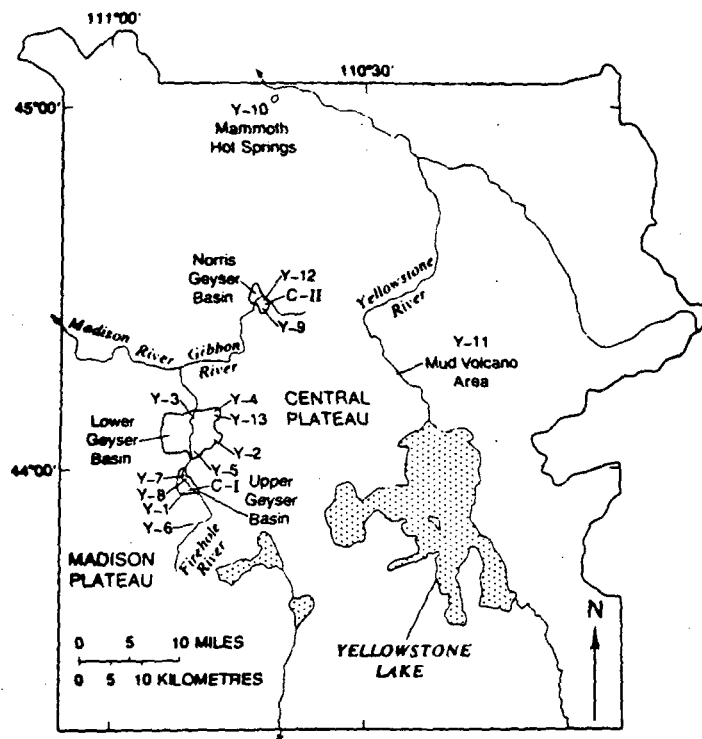


Fig. 8-5 Map of Yellowstone National Park showing holes drilled by the USGS (Y series) and the Carnegie Institute (C series).

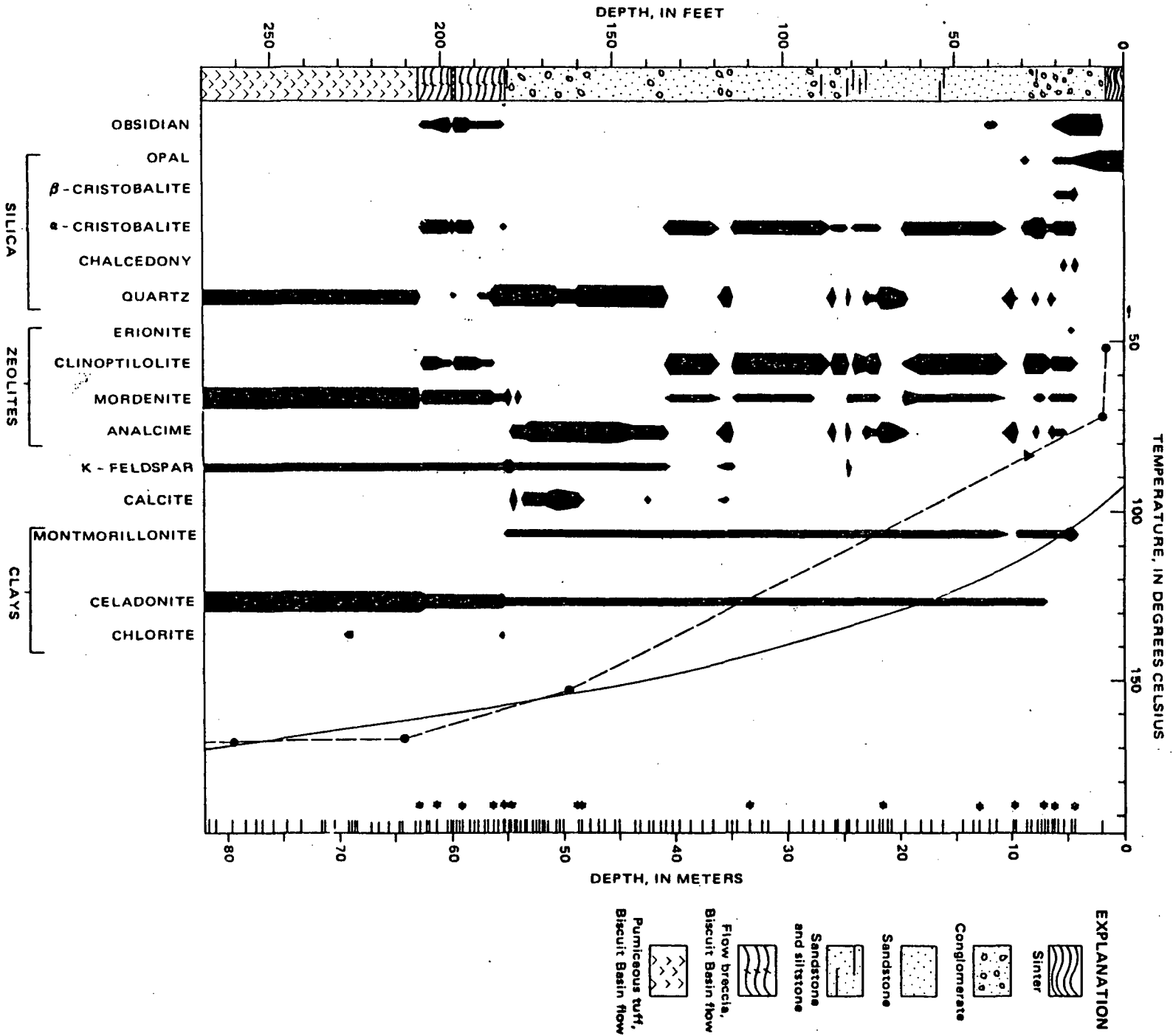
shown in Figure 8-6 (Keith et al, 1978). Much of the following discussion is also from that work. Since volcanic glass is meta-stable it tends to alter quite rapidly. The first alteration product is perlite which is formed through the process of hydration. This hydration causes expansion due to the absorption of water which can effectively seal off permeability and thus stop continued alteration. If the process does continue, the first new phase to form is clinoptilolite which requires little chemical change in the original starting material beyond the continued addition of water. Clinoptilolite and a lower silica zeolite, analcime, are mutually exclusive (Fig. 8-6) and analcime may form from clinoptilolite with the liberation of potassium which may form hydrothermal K-feldspar. Other authors have attributed hydrothermal K-feldspar to the boiling process as is demonstrated in Figure 8-4.

Clay minerals are the first direct replacements of obsidian, generally forming along hydration cracks or other areas of permeability. The first formed are montmorillonite and celadonite. These phases and interlayered montmorillonite-celadonite often replace clinopyroxene phenocrysts. The presence of celadonite is probably governed by the availability of ferrous and ferric iron and possibly the availability of potassium from the thermal fluids.

From their work in these hot-water systems the USGS workers (Honda and Muffler, 1970; Keith et al, 1978) have concluded that although temperature is very important in determining the alteration mineralogy, original composition, permeability, and the supply of thermal fluids is of equal significance.

Drill hole Y-11 penetrated the vapor-dominated hydrothermal system in the Sulfur Cauldron area of Yellowstone (White et al, 1971; Bargar and Muffler, 1982). Here the vapor-dominated system developed after a water-dominated

Fig. 8-6 Distribution of phases in drill hole Y-8 from Yellowstone National Park (Keith et al., 1978).



system as evidenced by the extensive areas of siliceous sinter which line and flank the Yellowstone River in the vicinity. Bargar and Muffler (1982) report that the Lava Creek Tuff is not as conspicuously altered as it is in other locations in Yellowstone, because it has undergone primary devitrification and vapor phase crystallization during its cooling, and thus it contains no glass. Two stages of alteration have been recognized in the core from this area. The early stage contains chalcedony, sepiochlorite, calcite, quartz, mordenite, fluorite, iron oxides and hydroxides, rhodochrosite, bastnaesite, and some beta-cristobalite, pyrite and montmorillonite. This assemblage is believed to be related to alteration associated with the older stage of hot-water dominated hydrothermal activity. The later stage of alteration contains the assemblage kaolinite, halloysite, alunite, opal, and some beta-cristobalite, montmorillonite, and pyrite.

HYDROTHERMAL ALTERATION

REFERENCES

- Bargar, K.E., 1978, Geology and thermal history of Mammoth Hot Springs, Yellowstone National Park, Wyoming: U.S. Geol. Survey Bull. 1444, 55 p.
- Bargar, K.E., and Beeson, M.H., 1981, Hydrothermal alteration in research drill hole Y-2, Lower Geyser Basin, Yellowstone National Park, Wyoming: Am. Mineral., v. 66, p. 473-490.
- Bargar, K.E., Beeson, M.H., Fournier, R.O., and Muffler, L.J.P., 1973, Present-day deposition of lepidolite from thermal waters in Yellowstone National Park: Am. Mineral., v. 58, p. 901-904.
- Bargar, K.E., and Muffler, L.J.P., 1983, Hydrothermal alteration in research drill hole Y-11 from a vapor-dominated geothermal system at Mud Volcano, Yellowstone National Park, Wyoming, in Reid, S.G. and Foote, D.J. (eds), Geology of Yellowstone Park area: Wyoming Geol. Assoc. Guidebook, p. 139-152.
- Beane, R.E., 1982, Hydrothermal alteration in silicate rocks, in Titley, S.R. (ed), Advances in geology of the porphyry copper deposits, southwestern North America: Tucson, U. of Arizona Press, p. 117-137.
- Boles, J.R. and Franks, S.G., 1979, Clay diagenesis in Wilcox sandstones of southwest Texas: implication of smectite diagenesis on sandstone cementation: Jour. Sed. Petrology, v. 49, p. 55-70.
- Brindley, G.W., 1981, Structures and chemical compositions of clay minerals, in Longstaffe, F.J. (ed), Clays and the resource geologist: Mineral. Assoc. Canada shortcourse handbook, v. 7, p. 1-21.
- Browne, P.R.L., 1970, Hydrothermal alteration as an aid in investigating geothermal fields: GEOTHERMICS - Special Issue 2, p. 564-570.
- Browne, P.R.L., 1978, Hydrothermal alteration in active geothermal fields: Ann. Rev. Earth Planet. Sci., v. 6, p. 229-250.
- Browne, P.R.L. and Ellis, A.J., 1970, The Ohaki-Broadlands hydrothermal area, New Zealand: Minerology and related geochemistry: Am. Jour. Sci., v. 269, p. 97-131.
- Burruss, R.C. and Hollister, L.S., 1979, Evidence from fluid inclusions for a paleogeothermal gradient at the geothermal test well sites, Los Alamos, New Mexico: Jour. Volc. and Geotherm. Res., v. 5, p. 163-177.
- Deer, W.A., Howie, R.A., and Zassman, J., 1966, An introduction to the rock-forming minerals: New York, Wiley, 528 p.
- Dunoyer de Segonzac, G., 1970, The transformation of clay minerals during diagenesis and low-grade metamorphism: a review: Sedimentology, v. 15, p. 281-346.

- Eberl, D., Whitney, G., and Khoury, H., 1978, Hydrothermal reactivity of smectite: *Amer. Mineral.*, v. 63, p. 401-409.
- Elders, W.A. and Bird, D.K., 1976, Investigations of the Dunes geothermal anomaly, Imperial Valley, California: Part II. Petrological studies: Active formation of silicified cap rocks in arenaceous sands in a low-temperature, near surface geothermal environment in the Salton Trough of California, U.S.A.: in Cadek, J. and Paces, T. (eds.), *Proceedings of the International Symposium on Water-Rock Interaction*, Geological Survey, Prague (1974), p. 15-157.
- Elders, W.A., Hoagland, J.R., McDowell, S.D., and Cobo, J.M., 1978, Hydrothermal mineral zones in the geothermal reservoir of Cerro Prieto: *Proceedings of the first symposium on the Cerro Prieto geothermal field*, Baja California, Mexico.
- Elders, W.A., Hoagland, J.R., and Olson, E.R., 1978a, Hydrothermal mineralogy and isotope geochemistry in the Cerro Prieto geothermal field, Mexico: III. Practical Applications, *Geothermal Resources Council Transactions*, v. 2, p. 177-180.
- Elders, W.A., Hoagland, J.R., Olson, E.R., McDowell, S.D., and Collier, P., 1978b, A comprehensive study of samples from geothermal reservoirs; petrology and light stable isotope geochemistry of twenty-three wells in the Cerro Prieto geothermal field, Baja, California, Mexico, University of California at Riverside/Institute of Geophysics and Planetary Physics, Report 77/26, 153 p.
- Ellis, A.J., 1971, Magnesium concentrations in the presence of magnesium chlorite, calcite, carbon dioxide, quartz, *American Journal of Science*, v. 271, p. 481-489.
- Ellis, A.J., 1979, Chemical geothermometry in geothermal systems, *Chemical Geology*, v. 25, p. 219-226.
- Ellis, A.J., 1979, Explored geothermal systems: in *Geochemistry of Hydrothermal Ore Deposits*; ed. H.L. Barnes, John Wiley and Sons, New York, p. 632-683.
- Ellis, A.J. and Mahon, W.A.J., 1964, Natural hydrothermal systems and experimental hot water/rock interactions: *Geochim et Cosmochim Acta*, v. 28, p. 1323-1357.
- Ellis, A.J. and Mahon, W.A.J., 1967, Natural hydrothermal systems and experimental hot/rock interactions: Part 2, *Geochim et Cosmochim Acta*, v. 31, p. 519-538.
- Ellis, A.J. and Mahon, W.A.J., 1977, *Chemistry and geothermal systems*, Academic Press, New York, 392 p.
- Ewers, G.R. and Keays, R.R., 1977, Volatile and precious metal zoning in the Broadlands Geothermal Field, New Zealand: *Economic Geology*, v. 72, p. 1337-1354.

- Facca, G. and Tonani, F., 1967, The self-sealing geothermal field: Bull. Volcanol., v. XXX, p. 271-273.
- Fenner, C.N., 1936, Bore-hole investigations in the Yellowstone Park: J. Geol., v. 44, p. 225-315.
- Grindley, G.W. and Browne, P.R.L., 1976, Structural and hydrological factors controlling the permeabilities of some hot-water geothermal fields: Proc. 2nd United Nations symp. on Devel. and Use of Geothermal Resources, San Francisco, CA, May 1975, p. 277-386.
- Helgeson, H.C., 1967, Solution chemistry and metamorphism, in Abelson, P.H. (ed) Research in Geochemistry, v. 2, New York, Wiley, p. 362-402.
- Helgeson, H.C., 1979, Mass transfer among minerals and hydrothermal solutions, in Barnes, H.L. (ed), Geochemistry of hydrothermal ore deposits, 2nd Edition, New York, Wiley-Interscience, p. 568-610.
- Helgeson, H.C., Brown, T.H., and Leeper, R.H., 1969, Handbook of theoretical activity diagrams depicting chemical equilibria in geologic systems involving an aqueous phase at one atm and 0° to 300°C: San Francisco, Freeman, Cooper, 253 p.
- Holland, H.D., 1967, Gangue minerals in hydrothermal deposits, in Barnes, H.L. (ed), Geochemistry of hydrothermal ore deposits: New York, Holt, Rinehart, and Winston, p. 382-436.
- Holland, H.D. and Malinin, S.D., 1979, The solubility and occurrence of non-ore minerals, in Barnes, H.L. (ed), Geochemistry of hydrothermal ore deposits, 2nd edition: New York, Wiley, p. 461-508.
- Honda, S. and Muffler, L.J.P., 1970, Hydrothermal alteration in core from research drill hole Y-1, Upper Geyser Basin, Yellowstone National park, Wyoming: Am. Mineral., v. 55, p. 1714-1737.
- Hower, J., 1981a, X-ray diffracton identification of mixed-layer clay minerals, in Lonstaffe F.J. (ed), Clays and the resource geologist: Mineral. Assoc. Canada Shortcourse handbook, v. 7, p. 60-80.
- Hower, J., 1981b, Shale diagenesis, in Longstaffe, F.J. (ed), Clays and the resource geologist: Mineral. Assoc. Canada shortcourse handbook, v. 7, p. 60-80.
- Jones, J.B. and Segnit, E.R., 1971, The nature of opal I. Nomenclature and constituent phase: J. Geol. Soc. Australia, v. 18, p. 57-68.
- Keith, T.E.C. and Muffler, L.J.P., 1978, Minerals produced during cooling and hydrothermal alteration of ash flow tuff from Yellowstone drill hole Y-5: Jour. Volcanol. and Geoth. Res., v. 3, p. 373-402.
- Keith, T.E.C., Thompson, J.M., and Mays, R.E., 1983, Selective concentration of cesium in analcime during hydrothermal alteration, Yellowstone National Park, Wyoming: Geochim et Cosmochim Acta, v. 47, p. 795-804.

- Keith, T.E.C., White, D.E., and Beeson, M.H., 1978, Hydrothermal alteration and self sealing in Y-7 and Y-8 drill holes in northern part of Upper Geyser Basin, Yellowstone National Park, Wyoming: U.S. Geol. Survey Prof. Paper 1054-A, 26 p.
- McDowell, S.D. and Elders, W.A., 1980, Authigenic layer silicate minerals in borehole Elmore 1, Salton Sea geothermal field, California, U.S.A.: Contrib. Mineral. Petrol., v. 74, p. 293-310.
- Meyer, C. and Hemley, J.J., 1967, Wall rock alteration, in Barnes, H.L. (ed), Geochemistry of hydrothermal ore deposits: New York; Holt, Rinehart, and Winston, p. 166-235.
- Muffler, L.J.P. and White, D.E., 1969, Active metamorphism of Upper Cenozoic sediments in the Salton Sea geothermal field and the Salton Trough, southeastern California: Geol. Soc. America Bull., v. 80, p. 157-182.
- Murata, K.J. and Larson, R.R., 1975, Diagenesis of Miocene siliceous shales, Temblor Range, California: U.S. Geol. Survey Jour. Res., v. 3, p. 553-566.
- Murata, K.J. and Norman, M.B., 1976, An index of crystallinity for quartz: Am. Jour. Sci., v. 276, p. 1120-1130.
- Renner, J.L., White, D.E., and Williams, D.L., 1975, Hydrothermal convection system, in White, D.E. and Williams, D.L. (eds), Assessment of Geothermal Resources of the United States-1975: U.S. Geol. Survey Circular 726, p. 5-57.
- Reynolds, R.C. and Hower, J., 1970, The nature of interlayering in mixed layer illite-montmorillonites: Clays and Clay Minerals, v. 18, p. 25-36.
- Schoen, R., White, D.E., and Hemley, J.J., 1974, Argillization by decending acid at Steamboat Springs Nevada: Clays and Clay Minerals, v. 22, p. 1-22.
- Slaughter, M. and Earley, J.W., 1965, Mineralogy and geological significance of the Mowry bentonites, Wyoming: Geol. Soc. America Sp. Paper 83, 116 p.
- Steiner, A., 1968, Clay mineras in hydrothermally altered rocks at Wairakei, New Zeland: Clays and Clay Minerals, v. 16, p. 193-213.
- White, D.E., Brannock, W.W., and Murata, K.J., 1956, Silica in hot-spring waters: Geochim et Cosmochim Acta, v. 10, p. 27-59.
- White, D.E., Fournier, R.O., Muffler, L.J.P. and Truesdell, A.H. 1975, Physical results of research drilling in thermal areas of Yellowstone National Park, Wyoming: U.S. Geol. Survey Prof. Paper 892, 70 p.
- White, D.E., Muffler, L.J.P., and Truesdell, A.H., 1971, Vapor-dominated hydrothermal systems compared with hot-water systems: Econ. Geology, v. 66, p. 75-97.

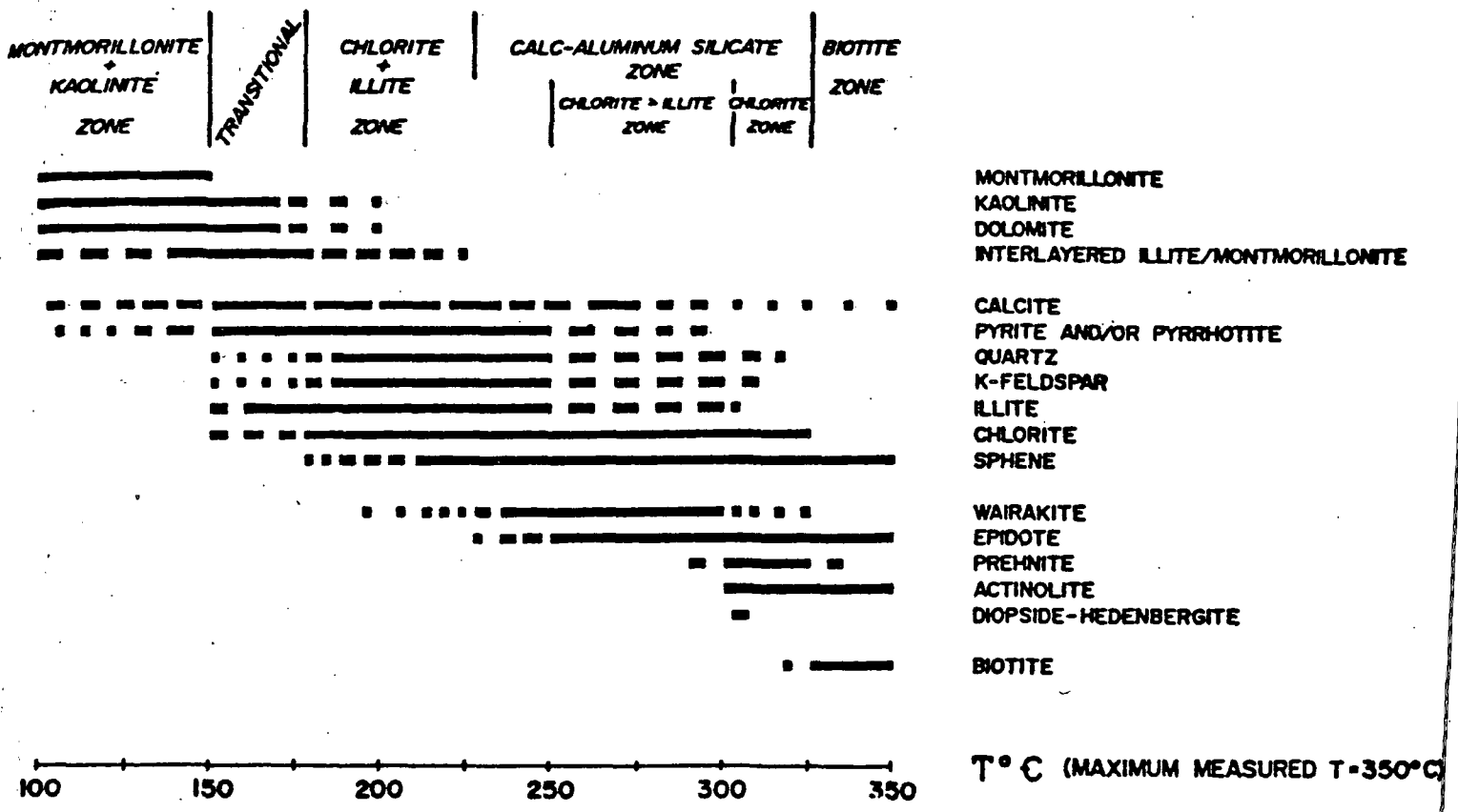


Figure 2. Mineral zones in sandstones at Cerro Prieto as a function of temperature.

Elders and others, 1979

Age Dating of Rocks and Minerals in Geothermal and Volcanic Environments

- I. Purpose of dating
 1. Measure time and duration of geological events
 - a) thermal events
 - volcanic eruption
 - magma emplacement
 - hydrothermal systems - alteration
 - b) tectonic events
 - uplift of rocks
- II. Basis of dating
 1. Qualitative relations
 - a) soil development, geomorphic position, lichenometry
 2. Quantitative methods
 - a) based on radioactive decay
 - b) measures time since system became closed to removal of daughter product of decay (blocking or retention temperature)
- III. Techniques of dating
 1. Conventional K-Ar
 - a) basis
 - b) suitable materials
 - c) analytic techniques
 - d) assumptions
 2. $^{40}\text{Ar}/^{39}\text{Ar}$
 - a) basis
 - b) analytic techniques
 - c) comparison with conventional K-Ar
 3. Fission track
 - a) basis
 - b) suitable materials
 - c) population method
 - d) external detection method
- IV. Interpretation of results
 1. Two fold problem
 - a) precision of laboratory analyses (dates) - the mysterious \pm
 - b) geologically meaningful interpretation (ages)
 - representative sampling
 - interpretability
 2. Tectonic events
 - a) uplift through isotherms
 3. Thermal events
 - a) igneous emplacement
 - b) hydrothermal systems

V.

Other techniques

1. Obsidian hydration
2. U disequilibrium
3. Dating waters (?)

QUALITATIVE DATING METHODS

BASED ON: STRATIGRAPHIC RELATIONS
DEVELOPMENT OF A GEOLOGICAL PARAMETER

EXAMPLES: GEOMORPHIC RELATIONS
SOIL HORIZONS
LICHEN GROWTH

QUANTITATIVE METHODS

CONVENTIONAL K-AR

$^{40}\text{AR}/^{39}\text{AR}$

FISSION TRACK

OTHERS

ABSOLUTE AGE DATING

BASED ON RADIOACTIVE DECAY

$$N = N_0 e^{-\lambda t}$$

λ = DECAY CONSTANT

CONCEPT OF HALF-LIVES

TIME IT TAKES 1/2 OF PARENT TO DECAY

$$T_{1/2} = \frac{\ln 2}{\lambda}$$

$T_{1/2}$ IN SYSTEMS DISCUSSED HERE

$${}^{40}\text{K} = 1.25 \times 10^9 \text{ YR}$$

$${}^{238}\text{U} = 4.47 \times 10^9 \text{ YR}$$

K-AR: < 30,000Y TO 4.5 BY

FISSION TRACK: 100Y TO μe

QUANTITATIVE DATING MEASURES TIME OF SYSTEM

"CLOSURE" - I.E. RETENTION OF DAUGHTER PRODUCTS

K-Ar - RETENTION OF Ar IN MINERAL GRAINS

CLOSED TO Ar LOSS

FISSION TRACK - RETENTION OF TRACKS IN MINERALS

CLOSED TO ANNEALING

CLOSURE - DEPENDENT UPON TEMPERATURE

COOLING RATE

PHYSICAL AND CHEMICAL SYSTEM
PARAMETERS

CONVENTIONAL K-AR

BASED ON DECAY OF ^{40}K TO ^{40}AR BY

ELECTRON CAPTURE AND POSITRON EMISSION

$^{40}\text{K} = 0.0119\%$ TOTAL K

MATERIALS SUITABLE FOR K-AR DATING VOLCANIC ROCKS

1) MINERALS

FELDSPARS: K-SPAR (130-200⁰C)

PLAGIOCLASE

MICA: BIOTITE (~ 280⁰C)

MUSCOVITE

AMPHIBOLE: HORNBLLENDE (~ 550⁰C)

2) BASALT

WHOLE ROCK

K MEASURED BY: FLAME PHOTOMETRY.

ATOMIC ABSORPTION

XRF

NEUTRON ACTIVATION

OTHERS - ICP

ANALYSES MADE OF SEPARATE SPLIT OF SAMPLE THAN THE
SPLIT ANALYZED FOR AR

^{40}Ar MEASURED BY ISOTOPE DILUTION

1) SEPARATE MINERALS

2) FUSE KNOWN AMOUNT IN VACUUM

3) ADD ^{38}Ar SPIKE

4) PURIFY GASSES: H_2O & CO_2 FROZEN

N_2 - Ti GETTER

H_2 - REACTED WITH
 Cu-CuO

5) MEASURES RATIOS: $^{40}\text{Ar}/^{38}\text{Ar}$

$^{40}\text{Ar}/^{36}\text{Ar}$

K-Ar Assumptions

- 1) No radiogenic ^{40}Ar has escaped since cooling
- 2) No excess ^{40}Ar has been added
- 3) Atmospheric ^{40}Ar corrected appropriately
- 4) Mineral closed to K
- 5) Isotopic composition changed only by K decay
- 6) Decay constants are known

Measures blocking temperatures of minerals



Argon Loss

- 1) Mineral lattice may not retain Ar thru time
- 2) Partial or complete melting
- 3) Metamorphism
- 4) Alteration
- 5) Chemical or mechanical weathering



CONVENTIONAL K-Ar FORMULAS

$${}^{40}\text{Ar}^* = {}^{38}\text{Ar}_S \left\{ \left(\frac{{}^{40}\text{Ar}}{38}\text{Ar} \right)_M - \left(\frac{{}^{40}\text{Ar}}{38}\text{Ar} \right)_S - \left[\frac{1 - \left(\frac{{}^{38}\text{Ar}}{36}\text{Ar} \right)_M \left(\frac{{}^{36}\text{Ar}}{38}\text{Ar} \right)_S}{\left(\frac{{}^{38}\text{Ar}}{36}\text{Ar} \right)_M \left(\frac{{}^{36}\text{Ar}}{38}\text{Ar} \right)_A - 1} \right] \times \left(\frac{{}^{40}\text{Ar}}{38}\text{Ar} \right)_A - \left(\frac{{}^{40}\text{Ar}}{38}\text{Ar} \right)_M \right\}$$

S = SPIKE

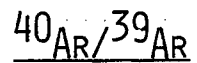
M = MIXTURE

A = ATMOSPHERIC

substitute to get date in:

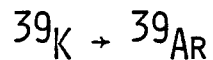
$$t = \frac{1}{\lambda} \ln \left[\frac{{}^{40}\text{Ar}^*}{{}^{40}\text{K}} \left(\frac{\lambda}{\lambda_e} \right) + 1 \right]$$





CAN DISTINGUISH GAIN OR LOSS OF AR
IDENTIFY DETAILS OF THERMAL HISTORY

MEASURE AR AND K ON SAME SAMPLE
IRRADIATE SAMPLE WITH STANDARD



ANALYZE IN MASS SPECTROMETER BY INCREMENTAL
HEATING

MEASURE RATIOS IN STANDARD AND SAMPLES

$$t = \frac{1}{\lambda} \ln \left[\frac{40\text{Ar}^*}{39\text{K}} \left(\frac{\lambda}{\lambda e} \right)^{J+F} \right]$$

J FROM STANDARD

CONVENTIONAL K-AR VS ^{40}Ar - ^{39}Ar

- CONVENTIONAL REQUIRES SEPARATE SAMPLES FOR K AND AR ANALYSES, ^{40}Ar - ^{39}Ar DOES NOT
- CONVENTIONAL GIVES INTEGRATED AGE OF ALL AR COMPONENTS IN GRAIN
- ^{40}Ar - ^{39}Ar GIVES DATA ABOUT DISTURBANCE
- ^{40}Ar - ^{39}Ar REQUIRES ACCESS TO REACTOR
- ^{40}Ar - ^{39}Ar PRECISION TO 0.25%

Fission Track

based on spontaneous fission of ^{238}U

fission fragments move through crystal lattice

creating 10 micron tracks that

can be etched for visibility with

1000x optical microscope

to calculate date, need: density of tracks

concentration of U

method gives - time mineral was at temperature

that allows retention of tracks

allows - quantification of thermal history of area



Fission Track Assumptions

- 1] Sufficient concentration of U**
- 2] Track stability known**
- 3] Not many inclusions, defects,
or lattice dislocations**
- 4] U distribution must be representative**



MINERALS FOR FISSION TRACK

ZIRCON (175 ± 25⁰C)

APATITE (105 ± 10⁰C)

SPHENE (290 ± 40⁰C)

EPIDOTE

GLASS - MAY BE INACCURATE

METHOD MEASURES, IN K-AR YEARS,
TIME SINCE MINERAL COOLED THROUGH
TEMPERATURE OF ANNEALING

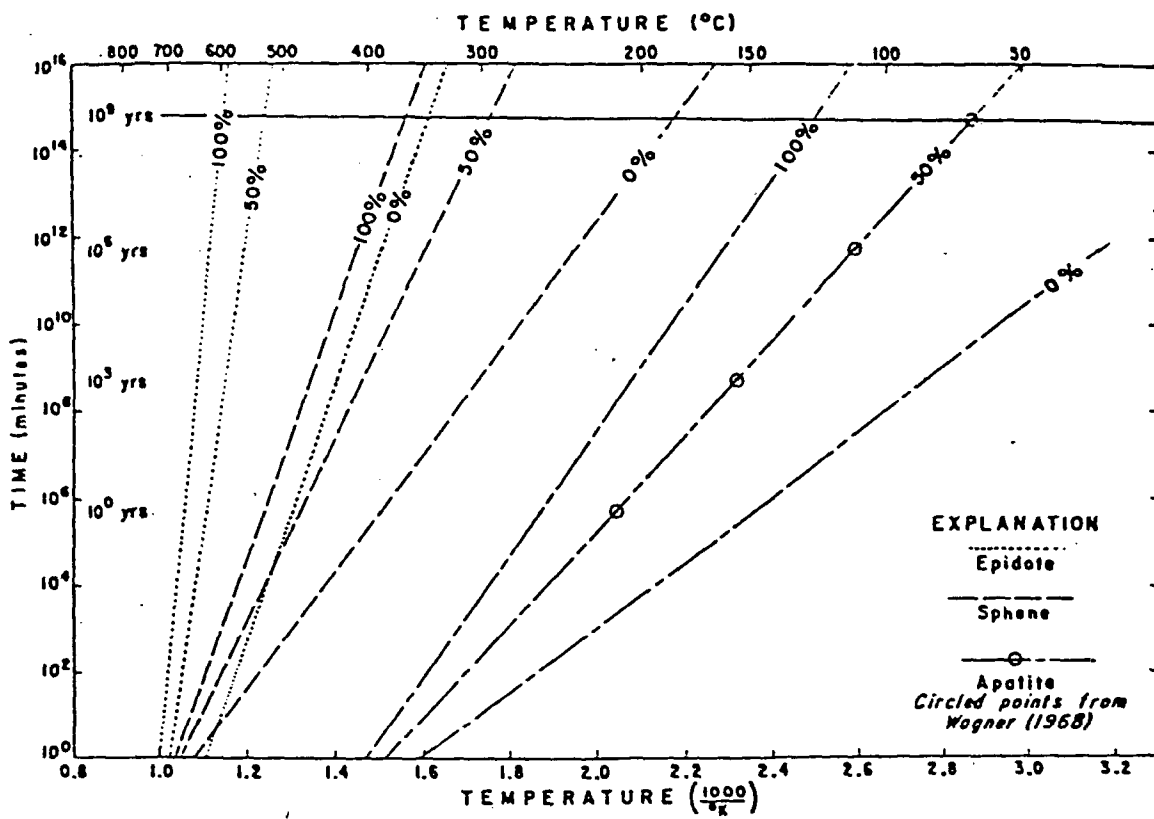


Figure 13. Extrapolated annealing data for spinel and apatite.

FISSION TRACK TECHNIQUE

POPULATION METHOD

- 1) MOUNT AND POLISH MINERALS
- 2) ETCH
- 3) COUNT NATURAL TRACKS
- 4) IRRADIATE
- 5) COUNT INDUCED TRACKS
- 6) ESTABLISH NEUTRON DOSE FROM MONITOR

Fission Track - External Detector

1) mount and polish minerals

2) etch

3) mount detector (annealed muscovite)

4) irradiate package (grain, detector, monitor)

5) remove and etch detectors

6) remount detector

7) count tracks





CALCULATE AGE:

$$t = \frac{1}{\lambda_a} \ln \left[1 + \left(\frac{P_s}{P_i} \right) \left(\frac{\lambda_a}{\lambda_f} \right) \frac{\psi \sigma}{I} \right]$$

$$= 6.446 \times 10^9 \ln \left[1 + 7.744 \times 10^{-18} \left(\frac{P_s}{P_i} \right) \psi \right]$$

P_s = spontaneous track density

P_i = induced track density

ψ = neutron dose

λ = ^{238}U alpha decay = $1.55125 \times 10^{-10} \text{ y}^{-1}$

λ_f = ^{238}U fission decay = $8.46 \times 10^{-17} \text{ y}^{-1}$

I = atomic ratio $^{238}\text{U} / ^{235}\text{U} = 137.8$

σ = ^{235}U cross section = $582 \times 10^{-24} \text{ cm}^2$

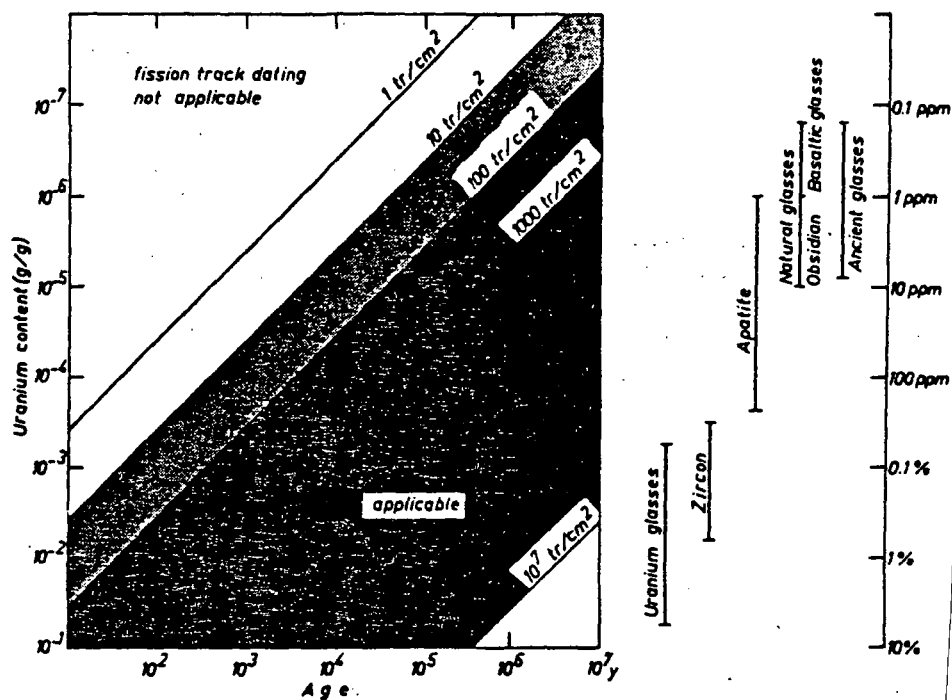


Fig. 3. Usefulness of a sample for fission-track dating in relation to its uranium content and its age. Counting of track densities below 100 tracks/cm² is very time-consuming

INTERPRETATION OF RESULTS

"DATES" vs "AGES"

BE AWARE OF THE \pm

REPRESENTATIVE SAMPLING IMPORTANT

CAN SEPARATE CLOSELY SPACED EVENTS
CAN IDENTIFY DIFFERENT GENERATIONS
CAN OBTAIN AGE FOR DURATION OF EVENT

K-Ar

different blocking temperatures may
yield different dates

if concordant - cooled quickly

if discordant - cooled slowly

partial metamorphism

date may not be meaningful



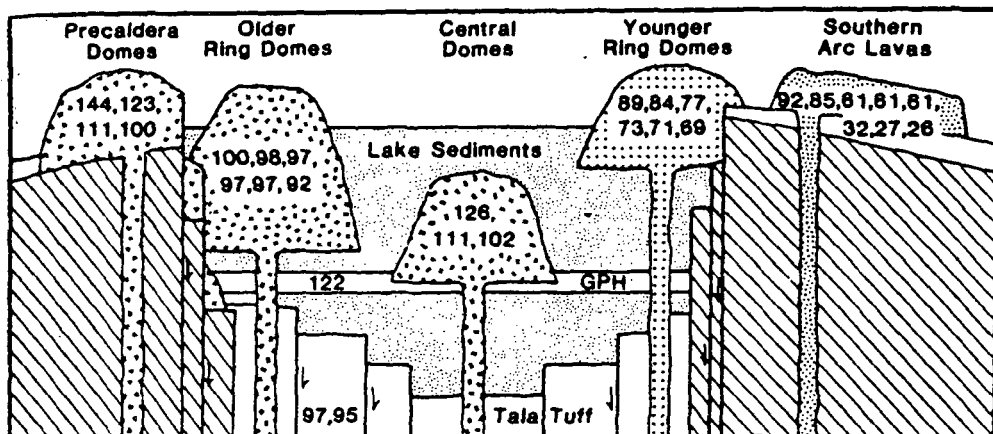


Figure 3. Schematic cross section with K-Ar dates. The central domes and giant pumice horizon (GPH) are stratigraphically approximately equivalent in age. The autobrecciated bases of the older ring domes are separated from the GPH by approximately 10 m of caldera-lake sediments, whereas there are approximately 50 m of sediments between the bases of the younger ring domes and the GPH. The lake sediments are capped by subaerial airfall tephra correlated chemically with the southern arc lavas. Overlapping relations within the southern arc lavas indicate they young from east to west, consistent with the 30-Ka dates on the easternmost dome (FF in Fig. 1). Although the dates are generally in accord with stratigraphic relations, the GPH and central domes and possibly the older ring domes give anomalously old ages due to extraneous argon. Patterns as in Figure 1.

Ma hood and Drake, 1982

KBS data

Table 1.--Summary of dates obtained from the KBS Tuff (m.y.).
(K-Ar dates recalculated to the new IUGS standard constants)

Total fusion K-Ar	Total fusion ⁴⁰ Ar/ ³⁹ Ar	⁴⁰ Ar/ ³⁹ Ar age spectrum
Area 105		
3.72±2.1 (FM) p	3.19±1.1 (FM) p	2.48±0.01 (FM) f (Regression analysis; four datum points).
2.46±1.0 (FM) p	2.31±0.5 (FM) p	
2.44±0.3 (FM) f	2.45±0.3 (FM) f	1.96±0.11 (FM) f (Full regression analysis; complex overprint spectrum).
2.42±0.3 (FM) f	0.53±0.33 (FM) f	
2.01±0.03 (B) f	1.60±0.19 (FM) f	
2.40±0.03 (B) f		
1.56±0.02 (B) f	1.87±0.19 (FM) f	
1.65±0.02 (B) f		
1.61±0.02 (B) f	2.11±0.19 (FM) f	
1.68±0.01 (B) g	1.09±0.29 (FM) f	
2.53±0.02 (B) f	1.58±0.12 (FM) f	
1.50±0.02 (B) f	1.39±0.14 (FM) f	
1.62±0.02 (B) f		
1.65±0.02 (B) f	2.17±0.10 (FM) f	
Area 131		
2.16±0.03 (B) f	0.93±0.54 (FM) f	1.57±1.0 (FM) f (Peak age; complex overprint spectrum).
1.83±0.02 (B) f	0.93±0.54 (FM) f	
1.84±0.07 (B) g		
1.81±0.02 (B) f	2.15±0.19 (FM) f	1.78±0.03 (FM) f (Average double line regression analysis; complex overprint spectrum).
1.85±0.03 (B) f	0.70±0.17 (FM) f	1.10±0.32 (FM) f (Full regression analysis; complex overprint spectrum).
1.73±0.03 (B) f		1.79±0.02 (FM) f (Four datum point regression analysis; complex overprint spectrum).
1.83±0.03 (B) f		1.96±0.03 (FM) f (Six datum points regression analysis; complex overprint spectrum).
Area 10		
6.90±0.05 (B) f		2.47±0.02 (FM) f (Average double line regression analysis).
1.54±0.02 (B) f		
1.60±0.01 (B) f		

Authors of original papers suggest possible detrital contamination. p = pumice sample, whole rock; f = sanidine-anorthoclase; g = glass. Bracketed dates are from a single sample. FM = Fitch and Miller (1970, 1975); Fitch, Hooker, and Miller (1976, 1978). B = Curtis and others (1975). Fission track date on zircon from Area 131 is 2.44±0.08 m.y., obtained by Hurford, Gleadow, and Naeser (1976).

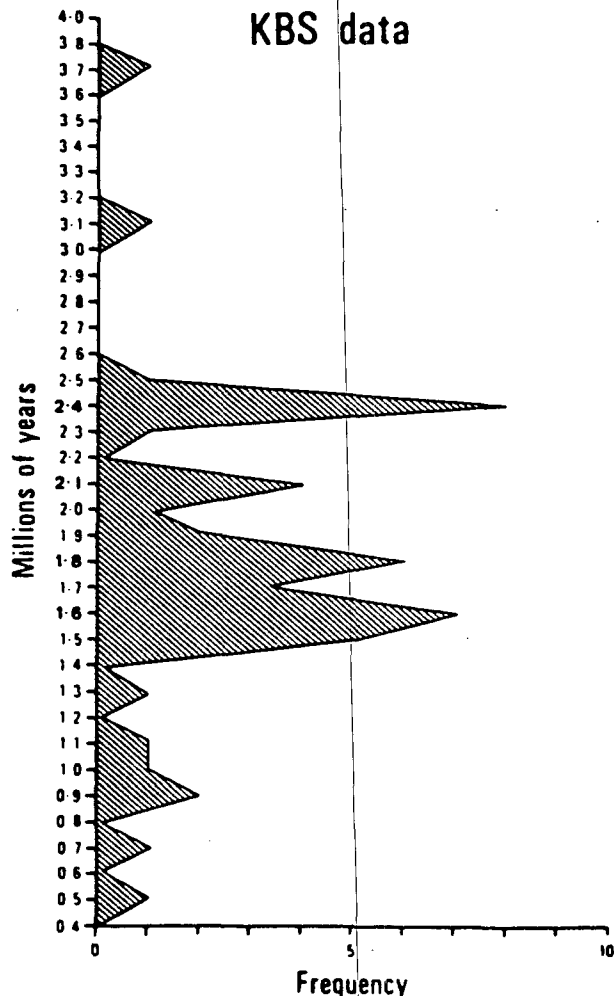
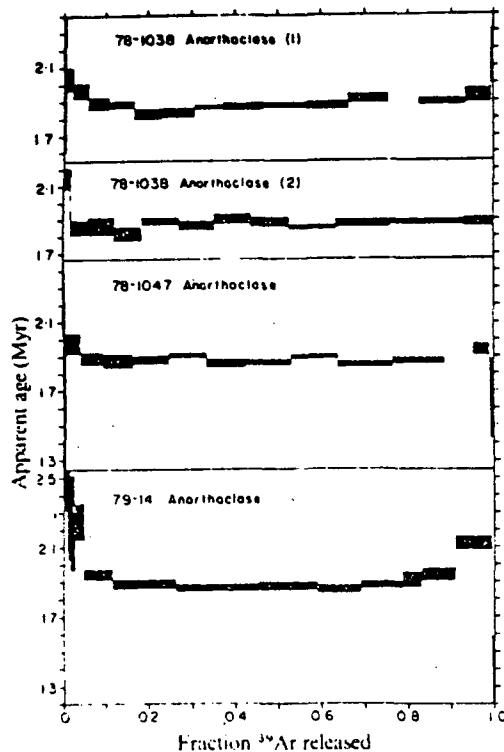


Figure 1.--Unweighted frequency distribution diagram of published dates from the KBS Tuff.



McDougall, 1981

Fig. 1. ⁴⁰Ar/³⁹Ar age spectra for anorthoclase from pumice clasts in the KBS Tuff. Data plotted as apparent age against fraction of ³⁹Ar released. Uncertainty of the age for each step, at the level of 1 s.d., indicated by thickness of bar.

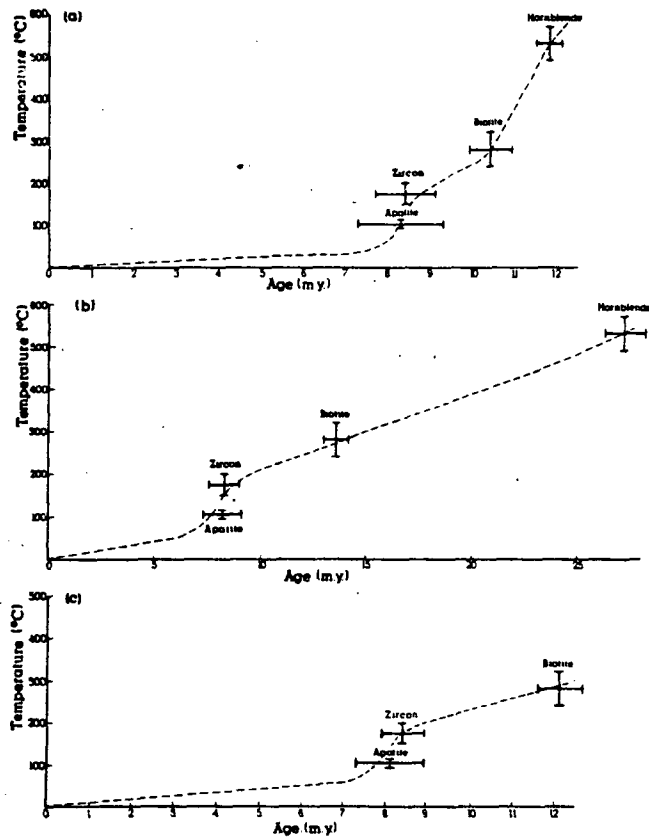


Figure 2. Cooling histories for three samples from the Mineral Mountains intrusive complex, Utah. K-Ar and fission track dates from Table 1 and Table 2 are plotted against closure temperature discussed in text. (a) sample 79-1 Biotite granite (Tbg); (b) sample 79-153 Hornblende granodiorite (hd); (c) 79-154 Quartz monzonite (Tqm). Error bars are those quoted in Tables 1, 2 and text. Dashed lines represent hypothetical cooling curve followed by each sample.

- Berger, G. W., and York, Derek, 1981, Geothermometry from $^{40}\text{Ar}/^{39}\text{Ar}$ dating experiments: *Geochem. Cosmochim. Acta*, v. 45, p. 795-811.
- Coleman, S. M., and Pierce, K. L., 1977, Summary Table of Quaternary Dating Methods: U.S. Geological Survey Map MF-904.
- Colman, S. M., Pierce, K. L., 1981, Weathering rinds on andesitic and basaltic stones as a Quaternary age indicator, western United States: U.S. Geol. Surv. Prof. Paper 1210, 56 p.
- Dalrymple, G. B., 1979, Critical tables for conversion of K-Ar ages from old to new constants: *Geology*, v. 7, p. 558-560.
- Dalrymple, G. B., and Lanphere, M. A., 1969, Potassium-Argon Dating: Freeman and Co., San Francisco, 258 pages.
- Dalrymple, G. B., Alexander, E. C., Jr., Lanphere, M. A., and Kraker, G. P., 1981, Irradiation of samples for $^{40}\text{Ar}/^{39}\text{Ar}$ dating using the Geological Survey TRIGA reactor: U.S. Geol. Surv. Prof. Paper 1176, 55 p.
- Dodson, M. H., 1979, Theory of cooling ages, in Jager, E., Hunziker, J.C., eds., *Lectures in Isotope Geology*: Springer-Verlag, New York, p. 194-202.
- Evans, S. H., Jr., and Nielson, D. L., 1982, Thermal and tectonic history of the Mineral Mountains intrusive complex: Geothermal Resources Council, *Trans.*, v. 6, p. 15-18.
- Faure, G., 1977, Principles of Isotope Geology: John Wiley and Sons, N. Y., p. 147-181, 267-281.
- Fitch, F. J., Hurford, A. J., Hooker, P. J., Miller, J. A., 1978, The KBS Tuff problem, in, Zartman, R. E., ed., *Short papers of the Fourth International Conference, Geochronology, Cosmochronology, Isotope Geology*: U.S. Geol. Surv. Open-file Rept. 78-701, p. 114-117.
- Friedman, I., 1968, Hydration rind dates rhyolite flows: *Science*, v. 159, p. 878-880.
- Harrison, T. M., and McDougall, Ian, 1980, Investigations of an intrusive contact, northwest Nelson, New Zealand - I. Thermal, chronological and isotopic constraints: *Geochem. Cosmochim. Acta*, v. 44, p. 1985-2003.
- Harrison, T. M., and McDougall, Ian, 1982, The thermal significance of potassium feldspar K-Ar ages inferred from $^{40}\text{Ar}/^{39}\text{Ar}$ age spectrum results: *Geochem. Cosmochim. Acta*, v. 46, p. 1811-1820.
- Hurford, A. J., and Green, P. F., 1982, A users' guide to fission track dating calibration: *Earth and Planetary Science Letters*, v. 59, p. 343-354.
- Izett, G. A., and Naeser, C. W., 1976, Age of the Bishop Tuff of eastern California as determined by the fission-track method: *Geology*, v. 4, p. 587-590.

- Mahood, G. A., and Drake, R. E., 1982, K-Ar dating young rhyolitic rocks: A case study of the Sierra La Primavera, Jalisco, Mexico: Geol. Soc. of Am. Bull., v. 93, p. 1232-1241.
- McDougall, I., 1981, $^{40}\text{Ar}/^{39}\text{Ar}$ age spectra from the KBS Tuff, Koobi Fora Formation: Nature, v. 294, p. 120-124.
- Naeser, C. W., 1978, Fission Track Dating: U. S. Geological Survey Open File Report 76-190.
- Naeser, C. W., Izett, G. A., and Obradovich, J. D., 1980, Fission-track and K-Ar ages of natural glasses: U. S. Geol. Surv. Bull., 1489, 31 p.
- Seward, Diane, 1979, Comparison of zircon and glass fission-track ages from tephra horizons: Geology, v. 7, p. 479-482.
- Silberman, M. L., White, D. E., Keith, T. E. C., and Dockter, R. D., 1979, Duration of hydrothermal activity of Steamboat Springs, Nevada, from ages of spatially associated volcanic rocks: U. S. Geol. Surv. Prof. Paper 458-9, 14 p.
- Steiger, R. H., and Jager, E., 1977, Subcommittee on Geochronology: convention on the use of decay constants in geo- and cosmochronology: Earth and Planetary Science Letters, v. 36, p. 359-362.
- Wagner, G. A., 1979, Archaeometric dating, in Jager, E., J. G. Honziker, eds., Lectures in Isotope Geology: Springer-Verlag, New York, p. 178-188.